

**HOST AND PATHOGEN TRANSCRIPTIONAL PROFILES OF ACUTE *Brucella*
melitensis INFECTION**

A Dissertation

by

CARLOS ALBERTO ROSSETTI

Submitted to the Office of Graduate Studies of
Texas A&M University
in partial fulfillment of the requirements for the degree of

DOCTOR OF PHILOSOPHY

August 2007

Major Subject: Veterinary Microbiology

**HOST AND PATHOGEN TRANSCRIPTIONAL PROFILES OF ACUTE *Brucella*
melitensis INFECTION**

A Dissertation

by

CARLOS ALBERTO ROSSETTI

Submitted to the Office of Graduate Studies of
Texas A&M University
in partial fulfillment of the requirements for the degree of

DOCTOR OF PHILOSOPHY

Approved by:

Chair of Committee,
Committee Members,

Head of Department,

L. Garry Adams
Renée M. Tsolis
Terry L. Thomas
James E. Womack
Gerald Bratton

August 2007

Major Subject: Veterinary Microbiology

ABSTRACT

Host and Pathogen Transcriptional Profiles of Acute *Brucella melitensis* Infection.

(August 2007)

Carlos Alberto Rossetti, D.V.M., Universidad de Buenos Aires;

M.S., Universidad de Buenos Aires

Chair of Advisory Committee: Dr. L. Garry Adams

The parallel gene expression profiles of *Brucella melitensis* and the host have not been elaborated. In this study, I analyze and discuss the transcriptional profiles of *B. melitensis* invasive-associated genes, the expression profile of intracellular *B. melitensis* and *B. melitensis*-infected non-phagocytic cells in the first 12 h post-infection (PI), and the *in vivo* temporal global transcriptome of both *B. melitensis* and the infected bovine host in the first 4 h PI. The initial study found that *B. melitensis* at late-log phase of growth were more invasive in non-phagocytic cells than at early-log or stationary growth phase. Microarray-based studies identified 454 *Brucella* genes differentially expressed between the most and the least invasive growth phases. Additionally, *B. melitensis* strains with transposon interrupted in loci BMEII0380 (*acrA*) and BMEI1538 (hypothetical protein) were found to be deficient in internalization compare with the wild-type strain. A second experiment was designed with the goal of characterizing host and pathogen transcriptome in parallel. For detecting intracellular *Brucella* gene expression, a combined protocol consisting of a linear amplification of sense-stranded RNA biased to pathogen transcripts to the previously enriched host:pathogen RNA

mixed sample, was developed. RNA samples were hybridized on human and *Brucella* cDNA microarrays, which analysis revealed a common down-regulation transcriptional profile at 4 h PI that was reverse at 12 h PI. The integrity of *B. melitensis* *virB* operon and the expression of host MAPK1 were confirmed as critical for early *B. melitensis* intracellular survival and replication in non-phagocytic cells. Finally, a temporal morphological and molecular characterization of the initial *B. melitensis*:bovine host interaction using a calf ileal loop model was performed. *B. melitensis* was isolated from intestinal Peyer's patches as soon as 15 min and from systemic blood after 30 min post-intra luminal inoculation. Microarray results revealed a common transcriptional profile in *Brucella*, but two different transcriptional profiles were identified in the host in the first 4 h PI. The importance of differentially expressed biological processes, pathways and individual genes in the initial *Brucella* pathogenesis is discussed.

DEDICATION

To my lovely wife Paola
and my two amazing sons Fernando and Pablo

ACKNOWLEDGMENTS

I am entirely grateful to my advisory committee's chair, Dr. L. Garry Adams for his initial trust in me and for his guidance throughout my doctoral studies. I also extend my acknowledgments to the other members of my Ph.D. Committee, Dr. Renée Tsohis, Dr. Terry Thomas and Dr. James Womack for their advice and support during the course of this study.

This research would not be possible without help from many other people. I thank all members of Dr. Adams' lab: Dr. Josely Figueiredo, Tamara Gull, Doris Hunter, Dr. Sangeeta Khare, Jairo Nunes, Roberta Pugh and Tiffany Fausett for their invaluable technical assistance; Dr. Sara D. Lawhon, for helpful discussions and critical reading; Alan Patranella for taking care of experimental animals; Linda McCallum for helping with surgical and anesthetic procedures; Rhonda Friedberg, Dr. Mitchell McGee and Dr. Stephen A. Johnston from the Western Regional Center of Excellence (WRCE) Pathogen Expression Core (Center for Innovations in Medicine, A.S.U.) for developing and printing the *B. melitensis* cDNA microarrays; Dr. Robin E. Everts and Dr. Harris A. Lewin, from W.M. Keck Center for Comparative and Functional Genomics, U.I.U.C. for printing the bovine cDNA microarrays; Dr. Tom A. Ficht for sharing *B. melitensis* mutants from his *B. melitensis* mutant's bank; Jonathan Lawson, for sharing protocols before publishing; Helga Bhatkar and Dr. Ross Payne, for guidance on TEM and SEM observation; and Dr. Cristi Galindo and Dr. Harold "Skip" Garner from U.T.S.W.

Medical School, Dallas, and Dr. Bryan Kamery and Dr. Ken Drake from Seralogix, Inc., Austin, for carrying out the microarray analysis.

Financial support for my Ph.D. program was provided by I.N.T.A. (Instituto Nacional de Tecnología Agropecuaria) – Fulbright Argentina fellowship, and NIH/NIAID Western Regional Center of Excellence and U.S. Department of Homeland Security -National Center of Excellence for Foreign Animal and Zoonotic Disease (FAZD) Defense grants.

TABLE OF CONTENTS

	Page
ABSTRACT	iii
DEDICATION	v
ACKNOWLEDGMENTS.....	vi
TABLE OF CONTENTS	viii
LIST OF FIGURES.....	xi
LIST OF TABLES	xiii
 CHAPTER	
I INTRODUCTION.....	1
General aspects of genus <i>Brucella</i>	1
Clinical manifestations of brucellosis	2
Cell biology of <i>Brucella</i> infection.....	3
<i>Brucella</i> virulence factors	8
The host response to <i>Brucella</i> infection.....	15
Models to study <i>Brucella</i> :host interaction	18
The goal.....	21
II IDENTIFICATION OF <i>Brucella melitensis</i> INVASIVE	
CANDIDATE GENES IN NON-PROFESSIONAL	
PHAGOCYtic CELLS BY MICROARRAY ANALYSIS	23
Introduction.....	23
Materials and methods	24
Results	32
Discussion	52

TABLE OF CONTENTS (continued)

CHAPTER	Page
III HOST AND <i>Brucella melitensis</i> TEMPORAL GENE EXPRESSION PROFILES IN AN <i>in vitro</i> MODEL OF INFECTION.....	65
Introduction	65
Materials and methods	66
Results	80
Discussion	111
IV TEMPORAL GLOBAL GENE EXPRESSION ANALYSIS OF THE <i>in vivo</i> INITIAL INTERACTION OF BOTH <i>Brucella melitensis</i> AND THE BOVINE HOST	125
Introduction	125
Materials and methods	126
Results	133
Discussion	159
V CONCLUSIONS.....	170
REFERENCES.....	173
APPENDIX A	213
APPENDIX B	226
APPENDIX C	231
APPENDIX D	235
APPENDIX E.....	239
APPENDIX F	252

TABLE OF CONTENTS (continued)

	Page
APPENDIX G	266
APPENDIX H	275
APPENDIX I	297
APPENDIX J	302
VITA	306

LIST OF FIGURES

FIGURE	Page
1	The ability of <i>B. melitensis</i> 16M at different phases of growth to invade HeLa cells 33
2	Fluorescent signal values of <i>B. melitensis</i> gDNA in microarrays co-hybridized with <i>B. melitensis</i> RNA at late-log and stationary growth phases 35
3	Fluorescent signal values of <i>B. melitensis</i> transcript or gDNA from differentially expressed genes at stationary and late-log phases of growth .. 38
4	Distribution of genes differentially expressed at late-log growth phase compared to stationary phase associated in cluster of ortholog genes (COGs) functional categories..... 39
5	Validation of DNA microarray results by quantitative RT-PCR 43
6	Hierarchical cluster of genes from <i>B. melitensis</i> grown to stationary and late-log phases 44
7	Expression profile chart for genes most highly up-regulated or down-regulated in late-log phase cultures of <i>B. melitensis</i> compared to stationary phase bacterial cultures 47
8	Principal component analysis (PCA) of gDNA and transcript levels in <i>B. melitensis</i> cultures collected at stationary and late-log phases of growth..... 50
9	Internalization ability of <i>B. melitensis</i> transposon interrupted in genes highly up-regulated in late-log growth phase in HeLa cells 53
10	Kinetics of <i>B. melitensis</i> 16M intracellular replication in HeLa cells..... 81
11	Inter-array comparison of signal consistency from <i>B. melitensis</i> RNA samples reverse transcribed with genome-directed primers (GDP) vs. random hexamer primers (RHP)..... 84
12	Validation of <i>Brucella melitensis</i> and host microarray results by quantitative Real-time PCR..... 103

LIST OF FIGURES (continued)

FIGURE	Page
13 Invasion phenotype and intracellular survival and replication of <i>B. melitensis virB3</i> mutant in HeLa cells.....	109
14 Phenotype of <i>B. melitensis</i> -infected HeLa cells transfected with MAPK1-validated siRNA molecules.....	112
15 Kinetics of infection with <i>B. melitensis</i> 16M.....	137
16 Integrity and composition of the host:pathogen RNA samples pre- and post-enrichment treatment.....	140
17 Distribution of genes differentially expressed in intracellular <i>B. melitensis</i> between 15 min and 4 h post-infection categorized by COGs functional categories	143
18 Distribution of host genes differentially expressed in <i>B. melitensis</i> -infected bovine Peyer's patch after 1 h post-infection categorized by Gene Ontology.....	148
19 Validation of <i>B. melitensis</i> microarray results by quantitative Real-time PCR.....	156
20 Validation of bovine microarray results by quantitative Real-time PCR.....	158

LIST OF TABLES

TABLE	Page
1	Identification of the sequences disrupted by transposon mutagenesis 25
2	Primers for Real-time PCR analysis of tested genes in <i>B. melitensis</i> 31
3	Genes significantly up-regulated in <i>B. melitensis</i> cultures grown in F12K tissue medium to late-log phase, compared to bacteria at stationary phase 48
4	Eigenvalue for each principal component 49
5	<i>Brucella melitensis</i> 16M genome-directed primers (<i>BmGDP</i>) 72
6	Primers for Real-time PCR analysis of genes in <i>B. melitensis</i> samples 78
7	Primers for Real-time PCR analysis of genes in HeLa cell samples 79
8	Results of pairwise graphical comparisons 87
9	Top scored <i>B. melitensis</i> pathways subnet analyzed and discovered candidate mechanistic genes from modeling at 4 and 12 h PI 105
10	Top scored host pathways subnet analyzed and discovered candidate mechanistic genes from modeling at 4 and 12 h PI 106
11	Primers for Real-time PCR analysis of genes in bovine Peyer's patch samples 134
12	Primers for Real-time PCR analysis of genes in <i>B. melitensis</i> samples 135
13	Number of genes differentially expressed by intracellular <i>B. melitensis</i> from 15 minutes to 4 h post-infection 142
14	Number of host genes differentially expressed in <i>B. melitensis</i> -infected bovine Peyer's patch from 15 min to 4 h post-infection 147
15	Set of host candidate genes identified <i>in silico</i> as important for infection of bovine Peyer's patch in the first 4 hours of <i>Brucella</i> :host interaction 160

CHAPTER I

INTRODUCTION

GENERAL ASPECTS OF GENUS *Brucella*

Bacteria from the genus *Brucella* are the etiological agents of brucellosis, a worldwide zoonotic disease that has a negative economic impact on animal production and human public health (41, 92). The brucellae are small aerobes non-motil Gram negative coccobacilli that are facultative intracellular pathogen *in vivo*. Based on its 16S rRNA sequence, *Brucella* spp. are included in the $\alpha 2$ subclass of the class Proteobacteria among with other plant (*Agrobacterium* and the Rhizobiaceae) and mammalian (*Bartonella* and the Rickettsiae) pathogens (161). The genus *Brucella* consists on 6 recognized species, based on their primary host: *B. melitensis* infects sheep and goats; *B. abortus*, cattle; *B. suis*, swine; *B. ovis*, sheep; *B. canis*, dogs and *B. neotomae*, desert wood rats (171). Recently, isolates from aquatic mammals have been proposed as new specie, but the official recognition is still pending (195). With the exception of *B. ovis* and *B. neotomae* that exclusively have pathogenic effects on their primary hosts, brucellae are able to infect other susceptible animals with similar pathogenic effect (66). For instance, *B. abortus* and *B. melitensis* infect other ruminants; *B. suis* infects a broader spectrum of animals including hares, reindeers, caribous, wild pigs and dogs,

This dissertation follows the style and format of Infection and Immunity.

while *B. canis* affects wild canids. All 4 species of *Brucella* are also virulent for humans and the first three are bioterrorist agents.

CLINICAL MANIFESTATIONS OF BRUCELLOSIS

Among animal species, most mammals are susceptible to brucellosis. The success of the infection and the severity of the clinical disease depend on: age; immunological competence of the host; animal host; infective dose; strain virulence; and species of *Brucella*. Natural infections occur primarily through mucosa membranes of the alimentary tract for *B. melitensis* and *B. abortus*, and the genital tract for *B. ovis*, *B. suis* and *B. canis* (2, 171). Following penetration of mucosal epithelium, invading brucellae are transported, either free or within phagocytic cells, to the regional lymph nodes. Failure to destroy *Brucella* within the primary lymph node results in persistence of infection and dissemination of the agent via lymph and blood (66, 171). *Brucella* may localize and produce lesions in multiple organs, i.e. bones, joints, eyes, and brain; however, the agent has a predilection for lymphoid tissues, mammary gland, reproductive tract, placenta and fetal organs (2, 66). Placentitis, abortion and temporary infertility are the principal clinical manifestations of brucellosis in pregnant females. *Brucella* infection in males causes orchitis and inflammation of the accessory sex organs resulting in permanent or temporary infertility.

The clinical manifestations of brucellosis are different in humans, resulting in intermittent fevers, chills, sweats, weakness, myalgia, osteoarthricular complications, endocarditis, depression and anorexia (243). Human brucellosis is an occupational-

related disease associated with accidental contact with infected animals, clinical specimens or foodborne disease associated with the consumption of contaminated animal products. The severity of the symptoms and signs vary depending on the species of *Brucella*: *B. melitensis* causes the most severe and acute symptoms, followed by *B. suis*, while *B. abortus* and *B. canis* tend to produce milder disease and subclinical infections in humans (243).

CELL BIOLOGY OF *Brucella* INFECTION

Brucella infects hosts principally by penetrating the natural mucosa from where it disseminates to the rest of the body (66). An experimental infection found that the oral cavity - pharynx and the intestine were the two main gates of entry for oral infection of *B. abortus* in calves (30). Conjunctivae, intranasal mucosa and vagina were also permeable to *Brucella* infection (156, 157, 181). The evaluation of the invasion process of *B. abortus* through calf intestinal Peyer's patches found that lymphoepithelial but not enteroabsorptive cells, engulfed individual brucellae that remain inside vesicles, phagolysosomes and large vacuoles (1). After transepithelial migration, many bacteria were observed alive inside neutrophils, mononuclear phagocytes or free in the interstitium and lymphatic vessels of lamina propria. The invasion process via conjunctiva was accompanied by an submucosal inflammatory reaction with the bacterium consistently being isolated from the parotid lymph node 2 to 4 days post-inoculation (66). These observations suggest that *Brucella* invades the host by

transepithelial migration, escape the submucosal defenses and disseminate free or inside phagocytic cells to regional lymph nodes by lymphatic drainage.

In addition to *in vivo* studies required for full understanding of *Brucella* pathogenesis, *in vitro* assays performed on cell lines or primary cultures are informative for a more complete understanding the host:agent relationship. The bacterial adhesion to cell membrane is an essential first step in the establishment of infection (199). *Brucella* attaches as a single organism to cultured epithelial cell lines via receptor molecules containing sialic acid or sulphated residues, and at 8 h post-infection begin to form microcolonies which subsequently become larger with extended time (31). It has been demonstrated that rough strains are more adherent and invasive to non-phagocytic cells than smooth ones (53), in part because the O-polysaccharide structure of the *Brucella* outer membrane protein would obscures unspecific ligands and consequently decreases the ability of the bacteria to bind the cell surface. Within a few minutes after binding non-professional phagocytic cells, *Brucella* is internalized by receptor-mediated phagocytosis (52, 53). Detailed studies have shown that the *Brucella* uptake by epitheloid-like cells is not a passive but an active mechanism, where the bacteria induces its own internalization by activating small GTPases of the Rho subfamily (i.e. Rho, Rac, Cdc42) and modulate rearrangements of the host cell actin cytoskeleton and microtubules (98). However, only a limited number of non-professional phagocytic cells in a monolayer are permissive to invasion (53, 180), suggesting heterogeneous susceptibility and/or invasiveness among cells and bacteria, respectively. After *in vivo* invasion of non-professional phagocytic cells, such as trophoblasts, *Brucella* localizes

and replicates within the rough endoplasmic reticulum without restricting basic cellular functions. However, after extensively intracellular replication infected cells develop signs of degeneration and necrosis, leading to a release of free bacteria into the media and the infection of the other cells proceeds (8). *In vitro* studies have found that during the first minutes after invasion, virulent *Brucella* transiently interacts with an intracellular compartment related to the early endocytic network that is gradually transformed in a multimembranous autophagic vacuole. Later, *Brucella* is delivered into a rough endoplasmic reticulum-like compartment in the perinuclear area, where massive intracellular replication occurs (53, 179). The benefits for the pathogen of being associated with the endoplasmic reticulum of non-professional phagocytic host-cell, an event also observed in *Toxoplasma gondii* (214), have not been identified yet, although the hypothesis of taking advantage of utilizing metabolites synthesized or translocated to this compartment is an attractive concept (93). The type IV-secretion system (T4SS) encoded by *virB* operon in virulent *Brucella* controls its own intracellular trafficking, bypassing late endosomal compartments and avoids its degradation by inhibiting phagosome-lysosome fusion in non-professional phagocytic cells (39).

Once infected, natural hosts and humans can remain infected for life. After translocating the epithelium layer, *Brucella* is endocytosed by local macrophages and transported to the regional lymph nodes. Failure to destroy the bacteria at this stage, results in dissemination to organs that are rich in elements of the reticuloendothelial system, such as spleen, bone marrow and lymph nodes (66). The chronic nature of the disease lies in the ability of virulent brucellae to survive and replicate inside

macrophages (194). On the contrary as observed in non-professional phagocytic cells, differences in mechanisms of binding and entering of each individual bacterium into macrophages determine its fate within intracellular compartments and the outcome of the infection (28, 190, 236). Opsonized *Brucella* binds professional phagocytic cells through complement and Fc receptors, whereas non-opsonized organisms seem to bind via lectin, fibronectin and/or other unknown receptors (28, 190). More recently, two papers have addressed the possibility that lipid rafts could serve as docking sites for non-opsonized *Brucella* to stabilize the bacteria-macrophage interaction previous to internalization (167, 236). As soon as the bacteria contact the macrophage membrane, F-actin and annexin I-associated structures transiently accumulate beneath or around the pathogen, regardless of whether the bacteria were previously opsonized or not (134). Phagocytosis occurs within few minutes after contact, and opsonized *Brucella*, but not non-opsonized, induce major morphological changes in the macrophages cell membrane consisting on membrane ruffles that surround and capture the bacteria, in a zipper-like interaction between receptors and ligands (134, 190). The initial formation of two types of *Brucella*-containing phagosomes, one tightly-fitting, representing the survival-permitting compartment, and other spacious, representing the killing compartment, was observed after *Brucella* engulfment (11, 190). The delayed phagocytosis observed in wild type *Brucella* compared with *virB* mutant was interpreted as a necessary time for the fully virulent pathogen to alter the plasma membrane in order to create a specialized organelle permissive for survival and replication (236). These *Brucella*-containing phagosomes briefly interact with early-endosomal compartments, and 1h post infection co-localize

with late-endosomal markers in cell lines (11, 17) but not in primary macrophages (33). Simultaneously, the delivery of the proton pump ATPase to the phagosome membrane causes a rapid acidification inside the vacuole, a condition necessary during the early phase of infection for survival and replication of *Brucella* in macrophages (11, 17, 183, 190). Paradoxically, the number of *Brucella* inside macrophages decreases in the first hours post-infection and only few phagocytosed organisms are capable of surviving, redirecting their intracellular trafficking and replicating inside phagosomes, a process highly dependent on a functional T4SS (11, 17, 33, 104, 190). This initial killing is probably due to the capability of macrophages to generate toxic oxygen-dependent mechanisms during phagocytosis (103). After the adaptation phase, *Brucella* begin replicating. Nevertheless, the *Brucella*-replicative niche in macrophages is controversial. It has been observed that *Brucella* replicates inside compartments with phagolysosomal characteristics (11), endoplasmic reticulum-like compartments (17, 33) and non-acidic phagosomes (17). Among all the differences reported, the replication inside phagolysosome vacuoles is the most curious, because experimental evidence seems to support the proposed that *Brucella* intracellular survival in macrophages resulting from an inhibition of *Brucella*-containing phagosome and lysosome membrane fusion (33, 166, 184, 190). However, the reported differences in *Brucella* intracellular trafficking within macrophages may in part be due to different cells (primary cultures vs. cell lines, human vs. mouse origin), *Brucella* strains and conditions used (opsonized vs. non-opsonized bacteria).

In addition to macrophages and cells of the reticulo-endotelial system, *Brucella* has predilection for the gravid uterus ultimately causing abortion with huge numbers of organisms being expelled in the fetus and fetal fluids (4). In the placenta, *Brucella* replicate initially in the phagosomes of erythrophagocytic trophoblasts of the placentome and later in the rough endoplasmic reticulum of the periplacentomal chorioallantoic trophoblasts (8). The subsequent fetus invasion and replication in placental cotyledones leads to extensive placentitis and abortion. Despite the the important role that trophoblasts play in brucellosis there is no detailed description of how *Brucella* invade and intracellularly traffick.

***Brucella* VIRULENCE FACTORS**

Brucella was first isolated in 1887, and today still little is known about the molecular mechanisms and the bacterial factors responsible for the clinical manifestations of brucellosis and host restriction. To date, the complete genome sequences of 4 strains of *Brucella* belonging to 3 different *Brucella* species (36, 51, 102, 175) and other related studies (128, 165, 185) provide an opportunity to initiate the identification and understanding of the mechanisms of *Brucella* pathogenicity and host specificity. Except for *B. suis* biovar 3 that has only 1 chromosome (128), other *Brucella* genomes consists of 2 circular chromosomes, coding from 3200 to 3400 ORFs. The largest chromosome (ChrI) is about twice the size of the other chromosome (ChrII) and it would seem that both chromosomes arose from a single ancestral chromosome via recombination between 2 rRNA operons (128). Comparisons of genomic sequences of *B.*

abortus, *B. melitensis* and *B. suis* genomes reveal extensive similarity (> 94%) to each other at the nucleotide level and gene organization (102), with *B. abortus* and *B. melitensis* being more closely related than to *B. suis* (36). In addition, single-nucleotide polymorphisms among *B. melitensis* and *B. suis* is very low (175). These observations suggest that the small number of differences among the 3 species sequenced might be responsible for their variable host preference and pathogenicity.

The genomes of the 3 species of *Brucella* sequenced document the absence of well characterized virulence factors present in other pathogenic bacteria such as capsules, pili and/or fimbriae, cytolysins, exotoxins, resistant forms, antigenic variation, phage-encoded toxins, lysogenic phages, virulent plasmids and pathogenicity islands (51, 102, 175). In spite of the lack of these classical virulence factors, *Brucella* is able to infect, replicate and persist inside the host, yet these effects have been attributed to a small number of identified virulent factors that are present and conserved across *Brucella* genome.

Brucella, like other bacterial pathogens, adapts their gene expression according to different environments, mediated in part by two-component regulatory systems. The two components of these systems generally are a sensor protein located in the cytoplasmic membrane that responds to an environmental stimulus, and a cytoplasmic response regulator which activates transcription factors that mediate changes in gene expression after binding specific DNA sequences (76). Three of 8 two-component regulatory systems encoded in the *Brucella* genome, have been described (58, 59, 216), but only one (BvrR/BvrS) is apparently involved in virulence. The two-component

regulatory system BvrR/BvrS, highly conserved in the 6 species of the genus (149), has been studied in *Brucella abortus*. The system was found to be critical for the control of polycation peptides resistance, invasion and intracellular survival in this specie (216). A more recent study found that BvrR/BvrS regulates the structure of outer membrane components important for homeostasis and virulence. The expression of at least 2 outer membrane proteins, Omp3a (formerly Omp25), well known for being involved in *Brucella* virulence (62, 127) and Omp3b, related to *B. melitensis* Omp31, a haemin-binding protein (47), was observed to be transcriptionally regulated by this two-component system (99). Another report suggests that the system also regulates the degree of lipid A acylation and is involved in recruiting and assembling surface bacteria molecules necessary for penetration, vacuole maturation and intracellular trafficking (149); however, the environmental factor “sensed” by the system is unknown.

A well recognized virulence factor in *Brucella* is lipopolysaccharide (LPS), a major component of the outer membrane, although its precise role in the pathogenesis of brucellosis is not clear yet (122). LPS has 3 domains: lipid A, the core oligosaccharide and the O antigen (or O chain). The O antigen appears to be the most important LPS component in *Brucella* virulence: it protects the bacteria from cellular cationic peptides (154), oxygen metabolites and complement-mediated lysis (40, 72), inhibits cytopathic effect on host cells (73, 176), impairs cytokine production from infected cells (122, 191) and is an *in vitro* down-regulator of T-cell activation (79). The presence or absence of the O chain in the LPS determines smooth or rough phenotypes respectively. Well characterized rough strains of *B. abortus*, *B. melitensis* and *B. suis* were attenuated for

survival *in vivo* (5, 91, 122, 155, 228), attributed in part because rough mutants of *B. abortus* are more susceptible than parental smooth strains to lysis mediated by complement (40). However, differences in survival of rough mutants of *B. abortus in vivo* were not consistent with those observed in complement mediated-lysis (5). Moreover, rough mutants of *B. melitensis* were found to be resistant to complement-mediated killing (72). Together, these results suggest that the differences in *in vivo* survival between smooth and rough strains of *Brucella* should be attributable to differences in intracellular survival rather than extracellular killing activities. Nevertheless, *in vitro* studies of replication of genetically defined rough mutants inside professional and non-professional phagocytes produced contradictory results (5, 82, 91, 147, 228). And it is not clear why naturally rough strains of *B. canis* and *B. ovis* are virulent in their primary hosts. Further studies are needed for better understanding of the contribution of LPS to the virulence of brucellae.

The importance of the O antigen for the proper uptake of *Brucella* and its intracellular fate has been recently reported (184, 236). These studies demonstrated that smooth but not rough *Brucella*, enter the host cells via lipid rafts, and from an unknown complementary mechanism, there is an inhibition of the phagosome-lysosome fusion and a modification in the intracellular trafficking. Lipid rafts are cholesterol-rich microdomains that participate in the organization of receptors and signaling molecules on cell membranes, being also used for many pathogens to adhere and invade the host cells (230). The connection among smooth *Brucella*, lipid rafts and phago-lysosome fusion is a new virulence factor called cyclic B-1,2-glucan. This molecule described in

Brucella abortus, is produced inside of phagosome and interacts with cholesterol molecules, disrupting the formation of lipid rafts on phagosomal membranes that prevent lysosomal fusion to the benefit of the pathogen (10).

Little is known about molecular mechanisms and factors involved in *Brucella* invasion. Recently, one surface protein of *B. abortus* associated with adhesion and invasion of non-professional phagocytic cells has been characterized (32). This adhesin called SP41 for Surface Protein 41kDa, is 433aa length and encoded by *ugpB* gene (BMEII0625). A wild-type strain of *B. suis* was 40 to 50 times more invasive to epithelial cell line than a *ugpB* mutant strain, indicating that invasion was affected in the absence of the gene product, i.e. SP41. Even if its counterpart is still unknown, the preliminary data suggest that this adhesin/invasin protein would interact with receptors containing sialic acid residues located in the host cell membrane. The presence of antibodies against SP41 in 70% of human patients with acute brucellosis indicates some role during initial stage of *in vivo* infection.

The T4SS is another major virulence factor in brucellae that has received special attention due to its importance in intracellular survival of the agent. The T4SS ancestrally related to bacterial conjugation and used to mobilize macromolecules across the bacterial membrane to the extracellular space or into other cells, has been found in the genome of the reference strains of the 6 *Brucella* species (169). T4SS have been found to play a key role in virulence for other pathogens such as *Agrobacterium tumefaciens* (133), *Bordetella pertussis* (238), *Legionella pneumophila* (234) and *Helicobacter pylori* (34) where the system is used to translocate effector proteins or

DNA that interfere with the host cell machinery. The exact role of T4SS in *Brucella* virulence is unclear. It has been demonstrated that the expression of *virB* operon, that encodes the secretion apparatus in *B. melitensis*, *B. abortus* and *B. suis*, is essential for intracellular survival and multiplication in professional and non professional phagocytic cells and for persistence in mice (22, 33, 50, 82, 109, 169, 213). *virB* is expressed intracellularly starting at 15 min and reaching the maximum expression at 5 h post-infection apparently by acidification of the *Brucella*-containing vacuola (22, 212) and is repressed intracellular at high bacterial density by a 12-carbon homoserine lactone (222). It has been hypothesized that the putative effector molecules secreted by T4SS remodel the phagosome compartment and perturb the intracellular trafficking in infected cells, allowing *Brucella* to establish a niche in which it multiplies (33, 39).

The presence of open reading frames encoding homologues of flagellar related proteins, were found in the 3 *Brucella* genomes sequenced (51, 102, 175). However, as *Brucella* has long been described as a non-motile bacterium and some of the ORFs are truncated and other important components of flagellar apparatus are missing. It is thought that flagellar genes are remnants from evolution (160). Nevertheless, the importance of flagellar genes in *Brucella* virulence was detected after the isolation of an *in vivo* and *in vitro* attenuated *B. melitensis* 16M mutant with disruption on *fliF* gene, which encodes a protein of a basal component of the flagellum (147). In a more recent report, the expression of *B. melitensis* genes that encodes for basal and distal part of the flagellar apparatus and the flagellar structure was detected in specific moments of growth phase and infection (84). Apparently, the expression of both flagellar genes and

T4SS are under the control of the quorum-sensing transcriptional regulator *vjbR* (BMEII1116), which in the presence of the quorum sensing signal molecule, down-regulates expression of these two virulence factors (48). Mutations of several flagellum genes produced phenotypes unable to persist in a murine intraperitoneal model of infection, which suggests some role of the flagellum apparatus in chronic infection. The biological function of *Brucella* flagellum has not been determined yet, and there is the possibility that the flagellar apparatus, due to the phylogenetic relationship between flagellar and type III secretion system, is involved in secretion rather than in motility (147).

The virulence factors described above are involved in invasion, intracellular replication or survival, but little is known about how *Brucella* modulates the host immune response to establish a chronic infection. However, a recent identification of a *B. abortus* immunomodulatory protein, PrpA, will partially help unravel the molecular mechanisms of persistence (217). This protein encoded by the locus BAB1_1800, belongs to the proline-racemase family and has the capacity to induce a T cell-independent B cell-nonspecific polyclonal activation. *In vitro*, it was observed that PrpA induced naïve mice-splenocyte proliferation while in the mouse model of infection this factor was involved in persistence and in the transient immune suppression within a limited period of time post-infection. Further analysis identified that the proliferative response of mice splenocytes results in a state of immune suppression modulated by IL10 cytokine secretion.

In the systemic search for virulence factors, many other genes which expression would seem to be required for full virulence of brucellae at different stage of the infection process, have been identified using transposon mutagenesis, signature-tagged mutagenesis or differential fluorescence induction, and described elsewhere (6, 12, 49, 50, 68, 82, 101, 109, 131, 132, 140, 146, 147, 193). However, their biological function in the context of the infection process is not always completely understood and further characterization of these potential virulent elements is needed to understand their role in *Brucella* pathogenicity.

THE HOST RESPONSE TO *Brucella* INFECTION

The host immune response to an infectious agent is divided in innate and adaptive. The first one consists on preexisting or rapidly responding chemical and cellular defense mechanisms and is non-specific, while the second one is specific against the infected agent but takes more time to become effective (225). Lately, innate immunity has been intense subject of study, basically because it was recognized as a central defense mechanism that influences the development of adaptive immunity and an important component of local immunity in mammals (77). Immunity against brucellae involves cellular and humoral response. The immediate innate immune response to *Brucella* spp. in naïve animals begins when *Brucella* lipoproteins (LP) contacts non-activated antigen-presenting cells (APC), mainly dendritic cells and local macrophages, through CD14 and Toll-like receptor 2 (TLR2) dependent mechanisms (90, 113). This initial contact generates a receptor-induced signaling that stimulates infected cells to

secrete cytokines such as $\text{TNF}\alpha$, IL1a, IL6 and IL12 that modulate the development of specific Type I cellular immune response to promote a clearance of the bacteria (56, 245). The set of cytokines secreted by *Brucella*-infected APC stimulate a T helper 0 cells (Th0), a subpopulation of CD4^+ α/β T lymphocytes, to differentiate them in Th1 cells, which result in IL2, IL18, $\text{TNF}\beta$ and $\text{IFN}\gamma$ secretion. All together, these cytokines stimulate activation of macrophages, promote B-cell switching of immunoglobulin and recruit more immune cells to the site of infection (119). Natural killer (NK) cells, neutrophils, CD8^+ and $\gamma\delta$ T lymphocytes are part of the secondary innate immune response and migrate immediately to the infection site to contribute to resolve the infection (56).

Secondary infection boosts a *Brucella*-specific immune response. At that point humoral response plays a major role, being *Brucella*-specific antibodies available to bind and opsonize the agent, facilitating uptake by phagocytic cells (71). On the other hand, specific CD4^+ T cells (Th1) secrete $\text{INF}\gamma$ that activates macrophages and enhances their killing activity (119, 126), and specific CD8^+ T lymphocytes (cytotoxic T cells) that recognize and kill *Brucella*-infected cells by binding them through the microbial antigen displayed on the surface (170). These cytotoxic T cells not only secrete proteolytic enzymes that trigger apoptosis in the infected cells, releasing the intracellular microbes that can then phagocytosed by activated macrophages, but they also produce substantial amounts of $\text{INF}\gamma$ involved in macrophage activation (246).

Natural resistance to brucellosis in domestic animal has been observed since 1940 (26, 224). Bovine *Slc11a1* (former *NRAMP1*) gene has been pointed out as a

candidate element for controlling intracellular replication of *B. abortus* in macrophages (15); however its biochemical function and how it contributes to resistance the infection remain unclear (242). Inheritance of *Brucella*-infection resistance involves more than one gene (3), but no other genetic element responsible for control of infection has been identified.

The global host response to *Brucella* infection was analyzed in murine macrophage-cell lines by microarray technology (69, 104). Eskra *et al.* (2003) identified 148 genes differentially expressed in RAW267.4 macrophage cell line at 4 h post-infection with *B. abortus*. Sixty nine of these genes were up-regulated, mainly genes encoded for pro-inflammatory cytokines and chemokines, and pro and anti-apoptotic factors, and 79 genes were down-regulated, mainly those encoded for cell cycling, proliferation and intracellular trafficking. In a more recent paper, He *et al.* (2006) analyzed a temporal transcriptional profile of the J774.A1 murine macrophage cell line infected with *B. melitensis*. The authors reported that the most significant changes in gene expression of *B. melitensis*-infected murine macrophages occurred early post-infection and the transcriptional profile returned to normal 24h post-infection. In concordance with Eskra *et al.*, they also found that genes involved in general cellular activities were down-regulated and genes involved in immune response, inflammation and cellular defense were up-regulated in infected macrophages compared with the control cells at 4 h post-infection. Microarray analysis also revealed that intracellular *B. melitensis* survival and replication may be a consequence of apoptosis inhibition by suppressing mitochondrial activity, thereby preventing activation of caspase cascades.

At the same time *Brucella* has developed its own strategies to avoid being recognized and eliminated by the host immune system. For instance, *B. abortus*, *suis* and *B. melitensis* were found to impair apoptosis in human and bovine macrophages, which preventing infected host cell elimination (73, 86, 96). Moreover, *Brucella* alters the production and secretion of cytokines of infected host cells (29, 127, 217), inhibits degranulation of neutrophils (19, 172), impairs NK cells activity (198) and modulates the host immune response (217). These are reasonably well defined examples of how the agent influences the host response, and ultimately the outcome of the infection.

MODELS TO STUDY *Brucella*:HOST INTERACTION

Most of the available information on molecular pathogenesis of *Brucella* and *Brucella*:host interaction originates from *in vitro* studies performed on primary cultures or cell lines of non-professional phagocytic cells such as epithelioid-like cells (179), fibroblasts (53) or trophoblasts (200), and professional phagocytic cells such as macrophages (11, 27), dendritic cells (20), lymphocytes (215) or neutrophils (172). However, *in vitro* studies may result in not only different but also contradictory results, in part because of the different conditions used or parameters employed. Although, *in vitro* studies reveal only a partial representation of the *in vivo* host:agent interaction, a caveat that must be kept in mind when experimental data are analyzed and interpreted. For example, when cell cultures are not in their original microenvironment, different gene expression and responses induced by injury are expected. Moreover, the majority of the cell lines derive from transformed cells, which are not truly representative of *in*

vivo tissue. Another limitation is that epithelial cells are polarized *in vivo*, where different surfaces are exposed to different environments and express different surface molecules. Quite the opposite, cellular surfaces are not differentiated in cell lines or primary cultures growth in monolayer, so that surface molecules are irregularly distributed. Polarized cell culture or three-dimensional cell cultures may partially resolve this problem (168). For example, *in vivo* mucosal surfaces are covered with a protective layer of viscous mucus, inhabited by resident microflora and bathed in solutions that are very difficult to mimic in an *in vitro* system. Additionally, *in vivo* cells are naturally organized in tissues formed by more than one cell layer and by different cell types, something that it is also very difficult to mimic *in vitro*. The host immune response is largely under represented in *in vitro* models. Despite all the limitations mentioned, *in vitro* studies do allow detailed studies and are useful for generating and testing hypotheses for subsequent *in vivo* evaluation.

On the other hand, *in vivo* studies are more time consuming, more expensive to develop and some of them require special facilities; but they are a *sine qua non* condition for fuller understanding of bacterial pathogenesis. Also to consider is the difficulty of identifying appropriate laboratory animals that reproduce the disease and developing lesions similar to those encountered in natural hosts (87). The most studied-model system for *in vivo Brucella*:host interactions is the murine model (14). In the mouse, *Brucella* persists in the spleen and lymph nodes after 8 weeks post-inoculation (87) which makes the model useful for studying the mechanisms of persistence. However, over time the agent is cleared and become undetectable, which is quite different than

what is observed naturally in primary hosts or humans. In addition, the model has other caveats, because the mouse is not a natural host of any *Brucella* species and consequently the response to infection is different than it is in natural host animal species (120). On the other hand, the mouse model has the advantage that there are an immense genetic tools and resources available. The guinea pig is another laboratory animal model widely used for *in vivo Brucella* studies. In contrast to mice, guinea pigs are much more susceptible to *Brucella* infection (88); however, results must be carefully interpreted. Under certain circumstances and with some limitations, information from laboratory animals can be extrapolated to man and natural host species (87).

In contrast to laboratory animal models, defined models of *Brucella* primary natural hosts for studying host:agent interaction have not been standardized. This results in greater variability making comparisons among labs more difficult, yet reflects more accurately the realities of *in vivo* infectious process in the natural host. Recently, a caprine model for studying ruminant brucellosis was proposed (65). According to the authors, colonization, pathogenicity and vaccine efficacy can be effectively monitored. In addition to the obvious advantages that this model has over murine model for studying ruminant brucellosis (goats are natural hosts and ruminants), the authors also mention some advantage over large ruminant's model: less expensive, requires less space and shorter gestation time.

Cattle are the natural host of *Brucella abortus*, but can also be infected by *B. melitensis* under specific epidemiological conditions (129, 231), and by *B. suis* experimentally (78). The alimentary tract is the major route in the transmission of *B.*

melitensis and *B. abortus* (2), having been the agent isolated from calf's intestine after an experimental oral infection (30). Calf ligated ileal-loop model has been clearly documented to be an excellent model for studying host:agent interaction for orally-ingested pathogens (21, 152, 201, 218). Our lab has been using the model extensively (204, 247), and we have found the model to be very informative for understanding primary *in vivo* host:*Brucella* interactions.

THE GOAL

The epithelium layer is the first barrier against *Brucella* infection. Precise and detailed descriptions on *Brucella* internalization and intracellular trafficking in non-professional phagocytic cells have been published, but a global temporal molecular characterization of these phenomena has yet to be accomplished. The overall objective of this study is to characterize the transcriptome of *Brucella* and *Brucella*-infected host cells during the initial infectious process for understanding the initial strategies employed for the pathogen to survive and replicate intracellularly and to identify perturbations of major gene(s) modulating critical cellular pathways during initial infection. The second chapter of this dissertation explores the invasiveness of *B. melitensis* in non-phagocytic cells and characterizes the transcriptional profile of *in vitro* *B. melitensis* cultures at different growth phases in cell culture media for the identification of candidate invasive-associated genes of *Brucella*. Moreover, 2 *B. melitensis* strains with transposon interrupted in different loci were found deficient in internalization compare with the wild-type strain. Chapter III characterizes the

transcriptome of *B. melitensis* and *B. melitensis* infected non-phagocytic host cells at 4 and 12 h post-infection in an *in vitro* model of infection. One candidate host and *Brucella* genes identified by dynamic Bayesian modeling analysis from the expressed transcriptomes as relevant for early brucellosis were knocked down in HeLa cells using siRNAs and transposon interrupted in *B. melitensis*, to verify their role in the early infection process and establish a phenotype. Chapter IV analyses the morphological and molecular temporal *B. melitensis* bovine host initial interaction *in vivo*. The importance of expressed pathways and genes in the context of initial *Brucella* pathogenesis is discussed.

CHAPTER II

IDENTIFICATION OF *Brucella melitensis* INVASIVE CANDIDATE GENES IN NON-PROFESSIONAL PHAGOCYtic CELLS BY MICROARRAY ANALYSIS

INTRODUCTION

Genomic analysis of *Brucella* species has largely failed to identify well-characterized virulence factors, such as capsules, pili and/or fimbriae, cytolysins, exotoxins, resistant forms, antigenic variation, phage-encoded toxins, lysogenic phages, virulent plasmids and pathogenicity islands, that are present in other pathogenic bacteria (51, 102, 175). In spite of the lack of these classical virulence factors, *Brucella* can readily infect, replicate and persist inside the host.

Natural *Brucella* infections occur primarily through adhesion and penetration of mucosal epithelium (2, 171). Detailed *in vitro* studies have demonstrated that *Brucella* bind sialic acid residues present on eukaryotic cells membrane (31) and are uptake by epitheloid-like cells by an active mechanism in which the organism induces its own internalization by activating small GTPases of the Rho subfamily and modulating rearrangements of the host cell actin cytoskeleton and microtubules (98). Recently, the first *Brucella* surface protein, called SP41, associated with invasion in non-phagocytic cells was characterized (32). Nevertheless, very little is known about the molecular mechanisms underlying *Brucella* adhesion and internalization in eukaryotic cells. Our goal in this study was to characterize the *Brucella melitensis* invasion-related

transcriptome as a preliminary approach for identifying pathogen candidate genes involved in the non-professional phagocytic cell invasion process.

MATERIALS AND METHODS

Bacterial strains, media and culture conditions. Smooth virulent *Brucella melitensis* 16M Biotype 1 (ATCC 23456) (American Type Culture Collection, Manassas, VA), re-isolated from an aborted fetus goat and its derivatives were maintained as frozen glycerol stocks. Mutants were created by transposon mutagenesis using two different transposon systems (Table 1) and constructed as previously described (5, 241). Individual 50 ml conical tubes were filled with 10 ml of cell culture media [F12K medium (ATCC) supplemented with 10% heat-inactivated fetal bovine serum (HI-FBS) (ATCC)], inoculated with 0.1 ml (1:100 for early-log cultures), 0.25 ml (1:40 for late-log cultures) and 1 ml (1:10 for stationary cultures) of a saturated culture of *B. melitensis* 16M and incubated at 37°C with 5% CO₂ overnight with loose lids and 200 rpm shaking. Growth curves of cultures were determined by comparing the optical density (OD) of the culture at 600nm with bacterial colony forming units (CFU). Bacterial numbers were assessed by plating a serial dilution on tryptic soy agar (TSA) (BD, Franklin Lakes, NJ) and incubating at 37°C with 5% CO₂ for 4 days. Kanamycin (100 µg ml⁻¹) (Sigma, St. Louis, MO) was used to supplement TSA media when necessary.

Determination of invasiveness. HeLa S3 cell line (ATCC CCL-2.2) between passages 8 and 15 was grown in F12K medium containing 10% HI-FBS at 37°C with 5%

TABLE 1. Identification of the sequences disrupted by transposon mutagenesis

Mutant	Transposon	Locus interrupted	Homologous protein
BME5D1	<i>Tn5</i>	BMEI1414	Perosamine synthetase (<i>wbkb</i>)
QW154H11	<i>Himar1</i>	BMEI1416	O-antigen export system ATP binding protein RfbB
BME5F3	<i>Tn5</i>	BMEI1538	Hypothetical protein
BME8A6	<i>Tn5</i>	BMEI1707	Mandelate racemase
QW81G10	<i>Himar1</i>	BMEII0025	Attachment mediating protein VirB1 homolog
QW70F8	<i>Himar1</i>	BMEII0034	Channel protein VirB10 homolog
QW184B9	<i>Himar1</i>	BMEII0380	Acriflavin resistance protein A precursor (<i>acrA</i>)
QW73H12	<i>Himar1</i>	BMEII0472	Membrane fusion protein MtrC

CO₂. Twenty-four hours prior to infection, the cells were suspended and cultured in 25 cm² plastic flasks (Corning, Corning, NY) at a concentration of 2x10⁶ cells/flask and replaced in the incubator. Before infection, cells from 1 flask were detached and counted. Infection with *B. melitensis* 16M or its derivatives was done by replacing the medium overlying the HeLa monolayers by a bacterial inoculum grown on cell culture media, at a multiplicity of infection of 1000 bacteria per cell (MOI 1,000:1). Bacteria were centrifuged onto the cells at 800 X g for 10 min followed by 30 min of incubation at 37°C. Then, cells were washed once with PBS to remove extracellular bacteria and re-incubated with F12K media supplemented with 100 µg ml⁻¹ of gentamicin solution (Sigma) for 1 hour. To determine the intracellular viable number of bacteria, infected

cultures were washed 3 times with PBS and then lysed with 0.1% Triton X-100 (Sigma). Lysates were serially diluted and cultured on TSA plates (supplemented with kamamycin as necessary) for quantitation of CFU.

Isolation of total RNA from *B. melitensis* 16M. Total RNA was isolated from 4 different cultures of *B. melitensis* 16M grown in F12K supplemented with 10% HI-FBS at late-log and stationary growth phase as previously described (189). Briefly, ice-cold ethanol/phenol solution was added to the *B. melitensis* culture and the bacteria recovered by centrifugation. The media was then removed and the pellet suspended in TE buffer–lysozyme solution containing 10% SDS (Ambion, Austin, TX). After 2 min of incubation, acid water-saturated phenol was added to the lysate and mixed, and the sample incubated for 6 min at 64°C. Tubes were kept on ice for at least 2 min and then centrifuged at maximum speed. The upper layer, containing the RNA, was transferred to a new tube, mixed with an equal volume of chloroform and then separated by centrifugation. The aqueous phase was mixed with 100% cold ethanol and stored at -20°C. After at least one hour of incubation, RNA was pelleted by centrifugation, washed in 80% ethanol and suspended in DEPC-treated water (Ambion) with 2% DTT and 1% RNase inhibitor (Promega, Madison, WI). Contaminant genomic DNA was removed by RNase-free DNase I treatment (Ambion) according to the manufacture’s instructions, and samples were stored at -80°C until used. The quality of the RNA samples was determined using the Agilent 2100 Bioanalyzer (Agilent, Palo Alto, CA).

Isolation and labeling of *B. melitensis* genomic DNA. A pellet from a saturated culture of *B. melitensis* 16M grown on tryptic soy broth (TSB) (BD) was washed with 25

ml of J-buffer [0.1M Tris pH 8.0; 0.1M EDTA; 0.15M NaCl] and then lysed in 1 ml of J-buffer containing 10% lysozyme solution (10mg/ml in 0.25M Tris, pH 8.0). After 10 min of incubation, DNA was released from the cells by sodium salt of N-lauroyl sarcosine (Sigma) followed by degradation of RNA by DNase-free RNase (Roche Applied Science, Indianapolis, IN), and digestion of proteins with proteinase K (Roche Applied Science). The resulting solution was transferred to a dialysis bag and dialyzed against TE [10mM Tris, pH 8.0 and 1mM EDTA] overnight at 37°C. DNA was subsequently extracted twice using neutral water-saturated phenol (Ambion) first and then twice with ether (Sigma) before dialyzing overnight against TE. DNA concentration was determined by absorption spectrophotometry at 260 nm (NanoDrop® ND-1000) (NanoDrop, Wilmington, DE) and stored at 4°C until used.

B. melitensis genomic DNA was labeled overnight by directed incorporation of Cy5-dCTP (Amersham Pharmacia Biosciences, Piscataway, NJ) during reverse transcription using random primers solution and Klenow fragment from BioPrime DNA labeling system kit (Invitrogen, Carlsbad, CA) and 50X dNTPs (1:2 dCTP) (Invitrogen). The reaction was stopped by adding 5 µl of stop buffer from the BioPrime kit and unincorporated Cy dye was removed using PCR purification kit (Qiagen, Valencia, CA), eluted in 1mM Tris pH 8.0 and kept at 4°C until used.

Construction of cDNA microarrays. A set of unique 70-base oligonucleotides representing 3,227 ORFs of *B. melitensis* strain 16M and unique / divergent genes from *B. abortus* and *B. suis* were designed at the Pathogen Expression Core and purchased from Sigma-Genosys (The Woodland, TX). Oligonucleotides were suspended in 3X

SSC (Ambion) at the final concentration of 40 μ M before robotic arraying in triplicate onto ultraGAPS coated glass slides (Corning) using a Spotarray 72 microarray printer (Perkin Elmer, Downer's Grove, ILL). Printed slides were steamed and UV cross-linked and stored in a desiccators until use.

Sample preparation and slide hybridization. The labeling and hybridization procedures were based on a adaptation of the protocol developed by The Institute for Genomic Research (105). Briefly, 10 μ g of total RNA from *B. melitensis* 16M grown in F12K to late-log and stationary growth phases were reverse transcribed overnight to amino-allyl cDNA using 6 mg of random hexamer primers (Invitrogen), 0.6 μ l 50X dNTPs (Invitrogen) / aa-dUTP (Ambion) mix (2:3 aa-dUTP:dTTP) and 400U Superscript III (Invitrogen). The reaction was stopped by incubating the samples with 1M NaOH at 65°C for 15 min and neutralized by adding 1M HCl. Unincorporated aa-dUTPs and free amines were removed by column passage (Qiagen). Speedvac-dried samples were rehydrated in 0.1M Na₂CO₃ buffer (pH 9.0) and labeled with Cy3-ester (Amersham Pharmacia Biosciences). After one hour incubation in the dark, uncoupled dye was removed using columns (Qiagen) and Cy3 incorporation calculated by NanoDrop®. Dried samples were suspended in nuclease-free water and mixed with 0.5 μ g of labeled gDNA to the final volume of 35 μ l. Samples were heated at 95°C for 5 min and then kept at 45°C until hybridize. Right after hybridization, 35 μ l of 2X formamide-based hybridization buffer [50% formamide; 10X SSC; 0.2% SDS] was added to each sample, well mixed and applied to oligoslides. The microarrays were kept in prehybridization buffer [5X SSC, 0.1% SDS; 1% BSA in 100ml of water] at 45°C for at

least 45 min followed by 4 washes in distilled water, one wash in 100% isopropanol and finally drying by centrifugation. Four slides for each condition were hybridized at 45°C for ~20 h in a dark humid chamber (Corning) and washed for 5 min at 45°C with low stringency buffer [1X SSC, 0.2% SDS] followed by two 5-min washes in a higher stringency buffer [0.1X SSC, 0.2% SDS and 0.1X SSC] at room temperature with agitation. Slides were dried by centrifugation at 800 X *g* for 2 min and immediately scanned.

Data acquisition and microarray data analysis. Immediately after washing, the slides were scanned using a commercial laser scanner (GenePix 4100; Axon Instruments Inc., Foster City, CA). The genes represented on the arrays were adjusted for background and normalized to internal controls using image analysis software (GenePixPro 4.0; Axon Instruments Inc.). Genes with fluorescent signal values below background were disregarded in all analyses. Data were analyzed using GeneSpring 7.0 (Silicon Genetics, Redwood City, CA), Significance Analysis of Microarrays (SAM) (Stanford University, Stanford, CA) and Spotfire DecisionSite 8.2 (Spotfire, Inc., Somerville, MA). Computational hierarchical cluster analysis and analysis of variance (ANOVA) were performed using Spotfire DecisionSite 8.2. ANOVA was also performed, as an additional filtering aid, using GeneSpring. For each software program used, data were first normalized by either mean (for Spotfire pairwise comparisons and SAM two-class comparisons) or percentile value (for GeneSpring analyses). Normalizations against genomic DNA were performed as previously described (219).

Microarray results validation. One randomly selected gene from every cluster

of ortholog genes (COGs) functional category ($n = 18$) that had differential expression between late-log and stationary growth phase by microarray results was analyzed by quantitative RT-PCR (qRT-PCR). Two micrograms from the same RNA samples used for microarray hybridization were reverse transcribed using TaqMan® (Applied Biosystems, Foster City, CA). For relative quantitation of target cDNA, samples were run in individual tubes in SmartCycler II (Cepheid, Sunnyvale, CA). One SmartMix bead (Cepheid) was used for 2 - 25 μ l PCR reaction along with 20 ng of cDNA, 0.2X SYBR Green I dye (Invitrogen) and 0.3 μ M forward and reverse primers (Sigma Genosys) designed by Primer Express Software v2.0 (Applied Biosystems) (Table 2) to produce an amplicon length of about 150 bp. For each gene tested, the individual calculated threshold cycles (Ct) in late-log and stationary samples were averaged among each condition and normalized to the Ct of the 16S rRNA gene from the same cDNA samples before calculating the fold change using the $\Delta\Delta C_t$ method (Applied Biosystems Prism SDS 7700 User Bulletin #2). For each primer pair, a negative control (water) and an RNA sample without reverse transcriptase (to determine genomic DNA contamination) were included as controls during cDNA quantitation. All samples were run on 1% agarose gel after qRT-PCR to verify that only a single band was produced. Array data were considered valid if the fold change of each gene tested by qRT-PCR was > 2.0 and in the same direction as determined by microarray analysis.

Statistical analysis. Determination of invasiveness of cultures of *B. melitensis* wild-type at different phases of growth was performed in triplicate on three independent experiments. Screening of mutant invasion in HeLa cells was performed once in

TABLE 2. Primers for Real-time PCR analysis of tested genes in *B. melitensis*

Functional categories	Locus ID	Gene product	Forward primers (5'-3')	Reverse primers (5'-3')
Cell division	BMEI0073	Cell division protein FtsX	CATCGAGGTGCTGCATTTTCAT	ATAGGATGCCACCAGGAGAA
Carbohydrate metabolism	BMEI0344	Phosphoglucosamine mutase/phosphoacetylglucosamine mutase/phosphomannomutase	CTTATCTCCGCGCTCCAGAT	CTGATTTACGCGTTTGTTC
Cell envelope	BMEI0402	31 KDA outer-membrane immunogenic protein precursor	GGCTTCACCCCGACTGAAC	GTTGGTGACGGCGTATTCTACA
Energy production	BMEI0475	Cytochrome C1	GCTGCAGCGGCTAATAATGG	CGGTCAAAAGCGAATGGATATAA
Nucleotide metabolism	BMEI0608	Thymidylate synthase	TGCCCTGTTGACGATGATGA	ATGCATCACCGGCAGCTT
Membrane transport	BMEI0642	Urea transporter	GTTTCTGGTCCTTGCAGCCTAT	ACGGCATTGTTGAGGAGGAA
Post-translational modification	BMEI0645	Urease accessory protein UreF	AGCCTCGGGCTTGCTTTT	TCGCCTCCAGCAGAATTTTT
AA metabolism	BMEI0730	Lactoylglutathione lyase	CAGCCCCCTCCGATACAGAT	AGTTCTCGCAGGTGGCATA
Cofactor transport	BMEI0842	Molybdenum cofactor biosynthesis protein C	CGCGCACTAGCCCCGATT	CGCCGCTTTTTTCGATCA
Transcription	BMEI1384	Transcriptional regulator, AraC family	CGCAGTTCACCAAGGCATT	GCGTGTTCAGAGGCGATCTT
Translation	BMEI1798	23S ribosomal RNA methyltransferase	CATGGGCTCGGTCTTTTCC	TGTTCAATGCCATTATCAGGAT
Signal transduction	BMEI2034	Sensor protein ChvG	GCCTGTTCCGCATTCCCTAT	GCGCATTGGAATCACCATTT
Lipid metabolism	BMEII0047	Lysophospholipase L2	GGCTATGTGCGCAGCTTCA	GGGAGGAGAGCCGTTCCA
Secondary metabolism	BMEII0079	Isochorismatase	CGCCTTGCCTGAAATATGT	GCGAATCGAGGCCGTAGAG
Cell motility	BMEII0150	Flagellin	GCGGTTGACAAGATCACTGTCA	CGAGAGAAGCAAGAGCGGTTT
Defense mechanism	BMEII0382	Acriflavin resistance protein D	TTGCAGGATCAGAATGCGATT	CATCCGACAGGCGGAAGA
DNA replication & repair	BMEII0663	Phosphohydrolase (MutT/NUDIX family protein)	CGGAGGTGGAGACCCAGAA	TCAAGCTGCGTATCCATCAAAA
Inorganic ion transport	BMEII1120	Iron(III)-binding periplasmic protein precursor	GCAAGAAGGGCCTCGAATTC	TTCGGGATGATGGTTTCCA
Control	AF220147	16S rRNA	CCTTACGGGCTGGGCTACA	TGATCCGCGATTACTAGCGATT

triplicate. Subsequent evaluations of invasion were performed on nine separate occasions only on mutants exhibiting statistically significant differences compared with the WT strain in the screening test. Statistical significance of differences was determined using Student's *t* test. A *p* value < 0.05 was considered significant.

RESULTS

***B. melitensis* 16M at late-log phase of growth was more invasive in non-professional phagocytic cells than early-log and stationary growth phases.** Under our growth conditions, logarithmically growing cultures (early-log) had 0.5×10^9 CFU/ml, late-log cultures had 2×10^9 CFU/ml and stationary-phase cultures had 5×10^9 CFU/ml. *B. melitensis* 16M cultures grown in tissue culture media were added directly to confluent monolayers of HeLa cells and co-incubated for 30 min and then washed and re-incubated 1 h with fresh media containing gentamicin to kill extracellular bacteria. In three different experiments, each performed in triplicate, late-log growth phase cultures were 2.2 ($p < 0.05$) and 4.8 ($p < 0.01$) times more invasive than cultures at early-log and stationary growth phases, respectively. The average number of intracellular bacteria recovered was 60 CFU at early-log, 130 CFU at late-log and 27 CFU at stationary growth phase per every 10^6 bacteria inoculated onto cells (Fig. 1).

***B. melitensis* express different sets of genes in late-log and stationary phases of growth in F12K tissue culture medium.** In order to understand the molecular differences in the invasion process, four biological replicates of cultures at the most (late-log) and the least (stationary) invasive growth phases were analyzed using

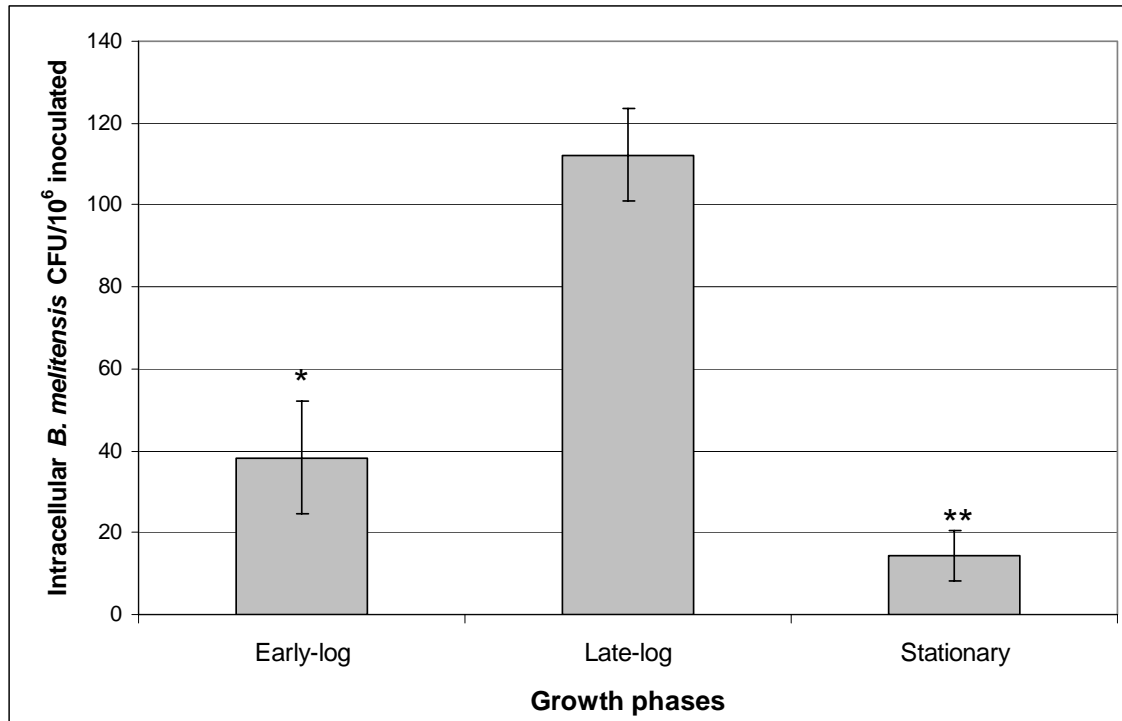


FIG. 1. The ability of *B. melitensis* 16M at different phases of growth to invade HeLa cells. *B. melitensis* 16M were grown overnight with shaking in F12K cell culture media supplemented with 10% (v/v) heat-inactivated fetal bovine serum to the early-log, late-log and stationary growth phases. HeLa cell infections were performed at MOI 1,000:1 with centrifugation for 10 min. Following 30 min incubation, extracellular bacteria were killed by 1 h gentamicin-treatment. Infected cultures were washed 3 times with PBS before lysing, and the lysates were serially diluted and cultured on TSA plates for quantitation of CFU. The intracellular number of late-log growth phase cultures of *B. melitensis* was significantly different from those grown to early-log (* = $p < 0.05$) and stationary (** = $p < 0.01$) growth phases. Results are presented as the number of CFU from internalized bacteria 30 min post-infection per every 10⁶ inoculated. Data presented are the mean + SD (error bars) of triplicate samples from one of 3 independent experiments with similar results.

cDNA microarray technology. Genomic DNA was used as an internal standardization control for each experiment in order to allow experiment to experiment comparisons (219). The experiments we report had little variability between gDNA signals from array to array, even under the two different conditions examined (i.e., late-log and stationary growth phase). The R^2 value for any two arrays (for gDNA Cy5 fluorescent values) was between 0.78 and 0.89, even before normalization. When the values for each conditional replicate were averaged (four arrays each for log phase and stationary growth phases), the resulting R^2 value was 0.88 (Fig. 2). Comparisons of RNA Cy3 fluorescent signals (log versus log and stationary versus stationary phases) yielded similar R^2 values (data not shown).

In order to further minimize the incidence of false positives and increase the consistency and reliability of the microarray analysis results, the data were analyzed separately using four different techniques: GeneSpring combinatorial analysis, Spotfire DecisionSite 8.2 pairwise comparisons, SAM two-class unpaired comparisons, and ANOVA. A change in gene expression was considered significant if the p value was less than 0.05, the fold change at least 2.0, and the gene expression alteration occurred for all replicate experiments. We further expected each gene to be significantly differentially expressed for at least two of the three replicate spots for each experimental array set (stationary versus late-log phase). Based on these criteria, genes that were deemed significant by all four analytical methods (GeneSpring, Spotfire DecisionSite 8.2, SAM, and ANOVA) were organized by COGs functional categories (NCBI *Brucella melitensis*

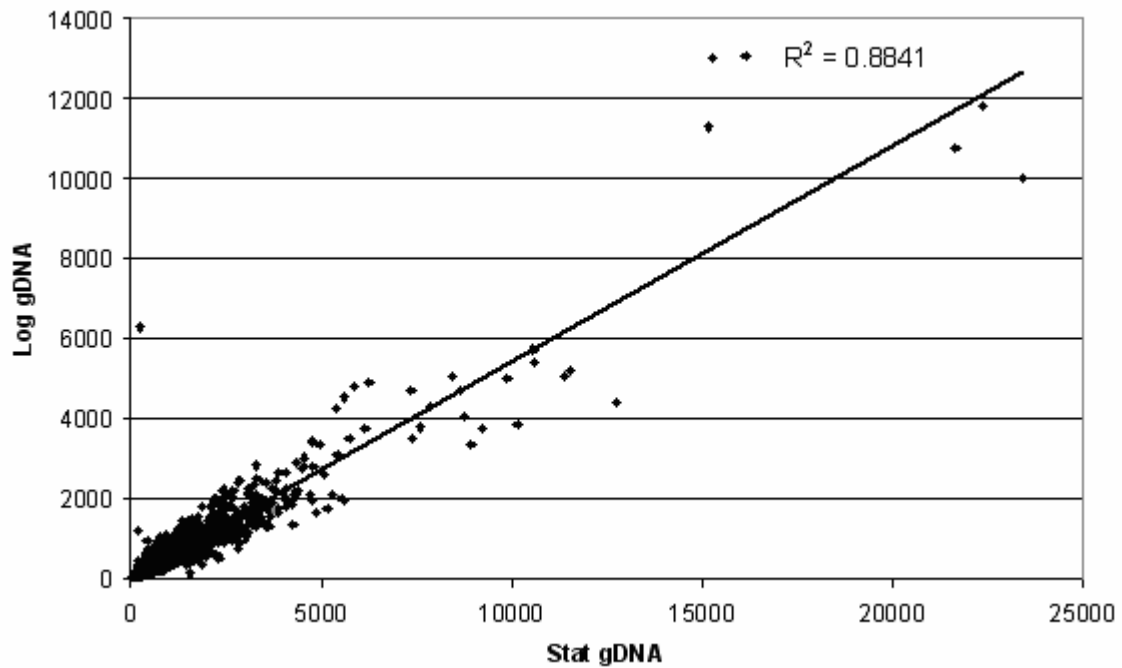


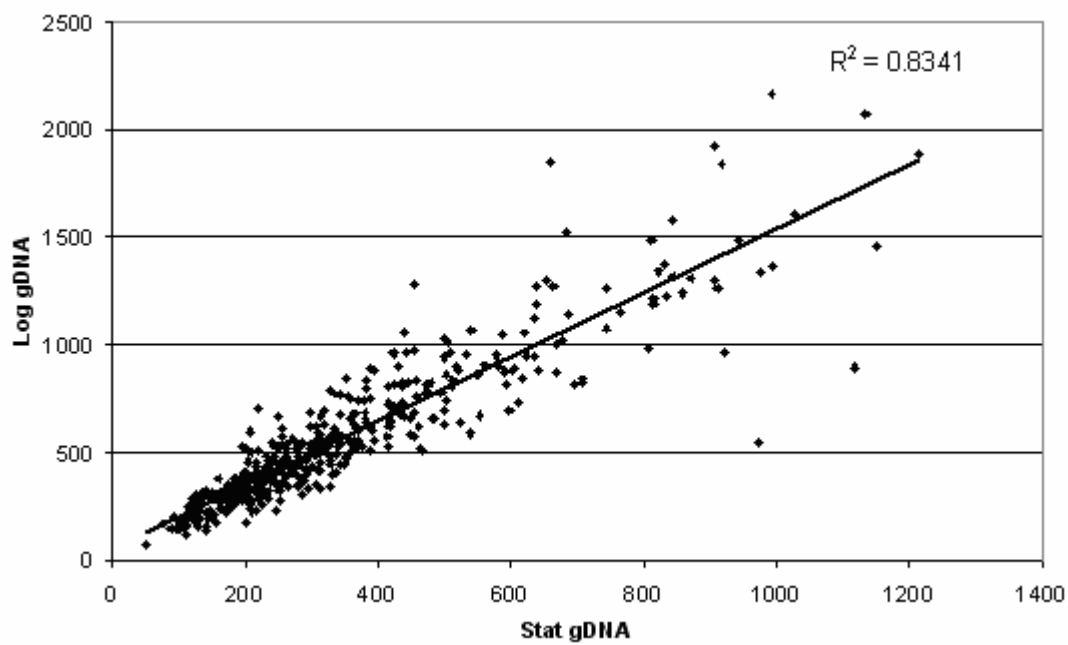
FIG. 2. Fluorescent signal values of *B. melitensis* gDNA in microarrays co-hybridized with *B. melitensis* RNA at late-log and stationary growth phases. Average Cy5 (gDNA) fluorescent signal values for *B. melitensis* grown in F12K tissue culture medium to late-log and stationary phases (4 arrays each) were plotted in Excel. Each dot represents the signal value for an individual spot on the array. Fluorescent signal values for gDNA co-hybridized with *B. melitensis* RNA extracted at stationary growth phase are indicated on the ordinate, and fluorescent signal values for gDNA co-hybridized with *B. melitensis* RNA extracted at late-log phase are on the abscissa. Stat refers to stationary phase, log refers to late-log phase, and gDNA refers to genomic DNA. The R-squared value (0.8841) is displayed in the upper right-hand quadrant of the graph.

16M genome project web page: http://www.ncbi.nlm.nih.gov/entrez/query.fcgi?db=genomeprj&cmd=Retrieve&dopt=Overview&list_uids=180) and compiled into a list that included 454 genes (different loci) that were up- or down-regulated when *B. melitensis* were grown to late-log phase, compared to stationary phase (Appendix A). A direct comparison of the signal intensity values of these genes indicate that the difference between log and stationary phases was specifically due to differential gene expression and not array spatial bias, as indicated in Figure 3. When the average gDNA intensity values for these 454 genes were plotted (stationary phase versus log phase), the R^2 value was 0.83 (Fig. 3A). However, the R^2 value for the same genes comparing instead the Cy3 fluorescence values (labeled cDNA amplified from RNA) was extremely low ($R^2 = 0.049$, Fig. 3B).

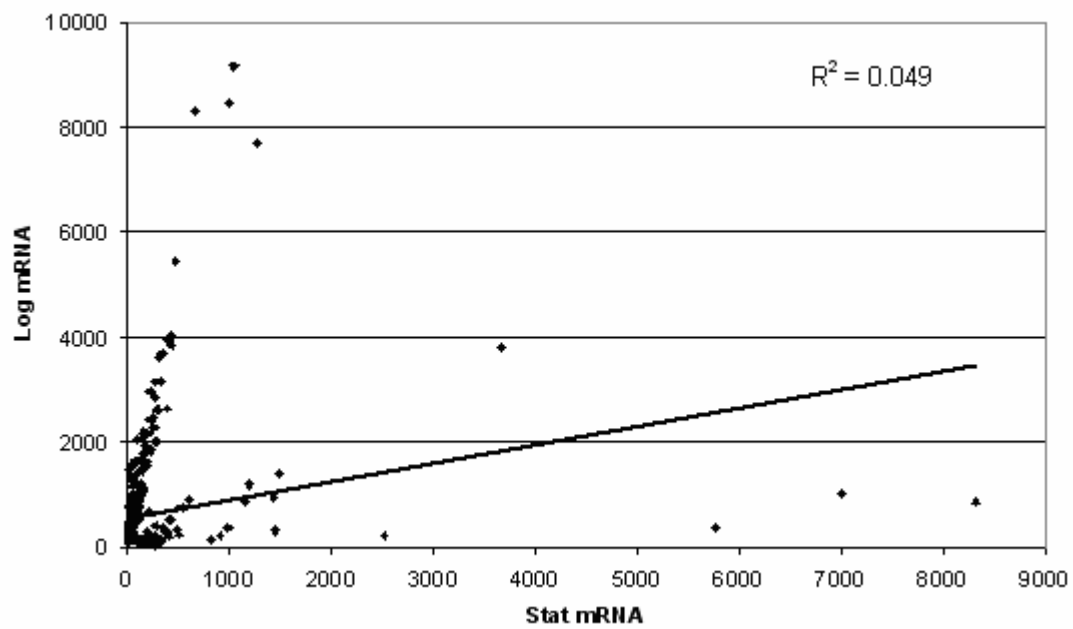
Of the 454 genes significantly altered in *B. melitensis* during late-log phase (14% of *B. melitensis* genome), 414 (91%) were up- and 40 (9%) were down-regulated, compared to when the bacteria were allowed to reach stationary phase of growth. The relative changes in gene expression ranged from a 386.5-fold induction of the Glycerol-3-phosphate regulon repressor gene (BMEII1093) to a 60.5-fold down-regulation of the locus BMEII0615 (hypothetical protein). The vast majority of these up-regulated genes were those associated with DNA replication, transcription and translation (57 genes), nucleotide, amino acid, lipid and carbohydrate metabolism (65 genes), energy production and conversion (24 genes), membrane transport (56 genes) and cell envelope, biogenesis and outer membrane (26 genes), while the 40 down-regulated genes were distributed among several COGs (Fig. 4). These results suggest a more active

FIG. 3. Fluorescent signal values of *B. melitensis* transcript or gDNA from differentially expressed genes at stationary and late-log phases of growth. Average Cy5 (gDNA) or Cy3 (transcript) signal values for *B. melitensis* grown in F12K tissue culture medium to late-log and stationary phases (4 arrays each) were plotted in Excel. Each dot represents the signal value for an individual spot on the array, determined to be significantly differentially expressed between late-log and stationary phases. **(A)** Comparison of genomic DNA levels of significant genes at stationary and late-log phases of growth. Stationary phase gDNA signal values are on the ordinate, and late-log phase signal values are on the abscissa. The R-squared value (0.8341) is displayed in the upper right-hand quadrant of the graph. **(B)** Comparison of transcript levels of significant genes at stationary and late-log phases of growth. Stationary phase transcript signal values are on the ordinate, and late-log phase signal values are on the abscissa. Note the very low R-squared value (0.049), displayed in the upper right-hand quadrant of the graph. Stat refers to stationary phase, log refers to late-log phase, and gDNA refers to genomic DNA.

A



B



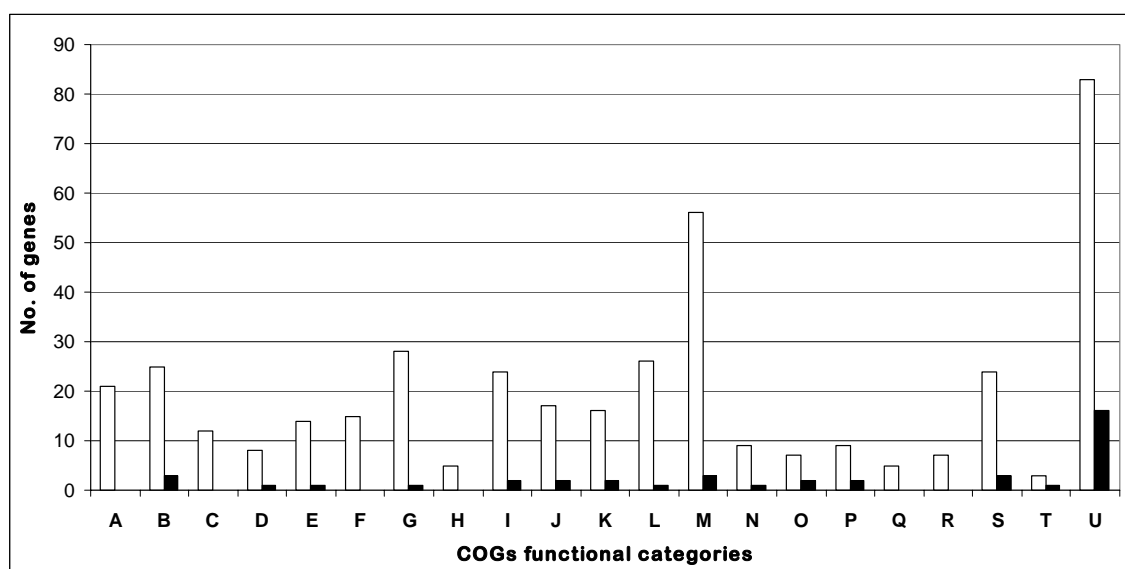


FIG. 4. Distribution of genes differentially expressed at late-log growth phase compared to stationary phase associated in cluster of ortholog genes (COGs) functional categories. Functional classifications are as follow: A, DNA replication, recombination and repair; B, Transcription; C, Translation, ribosomal structure and biogenesis; D, Nucleotide metabolism; E, Carbohydrate metabolism; F, Lipid metabolism; G, Amino acid metabolism; H, Secondary metabolites biosynthesis, transport and metabolism; I, Energy production and conversion; J, Inorganic ion transport and metabolism; K, Cofactor transport and metabolism; L, Cell envelope, biogenesis and outer membrane; M, Membrane transport; N, Defense mechanism; O, Signal transduction; P, Post-translational modification and secretion, protein turnover and chaperones; Q, Cell division; R, Cell motility and chemotaxis; S, General function prediction only; T, Predicted by homology; U, Unknown function. Open bars, up-regulated genes; solid bars, down-regulated genes.

metabolism of the *Brucella* cultures at late log phase of growth compared to cultures at stationary phase.

The highest bacterial replication observed at late-log compare to stationary growth phase is coincident with the up-regulation of genes encoding for DNA replication such as DNA polymerase (BMEI1321, BMEI1942, BMEII0290), *dnaA* (BMEI1362), a single strand binding protein (BMEI0880), DNA helicase (BMEI1485) and DNAtopoisomerase (BMEII0676), genes involved in pyrimidine (BMEI0609, BMEI1639) and purine (BMEI1575/6, BMEII0088) metabolism, and cell division-involved genes like *ftsX* (BMEI0073), *parB* (BMEI0010) and *minE* (BMEII0925).

Transcriptional regulators allow bacteria to express certain genes in response to specific signals. Twenty-one genes encoded transcriptional regulators belonged to AraC, AsnC, BetI, DeoR, GntR, IclR, LysR, LuxR, MarR, MerR and RpiR families were up-regulated in late-log *B. melitensis* cultures. Some families are known to be involved in positive regulation of gene expression (LuxR, AraC), others families are involved in repression (DeoR, MerR), while members of other families (IclR, LysR) could be activators or repressors of expression (187). Their role in *Brucella* internalization is still unknown. As expected, the locus encoding for the alternative sigma 32 factor (BMEI0280) that allows bacteria survive in general stress situations, was observed up-regulated in stationary cultures, while the locus BMEI1789 encoding for a subunit of another alternative sigma 54 factor (*rpoN*), which generally allows transcription of those genes involved in utilization of nitrogen and carbon sources and energy metabolism, was up-regulated in late-log phase cultures. The role of *rpoN* in *Brucella* remains to be

elucidated (55). Altogether, these data highlight the importance of finding the target genes of these transcriptional regulators in order to better understanding the *Brucella* physiology and metabolism.

A significant number of genes (26) directly involved in cell envelope/outer membrane biogenesis were differentially expressed at late-log compare to stationary phase of growth such as those encoding for outer membrane proteins (BMEI0402, BMEI0786), lipoproteins (BMEI0991, BMEI1079), LPS (BMEI0418, BMEI0586, BMEI0833, BMEI1414) and peptidoglycan biosynthesis (BMEI0271, BMEI0576). ORFs encoding membrane transport elements were the COGs functional category with more up-regulated expressed genes. Among them, genes encoding for amino acid (BMEI0263/4, BMEI0098/9, BMEI0861-4) carbohydrate (BMEI1580, BMEI1713, BMEI0621/2/4) and uncharacterized transports (BMEI1554, BMEI0481/3, BMEI0662) were the predominant up-regulated groups. Three genes encoding proteins for the *virB* operon-type IV secretion system (T4SS), such as *virB1* (BMEI0025), *virB3* (BMEI0027) and *virB10* (BMEI0034) were up-regulated, and one (BMEI0033) was down-regulated. Altogether, these data indicate an active conversion of metabolites to components of the cell envelope structure at late-log phase, which could influence in the initial *Brucella*:host cell interaction, facilitating attachment and entry into host cells.

Other conclusive remarks arising from the evaluation of microarray data analysis are the up-regulation of 9 protein-encoding ORFs involved in defense mechanisms (most against acriflavin protein) and 5 genes implicated in flagellar apparatus expression such as *fliC* (BMEI0150), *fliF* (BMEI0151), *fliN* (BMEI1112), *flhA* (BMEI0166) and *flgD*

(BMEI0164). Besides, there were 100 genes, 84 up- and 16 down-regulated differentially expressed with uncharacterized function in late-log phase compare with the stationary phase of growth. They represent a 22% of the genes differentially expressed, and may encode transcripts with previously unrecognized roles in *B. melitensis* adhesion and internalization.

Validation of microarray results. To confirm the microarray results, we randomly chose 18 differentially expressed genes (one from each COGs functional category) and conducted qRT-PCR. Based on qRT-PCR results, 15 of these genes (83%) were altered greater than 2.0-fold and in the same direction as was determined by microarray analysis, two other genes (BMEI0402 and BMEI0642) were determined to be differentially expressed and in the same direction of microarray analysis, but the fold change was lower than 2, and no significant difference in the expression level of BMEI0344 was observed using qRT-PCR (Fig. 5).

Late-log *B. melitensis* genes follow a similar expression pattern. In order to identify groups of genes with similar expression patterns, we performed hierarchical clustering analysis using Spotfire DecisionSite 8.2. Specifically, we were interested in identifying patterns of gene expression between bacteria grown in F12K tissue culture medium at late-log and stationary phases. Clustering analysis was performed on normalized Cy3 (cDNA amplified from total RNA) signal intensity values from the four log phase samples and four stationary phase samples and generated the cluster shown in Figure 6. As shown, all four samples from the log phase of growth clustered together, apart from those collected at stationary phase. This indicated that these 136 co-clustered

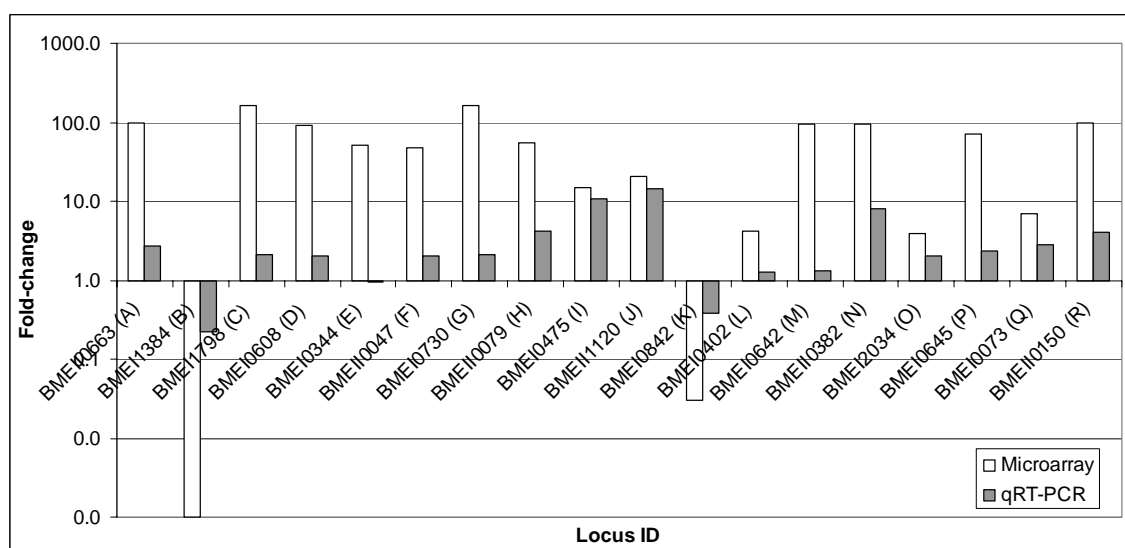


FIG. 5. Validation of DNA microarray results by quantitative RT-PCR. cDNA was synthesized from the same RNA samples used for microarray hybridization. Eighteen randomly selected ORFs that were differentially expressed based on microarray analysis between late-log and stationary growth phase were validated by quantitative RT-PCR. Fold-changes were normalized to the expression of *B. melitensis* 16S rRNA and calculated using the $\Delta\Delta C_t$ method. Seventeen out of 18 ORFs tested showed fold-changes in the same direction by both methodologies and 15 of them were also altered greater than 2-fold. Functional classifications are as follow: A, DNA replication, recombination and repair; B, Transcription; C, Translation, ribosomal structure and biogenesis; D, Nucleotide metabolism; E, Carbohydrate metabolism; F, Lipid metabolism; G, Amino acid metabolism; H, Secondary metabolites biosynthesis, transport and metabolism; I, Energy production and conversion; J, Inorganic ion transport and metabolism; K, Cofactor transport and metabolism; L, Cell envelope, biogenesis and outer membrane; M, Membrane transport; N, Defense mechanism; O, Signal transduction; P, Post-translational modification and secretion, protein turnover and chaperones; Q, Cell division; R, Cell motility and chemotaxis.

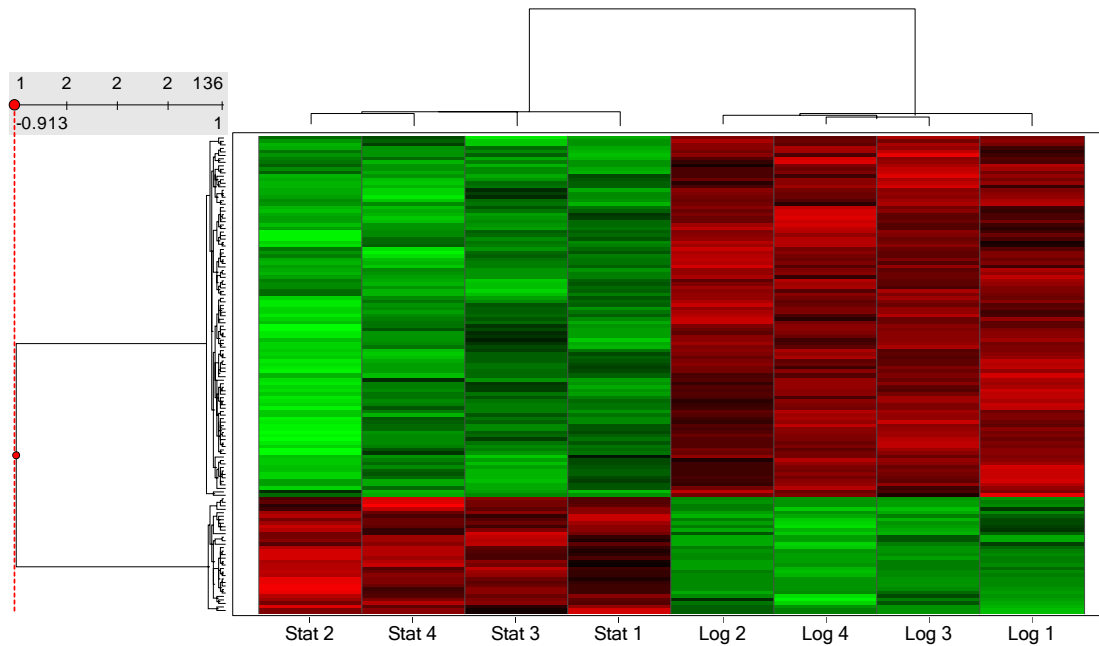


FIG. 6. Hierarchical cluster of genes from *B. melitensis* grown to stationary and late-log phases.

Hierarchical clustering was performed on normalized Cy3 (transcript) signal intensity values from 8 arrays using Spotfire DecisionSite 8.2 software. Stat 1 – Stat 4 represent the four stationary phase replicate bacterial samples, and Log 1 – Log 4 represent the four late-log phase replicate samples. Higher signal values are shown in red, and lower signal values are shown in green.

genes were indeed differentially expressed between the two growth conditions. Moreover, the majority of differentially expressed genes were up-regulated in log phase compared to stationary phase (bright red color), consistent with the statistical analysis results (Appendix A). Co-clustered *B. melitensis* genes that were up-regulated during late-log growth phase included those encoding proteins involved in energy production and conversion, synthesis of cell envelope structural constituents, motility, metabolite influx and drug efflux, and transcriptional regulation. Co-clustered genes that were down-regulated included those involved in transcription regulation and metabolism (data not shown).

In order to visually characterize and compare genes induced during different phases of culture, we used Spotfire DecisionSite 8.2 to create profile charts for genes that were consistently up-regulated or down-regulated in late-log phase of *B. melitensis* cultures (Fig. 7A and B), compared to stationary phase bacterial cultures. The 20 spots, representing 10 genes that most closely resembled the pattern of expression shown in Figure 7A (i.e., up-regulated in late-log phase cultures, compared to stationary phase cultures) are presented in Table 3. Six of the 10 genes (denoted by asterisk in Table 3) were also expressed during stationary phase, although to a lesser extent. The 20 down-regulated genes (Fig. 7B), on the other hand, all encode uncharacterized hypothetical proteins, and thus shed no light on potential patterns of down-regulation. Overall, the profiling results were similar to the fold-change data (Appendix A) and the clustering results (Fig. 6).

FIG. 7. Expression profile chart for genes most highly up-regulated or down-regulated in late-log phase cultures of *B. melitensis* compared to stationary phase bacterial cultures. (A) An expression profile chart of the most highly up-regulated genes during late-log phase, was created using Spotfire DecisionSite 8.2 software. The ordinate represents normalized signal intensity values for each spot (gene), and experiment number/type is indicated on the abscissa. Stat 1 – Stat 4 represent the four replicate bacterial culture samples collected at stationary phase, and Log 1 – Log 4 represent the four replicate bacterial culture samples collected at late-log phase. Genes represented in the profile chart are listed in Table 3 with functions. (B) An expression profile chart of the most highly down-regulated genes during late-log phase.

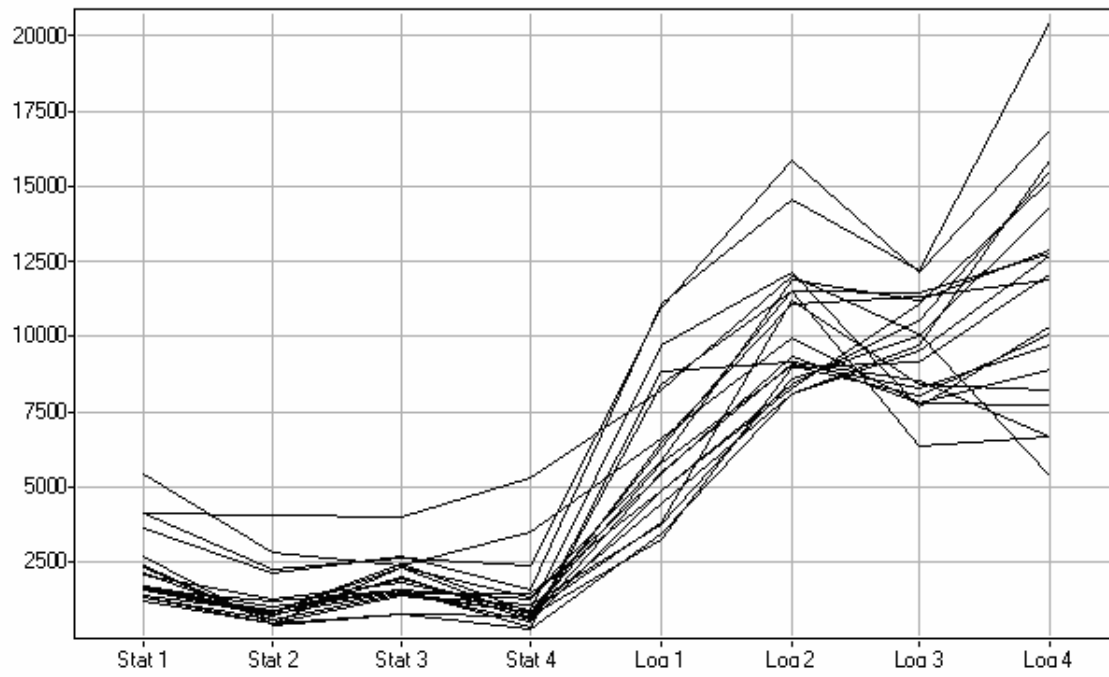
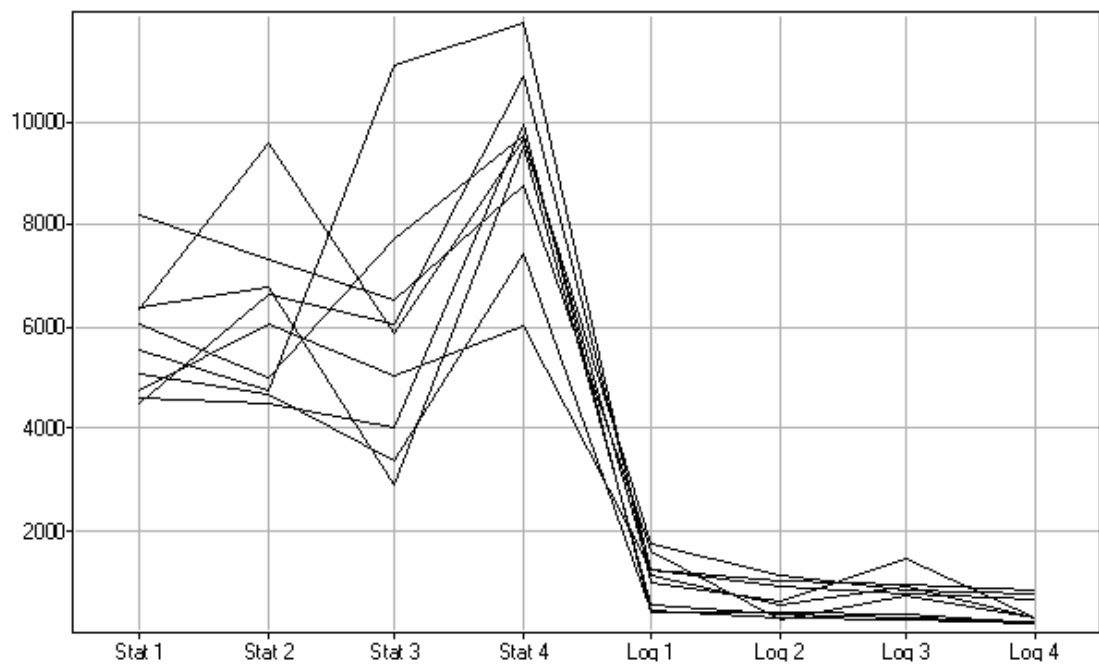
A**B**

TABLE 3. Genes significantly up-regulated in *B. melitensis* cultures grown in F12K tissue medium to late-log phase, compared to bacteria at stationary phase

Locus	Gene product	Function	No. of Spots
BMEI1977	1-acyl-sn-glycerol-3-phosphate acyltransferase*	Cell envelope: Biosynthesis and degradation of surface polysaccharides and lipopolysaccharides	2
BMEII0249	Dihydrodipicolinate reductase*	L-lysine synthesis	1
BMEI1297	DNA-directed RNA polymerase omega subunit*	Transcription regulation	1
BMEI1622	Hypothetical protein	Unknown	3
BMEI0362	Hypothetical protein*	Unknown	3
BMEI2005	Phenylalanyl-tRNA synthetase alpha subunit*	Protein biosynthesis	3
BMEII1003	Putative O-antigen transporter	Cell envelope metabolism transport of LPS components	3
BMEII0529	Surface protein	Unknown	2
BMEII0962	Taurine transport permease protein TauC*	ABC-type transport system required for uptake of aliphatic sulfonates	1
BMEII1065	Transcriptional regulatory protein, LysR family	Transcription regulation	1

No. of spots refers to the number of replicate spots (from Figure 7A) that represented each of the gene products shown. Asterisks denote genes that were also expressed during stationary phase, but to a much lesser extent.

Application of principal components analysis to assess global trends in *B. melitensis* transcriptional responses and to functionally group bacterial growth phase-specific genes. In order to reduce the dimensions of the data and describe the general trend of gene expression changes induced in *B. melitensis* cultures when grown in F12K tissue culture medium, we performed principal component analysis (PCA) using Spotfire DecisionSite 8.2 software. Three components were sufficient to describe 100% of the variability between treatments, with the three new axes (PC1, PC2, and PC3) accounting for 85.8%, 8.0% and 6.2% of the variability, respectively (Table 4).

TABLE 4. Eigenvalue for each principal component

Principal Component	Eigenvalue	Eigenvalue (%)	Cumulative Eigenvalue (%)	No. of genes
PC1	16.381	85.808	85.808	2,769
PC2	1.522	7.974	93.782	257
PC3	1.187	6.218	100.000	203

The three components are shown graphically in Figure 8. We interpreted the first principal component (PC1) to represent those genes that were not significantly expressed in *B. melitensis* cultures during either phases of growth. We interpreted PC2 to represent genes that were expressed during both late-log and stationary phases, although slightly higher or lower in the latter for some genes. We considered the third principal component (PC3) to primarily represent genes that were expressed only in late-log cultures (i.e., up-regulated during late-log phase of growth compared to the stationary phase). Overall, the PCA data corroborated the results obtained using GeneSpring, Spotfire, SAM, and which also suggested that the most significant difference between late-log and stationary phases was the induction of genes specifically in the log phase that were down-regulated upon entry into the stationary phase of growth.

PCA has previously been shown to be a powerful tool for grouping similarly expressed genes into functional sets (44). We interpreted the PCA results (based on component loadings) in order to attach biological meaning to the components and organized the genes that were most highly correlated with PC2 and PC3 based on eigenvalue percentages, into two separate lists of 257 and 203 genes, respectively. In



FIG. 8. Principal component analysis (PCA) of gDNA and transcript levels in *B. melitensis* cultures collected at stationary and late-log phases of growth. PCA was performed using Spotfire DecisionSite 8.2 software. Three components were sufficient to describe all the variation between sample types. Data reduction (from many dimensions down to 2 dimensions) results in a representation of the data (as shown graphically) that can be interpreted as a description of gene expression changes (compared to gDNA levels). The three components, (PC1, red), (PC2, blue), and (PC3, yellow), can be viewed as groups of *B. melitensis* genes that behave similarly between the various conditions: not expressed in either stationary or late-log phases of growth (PC1), expressed in both phases of growth (PC2), expressed only during late-log phase (i.e., not during stationary phase) (PC3). gDNA represents the level of the gene in the bacterial genome, Stat represents the level of the gene transcript at stationary phase, and Log represents the level of the gene transcript at late-log phase.

other words, we grouped together those genes whose expression patterns most resembled that of PC2 and PC3, as depicted in Figure 8. The majority of genes highly loaded on component 2 (expressed during both phases of bacterial growth) were related to protein synthesis, sugar metabolism, electron transport, motility, and intermediary metabolism, as expected (data not shown). Of the 257 genes that most highly correlated with PC2, 153 were also determined to be significantly expressed in both late-log and stationary phases of *B. melitensis* growth, based on GeneSpring, Spotfire, SAM, and ANOVA analyses (data not shown). Of the 203 genes most highly loaded on component 3 (PC3), 118 were also included in the most statistically significant altered gene list (Appendix A) and coded for proteins involved in cell wall synthesis, energy metabolism and transport of metabolites, metals, and drugs. Overall, the results were similar to what was obtained using hierarchical clustering (Fig. 6).

Phenotypic characterization of *B. melitensis* strains mutated in genes highly up-regulated in late-log growth phase in HeLa cells. The above results suggested the possibility that some of the 454 genes differentially expressed between late-log and stationary growth phases might influence the invasion process of *B. melitensis* in HeLa cells. To test this hypothesis, we evaluated *in vitro* the internalization performance of 8 transposon interrupted mutants of *B. melitensis* 16M genes highly up-regulated in late-log growth phase. The criterion for election of the mutants was based on magnitude of fold-change expression and availability of the mutant strain with transposon interruption in the locus expressed on our *B. melitensis* mutant bank. The transposon mutants tested (Table 1) were interrupted in the following loci (fold-change as shown in Appendix A

are indicated between parenthesis): BMEI1414 (> 133.4-fold), BMEI1416 (207.7-fold), BMEI1538 (> 146.3-fold), BMEI1707 (> 42.5-fold), BMEII0025 (> 9.0-fold), BMEII0034 (> 81.6-fold), BMEII0380 (267.76-fold) and BMEII0472 (> 86.7-fold). All mutant strains had growth curves similar to the wild type strain when grown in F12K tissue culture media supplemented with 10% HI-FBS (i.e. late-log cultures had 2×10^9 CFU/ml). Cultures were inoculated directly onto confluent monolayer of HeLa cells, co-incubated for 30 min and then washed and re-incubated 1 h with fresh media containing gentamicin for killing extracellular bacteria. After lysing infected cell cultures with 0.1% Triton X-100, invasive bacteria were assessed by plating a serial dilution on TSA supplemented with kanamycin and incubating at 37°C with 5% CO₂ for 4 days. The screening invasion assays revealed that 4 mutants BME5F3, BME8A6, QW70F8 and QW184B9, were statistically significantly deficient ($p < 0.05$) for internalization, compared to the parental strain. The invasiveness of these 4 mutants was re-evaluated in 9 independent assays, being BME5F3 (BMEI1538::*Tn5*) and QW184B9 (BMEII0380::*HimarI*) statistically significantly deficient for internalization compared to the wild type ($p < 0.01$) (Fig. 9). These results suggest that 25% (~ 100) of the most highly up-regulated genes in late-log phase may have influence in *Brucella* internalization in non-phagocytic cells.

DISCUSSION

The molecular mechanisms involved in the initial *Brucella*:non-phagocytic host cell interaction are not well characterized. HeLa cells have been used as a model for

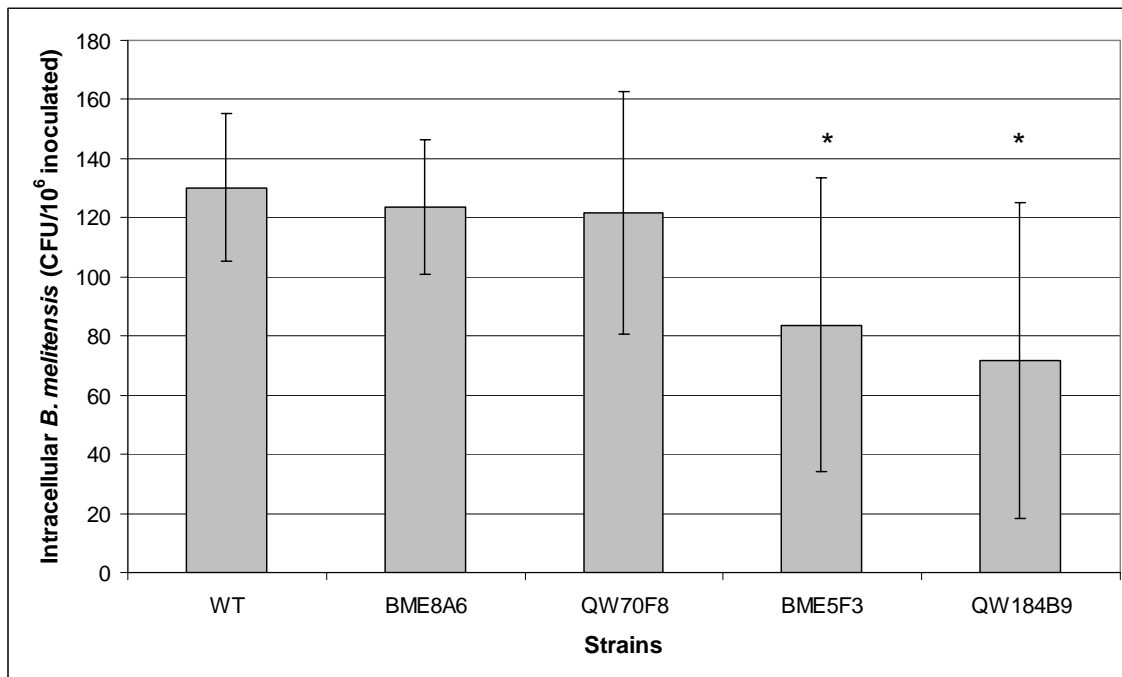


FIG. 9. Internalization ability of *B. melitensis* transposon interrupted in genes highly up-regulated in late-log growth phase in HeLa cells. HeLa cells were infected at MOI 1,000:1 by adding *B. melitensis* 16M grown to the late-log phase onto cells and spinning down for 10 min. After 30 min incubation, extracellular bacteria were killed by 1 h gentamicin-treatment. Infected cultures were washed 3 times with PBS before lysing, and the lysates were serially diluted and cultured on TSA (TSA supplemented with kanamycin for mutants) plates for quantitation of CFU. The invasiveness of *B. melitensis* 16M with transposon insertion in locus I1538 (BME5F3) and II0380 (QW184B9) were significantly different (* = $p < 0.01$) than the parental strain. Results are presented as the number of CFU from internalized bacteria 30 min post-infection per every 10⁶ inoculated. Means + SD (error bars) of 9 independent assays are shown.

studying adhesion and internalization of *Brucella* sp. in non-professional phagocytic cells (31, 98). These studies found that brucellae bind to cellular receptors containing sialic acid residues and induce their own uptake by a local rearrangement of the host cell cytoskeleton around the invading organisms. The ability of the bacteria to adhere and penetrate eukaryotic cells is a very well orchestrated process that requires several factors/elements in order to be successful (42). To date, only a few *Brucella* elements involved in cell invasion have been identified (10, 32, 54, 216). This study was performed with the goals of characterizing the *Brucella* invasion-related transcriptome in non-phagocytic cells and identifying bacterial candidate genes involved in the invasion process.

Successful establishment within the host requires facultative intracellular pathogens to rapidly adjust to different environmental conditions by a coordinated expression of a large number of genes necessary for the adaptation between the extracellular and intracellular phases of infection. To more efficiently identify invasive differences between cultures at different phases of growth and eliminate from consideration any elements that might be expressed as a consequence of bacterial pre-infection manipulation (centrifugation, washes, transfer to fresh media) or host:agent interactions, we grew the bacteria directly in the infective media used to inoculate the HeLa cell cultures and allowed them to interact only for a short period of time (30 min). We also used a higher MOI (1,000:1) than other studies (32, 50), because *B. melitensis* was not highly internalized by epithelioid-like HeLa cells during the first 30 minutes post-infection at lower MOIs under our experimental conditions.

Our initial experiment found that cultures of *B. melitensis* at late-log growth phase were more invasive to non-phagocytic cells than cultures at early-log and stationary growth phases. Similar results were observed for other invasive pathogens, such as *Salmonella* spp. or *Yersinia enterocolitica* (143, 177). As we demonstrated here, the *Brucella* transcriptome, and consequently the virulence of the organism, are modified during the different stages of the growth curve. This modification may also be influenced by the media used (*B. melitensis* growth curve was different in tryptic soy broth (TSB); data not shown), therefore the growth curve and the highest rate of infection must be determined for each condition employed.

The relationship between growth phase and invasiveness is dependent on the availability of bacterial virulence factors at any given time. For instance, *Shigella flexneri* is more invasive during the early phase of their exponential growth, because invasion proteins (Ipa) are secreted in higher amounts during this growth phase (162), while *Salmonella enterica* and *Legionella pneumophila* have their secretion systems assembled and effector proteins properly stored in the cytoplasm only at the late exponential and stationary growth phases, respectively (42, 85, 159). In order to understand why our system evoked greater invasiveness in *B. melitensis* cultures at late-log phase, we conducted a global gene expression detection study using cDNA microarray technology. Microarray analysis revealed that 454 genes were significantly differentially expressed between the most and least invasive cultures (Appendix A); however the roles of most of these genes are not well defined in *Brucella* pathogenesis. The vast majority of the observed changes in gene expression were related to the

bacterial response to the increased growth conditions in tissue culture media. For instance the up-regulation of genes associated with transcription and translation, nutrient metabolism, transport, and energy production and conversion correspond to a more active metabolism of the cultures at late-log phase of growth, compared to cultures at stationary phase. As was expected, several cell division- and DNA synthesis-related genes were also up-regulated in late-log phase, when the bacterial population was still actively growing. On the other hand, genes down-regulated in late-log phase were more heterogeneous in nature, demonstrating no predominant functional category. In concordance with the literature, the increased expression of the locus BMEI0280 encoding the alternative sigma 32 factor was observed in stationary cultures. Sigma 32 factor regulates the transcription of heat shock genes, which allow the bacteria to survive not only an abrupt increase in temperature, but also general stress situations, such as nutrient limitations during stationary growth phase (244).

In seeking to identify possible contributors to the increased invasiveness of *B. melitensis* at late-log phase, the conversion of metabolites to components that alter cell envelope structure must be considered. Altered outer membrane/cell wall topology would be expected to influence the initial bacteria:host cell interaction and might facilitate attachment and entry into host cells. In our study, a significant number of genes directly involved in cell envelope/outer membrane biogenesis were differentially expressed (Appendix A). One of the genes up-regulated at late-log growth phase was the locus BMEI0402. The product of this gene has not been characterized yet; however it presents high homology (63% sequence identity) to an immunogenic outer membrane

protein Omp31 (BMEII0844) (233). Omp31 is a haemin-binding protein (47), which binds to and extracts iron from the host. Iron has been identified as a required element for epithelial invasion in microbial pathogens (18, 81, 106), and the expression of this locus along with another iron-related genes in late-log cultures (BMEI0176-177, BMEII0536, BMEII0567, BMEII0583, BMEII0704, BMEII0883, BMEII1120, BMEII1122) may influence the internalization ability of brucellae. SP41 is another surface-exposed outer membrane protein recently reported to be important for *Brucella* adherence to and invasion of non-phagocytic cells (32). This protein is encoded by the *ugpB* gene (BMEII0625), which most likely belongs to an operon (BMEII0621-625) that encodes for a sn-glycerol-3-phosphate ABC transporter (<http://www.tigr.org/tigr-scripts/operons/operons.cgi>). In our study, the transcripts predicted to encode for the transport system [*ugpC* (BMEII00621) (ATP-binding protein), *ugpE* (BMEII0622) and *ugpA* (BMEII0624) (permease proteins)] were highly up-regulated (> 50 fold) in late-log cultures when compared to stationary cultures. However, the transcript from the gene *ugpB* that encodes for the OMP was not differentially expressed, and the other *ugpE* gene (BMEII0623) was down-regulated. These and previous data strongly suggest an active role of the whole sn-glycerol-3-phosphate ABC transport system in *Brucella*:host initial interaction, which will require further confirmation in future studies.

Two of the mutants tested had transposon-interrupted genes whose products influence cell envelope/outer membrane biogenesis, but none of them were found to have a role in invasion. The mutant BME5D1 has a disruption of the locus BMEI1414 that encodes for perosamine synthetase. This enzyme is involved in the biosynthesis of

the O- side chain of *Brucella* LPS, and a mutant deficient for this gene was not found to be defective for internalization in bovine macrophages, compared to the parental strain (91). The other mutant (BME8A6) has a transposon inserted in the locus BMEI1707 that encodes for the enzyme mandelate racemase, which catalyzes the interconversion of the enantiomers of mandelate via an enol intermediate. No references in the literature were found to suggest that this enzyme is involved in bacterial invasion or virulence. Our results found a lower, albeit non-significant, invasive rate compared to the wild type strain in 9 independent assays. The possibility that this enzyme plays a dual role in metabolism and invasion or indirectly contributes to increased invasiveness in *Brucella* is not entirely unlikely, as the major glycolytic enzyme enolase was found to be surface-expressed and secreted, facilitating immune cell migration and pathogenic bacterial dissemination via activation of plasminogen, in addition to its main role in metabolism (89, 174, 209).

Rapid adaptive physiological response to multiple environmental and cellular signals in bacteria is mainly mediated by transcriptional regulators. Prokaryotic genes putatively coding for transcriptional regulators are grouped in families based on sequence similarity and functional criteria. Twenty-one transcripts, belonging to 11 families of transcriptional regulators, were differentially expressed in our study (Appendix A). It was recently reported that *B. melitensis* mutants for 12 of these 21 transcriptional regulators were not attenuated after one-week of infection in mice (101). However, none of these transcriptional regulators have been tested for internalization ability in non-phagocytic cells. Therefore, contribution of these genes to invasion

remains unknown. A well-known family of transcriptional activators that regulates various functions in microbes is LuxR (61). There are 2 loci (BMEI1758 and BMEI1116) that encode transcripts belonging to this family of transcriptional regulators in the *B. melitensis* genome. One (*vjbR*, BMEI1116) has been identified as a major regulator of the *virB* operon and flagella genes (48), while the function of the other remains unknown. In spite of detecting some *virB* and flagella genes up-regulated in our study, the transcriptional regulator *vjbR* was not differentially expressed, which would suggest that other transcriptional regulator(s) may participate in the expressional control of both the flagella and T4SS, as was discussed by Delrue *et al.* (2005). However, the locus BMEI1758 that encodes a 238 aa protein only found in *Brucella* species (no homology to proteins from other microorganisms), was up-regulated 221-fold in the late-log phase of growth. Determining the importance of this and other transcriptional regulators in late-log growth phase cultures in the initial host:agent interaction could be the first step to identifying the effectors gene(s) they regulate.

Another form of microbial transcriptional gene control is the two-component regulatory system, which involves a cytoplasmic membrane-located sensor protein and a cytoplasmic response regulator protein (16). Eight ORFs encoding for two-component response regulators have been identified in the *B. melitensis* 16M genome (51). Of particular interest is the up-regulation of the locus BMEI2034 (sensor protein ChvG), which is located immediately downstream of the ChvI/ChvG two-component system (BMEI2036-35), a *B. melitensis* homolog of the well-characterized BvrR/BvrS 2-component regulatory system that controls cell invasion and intracellular survival in *B.*

abortus (99, 216). Currently available data indicate that the locus BMEI2034 is located in the same operon as the sensor protein ChvG (locus BMEI2035) (<http://www.tigr.org/tigr-scripts/operons/operons.cgi>); however, only BMEI2034 (not BMEI2035), was detected as differentially expressed between late-log and stationary growth phases in this study. The role of ChvG/ChvI in *B. melitensis* virulence has not been studied, but their homology with other 2-component response regulators of other pathogens would suggest an important role in virulence regulation. On the other hand, the influence of the signal transduction systems differentially expressed in this study could not be evaluated due to the unknown molecular regulation of these response regulators in *B. melitensis*. Addressing these issues would be expected to enormously clarify *B. melitensis* virulence mechanisms.

Several motility-related genes were more highly expressed at late-log phase compared to stationary phase, including kinesin-like protein, chemotaxis MotD protein and genes related to flagellum apparatus synthesis and functions, e.g. flagellin itself (96.6-fold). Flagellin has been well-characterized as a contributor to bacterial virulence through chemotaxis, adhesion to and invasion of host cells (186). The extent to which flagellar machinery participates in the invasive process seems to depend at least partly on the species of bacteria and/or the host cell type. For instance, flagellar-associated motility in *Salmonella* is not required but accelerates invasion of Caco-2 colonic epithelial cells (229) whereas the invasion of *Acanthamoeba astronyxis* by *Bukrholderia pseudomallei* absolutely requires an intact flagellum apparatus (114). In the case of *B. melitensis*, a previous study has demonstrated that flagella expression is growth curve

dependent and required for persistent disease in a mouse model but not for invasion in cellular models (84). In the previous study was reported that a functional flagellum was assembled in early-log growth phase cultures but not at later time points. In our study, we did not analyze gene expression at early time points, but our results clearly indicate flagellar genes expressed in late-log phase cultures but not in stationary cultures. The differences in flagellum gene expression between the previous study and ours could be attributed to evaluation of different steps of the process (protein expression versus gene expression), different culture media, or post-transcriptional regulation mechanisms. We were not able to evaluate the role of *B. melitensis* flagellar gene expression in invasion under our experimental conditions, but undoubtedly, the presence of flagellar machinery and other adhesion/motility factors in some phases of the growth curve and their exact contribution to the *Brucella* invasion process warrant further studies.

Genes coding for specific or general transporters were differentially expressed in late-log growth phase cultures, compared to stationary phase cultures. Among those most frequently observed were the ABC transporters, which are used by bacteria to import or export different compounds such as ions, polypeptides or carbohydrates through their membranes (45) and those used in the transport of nutrients, the latter which is directly related to the physiological state of the bacteria (i.e. growth curve) and the environment (i.e. culture medium). Among the mutant strains tested was QW154H11 that has a transposon-interrupted locus BMEI1416. This locus codes for an ATP binding protein of the O-antigen export system. Our initial assays suggested that this ABC transporter system plays little or no role in *B. melitensis* invasion, and no publications

were found linking it with virulence in bacteria. Another up-regulated transporter was the acriflavin system. Acriflavin resistance pumps belong to a non-ABC multidrug-resistance efflux pumps. They not only confer bacteria protection to antibiotics but also defend them from natural substances produced by the host and play a direct role in bacterial pathogenesis (178). In this study, 3 (AcrA, AcrB, AcrD) of 7 Acriflavin resistance proteins observed in *B. melitensis* genome (51) were up-regulated in late-log growth phase cultures. Medium and growth-phase were reported to play an important role in the expression of the tripartite system AcrAB-TolC efflux pump in *E. coli* (13). Moreover, previous *in vitro* and *in vivo* studies using plant and other animal pathogens have shown the participation of the AcrAB-TolC efflux pump in adherence to, invasion of and persistence (24, 25). Not surprisingly, under our experimental conditions the mutant QW184B9 with a transposon interrupted in the locus BMEI0380 that encodes AcrA had significantly decreased internalization when compared with the parental strain. Participation of this multidrug-resistance efflux pump in *B. melitensis* invasion of non-phagocytic cells will require further clarification. Also, a *B. melitensis* strain QW73H12 mutated in the membrane fusion protein MtrC, a homolog of HlyD secretion protein, was evaluated for invasiveness. Proteins from this family are anchored in the cytoplasmic membrane with a highly conserved large periplasmic domain and are an important part of the transport apparatus of type I secretion systems (108). The role of MtrC protein in *Brucella* physiology has not been addressed yet, but our data suggest that it would not likely play a role in adhesion and internalization in spite of being highly up-regulated in the most invasive cultures.

The *virB* operon has been reported to be essential for intracellular survival and multiplication of *Brucella* (22, 50, 169, 213), but its role in adherence and internalization is contradictory (39, 236). In our study, some genes from the operon (*virB1*, 3 and 10) were up-regulated in late-log growth phase cultures compared to the stationary phase of growth. Building on the concept that highly up-regulated genes influence the invasive process under our experimental conditions, we infected non-phagocytic cells with a *B. melitensis* transposon interrupted in *virB1* and *virB10* genes. However, none of the mutants demonstrated differential invasion rates in HeLa cells, compared to the WT strain, which is in agreement with other previous experiments that have shown that *virB* did not influence *B. abortus* internalization in non-phagocytic cells (39).

Finally, genes up-regulated in late-log phase encoding hypothetical proteins whose function is unknown or barely predicted deserve some special consideration. This group of “hidden genes” may contain some of the heretofore unknown virulence factors utilized for *B. melitensis* to invade and infect the host. Here we found that a *B. melitensis* transposon interrupted in the locus BMEI1538 (BME5F3) that encodes for a hypothetical protein of 77aa with no detected homology, partially lost the capacity to be internalized by non-phagocytic cells. These preliminary data suggest that the product of this locus as well its role in *B. melitensis* invasion in non-phagocytic cells is deserving of special attention.

In conclusion, our studies reveal that *B. melitensis* grown in cell culture media at late-log phase are more invasive in non-phagocytic cells than cultures grown at early-log or stationary growth phases. cDNA microarrays provide informative differential

transcription profiles of *B.melitensis* cultures grown at late-log vs. stationary growth phase. Using a few specific examples we were able to confirm that highly expressed genes at late-log growth phase were involved in the invasion phenotype of *B. melitensis* cultures in non-professional phagocytic cells. Future studies on *Brucella* invasion and virulence will be aimed at more precisely delineating the roles of the genes discovered in this study.

CHAPTER III

HOST AND *Brucella melitensis* TEMPORAL GENE EXPRESSION PROFILES

IN AN *in vitro* MODEL OF INFECTION

INTRODUCTION

Brucella infects hosts principally by penetrating mucosal surfaces from which it disseminates to the rest of the body (66). *In vitro* assays performed on cell lines or primary cultures are useful for understanding the details of host:agent interactions. The HeLa cell line has been used to understand adhesion, internalization, intracellular trafficking, survival, and replication of brucellae in non-professional phagocytic cells. These studies have shown that individual *Brucella* initially attach to non-professional phagocytic cells via receptor molecules containing sialic acid or sulphated residues (31) and within a few minutes are internalized by receptor-mediated phagocytosis (52, 53). After invasion, virulent *Brucella* transiently interact with an intracellular compartment related to the early endocytic network that is gradually transformed in a multimembranous autophagic vacuole. Subsequently, *Brucella* is delivered to rough endoplasmic reticulum-like compartment in the perinuclear area, where massive intracellular replication occurs (53, 179).

Despite the published precise and detailed descriptions of *Brucella* internalization and intracellular trafficking in non-professional phagocytic cells, there is no global or temporal molecular characterization of these phenomena. The goals of this study were to characterize the transcriptome of *Brucella* and *Brucella*-infected host cells

during acute infection in order to understand the initial strategies employed for intracellular pathogen survival and replication and to identify perturbations of major gene(s) modulating critical cellular pathways during the initial infection.

MATERIALS AND METHODS

Bacterial strains, media and culture conditions. Smooth virulent *Brucella melitensis* 16M Biotype 1 (ATCC 23456) re-isolated from an aborted fetus goat, and its derivative a *B. melitensis* 16M II0027 *virB3* homolog::*HimarI* (*virB* mutant) (241) were maintained as frozen glycerol stocks. Saturated cultures of strains were sub-cultured into 50 ml conical tubes filled with 10 ml of cell culture media [F12K medium (ATCC) supplemented with 10% heat-inactivated fetal bovine serum (HI-FBS) (ATCC)] at a ratio of 1:200, and incubated at 37°C with 5% CO₂ overnight with shaking until they reached the late-log growth phase (OD 0.4).

Kinetics of *B. melitensis* in HeLa cells. HeLa cell infection was conducted as explained in Chapter II. Briefly, the HeLa S3 cell line (ATCC CCL-2.2), between passages 8 and 15, was grown in F12K medium containing 10% HI-FBS at 37°C with 5% CO₂. Twenty-four hours prior to infection, cells were cultured in 24 well plates (Corning) at a concentration of 1×10^5 cells/well and replaced in the incubator. Before infection, cells from 1 well were detached and counted. Infection with *B. melitensis* was done by replacing the medium overlying the HeLa monolayers with a bacterial inoculum grown in cell culture media, at a multiplicity of infection of 1,000 bacteria per cell (MOI 1,000:1). Bacteria were centrifuged onto the cells at 800 X *g* for 10 min followed by 30

min of incubation at 37°C. Then, cells were washed once with PBS to remove extracellular bacteria and re-incubated with F12K media supplemented with 100 µg ml⁻¹ of gentamicin solution (Sigma) for 1 hour. After antibiotic treatment, infected cultures were washed 3 times with PBS, 1 ml of cell culture media added and replaced in the incubator. To determine the kinetics of *B. melitensis* WT and the *virB* mutant in the first 12 h, the viable number of intracellular bacteria was determined at 0, 4, 8 and 12 h post-infection (PI) by lysing infected cultures with 0.1% Triton X-100 (Sigma). Lysates were serially diluted and cultured on TSA plates (supplemented with kamamycin as necessary) for quantitation of colony-forming units (CFU). Duplicate wells containing bacterial suspensions alone were used as a control for bacterial growth.

Induction of RNAi in HeLa cells. The day before transfection, HeLa cells were cultured in 24 well plates at a concentration of 4x10⁴ cells/well in 0.5 ml of cell culture medium and replaced in the incubator. The following day, 50 µl of serum-free cell growth medium (Invitrogen) was mixed in separate compartments with 30 nM and 100 nM of *Silencer*[®] mitogen-activated protein kinase 1 (MAPK1) (ID 1449) and MAPK1 (ID 1544) Validated siRNA (Ambion) for each 24 wells of cells to be transfected. Simultaneously, 1 µl of TransFecting lipid reagent (Bio-Rad, Hercules, CA) was diluted into 50 µl of serum-free cell growth medium for each 24-well culture to be transfected. The diluted siRNA was combined and gently mixed with the diluted transfecting reagent. After 20 min incubation at RT, the culture media was removed from the wells and replaced by 100 µl of the siRNA-TransFecting complexes, rocked for 1 min and then filled with 400 µl of F12K cell culture media supplemented with 10% HI-FBS. The

next day, the media in the wells was replaced for 0.5 ml of fresh cell culture medium. Forty-eight hours after transfection, HeLa cells were infected with *B. melitensis* 16M and invasion and survival of intracellular bacteria was determined as described above. Infection of non-transfected cells and HeLa cells transfected with 30 nM *Silencer*[®] negative control #1 siRNA (Ambion) were used as controls. For validation of RNAi efficiency, RNA from transfected cells was extracted at the same time of infection (i.e. 48 h post-transfection) using RNeasy kit (Qiagen) and eluted in 50 µl of DEPC-treated water with 2% DTT and 1% RNase inhibitor (Promega). RNAs extracted from HeLa cells transfected with 30 nM of *Silencer*[®] GAPDH siRNA control and negative control #1 siRNA (Ambion) were used for validation of knocked down gene expression. Contaminant genomic DNA was removed by RNase-free DNase I treatment (Ambion) according to the manufacture's instructions, and samples were stored at -80°C until used. The concentration of RNA was quantitated by NanoDrop[®] ND-1000 (NanoDrop), and the quality RNA was assessed using the Agilent 2100 Bioanalyzer (Agilent). Target mRNA levels were measured by qRT-PCR as explained below using the following primers: MAPK1 (Forward 5'-TGGATTCCTGGTTCTCTCTAAAG-3', Reverse 5'-GGGTCTGTTTTCCGAGGATGA-3'), GAPDH (Forward 5'-AAAACCTGCCAAATATGATGACA-3', Reverse 5'-AGCTTGACAAAGTGGTCGTTGA-3') and β-actin (Forward 5'-GCAAATGCTTCTAGGCGGACTA-3', Reverse 5'-CTGTCACCTTCACCGTTCCA-3') (Sigma Genosys).

Isolation of total RNA from HeLa cells. Total RNA from infected and non-

infected cell cultures was extracted at 4 and 12 h PI by removing the culture media, washing with PBS and adding 1 ml of TRI-Reagent® (Ambion) onto each cell monolayer (5×10^6 cells cultivated in 25 cm^2 tissue culture flasks). After 5 min at room temperature (RT), the suspension was transferred to a 1.5 ml vial and 200 μl of chloroform added and kept at RT for 10 min. Then, the tubes were centrifuged at 10,000 X g at 4°C for 15 min and the aqueous phase transferred to a fresh tube containing 0.5 ml of 100% isopropanol. After vortexing, the samples were kept at RT for 10 min and then centrifuged at 10,000 X g at 4°C for 10 min, the supernatant discarded and the pellet washed in 75% ethanol. Following centrifugation at 10,000 X g at 4°C for 5 min, the supernatant was discarded and the pellet re-suspended in DEPC-treated water with 2% DTT and 1% RNase inhibitor (Promega). Contaminant genomic DNA was removed by RNase-free DNase I treatment (Ambion) according to the manufacture's instructions, and samples were stored at -80°C until used. The concentration of RNA was quantitated by NanoDrop® ND-1000, and the quality of RNA was determined using the Agilent 2100 Bioanalyzer.

Enrichment and sense-strand amplification of *B. melitensis* total RNA from infected HeLa cell cultures. *B. melitensis* total RNA was initially enriched and then amplified from 50 μg of total RNA from *B. melitensis*-infected HeLa cells at 4 and 12 h PI. The enrichment procedure was performed using the MICROBEnrich® kit (Ambion) according to the manufacturer's instructions. After enrichment, the RNA was precipitated in 100% ethanol at -20°C for at least 1 h, centrifuged for 30 min at 10,000 X g at 4°C, followed by two ice-cold 70% ethanol washes. After 5 min centrifugation at

10,000 X *g* at 4°C, the RNA was re-suspended in 25 µl of DEPC-treated water and immediately amplified in a 3 step-protocol. This protocol enables amplification of sense-stranded prokaryotic transcripts, which was essential for our downstream microarray studies. In the first step, the protocol utilizes genome-directed primers (GDP: see below) to bias the reverse transcription to bacterial transcripts and the overhang tailing activity of Moloney murine leukemia virus (MMLV) reverse transcriptase to add the T7 promoter to cDNAs during reverse transcription. Then, the second-strand cDNA is synthesized and finally, *in vitro* transcription is carried out using a T7 polymerase. The protocol has been described in detail (141). Briefly, the total amount of RNA after the enrichment procedure was reverse transcribed to cDNA in a 50 µl reaction using 42 µM of *B. melitensis* genome-directed primers (*BmGDP*), 5 µl of 50X dNTPs (10mM each) (Invitrogen), 2.5 µl of PowerScript (Clontech, Palo Alto, CA), 2.5 µl of RNAsin (Promega), and 42 µM of T7 promoter-template switching primer (T7-TS) (5'-CGAAATTAATACGACTCACTATAGGGAGAGTACGCGGG-3') (Sigma Genosys). The *BmGDP* and the RNA were mixed and heated at 70°C for 10 min before being placed on ice for > 3 min and addition of the T7-TS and the reverse transcription reagents. The first-strand and the template switching reaction were performed at 42°C for 90 min in a thermocycler with a non-heated lid. In the next step, the second-strand cDNA was synthesized by adding 1X final concentration of 10X Advantage 2 Polymerase buffer (Clontech), 1X final concentration of 50X dNTPs mix (10mM each) (Invitrogen), 2U of Rnase H (Roche) and 1X final concentration of 50X Advantage 2 Polymerase mix (Clontech) to the final reaction volume of 150 µl. The components were

mixed and the reaction incubated in a heated-lid thermocycler with the following cycle: 37°C for 5 min, 94°C for 2 min, 65°C for 1 min and 75°C for 60 min. Double-stranded cDNA was purified using PCR purification kit (Qiagen), eluted in 100 µl of nuclease-free water and concentrated to 15 µl in a speed-vac with no heat. In the last step, the *in vitro* transcription, using the double-stranded cDNA as template and T7 Megascript kit (Ambion) in 40 µl reactions with an additional 400U of T7 polymerase (Ambion) and 20U of Rnase inhibitor SUPERase-In (Ambion), was carried out at 37°C for 16 h. RNA was cleaned and recovered using RNeasy kit (Qiagen) and eluted in 100 µl of nuclease-free water with 40U of SUPERase-In. The concentration RNA was determined, and the samples were stored at -80°C until used.

Isolation of total RNA and gDNA from cultures of *B. melitensis* 16M.

Intracellular *B. melitensis* gene expression was compared to the gene expression of the inoculum (i.e., cultures of *B. melitensis* 16M grown in F12K media supplemented with 10% HI-FBS at late-log growth phase) and *B. melitensis* gDNA was used for normalization of the bacterial gene expression profile. Isolation of total RNA and gDNA from *Brucella* cultures was done as previously described (Chapter II).

Design of *B. melitensis* genome-directed primers (*BmGDP*). The GDP-Finder is a computer-based algorithm (<http://www.innovationsinmedicine.org/software/GDP/>) that predicts the minimal number of primers to specifically anneal to all ORFs in a given genome (220). For the *B. melitensis* genome the algorithm predicts 89 reverse primers of 8-mer oligonucleotides searching for the first 500 bp of each complementary sequence of each ORF anneal to the 3,198 ORFs (Table 5). Primers were commercially

TABLE 5. *Brucella melitensis* 16M genome-directed primers (*BmGDP*)

Order	Primers	Unique No. of ORFs covered	No. ORFs covered	Percent complete
1	CGGCAAGC	291	291	9.10
2	CCAGCGCC	248	539	16.85
3	CGCCGCGC	223	762	23.83
4	CCTTGCCG	201	963	30.11
5	GCGCGCGC	171	1134	35.46
6	GCCGAAA	161	1295	40.49
7	CGCCGCCG	133	1428	44.65
8	GGCGCGGC	122	1550	48.47
9	GCGCCAGC	110	1660	51.90
10	TTCCGGCA	97	1757	54.94
11	GCTTGCGC	93	1850	
12	CGATCAGC	85	1935	
13	GCCGCCAT	76	2011	
14	TTCGGCAA	70	2081	
15	CCTTGCGG	68	2149	
16	CGATGATG	64	2213	
17	CCGCGCCG	56	2269	
18	CATCGGCA	53	2322	
19	CGGCGGCA	47	2369	
20	CCAGATCG	43	2412	75.42
21	GCTTGCCG	40	2452	
22	CCAGAAGC	40	2492	
23	GCGATGCG	38	2530	
24	GCGCGCGG	33	2563	
25	CCTTCGGC	32	2595	
26	CATCGCGC	30	2625	
27	CGCCTTCA	28	2653	
28	TTCCAGCG	27	2680	
29	CTTCCTTG	27	2707	
30	AGGCCGAT	25	2732	85.43
31	CCATGCCG	23	2755	
32	TTCCTGCG	22	2777	
33	AATGCCGC	20	2797	
34	GCGCGAAA	17	2814	
35	CCATTGCG	18	2832	
36	CCGCCAGC	18	2850	
37	TTCGGAAA	18	2868	
38	CAGCGCAT	15	2883	
39	GCCTTTTC	15	2898	
40	GCGGAAA	15	2913	91.09
41	GATGCGGC	14	2927	
42	GCCAAGCG	13	2940	
43	GCCTGCGC	12	2952	

44	CGGCATCG	12	2964	
45	CGCCATCG	10	2974	
46	GCCAGAAC	11	2985	
47	TGAAGCGG	11	2996	
48	GCACCAGC	8	3004	
49	CGGCAGAT	10	3014	
50	CCGCCTTC	9	3023	94.53
51	CTTGATGA	9	3032	
52	AAACCGGA	9	3041	
53	AAGCGGCA	8	3049	
54	GCGGCGCC	8	3057	
55	GCGCTCGC	6	3063	
56	CCGCTTTC	7	3070	
57	TCAATGGC	7	3077	
58	TCTTCAA	7	3084	
59	ATGGCGGC	5	3089	
60	GCCGCCAA	6	3095	96.78
61	TTTTCGCC	6	3101	
62	GAAATCAA	6	3107	
63	AAGCAAGG	6	3113	
64	TTCGGCCA	5	3118	
65	TTCATCGA	5	3123	
66	GCCGAGAA	3	3126	
67	GAAATCCG	5	3131	
68	CCAATGCA	5	3136	
69	GGCGGCGA	3	3139	
70	CGGCGATG	4	3143	98.28
71	CGAGATCG	4	3147	
72	TTGCGCAG	4	3151	
73	AAGCCCGC	4	3155	
74	TCACGCCG	4	3159	
75	CGCAATAT	4	3163	
76	AATGAAA	3	3166	
77	CATCGATG	3	3169	
78	GCGACAGC	3	3172	
79	CAGCCGGA	3	3175	
80	CCATATCC	3	3178	99.37
81	CCCGCGCA	3	3181	
82	TGCTCATC	3	3184	
83	ACTGTTCC	3	3187	
84	GATGATCG	2	3189	
85	CGACCAGC	2	3191	
86	TGATATCG	2	3193	
87	AATTTCCG	2	3195	
88	CGCAATAA	2	3197	
89	GCATTGGC	1	3198	100.00

synthesized (Sigma Genosys) and used for reverse transcription during the first step of RNA amplification and for labeling the cDNA.

Samples preparation and slide hybridization. The labeling and hybridization procedures are an adaptation of the protocol developed by The Institute for Genomic Research (105) and were extensively described in Chapter II. Briefly, 10 µg of total RNA from *B. melitensis* 16M or HeLa cells were reverse transcribed overnight to amino-allyl cDNA using 1.5 µg of *BmGDP* (samples to be hybridized on pathogen arrays) or 6 mg of random hexamer primers (samples to be hybridized on host arrays) (Invitrogen), 0.6 µl 50X dNTPs (Invitrogen) / aa-dUTP (Ambion) mix (2:3 aa- dUTP: dTTP) and 400U Superscript III (Invitrogen). The reaction was stopped by incubating the samples with 1M NaOH at 65°C for 15 min and neutralized by adding 1M HCl. Unincorporated aa-dUTPs and free amines were removed by column passage (Qiagen) and dried using a Speed-Vac.

Dried samples were re-hydrated in 0.1M Na₂CO₃ buffer (pH 9.0) and labeled with Cy3-ester (experimental *B. melitensis* RNA and reference HeLa RNA) or Cy5-ester (experimental HeLa RNA) (Amersham Pharmacia Biosciences). After one hour incubation in the dark, uncoupled dye was removed using columns (Qiagen) and dye incorporation calculated by NanoDrop[®]. *B. melitensis* gDNA was labeled overnight by direct incorporation of Cy5-dCTP (Amersham Pharmacia Biosciences) during reverse transcription using random primers and Klenow fragment (see Chapter II for details). Dry, labeled cDNA samples to be hybridized on *B. melitensis* microarrays were resuspended in nuclease-free water and mixed with 0.5 µg of labeled *B. melitensis*

gDNA to the final volume of 35 μ l. Samples were heated at 95°C for 5 min and then kept at 42°C until hybridization. Following incubation at 42°C, 35 μ l of 2X formamide-based hybridization buffer [50% formamide; 10X SSC; 0.2% SDS] was added to each sample, well mixed, and applied to a custom 3.2K *B. melitensis* oligo-array. The dried, labeled cDNA samples from experimental HeLa RNA and universal human reference RNA (Stratagene, La Jolla, CA) were re-suspended in 20 μ l of nuclease-free water (experimental RNA) or human genomic DNA Cot1 (Invitrogen) (reference RNA), mixed and heated at 95°C for 10 min followed by 10 min at 60°C and another 10 min at 25°C. Samples were kept at 42°C until hybridization. Following incubation at 42°C and immediately before hybridization, 40 μ l of 2X formamide-based hybridization buffer was added to each sample. The samples were then hybridized to a commercially available 10K human ESTs microarray (Microarray Center, Ontario, Canada). Slides were hybridized at 42°C for ~20 h in a dark, humid chamber (Corning) and washed for 10 min at 42°C with low stringency buffer [1X SSC, 0.2% SDS] followed by two 5-min washes in a higher stringency buffer [0.1X SSC, 0.2% SDS and 0.1X SSC] at room temperature with agitation. Slides were dried by centrifugation at 800 X g for 2 min and immediately scanned. Prior to hybridization, microarrays were pre-treated by washing in 0.2% SDS, followed by 3 washes in distilled water and kept in prehybridization buffer [5X SSC, 0.1% SDS; 1% BSA in 100ml of water] at 42°C for at least 45 min. Immediately before hybridization, the slides were washed 4 times in distilled water, dipped in 100% isopropanol and dried by centrifugation.

Data acquisition and microarray data analysis. Following the stringency

washes and centrifugation, the microarrays were scanned using a commercial laser scanner (GenePix 4100). The genes represented on the arrays were adjusted for background and normalized to internal controls using image analysis software (GenePixPro 6.0). Genes with fluorescent signal values below background were disregarded in all analyses. Pathogen arrays were normalized against *B. melitensis* genomic DNA as previously described (219). Data were analyzed using GeneSifter (VizX Labs, Seattle, WA). The signal values of every gene (triplicate spots in 4 arrays = 12 spots) for each experiment (i.e. 4 and 12 h) were averaged, the fold-change calculated, and Student's t test performed. At each time point, genes determined to be expressed at statistically significant levels on pathogen arrays hybridized with probes generated from *B. melitensis*-infected cells (fold-change > 2 and *p* value < 0.05) were subtracted from the final list of differentially expressed genes.

Only a few host genes were detected as differentially expressed between infected and control samples using traditional statistical methods; therefore, different criteria were used to identify those genes differentially expressed in the host. Host arrays were initially normalized against universal human reference RNA and resulting data analyzed using Seralogix's suite of gene expression analysis and modeling tools (www.seralogix.com). Differentially expressed genes were found to be significant based on Seralogix's Bayesian z-score method. With this method, genes are ranked and ordered according to their expression magnitudes. A Bayesian predicted average variance value is used in the z-score method. Actual measured variances associated with each gene are used to compute a Bayesian averaged predicted variance value for each of

the ordered genes. The Bayesian variance is determined using a sliding window algorithm that averages 50 variances directly on the ascending and descending ordered sides of each gene of interest. Significantly changed genes were determined with the Bayesian z-test ($p < 0.05$).

For the identification of Biosignature Dynamic Bayesian Network modeling, mechanistic gene discovery and pattern/pathways recognition used a framework of integrated software tools (XManager, XConsole & XBuilder) and relational database storage specialized for management and analysis of biosignature data (Biosignature Analysis Framework) developed by Seralogix, Inc.

Microarray results validation. Five randomly selected genes from *B. melitensis* and HeLa cells with differential expression at 4 and 12 h PI ($n = 20$) by microarray results were analyzed by quantitative RT-PCR (qRT-PCR). Two micrograms from the same RNA samples used for microarray hybridization were reverse transcribed using TaqMan® Reverse Transcription Reagents (Applied Biosystems). For relative quantitation of target cDNA, samples were run in individual tubes in SmartCycler II (Cepheid). One SmartMix bead (Cepheid) was used for 2 - 25 μ l PCR reactions along with 20 ng of cDNA, 0.2X SYBR Green I dye (Invitrogen) and 0.3 μ M forward and reverse primers (Sigma Genosys) designed by Primer Express Software v2.0 (Applied Biosystems) (Tables 6 and 7) to produce an amplicon length of about 180 bp. For each gene tested, the individual calculated threshold cycles (Ct) were averaged among each condition and normalized to the Ct of the GAPDH and *gyrA* genes for host and pathogen respectively, from the same cDNA samples before calculating the fold change using the

TABLE 6. Primers for Real-time PCR analysis of genes in *B. melitensis* samples

Locus ID	Gene product	Forward primers (5'-3')	Reverse primers (5'-3')
BMEI0371	RNA polymerase S70	AGGCATGGGCCAAGCA	AGATCAAGCGTGCCATATTGC
BMEI0583	Cell division protein FtsQ	TCAAGGGTTTTGTGGACCAGAT	TGTTTTTCCCGATCAAGCTTCT
BMEI0884	Gyrase A	AAGGCCTCGATGATCGAGAAG	ACGAGGTCTGCAAAGGCGTATA
BMEI1426	Putative undecaprenyl-phosphate alpha	TGCACTTATCATCGCAATCAATG	GAACAGGGCAAAACCGAGAA
BMEI1440	Thio:disulfide interchange protein DsbA	CGAAATTGGCCGGTTTTACA	CCCGACATCTCCTCAAACGA
BMEI1645	Acridflavin resistance protein B	CTGATCCGCCAGGAACTCA	CACCTGAACCGGCAATCG
BMEII0260	GTP-binding protein LepA	AGGGCTATGCCTCGTTTCA	ATATGTTGCGGGATCAGTTTCT
BMEII0346a	Transcriptional regulator, AsnC family	GATCGCGAGATTCTGGCTATTC	TCGCCCCGATGATATTGCT
BMEII0346b	Transcriptional regulator, AsnC family	ATATCATCCGGGCGATGATACT	GCCAAAACATCCCGCAAAC
BMEII0974	Nitrous-oxide reductase	TCAGTTGCCGAACCAGCATA	GGCGACCTTCATCGTTTCAC

TABLE 7. Primers for Real-time PCR analysis of genes in HeLa cells samples

GenBank accession #	Gene symbol	Gene product	Forward primers (5'-3')	Reverse primers (5'-3')
NM_000623	BDKRB2	Bradykinin receptor, beta 2	TAACATGAAGTCGTTGTGAGGGTTA	CCGGCTCCCAATACTGATTC
NM_001735	C5	Complement component 5	TGTAGTTCACAAAACCAGTACCTCTGA	CACCGCATGAGAGGATCCA
NM_001511	CXCL1	Chemokine ligand 1	TTCACCCCAAGAACATCCAAA	CTCCCTTCTGGTCAGTTGGATT
NM_006116	MAP3K7IP1	Mitogen-activated protein kinase kinase kinase 7 interacting protein 1	GGCAGCTGAGATGAACTGTCTTT	CCCGACCCTTCTCCTATGC
NM_003246	THBS1	Trombospondin 1	GATCCCACCCCTTACTCATCAC	AGCTGGTGCTCACTGAGATGGT
NM_000212	ITGB3	Integrin, beta 3	GAGGATGTCTGGGCCACTCA	TGAGGGTGTGGAATTAGGAGGTA
NM_002745	MAPK1	Mitogen-activated protein kinase 1	TGGATTCCCTGGTTCTCTCTAAAG	GGGTCTGTTTTCCGAGGATGA
NM_002539	ODC1	Ornithine decarboxylase 1	TGTTGCTGCTGCCTCTACGT	GTGGCGTTTCATCCCCTCT
NM_006206	PDGFRA	Platelet-derived growth factor receptor, alpha polypeptide	ATATTCTTTAGTGGAGGCTGGATGTG	CCGAAAACCTGGCCGATCA
NM_181523	PIK3R1	Phosphoinositide-3-kinase, regulatory subunit, polypeptide 1	GGAAGCAGCAACCGAAACAA	AGTTATAGGGCTCGGCAAAGC

$\Delta\Delta C_t$ method (Applied Biosystems Prism SDS 7700 User Bulletin #2). For each primer pair, a negative control (water) and an RNA sample without reverse transcriptase (to determine genomic DNA contamination) were included as controls during cDNA quantitation. *Brucella* arrays data were considered valid if the fold-change of each gene tested by qRT-PCR was > 2.0 and in the same direction as determined by microarray analysis. Due to different microarray analysis conducted for HeLa cells gene expression detection (genes were differentially expressed based on z-score and not on fold-change), host array data were considered valid if the fold change of each gene tested by qRT-PCR was expressed in the same direction as determined by microarray analysis.

RESULTS

The intracellular replication of *B. melitensis* in HeLa cells begins after an initial adaptation period of 4h post-infection. Kinetics of *B. melitensis* 16M intracellular replication in non professional phagocytic cells was evaluated during the first 12 h PI. At 4 h PI, the number of intracellular *Brucella* recovered was not significantly different ($p > 0.05$) compared with the number recovered at invasion (T0). However the number of intracellular *Brucella* present between 4 and 12 h PI increase 70% ($p < 0.05$) (Fig. 10). The number of *B. melitensis* CFU present in growth control wells increased almost twice at 4 h and ~ 1 log in the first 12 h compared with the original inoculum (data not shown). These results indicate that under these experimental conditions, the intracellular replication of *B. melitensis* in HeLa cells begins after an initial adaptation period of 4h PI.

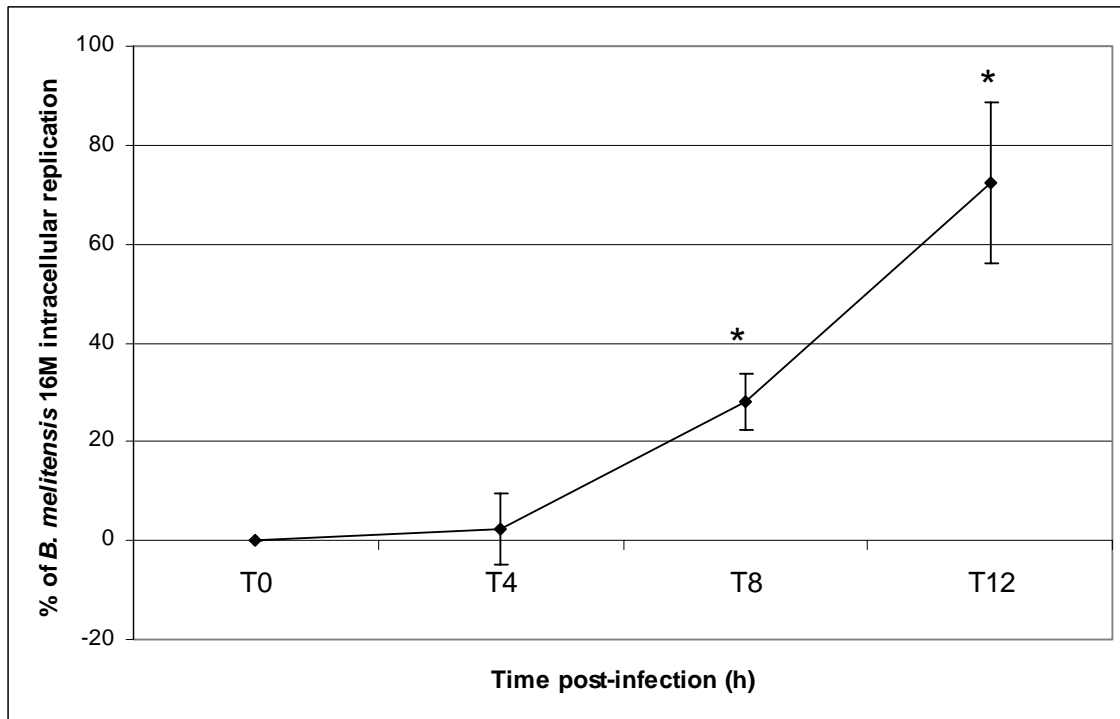
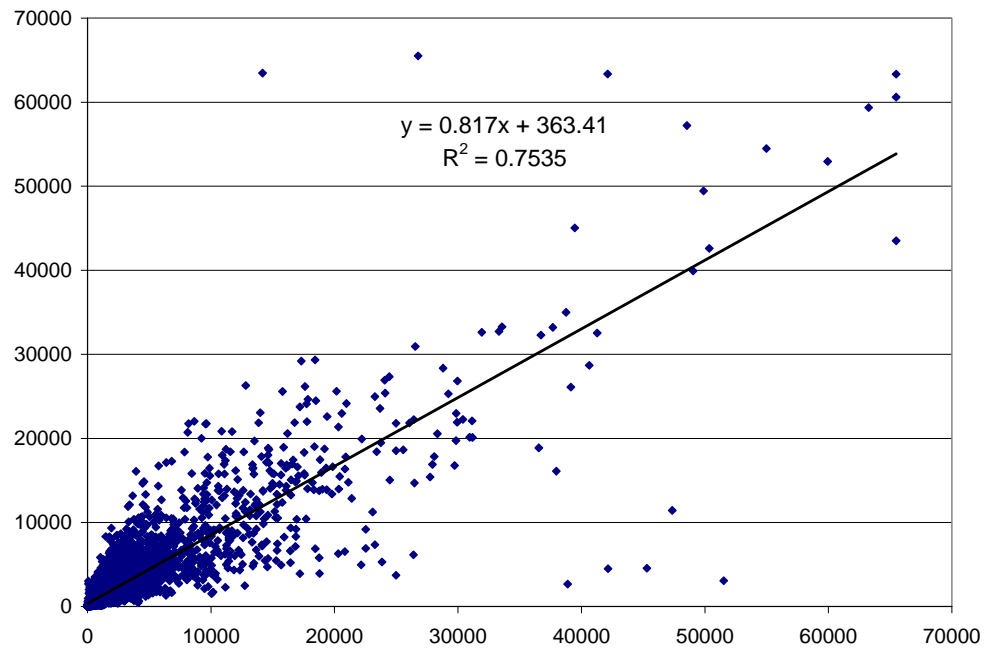
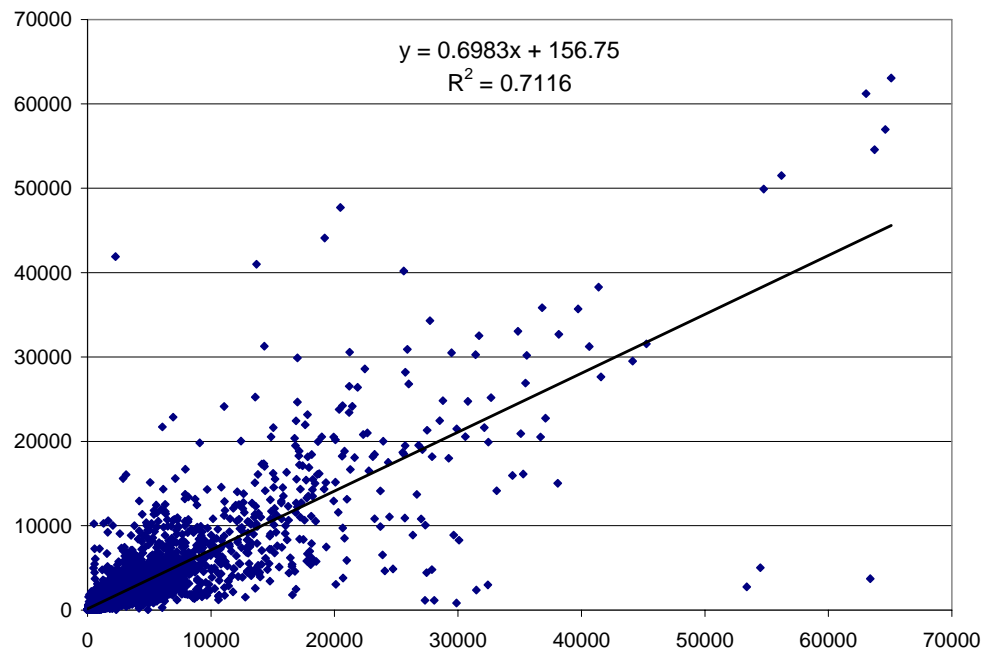


FIG. 10. Kinetics of *B. melitensis* 16M intracellular replication in HeLa cells. HeLa cells were infected at MOI 1,000:1 by replacing the media overlying the cells by a culture of *B. melitensis* 16M at late-log growth phase. After 30 min-interaction, cells were washed with PBS and incubated 1 h with gentamicin to kill extracellular bacteria. Cells were lysed at 0 (T0), 4 (T4), 8 (T8) and 12 (T12) hours PI and lysates serially diluted and cultured on TSA plates for quantitation of intracellular viable number of bacteria. The intracellular number of *B. melitensis* at 8 and 12 h PI was significantly different than those at T0 (* = $p < 0.05$) indicating that the intracellular replication of *B. melitensis* in HeLa cells began after an initial adaptation period of 4 h PI. Results are presented as the % of CFU compared with the T0. Data presented are the mean + SD (error bars) of triplicate samples of 3 independent experiments and statistical significance of differences was determined using Student's *t* test (p value < 0.05 was considered significant).

Genome-directed primers (GDP) generate more sensitive and specific probes of *B. melitensis* transcripts than random hexamer primers (RHP). Talaat *et al.* (2000) demonstrated the potential usefulness of GDP for detection of pathogen gene expression *in vivo*. In a technical experiment designed to determine the usefulness of the GDP for generation of cDNA from *B. melitensis* RNA and subsequent hybridization to microarrays, a primer set generated from GDP-Finder software was compared with a commercially available set of RHP. Each method was used on two identical *B. melitensis* RNA samples isolated from late-log phase cultures and the resulting cDNA was labeled with Cy3 and co-hybridized with Cy5-labeled genomic DNA (gDNA) on two arrays for each primer type. For inter-array comparison, 63 (of 9,681) genes with signals values flagged “bad” by GenePix 6.0 were removed across all four data sets to make them comparable. The consistency of the signal from samples reverse transcribed with GDP was slightly higher ($R^2 = 0.7535$) compared to RHP samples (0.7116) (Fig. 11A and B). Linear regression analysis also revealed a slightly higher advantage for GDP (p value of 1.12×10^{-72} , T statistic of 18.2) over RHP (p value of 1.0×10^{-14} , T statistic of 7.7). Likewise, correlation analysis indicated that GDP (87%) was slightly more consistent than RHP (84%) and the consistency was greater when considering average signal intensity values (GDP = 1665 & 1724 vs. 1912 & 1492 of RHP), average standard deviation (490 vs. 540) and standard deviation of average intensities (41 vs. 297). We also compared the average ratio between experimental replicates (1.3 for GDP and 0.91 for RHP), as well as the average signal log ratio between each experimental replicate and the co-hybridized gDNA (0.77 and 0.69 for GDP and 0.69 and 0.83 for RHP).

FIG. 11. Inter-array comparison of signal consistency from *B. melitensis* RNA samples reverse transcribed with genome-directed primers (GDP) vs. random hexamer primers (RHP). The consistency of the signal generated from a Cy3-labeled *B. melitensis* cDNA using a primer sets predicted from GDP-Finder software (GDP) was compared with a Cy3-labeled *B. melitensis* cDNA made by a commercially available set of RHP. Each method was used on two sets of identical *B. melitensis* RNA samples isolated from late-log phase cultures and the resulting cDNA was labeled with Cy3 and co-hybridized with Cy5-labeled genomic DNA (gDNA) to two *B. melitensis* oligoarrays for each primer type. Signal consistency from samples reverse transcribed with GDP was slightly higher ($R^2 = 0.7535$) **(A)** compared to RHP samples (0.7116) **(B)**.

A**B**

While the average ratio between experimental samples was higher for GDP than for RHP, the standard deviation of signal log ratios, which is a more reliable measure of consistency between arrays, was lower (0.06 for GDP and 0.10 for RHP). These results indicate greater consistency between arrays hybridized with samples reverse transcribed using GDP rather than RHP.

Then, we examined the consistency between replicate spots on each array (intra-array comparison). To streamline the comparison, genes that were flagged as “bad” and any “matching” replicate spots, were removed across all arrays. Eighty one spots were eliminated which left 9,600 spots, representing 3,200 different genes (genes spotted in triplicate). The comparison of the average signal values (GDP = 1,668 & 1,726, RHP = 1,915 & 1,494), their standard deviations (42 v 298) and the average standard deviation between replicate spots (GDP = 257 & 190, RHP = 296 & 290) essentially confirm a higher intra-array consistency for the GDP over the RHP samples. As a final measure of consistency/variability between arrays, we separated all of the replicate spots and treated them as replicate samples/arrays in order to gauge the trend of consistency across all replicate spots: two replicates (arrays) with triplicate spots for each, yields 6 “theoretical arrays” for each condition (GDP and RHP). The average R^2 value was much higher for GDP (0.83) compared to RHP (0.74), despite similar standard deviations (0.10 for GDP and 0.09 for RHP). These results indicated that GDP replicate spots were more similar to one another than were RHP replicate spots. Altogether, these results indicate that the reverse transcription of *B. melitensis* RNA using GDP generates more specific and sensitive probes than those generated with RHP.

Enrichment and amplification (E&A) RNA methodology is useful for downstream microarray application. Characterization of the transcriptome of intracellular *Brucella* is challenging due to the difficulty in obtaining sufficient quantities of good quality, pathogen RNA that is free of contaminating eukaryotic host RNA for further studies. To address this issue, we developed a 2-step protocol in which *Brucella* RNA is first enriched from a host:pathogen mixed RNA sample, and the remaining RNA is amplified in three steps as described in the Materials and methods. Before applying the E&A protocol to an *in vitro* system of infection, we wanted to evaluate whether bias was introduced and the reproducibility of the protocol. To answer these questions, we spiked 2 different samples of 25 µg of total RNA extracted from HeLa cells culture with 200 ng of *B. melitensis* RNA extracted from a late-log culture (host:pathogen RNA = 125:1). The mixed RNA samples were initially enriched using MICROBEnrich® kit, which decreased the RNA concentration more than 88% (from 25 µg to 2.55 and 3 µg of total RNA). Then, 0.1 volume of the remaining RNA (i.e. 0.25 and 0.3 µg of total RNA) was amplified. One round of amplification yielded more than 80 µg of amplified sense total RNA from each sample (> than 260-fold amplification). Two aliquots of 10 µg from every E&A RNA sample were indirectly labeled and co-hybridized against a *B. melitensis* gDNA on *B. melitensis* microarrays (4 arrays). The degree of bias introduced by the enrichment and amplification was determined by evaluating the performance of the E&A RNA samples against identical labeling and hybridization protocol from non-treated *B. melitensis* RNA (i.e. RNA extracted from a late-log culture).

Prior to all analysis procedures, spots that were flagged as “bad” were removed leaving a total of 3,120 good spots (out of the original 3,227). We employed genomic normalization to improve data quality and to compare multiple samples in a minimum of experiments (219). To compare the consistency of gene expression for each sample type, the signal values for each slide were graphed pairwise and fitted with trend lines. The resulting R^2 values (slopes) represented the level of consistency (similarity) between each slide, which was similar for biological and technical replicates (Table 8). The overall level of consistency for controls was less than for experimental replicates between slides. Also inter-slide variability was higher than intra-slide variability. E&A treatment decreased this variability, which suggests that some level of noise for the *B. melitensis* control slides might have been due to noise interference. We next examined the average signal values for *B. melitensis* control and for E&A mixed RNA. The results revealed higher signals in control samples (987.5 vs. 800.5), but the difference was small and indicates that amplification does not necessary correspond with higher signal.

TABLE 8. Results of pairwise graphical comparisons

Samples	R^2 value	
	Control (Cy5)	Experimental (Cy3)
Slides (inter)		
<i>B. melitensis</i> control	0.49	0.58
HeLa: <i>Bmel</i> E&A	0.52	0.79
Arrays (intra)		
<i>B. melitensis</i> control	0.88	0.86
HeLa: <i>Bmel</i> E&A	0.86	0.97

In order to evaluate the bias introduced by the enrichment and amplification process and the reproducibility of the protocol, we first calculated the correlation (r) between the fluorescence intensity in E&A vs. control samples and then compared the expression profiles of hybridizations of 2 independently amplified RNA samples. Our results show a reasonable correlation ($r = 0.5858$) between the expression profile of the samples E&A against the control sample, and a high degree of correlation between independent replicates ($r = 0.9063$). Altogether, these results suggest that our protocol is highly reproducible with an acceptable level of maintenance of the original information. Considering other reports that underestimate the magnitude of the bias as long as it is highly reproducible (240), our results from preliminary experiments indicate that enrichment of the original RNA sample followed by the biased amplification of pathogen transcripts is sufficient to accurately characterize the transcriptome of intracellular pathogens in an *in vitro* or *in vivo* system of infection.

Another variable we considered was that the enrichment protocol does not remove all of the eukaryotic RNA and the primers (GDP) used for reverse transcription (first step of amplification and labeling) do not exclusively anneal to *Brucella* transcripts. Therefore, there was the possibility that RNA molecules from HeLa cells overlapped with sequences of the *B. melitensis* transcripts, cross-hybridized with probes on *B. melitensis* oligoarrays. To identify the number of falsely detected genes due to contaminating eukaryotic RNA, total RNA isolated from HeLa cells culture was labeled and hybridized on *B. melitensis* microarrays under the same conditions as RNA isolated from *Brucella* cultures. Initially, we observed a reduced amount of cDNA generated (3.8

vs. 9 μ g from 10 μ g of HeLa RNA using GDP or RHP, respectively) which indicate some restriction of annealing of GDP to eukaryotic RNA. After hybridization, only 105 of 3120 genes (3.3%) were consistently detected (raw signal values above 500 for all 6 replicates -triplicate arrays on duplicate slides-) due to contaminating eukaryotic RNA vs. 34% of genes consistently detected when *B. melitensis* RNA was used. This experiment shows that although there is some cross-hybridization between cDNA generated from eukaryotic RNA and the oligonucleotides (oligospots) printed on pathogen arrays, overall, the E&A protocol is consistent and accurate for detecting intracellular *B. melitensis* gene expression in an *in vitro* and *in vivo* system of infection.

The intracellular *B. melitensis* transcriptome indicates a stress response at 4 h post-infection that is reversed at 12 h post-infection. The intracellular *B. melitensis* total RNA was initially enriched and then amplified from total RNA of *B. melitensis*-infected HeLa cells at 4 and 12 h PI. Four biological replicates of experimentally enriched and amplified RNA from every time point were indirectly labeled and co-hybridized against *B. melitensis* gDNA to a custom 3.2K *B. melitensis* oligo-array. As we discovered in our preliminary data, there was a possibility that some HeLa transcripts cross-hybridize with probes on *B. melitensis* microarrays. For that reason, the original total RNA from *B. melitensis*-infected HeLa cells were also co-hybridized against *B. melitensis* gDNA to *B. melitensis* oligo-arrays, and those oligospots with signal were considered non-specific and eliminated from all analysis to avoid false positive gene detection. The intracellular *B. melitensis* gene expression was compared to the gene expression of the inoculum (i.e. *in vitro*-grown cultures of *B. melitensis* at late-log phase

of growth). Based on this criterion, statistical analysis of microarray results revealed that 161 *B. melitensis* genes were detected as differentially expressed (fold-change > 2 and $p < 0.05$) at 4 h PI (Appendix B). The relative changes in gene expression ranged from a 142.5-fold induction of the *narG* gene (BMEII0949) to a 60.9-fold down-regulation (0.01643) of the locus BMEI0299 (hypothetical protein). The vast majority of the differentially expressed genes (126 genes, 78%) were down-regulated. In concordance with our kinetic studies of *B. melitensis* intracellular replication in HeLa cells, where very low bacterial replication was observed in the first 4 h PI, cell division genes *ftsQ* (BMEI0583) and *ftsA* (BMEI0584) were down-regulated as well as genes involved in DNA replication, transcription and translation, transport and intermediate metabolism, and cell envelope, biogenesis and outer membrane activities. Ultrastructural studies in HeLa cells have shown that virulent *Brucella* are located inside the stressful environment of autophagic vesicles at 4 h PI (179), and data from our microarrays agree with this finding. For example, the observed down-regulation of the ribosomal protein genes and RNA polymerase (BMEI0750) are signs of amino acid starvation, consistent with the poor nutritional intravacuole microenvironment found by *Brucella* (132). In addition *ppx* (BMEII0598) which encodes an exopolyphosphatase, the enzyme responsible for hydrolysis of the terminal phosphate of guanosine pentaphosphate (pppGpp) to form guanosine tetraphosphate (ppGpp), a major regulator of bacterial adjustment to stress (130) was significantly upregulated in our microarray data.

The up-regulation of the gene *czcD* (BMEI1438) and the catalytic subunits of the denitrifying reductase genes (BMEII0949, BMEII0974 and BMEII0998) are also

consistent with growth within autophagic vesicles. Host cells deliver divalent cations from the cytosol to the phagosome compartment to kill invaders that are taken up by bacteria through constitutively expressed transporters. CzcD is an integral membrane protein and part of the Co/Zn/Cd efflux system component that reduces the intracellular concentration of toxic heavy metals via active cation efflux to the extracellular media. Conversely, the low oxygen level inside the phagosome, demands the pathogen to adapt from aerobic metabolism to microaerobic or anaerobic metabolism to survive. Analysis of our microarrays found up-regulation of genes encoding the catalytic subunits of enzymes involved in electron transport during nitrate respiration such as *narG* (BMEI0949), *norB* (BMEI0998) and *nosZ* (BMEI0974) that allow *Brucella* to survive under low-oxygen conditions by respiration of nitrate (100). In addition to its role in denitrification, the protein encoded by *norB* reduces nitric oxide (NO) to nitrous oxide (N₂O). This could help decrease the presence of intravacuolar NO, an important host cell defense element in the autophagic vacuole, thereby increasing *Brucella*'s intracellular survival. Also down-regulated at 4 h PI, were *B. melitensis* genes that encoded an iron uptake protein (BMEI0375 and BMEI0844). Iron is an essential cofactor in various biosynthetic and bioenergetic pathways and is also important for bacterial growth. The down-regulation of BMEI0375 and BMEI0844 suggests further confirmation of the slow growth by *Brucella melitensis* during this initial intracellular phase. Curiously, one gene whose expression was enhanced in *Brucella* exposed to stressful situations, *clpX* (BMEI0875) (132), was down-regulated in our analysis. Overall, these results suggest

that after internalization, *B. melitensis* encounters a hostile environment that obliges them to adapt their metabolism to survive.

At 12 h PI, 115 *B. melitensis* genes were detected as differentially expressed (fold-change > 2 and $p < 0.05$) (Appendix C). Like the results at 4 h PI, *narG* (BMEI0949) was the highest expressed gene (103.3) and the most down-regulated gene was *ptsP* (BMEI0190), whose product is involved in the regulation of carbon and nitrogen utilization, with -13.5-fold (0.0739). As opposed to the profile at 4 h PI, at 12 h PI the majority of the differentially expressed genes (86 genes, 75%) were up-regulated. The greatest number of transcriptional changes at 12 h PI occurred in genes whose products are associated with DNA replication, transcription, transport and intermediate metabolism, as well as energy production and conversion. This molecular information combined with the intracellular replication of *B. melitensis* observed in infected HeLa cells, collectively indicate that by 12 h PI the bacteria have adapted to the intracellular environment and are actively replicating. Only 3 transcripts for ribosomal proteins (BMEI0202, BMEI0759 and BMEI0823) had decreased expression at 12 h PI, compared to 17 at the earlier time point. Also at the 12 h PI, no translation factors or tRNA synthetases were observed to be down-regulated which is indicative of translation re-activation.

In our data at 12 h PI, seven transcriptional regulators had enhanced expression in intracellular *Brucella*. Consistent with our data, two of them (BMEI0169 and BMEI0320) were previously identified as necessary for intracellular *Brucella melitensis* survival and replication both *in vivo* and in cell culture models (101). Another regulator

with enhanced expression at 12 h PI was *nikR*. In *Helicobacter pylori*, the product of this gene transcriptionally represses the expression of a nickel transport system, but induces urease expression by binding to the *ureA* promoter (67). In our study, *ureA* (BMEI0649) was highly up-regulated (10.57), therefore it is possible that *nikR* also transcriptionally activates urease expression in *Brucella*. Experimental evidence indicates that urease likely does not play a role in the intracellular survival of *Brucella* (202) but further investigation is warranted.

There were 4 genes differentially expressed with possible involvement in *Brucella* intracellular survival: *acrB*, *motD*, *phoQ*, and *ftsQ*. *acrB* (BMEI1645) encoding acriflavin-resistance protein B and is part of the efflux pumps, which protect the organism from antibiotics and other substances produced by the host, was up-regulated. The up-regulation of this transcript suggests the protein might be important in *Brucella* pathogenesis as it is in *Salmonella* (24). *motD* (BMEI10156) (or *fliK*) encodes a regulator of flagellar hook length in the alpha subgroup of the *Proteobacteria* (64) was up regulated, and its expression is essential for proper formation of bundles of the flagellum filaments. Previous work demonstrated the requirement of flagellum expression for persistence of *Brucella* in the mouse model of infection (84). *phoQ*, which encodes a sensor protein whose participation in *Salmonella* virulence is well established, was also up-regulated, but its regulatory role in *Brucella* virulence factors is unknown. Similar to the observations at the 4 h PI, *ftsQ* transcription was down-regulated; but to a lesser degree than it was in the other time point (-5.63 vs -10.25), possibly due to the intracellular replication of *Brucella*.

One iron transport system gene (*frpB*, BMEII0105) was up-regulated at 12h, consistent with the requirement in *Brucella* for this ion during replication. Also genes encoding transporters of carbohydrates, lipids and amino acids and as well as metabolic genes were up-regulated. Genes encoding for different components of amino acid ABC-transport systems were the most extensively differentially expressed, with 5 being (BMEI1627, BMEI1728, BMEII0070, BMEII0196, BMEII0631) up-regulated and 1 down-regulated (BMEII0038) suggesting either the need for amino acids in protein synthesis during this active growth period or possibly suggesting the use of amino acids as carbon sources. Together, these results indicate a reactivation of *Brucella* gene expression at 12 h PI (replicative period) compared with the earlier adaptation period. Considering the results from the growth kinetic studies with the microarray data, we conclude that there is a down-regulation of the pathogen transcriptome during the adaptation period which is reversed at the later time point, in concordance with *Brucella* intracellular replication.

Analysis of our microarray data also identified the modification of genes encoding a group of 50 proteins with unknown, predicted or moderately known functions at the 4 h PI. Further, 45 transcripts whose encoded proteins have unknown or poorly characterized functions were also differentially expressed 12 h PI compared to the control sample. These novel findings may have implications for *Brucella* virulence or intracellular survival and warrant further study.

***B. melitensis*-infected HeLa cells have a down-regulated expression profile at 4 h transitioning to an activated transcriptional profile at 12 h post-infection.** Four

biological replicates of RNA isolated from *B. melitensis*-infected HeLa cells from every time point were indirectly labeled and co-hybridized against human universal RNA reference to a commercial 10K human array. Gene expression was indirectly compared with RNA isolated from non-infected HeLa cells treated similarly. Due to the low infection rate (1 out of 10 cells or less), classical statistical analysis using commercially available software only detected 26 (13 up- and 13 down-regulated) and 13 (1 up- and 12 down-regulated) genes differentially expressed (fold-change > 1.5 , p value < 0.05) at 4 and 12 h PI, respectively (data not shown). To increase the detection of differentially expressed genes, we applied a more sensitive analysis for host microarray results. Using the Bayesian z-test, 157 (48 up- and 109 down-regulated) and 957 (733 up- and 224 down-regulated) host genes were differentially expressed at 4 and 12 h PI respectively (Appendixes D and E). At 4 h PI, we found that activities like DNA replication and repair, transcription, cell cycle progression/cell proliferation and differentiation, and intermediate metabolism are down-regulated. These findings reflect a scenario similar to the decreased replication and metabolic activity that *Brucella* undergo at this time point and suggests that both host cells and intracellular pathogen undergo a period of adaptation during the early stage of infection. Six genes involved in DNA replication and repair and 17 involved in regulation of transcription were down-regulated and only 2 genes (EWSR1 and PGBP1) related to these functions were up-regulated. According to our microarray data, translation does not seem to be affected after 4 h PI. Only 4 genes from this category were differentially expressed. Conversely, the data indicate that the cell cycle arrests and cell proliferation is diminished as reflected by the 15 genes

involved in these functions that were down-regulated. Additionally 2 negative regulators of cell proliferation (AIM2 and CTBP1) were up-regulated. This transient down-regulation of the cell cycle/cell division and proliferation during *B. melitensis* infection may permit the cell to check and repair internal processes before progressing. Two genes down-regulated from this group are important during pregnancy, the ultimate organ targeted by *Brucella* systemic infection. HPGD is a prostaglandin-inactivating enzyme, and it is down-regulated during term or prematurely delivery, associated with the high expression of prostaglandins (125). Intracellular *Brucella* may utilize prostaglandins for its own benefit, or alternatively and more likely, *Brucella*-induced HPGD down-regulation could be partially responsible for any role of prostaglandins in *Brucella* abortion. The other down-regulated gene encodes PLGF (placental growth factor), which is important for placental permeability and vascularization. *Brucella* abortion is characterized by impaired placental function. *Brucella* prevents delivery of oxygen and nutrients to the fetus and/or removal of waste products from the fetus (66). It is also possible that down-regulation of the PLGF in infected cells contributes to *Brucella*-induced abortion.

Previous investigations found that *Brucella* are able to inhibit programmed cell death on macrophages (96). In our study, it is unclear whether *Brucella* infection induces or inhibits apoptosis in HeLa cells at 4 h PI. Three anti-apoptotic genes (GSTP1, SERINC3 and GADD45) were down-regulated suggesting a pro-apoptotic profile. At the same time, 1 anti-apoptotic gene (PIWIL2) was up-regulated and 4 pro-apoptotic genes (TFPT, CASP8, BCAP31 and RUNX3) were down-regulated making interpretation

difficult. Additionally, SDCCAG3, which positively influences the presentation of Tumor Necrosis Factor (TNF)-receptor on the cell surface and makes the cells more vulnerable to TNF-mediated apoptosis, was up-regulated in infected cells 4 h PI, but TNF was not affected.

Immune and inflammatory responses are key functions for control and elimination of infections. Our studies found that these functions are basically down-regulated in *Brucella*-infected HeLa cells at 4 h PI. Expression of C5, a complement component with multiple functions in inflammatory response, including positive regulation of chemotaxis and part of the membrane attack complex (MAC) perforin system, was down-regulated 2.75 fold. Coincident with that MASP1, which has an important function in the immune response by recognizing the sugar residues on the pathogens surface and activates the classical pathway of the complement cascade (205), were also observed down-regulated. Further, CXCL1, a gene that encodes a chemokine implicated in many cellular functions besides immune response such as cell proliferation, chemotaxis and intracellular signaling, and one defensin gene (DEFB126) encoding an antimicrobial peptide, were down-regulated. These data suggest that the host fails to mount a local or a general defense response against the invading pathogen in the first 4 h PI. Collectively, our microarray results indicate that at four hours post infection, the physiologic and metabolic processes of non-phagocytic cells are disturbed by the presence of the pathogen.

Contrary to events at 4 h PI, infected cells at 12 h PI predominantly had up-regulation of most functions. Our analysis found 957 genes differentially expressed, 733

being up-regulated and 224 down-regulated (Appendix E). Functions, such as DNA replication, mRNA processing, transcription, cell cycle/cell division/cell proliferation, cell adhesion and intermediate metabolism which were down-regulated at 4 h PI, were clearly up-regulated at 12 h PI, indicating that HeLa cells had adapted to the intracellular presence of the *Brucella* and the replication of the pathogen seems not to interfere with their physiological pathways.

Transcription in general was up-regulated in infected cells at this time point. Host microarray data revealed 773 genes (81%) with increased expression as compared to the control cells. However, this transcriptional activation does not seem to correlate with protein expression, since genes whose products are involved in translation (translation initiation factors, tRNA synthetase) and protein biosynthesis (ribosomal proteins) were down-regulated. It has been demonstrated that *Brucella* replicate within the endoplasmic reticulum, therefore it is possible that a down-regulation of host translation is a *Brucella* strategy for replication. Additionally, several host genes related to protein catabolism were up-regulated (GLS, PRSS1, UCHL1, USP15 and 32, and others). A possible interpretation may be that *Brucella* inhibit host translation but increase protein catabolism to provide amino acids for its own benefit.

Cell-cell adhesion (cadherins, contactins) and cell-matrix adhesion (collagen, integrins) were also clearly up-regulated. Thirty-two genes encoding proteins involved in these activities were up-regulated and only 2 genes were down-regulated. This result may be a pathogen effect to prevent epithelium detachment, because *in vivo Brucella* pass through the mucosal epithelium to colonize deeper tissues, causing only minimal

tissue injury. To this end, the up-regulation of 17 cytoskeleton and cytoskeleton organization genes such as MAP1B, NEB, PFN2, VIL1 may be partially responsible for the increased adhesion response.

Similar to our findings at the 4 h PI, it was unclear whether infected HeLa cells undergo apoptosis at 12 h. Seven pro-apoptotic genes were up-regulated (BNIP31, CD38, MDM4, MAGEH1, PRG1, TP53, TP53BP2) and 5 anti-apoptotic genes were down-regulated (BCL2L1, BIRC3, BAG1, CSE1L, TEGT), which could be interpreted as a host defensive mechanism to prevent *Brucella* from establishing an intracellular niche. However, 3 up-regulated strong, apoptosis-inhibition genes (BCL2, BIRC4, DAD1) and 2 down-regulated apoptosis-inductor genes (ANXA1 and CASP1) could also indicate a pathogen counterbalance to avoid being released to the extracellular media. Collectively, our data indicate that under our experimental conditions neither pro- nor anti-apoptotic profile could be clearly associated with *B. melitensis*-infected cells in the first 12 h PI. Microscopic observations from experimental infections disclosed that non-phagocytic cells infected with virulent *Brucella* do not activate their apoptotic program. Instead, extensive bacterial replication generates necrosis and *Brucella* are released to the extracellular media after 48 h PI (8, 53). In addition, our data indicate that infected cells have a higher transcriptional profile for cell division and proliferation than non-infected cells. It is possible that an enhanced rate of division of host cells allows *Brucella* to remain intracellular while the cells divide.

The ability to mount an immune response recovered in the infected host cells at 12 h PI. Three interleukin receptor genes were up-regulated; IL1R1 and IL1F5 are

agonist and antagonist receptors for IL1 family molecules, respectively. IL1R1 is an important mediator involved in cytokine induction of immune and inflammatory responses, while IL1F5 inhibits cytokine production through inhibition of NF-KB activation (164). The other interleukin-receptor gene encodes the interleukin-2 receptor gamma chain (IL-2R gamma), an essential component of high- and intermediate-affinity IL-2 receptors, and also a functional component of the IL-4 receptor which associates with the IL-7 receptor (197). It was reported that *Brucella* lipoproteins induce a cytokine-mediated inflammation through binding of IL2R (90), thus our findings confirm previous observations. Another up-regulated receptor molecule was IRF4, which activates the transcription of several cytokines, such as IL2, IL 4, IL10, IL13 and modulates T cell differentiation (112). Several other genes that encode transcripts for T and B cell activation (CD8B1, CD28, CD86, IRF4, ICOSLG, TNFRSF17) and inflammatory response (C5, CCL16, CMTM7) were also up-regulated. The increased activity of host defenses against the pathogen was also reflected in the up-regulation of genes involved in phagocytosis (AHSG), bacteria cell wall degradation (LYZ) and oxidative burst of neutrophils (NCF1). The up-regulation of complement and the formation of the membrane attack complex were also active as reflected by the up-regulation of the complement components 2 and 5 (C2, C5) and the down-regulation of 2 genes whose products inhibit complement activation (CD46 and CD59). Other immune function related genes that were up-regulated included the antigen processing and presenting class I and II (HLA-A, HLA-B, HLA-DQA1, HLA-DRB1). MHC-I is present in all nucleated cells of the body while MHC-II expression is restricted to the immune

cells. It has been observed in infected macrophages that *Brucella* LPS interferes with MHC-II presentation of peptides to specific CD4⁺ T cells but has no effect on MHC class I antigen presentation (138); but its role in *Brucella*-infected HeLa cells has not been studied. Among the down-regulated genes were 2 pro-inflammatory cytokines (IL8 and IL18) and 4 interferon-induced genes. All these data indicate that host cells recovered immune and inflammatory responses by 12 h PI.

Modified expression of host genes related to the nervous system occurred at 12 h post-*Brucella* infection. Thirty-two genes (5.8% of the genes with known function associated with neural system development (NES, NGFR), neuronal differentiation (CDK5RAP1, NRG3), synaptic transmission (CHRNA2, NPFF) or intracellular trafficking in neural cells (GDI1) were differentially expressed (30 up- and 2 down-regulated). Understanding these data is challenging, but effects on these genes may be related to the neuro-modulation of the immune responses (94, 148). To summarize, the data indicate that at 12 h PI epithelial-like cells had a significantly up-regulated transcriptional profile and the intracellular presence of *Brucella melitensis* does not seem to interfere with normal physiologic and metabolic processes.

Validation of microarray gene expression results. To confirm the microarray results, we randomly chose 10 *B. melitensis* and 10 infected HeLa cells differentially expressed genes (5 from each time point) and conducted qRT-PCR. Validation of *B. melitensis* microarray gene expression results was done using cDNA reverse transcribed from the same enriched and amplified RNA samples used for microarray hybridization. The quantity of cDNA for each target gene was normalized to the quantity of gyrase A

(*gyrA*, BMEI0884) cDNA in each sample. *gyrA* was determined to be a stable expressed housekeeping gene in our microarray experiments and also in other bacteria (23). Quantitative Real-time PCR results confirmed 90% of the *Brucella* genes tested to be greater than 2.0-fold up- or down-regulated and in the same direction as was determined by microarray analysis (Fig. 12A and B) and that the 100% of the host genes tested were altered in the same direction as determined by microarray analysis (Fig. 12C and D). The only gene that was not validated by qRT-PCR was BMEI0346 (Transcriptional regulator protein, AsnC family). No significant difference in the expression level was observed using 2 different sets of primers, indicating possible false positive detection by microarray analysis or suboptimal qRT-PCR conditions for this particular gene as well.

Dynamic Bayesian modeling analysis of microarray data reveals host and pathogen biosignature mechanistic candidate genes. Mathematical modeling has great potential for discovering and understanding disease mechanisms and biological processes. A dynamic Bayesian modeling analysis was conducted to identify host and *Brucella* pathways, pathways subnets and candidate genes important for *B. melitensis* infection. The analysis identified 19 and 16 highly activated gene ontology (GO) biological processes (downloaded from TIGR Comprehensive Microbial Resources; <http://cmr.tigr.org/CMR/Downloads>) comprising 298 and 160 distinct mechanistic genes at 4 and 12 h PI, respectively in *Brucella*, and 69 and 77 highly activated biological process (downloaded from Gene Ontology Consortium Database; <http://www.geneontology.org>) with 49 and 50 distinct mechanistic genes at 4 and 12 h PI in HeLa cells (data not shown). Using the same bioinformatic platform, 15 and 13 top

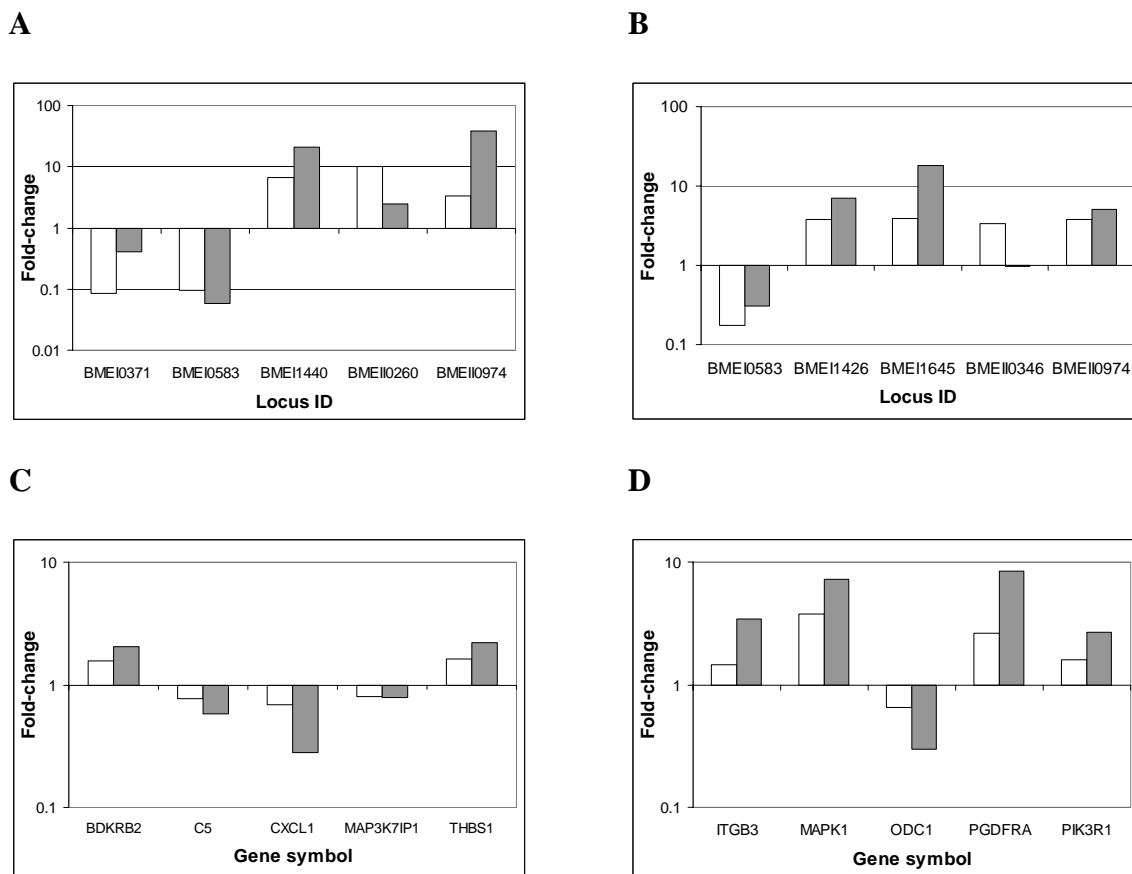


FIG. 12. Validation of *Brucella melitensis* and host microarray results by quantitative Real-time PCR. cDNA was synthesized from the same RNA samples used for microarray hybridization. Ten randomly selected ORFs differentially expressed as detected by microarrays in intracellular *B. melitensis* and in *B. melitensis*-infected HeLa cells at 4 and 12 h PI compared with the inoculum and control cells respectively, were validated by quantitative RT-PCR. Five of 5 *B. melitensis* ORFs (100%) tested at 4 h PI (**A**) and 4 of 5 ORFs (80%) tested at 12 h PI (**B**) had fold-change greater than 2-fold and in the same direction by both methodologies. Ten of 10 HeLa genes tested at 4 (**C**) and 12 (**D**) h PI had fold-change altered in the same direction by microarray and qRT-PCR. Open bars, microarray fold-change; dark gray bars, qRT-PCR fold-change.

scored pathways subnet from the 111 and 171 pathways associated with gene probes on the *B. melitensis* and human microarrays respectively, were selected and analyzed and the modeling disclosed mechanistic genes for each pathway determined. On the pathogen side (Table 9), pathways already known to be implicated in *Brucella* virulence, like flagellar assembly, LPS biosynthesis or T4SS, together with to-date-unknown pathways for virulence such as valine, leucine and isoleucine degradation or polyketide sugar unit biosynthesis pathways were scored on the top 15 list and predicted to have some implication in *Brucella* virulence. Interestingly, the top 15 pathways scored were similar at 4 and 12 h PI, and a high proportion of the genes (56%) was important for *Brucella* pathogenesis at both time points. In concordance with *Brucella* signaling pathways, the software not only predicted known host pathways involved in infectious disease response, like Toll-like receptor or cytokine-cytokine interaction signaling pathways but also others unknown such as axon guidance or GnRH signaling pathways (Table 10). The top 13 scored host pathways had broader temporal and integral differences than in the pathogen pathway analysis. For instance, 9 of 13 pathways overlap over time and only MAPK1 was predicted to be mechanistic at 4 h and 12 h PI. Another difference of the *Brucella* signaling pathways analysis was that some genes were predicted to be key regulators in different pathways at the same time point. For instance, MAPK1 had up in 6 of the top 12 pathways analyzed at 12 h PI. Overall, study of signaling pathways using dynamic Bayesian modeling analysis not only predicted some known host and pathogen pathways involved in *Brucella* virulence but also

TABLE 9. Top scored *B. melitensis* pathways subnet analyzed and discovered candidate mechanistic genes from modeling at 4 and 12 h PI

Pathway	Source	Mechanistic genes	
		4 h	12 h
ABC transporters	bme 02010	Ribosa ABC transporter (<i>rbsA</i> , <i>rbsB</i> , <i>rbsC</i>) and Oligopeptide ABC transporter (<i>oppA</i> , <i>oppB</i> , <i>oppC</i> , <i>oppD</i> , <i>oppF</i>)	Oligopeptide ABC transporter (<i>oppB</i> , <i>oppC</i> , <i>oppF</i>) and Branched-chain amino acid ABC transporter (<i>livF</i> , <i>livH</i> , <i>livM</i>)
Aminoacyl-tRNA biosynthesis	bme 00970	BMEI0987	BMEI0987
Fatty acid metabolism	bme 00071	BMEI1746, BMEI1747, BMEI10124	BMEI1746, BMEI10141
Flagellar assembly	bme 02040	BMEI0324, BMEI10150, BMEI10151, BMEI10159, BMEI10160, BMEI10161, BMEI10165, BMEI10166, BMEI10167, BMEI1087, BMEI1109	BMEI0324, BMEI10151, BMEI10160, BMEI10166, BMEI1087, BMEI1109, BMEI0145, BMEI0854, BMEI0856, BMEI0857, BMEI0925, BMEI1746, BMEI1747, BMEI10060, BMEI10141, BMEI10242, BMEI10744, BMEI10745
Glycolysis/ Gluconeogenesis	bme 00010	BMEI1746, BMEI10241, BMEI10608	BMEI1747, BMEI10060, BMEI10141, BMEI10242, BMEI10744, BMEI10745
Lipopolysaccharide biosynthesis	bme 00540	BMEI0831, BMEI0833, BMEI0835, BMEI1115, BMEI1904, BMEI1028	BMEI0831, BMEI1115, BMEI1904, BMEI1028, BMEI1029
Novobiocin biosynthesis	bme 00401	BMEI1308, BMEI1309	BMEI1308, BMEI1309
Oxidative phosphorylation	bme 00190	BMEI0076, BMEI0248, BMEI0250, BMEI0251, BMEI1185, BMEI1205, BMEI1543, BMEI1544, BMEI1546	BMEI0076, BMEI0248, BMEI0250, BMEI0251, BMEI1185, BMEI1544, BMEI1546
Polyketide sugar unit biosynthesis	bme 00523	BMEI10830, BMEI10836	BMEI0440, BMEI10830, BMEI10836
Protein export	bme 03060	BMEI0121, BMEI0680, BMEI0743, BMEI0777, BMEI1076, BMEI1077, BMEI2055	BMEI0680, BMEI0743, BMEI0777, BMEI1076, BMEI1077, BMEI2055
Purine metabolism	bme 00230	BMEI0647, BMEI0649, BMEI1430	BMEI0649, BMEI1430, BMEI1653
Two-component system	bme 02020	BMEI0865, BMEI0866, BMEI0978, BMEI0979, BMEI1804, BMEI10523, BMEI10554, BMEI10971	BMEI0866, BMEI0979, BMEI1582, BMEI1804, BMEI10523, BMEI10554
Type IV secretion system	bme 03080	BMEI10026, BMEI10027, BMEI10028, BMEI10030, BMEI10033, BMEI10034	BMEI10027, BMEI10028, BMEI10030, BMEI10033
Tyrosine metabolism	bme 00350	BMEI1125	BMEI1125, BMEI1882
Valine, leucine and isoleucine degradation	bme 00280	BMEI0125, BMEI0158, BMEI0203, BMEI0204, BMEI0426, BMEI0456, BMEI0466, BMEI0736, BMEI1067, BMEI1858, BMEI1919, BMEI1924, BMEI1927, BMEI1928, BMEI1945, BMEI1945, BMEI1945, BMEI10613, BMEI10748, BMEI1021, BMEI1101	BMEI0125, BMEI0158, BMEI0203, BMEI0204, BMEI0426, BMEI0736, BMEI1919, BMEI1927, BMEI1928, BMEI1945, BMEI10002, BMEI10061, BMEI10497, BMEI10613, BMEI1101

TABLE 10. Top scored host pathways subnet analyzed and discovered candidate mechanistic genes from modeling at 4 and 12 h PI

Pathway	Source	Mechanistic	
		4 h	12 h
Calcium signaling pathway	hsa04020	PRKACB	CD38, PDGFRA
Complement and coagulation cascade	hsa04610	MASP1, C5	FGA, F3, F7, SERPINA5
Cytokine-cytokine receptor interaction	hsa04060	IL1R1, CXCL1	
EMC-receptor interaction	hsa04512	LAMC1, THBS1	ITGB3, ITGB5, SPP1
GnRH signaling pathway	hsa04912	PRKACB	MAPK1
Insulin signaling pathway	hsa04910	PHKB	MAPK1
MAPK signaling pathway	hsa04010	MAP3K7IP1, NR4A1, JUND, MAPK1, MAPK8, MAPK11	STMN1, MAPK1
Regulation of actin cytoskeleton	hsa04810	BDKRB2	FGF7, PDGFRA, MAPK1, PIK3CG
Toll-like receptor signaling pathway	hsa04620	MAP3K7IP1	PIK3CG, PIK3R1, CD86
Urea cycle and metabolism of urea groups	hsa00220	GTP	ODC1
Axon guidance	hsa04360		MAPK1
T-cells receptor signaling	hsa04660		PIK3CG, PIK3R1
VEGF signaling pathway	hsa04370		MAPK1

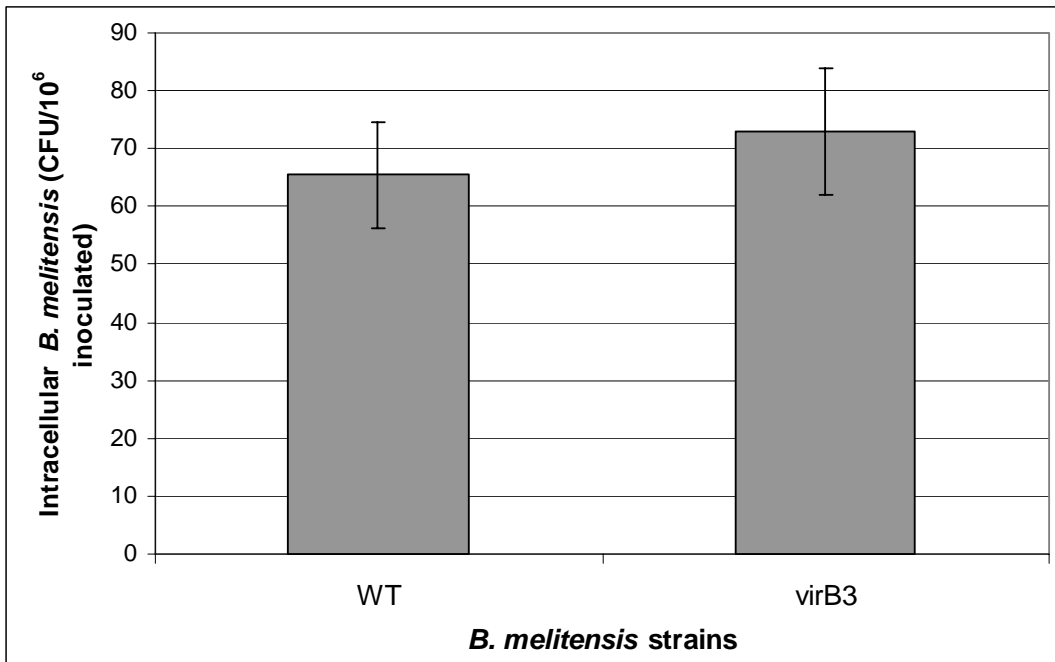
Pathways description was based on KEGG (<http://www.genome.jp/kegg/pathway>)

identified other possible underlying pathways whose involvement in *Brucella* infection will require further elucidation.

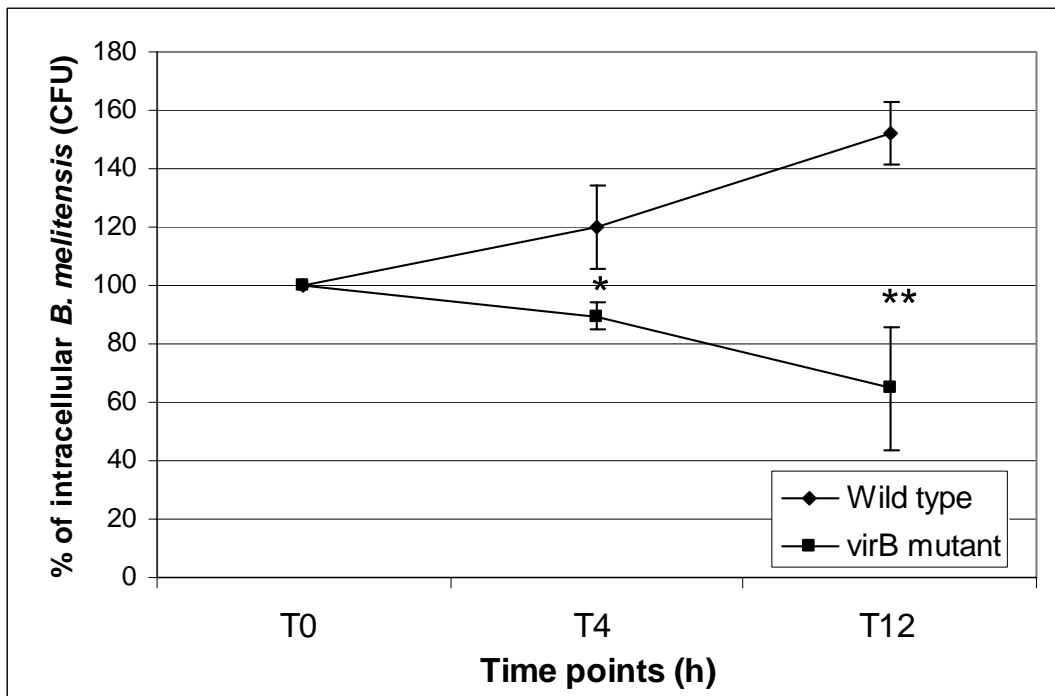
***virB* operon influences *Brucella* intracellular survival and replication but not invasion of HeLa cells in the first 12 h post-infection.** One of the pathways predicted *in silico* as mechanistic for *Brucella* intracellular survival is the type 4 secretion system (T4SS) (Table 9). *Brucella* strains mutated in the *virB* operon (which encodes a T4SS) were previously reported to be attenuated for virulence in cell culture and in the mouse model of infection (169, 213). However, the importance of *virB* in *B. melitensis* survival and replication in non-professional phagocytic cells during the first 12 h PI has not been studied. To evaluate the role of *virB*, we selected a *B. melitensis* transposon-interrupted in *virB3* homolog locus (BMEII0027) from our *B. melitensis* mutant bank and its phenotype was compared in parallel with the isogenic *B. melitensis* WT treated equally. First, we analyzed the influence of *virB* in the internalization of *B. melitensis* in HeLa cells. There were no differences ($p > 0.05$) in the number of internalized *B. melitensis* WT or mutant (Fig. 13A), indicating that *virB* is not required for *B. melitensis* invasion in non-professional phagocytic cells. However at 4 and 12 h PI, the number of intracellular *virB* mutants recovered was significantly lower ($p < 0.05$) than the number of WT recovered (Fig. 13B), indicating that *virB* operon is important for intracellular survival and replication of *B. melitensis* in HeLa cells during the first 12 h PI. The CFU of *B. melitensis* WT and mutant in growth control wells increased at a similar rate (almost 1 log at 12 h) compared with the original inoculum (data not shown). These findings indicate that loss of *virB* was responsible for the intracellular growth repression

FIG. 13. Invasion phenotype and intracellular survival and replication of *B. melitensis virB3* mutant in HeLa cells. HeLa cells were infected with *B. melitensis virB3* mariner transposon *Himar1*-interrupted at MOI 1,000:1 as explained in Materials and methods. The invasive phenotype and the intracellular viable number of bacteria were determined at 0, 4 and 12 h PI. Results were compared with HeLa cell cultures infected with *B. melitensis* WT in parallel. **(A)** The invasive phenotype of the *virB* mutant was similar than the WT ($p > 0.05$). Results are presented as the number of CFU from internalized bacteria per every 10^6 bacteria inoculated. **(B)** The intracellular viable number of *B. melitensis virB* mutant was significantly lower than the WT at 4 ($* = p < 0.05$) and 12 h ($** = p < 0.01$) post-infection. *Brucella* CFU at 4 and 12 h PI are presented as a percentage (%) of internalized bacteria. Data presented are the mean + SD (error bars) of 4 independent experiments done in triplicate and statistical significance of differences was determined using Student's *t* test ($p < 0.05$ was considered significant).

A



B



in the mutant strain but was not required for extracellular growth. These results are in consistent with the prediction from our mathematic modeling, and indicate that under these experimental conditions *virB* operon is essential for intracellular survival and replication, but not invasion, of *B. melitensis* in HeLa cells in the first 12 h PI.

Host MAPK1 is important for intracellular survival of *B. melitensis* in HeLa cells. Mitogen-activated protein kinase 1 (MAPK1 or ERK 1/2) controls many biological functions (124). Statistical analysis of our microarray experiments (also confirmed by qRT-PCR) revealed that MAPK1 was up-regulated at 4 and 12 h PI (Appendixes D and E). Further computational analysis predicted that this gene is important in *Brucella* pathogenesis (Table 10). However, the computational prediction does not indicate if the expression of MAPK1 favors or inhibits pathogen infection. To experimentally test the role of MAPK1 in *B. melitensis* pathogenesis in our non-professional phagocytic cell model, HeLa cells were independently transfected with either of 2 different MAPK1-validated siRNA molecules and 48 h later were infected with *B. melitensis* WT. The expression of MAPK1 measured by qRT-PCR in cell cultures transfected with either molecule of MAPK1-validated siRNA was knocked down more than 90% compared with the expression of the gene in non-transfected cells or cells transfected with negative and positive control siRNA molecules (siRNA molecules with no homology on eukaryotic genome, and GAPDH, respectively) (data not shown). The phenotype of *B. melitensis*-infected MAPK1-siRNA transfected HeLa cells was compared with the phenotype of *B. melitensis*-infected HeLa cells non-transfected and transfected with negative control siRNA (Fig. 14). HeLa cells transfected with a negative control of

siRNA molecules were more permissive to *Brucella* invasion than the other cell cultures but there was no effect on the intracellular *B. melitensis* survival and replication. The viable number of *Brucella* recovered at T0 in HeLa cells transfected with MAPK1 (ID 1449) - validated siRNA was only 40% of that recovered from non-transfected HeLa cells (control) ($p < 0.01$). Additionally, the intracellular replication of *Brucella* at 4 h PI was repressed in HeLa cell cultures transfected with siRNA-MAPK1 (ID 1449). To verify that MAPK1 was involved in *Brucella* invasion and intracellular replication after 4 h PI, we evaluated a second MAPK1 (ID 1544)-validated siRNA molecule in parallel under the same experimental conditions. In this case the number of invasive organisms was similar to that from the non-transfected cells ($p > 0.05$), but the CFU of *B. melitensis* recovered at 12 h PI was lower than that recovered at 4 h. These results do not fully define the role of MAPK1 in *Brucella* invasion process, but in accord with our predictive algorithm, indicate its importance in *Brucella* survival in non-professional phagocytic cells after 4 h PI.

DISCUSSION

Prior to this study, the *Brucella* and the host temporal transcriptomes during early interaction were unknown. Here, using cDNA microarray technology, we analyzed in parallel the transcriptional profile of both host and *Brucella* at 4 and 12 h PI.

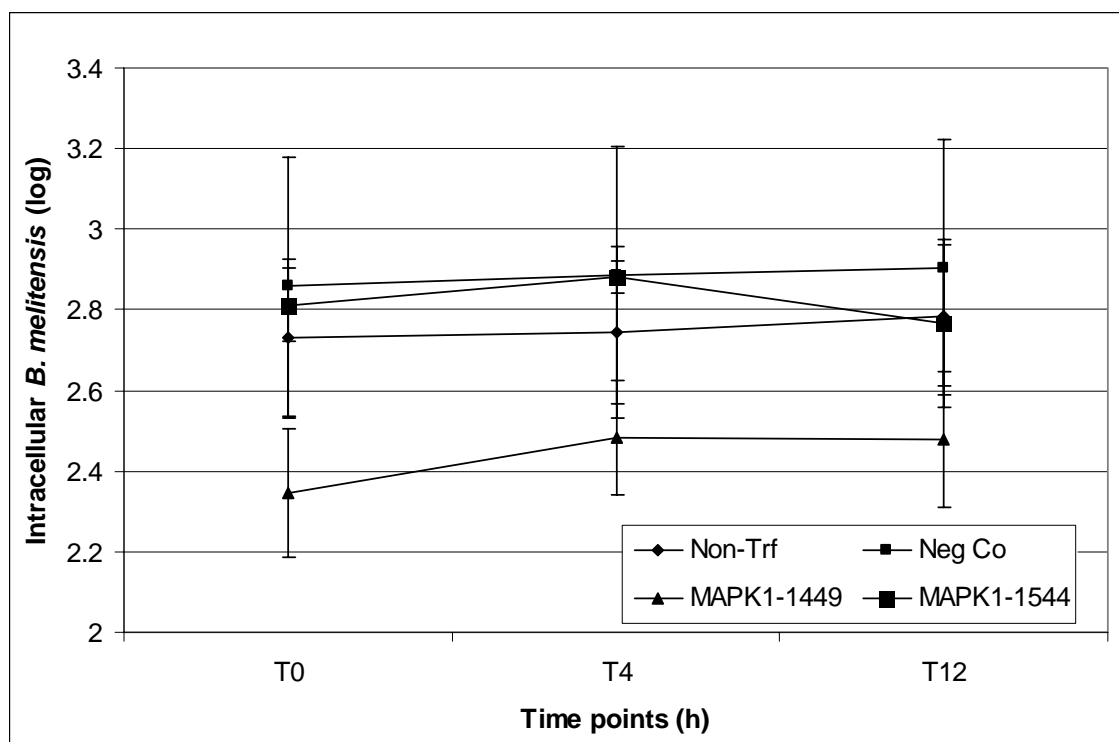


FIG. 14. Phenotype of *B. melitensis*-infected HeLa cells transfected with MAPK1-validated siRNA molecules. HeLa cells were independently transfected with 2 different MAPK1-validated siRNA molecules (1449 –triangles- & 1554 – big squares-) and 48 h later infected with *B. melitensis* WT cultures. Non-transfected (diamonds) and cell cultures transfected with siRNA-negative control (small squares) were used as controls of infection. The expression of MAPK1 measure by qRT-PCR was knocked-down more than 90% in cells transfected with both MAPK1-siRNA molecules. Cell cultures were infected and treated as explained in Materials and methods. The results suggest the importance of MAPK1 in *Brucella* intracellular survival in non-professional phagocytic cells after 4 h post-infection. Data are presented as logarithmic scale and results are the mean + SD (error bars) of 5 independent experiments done in duplicate.

Based on our initial experiments, which revealed that late-log cultures of *B. melitensis* grown in cell culture media are more invasive to HeLa cells than early-log or stationary cultures (see Chapter II), we infected HeLa cells with cultures at the optimal phase of growth and analyzed their intracellular kinetics. Our results demonstrate that *B. melitensis* survive, but are unable to replicate in the first 4 h PI (adaptive period). Following this initial period, *Brucella* begin to replicate intracellularly (replicative period). The initial lag period is due to a host:agent interaction and not a bacteria growth deficiency since the bacteria cultures continued growing in a control wells. We interpret this initial “non-replicative” period as the time necessary for the pathogen to adapt from the extracellular life style to the intracellular environment. Previous studies found different kinetics of *Brucella* cultures in non-professional phagocytic cells in the first 12 h PI. For instance, Detilleux *et al.* (1990a) reported intracellular replication of *B. abortus* cultures in the first 8 h PI, followed by a decreasing number of viable intracellular brucellae. Pizarro-Cerdá *et al.* (1998a) and Delrue *et al.* (2001) observed that the *B. abortus* and *B. melitensis* lag period was two times longer than we report here. However O’Callaghan *et al.* (1999) and Sieira *et al.* (2000) reported a similar intracellular kinetic profile of *B. suis* and *B. abortus* in HeLa cells as in our study. It is possible that the differences in the length of the adaptive period were based on the cultures (growth phase, media), cell types (HeLa or Vero cells) or the infection conditions used (initial time of *Brucella*:host cell interaction).

To understand the molecular behavior of the host and pathogen during their first 12 h PI, we studied their transcriptional profile at the adaptation (4 h PI) and at the

replicative phases (12 h PI). Modern technology has made the gene expression detection from mammalian systems straightforward and robust. However, the study of transcriptional profile of intracellular bacteria is challenging due to the difficulty of obtaining adequate high quality pathogen RNA free of eukaryotic-RNA for downstream applications. In order to address this problem, we initially demonstrated the usefulness of *BmGDP* for generating sensitive and specific probes of *B. melitensis* transcripts from an *in vitro* culture for gene expression profile studies using DNA microarray analysis. We also generated *BmGDP* probes from RNA isolated from non-infected HeLa cells (although in less amount than with random primers), and some cross-hybridization along with false positive detection was observed when those probes were hybridized on *B. melitensis* microarrays. These results indicate that the *BmGDP* primers set do not specifically anneal only to *B. melitensis* transcripts nor does hybridization to the *Brucella* arrays select against all eukaryotic transcripts. To reduce the interference of the host RNA from the heterogeneous population of RNA, we used a commercial kit (*MICROBEnrich*) to significantly reduce the eukaryotic RNA and enrich the *Brucella* RNA. However, some mammalian RNA was still present in the samples after treatment, which could interfere with pathogen gene expression detection. In addition, the enrichment procedure does not address the challenge of a small amount of *Brucella* RNA present in the initial material (*B. melitensis*-infected cells or tissues), which is about 1:1,000 or less (i.e. 10 ng in 10 µg of total RNA). This low level of pathogen RNA was insufficient for microarray studies. To increase the *Brucella* RNA concentration and simultaneously equilibrate the host:pathogen RNA ratio, we applied a linear

amplification of sense-stranded RNA protocol biased to pathogen transcripts in the previously enriched RNA sample. We then evaluated the reproducibility of the methodology by measuring the correlation between the gene expression detected in an original sample (non-enriched non-amplified *B. melitensis* RNA) vs. an E&A host:pathogen mixed RNA sample (i.e. *B. melitensis* RNA spiked with HeLa RNA 1:125). Bearing in mind that the presence of contaminant eukaryotic RNA and the extra handling of the samples could introduce some degree of bias into the population of treated RNA (153), the analysis of our results yielded an acceptable correlation ($r = 0.58589$) between these 2 samples with high reproducibility of the technique (correlation between independent replicates = 0.9063). Correlation studies of pathogen gene expression from treated mix host:pathogen RNA sample with the original pathogen RNA sample as we present here, have not been previously reported. Studies focused on validation of methodology for RNA amplification in the sense orientation have shown correlation between “pure” samples before and after amplification. Making the same comparison (i.e. unamplified vs. amplified *B. melitensis* RNA), our study yielded a higher correlation level compared to other studies ($r = 0.81398$ vs. 0.77, Lawson & Johnston, 2006, or 0.8009, Marko *et al.*, 2005). Amplification of the mixed RNA samples without previous enrichment did not work well in our hands (the lowest correlation compare against the original *B. melitensis* RNA sample, $r = 0.38296$). These results differ from other studies that have found a more complete bacteria global expression profile applying a direct amplification on the host:pathogen mixed sample (142). A possible explanation may be that in their study the number of bacteria, and the

bacterial RNA, was much higher than in our experiment and as a consequence, the bacterial:host RNA ratio was lower, with less contaminant eukaryotic RNA. Given that the *B. melitensis*:eukaryotic RNA ratio from *in vitro* or *in vivo*-infected samples is at least 10 times lower than in our simulated system and the possibility that eukaryotic RNA may interfere with pathogen gene expression detection, our strategy was to hybridize in parallel with the E&A sample, the original (untreated) infected sample on the *Brucella* oligoarray and disregard from future analysis all those spots that produced a signal in the untreated sample. The concept for using the original RNA samples as a control for cross-hybridization as opposed to non-infected HeLa cells, was based upon the evidence that the transcriptional profile of the infected host cells changes due to infection and would have different levels of cross-hybridization. This novel alternative, which has not been reported in previous studies that have evaluated the *in vivo* or *in vitro* transcriptional profile of intracellular bacteria (37, 139, 221, 226), decreases the sensitivity but increases the specificity of the system (i.e. some true positive expressed pathogen genes might be disregarded from the analysis but detected genes will be unambiguously pathogen genes).

A general overview from the combined analysis of the results from the host and pathogen transcriptional profiles indicate that both non-phagocytic cells and *Brucella* undergo an adaptation period during the first 4 h PI but is overcome by 12 h PI permitting *Brucella* to replicate intracellularly while minimally effecting on host physiological processes. Our studies identify down-regulation in all of the functional groups analyzed in *B. melitensis* at 4 h PI, similar to that observed in HeLa cells at the

same time point. It is difficult to say if these transcriptional modifications occurred as a consequence of the interaction (i.e. pathogen on the host or vice versa), or if they are self regulated. It has been clearly demonstrated that bacteria can modify host responses (75, 163, 210), but the opposite effect has not received the same attention. There are well defined examples of how *Brucella* influences the host response (19, 29, 79, 96, 166, 198, 217), but all of these studies focused on phagocytic cells. In non-phagocytic cells, *Brucella* escapes from the endocytic pathway, exploits the autophagic machinery of the host cell and transits to the endoplasmic reticulum where multiplication occurs (179). *Brucella* itself is responsible for modifying intracellular trafficking, since attenuated strains follow a different pathway. A type IV secretion system, encoded by the *virB* operon, is essential for *Brucella*'s modification of intracellular trafficking in HeLa cells (39). The *virB* promoter is induced intracellularly in macrophages after internalization and reaches peak expression at 5 h PI (22, 212). In our study, the microarray technique was not able to identify *virB* differentially expressed in intracellular *Brucella*. One possibility could be that the *virB* expression inside non-phagocytic cells follows a different kinetic than in macrophages. Another potential reason may be that in our initial study of *B. melitensis* gene expression in culture media (see Chapter II), we detected some of the *virB* genes (*B1*, *B3*, *B10*) up-regulated at late-log phase of growth. In this study, intracellular gene expression was compared with the inoculum (i.e., *B. melitensis* culture at late-log phase). Our results reflect only genes at least 2 fold differentially expressed as compare with the control, therefore it is possible that the changes in the *virB* operon are present but do not meet the 2-fold cut-off criterion. Independently, the

T4SS was identified in further computational analysis, and confirmed later in the *in vitro* model of infection, as a key pathway for *B. melitensis* survival and replication in HeLa cells in the first 12 h PI. Similar observations were reported for *B. abortus* (213) and *B. suis* (169). Our computational prediction found that some but not all of the *virB* genes are mechanistic for survival and replication in the first 12 h PI (Table 9). *virB* genes are organized in one operon that is transcribed as a polycistronic mRNA (22, 213). Due to the size of the transposon used to create the mutant (~1.3 kb), it likely has a polar effect on downstream genes. To further characterize the role of every *virB* gene in the initial steps of the infection, we are in the process of making non-polar mutants for individual *virB* genes that will be later tested under the same experimental conditions.

Impairment of phago-lysosome fusion is a major mechanism that allows intracellular survival of *Brucella*. It has been shown that *Brucella* lipopolysaccharide (LPS) – O side chain is involved in the prevention of phago-lysosome fusion in the first few hours following phagocytosis, resulting in the rapid acidification to the *Brucella*-containing vacuole and the expression of true virulence genes such as the *virB* operon (183, 184). However, virtually nothing is known about specific molecules and targets involved in *Brucella* phago-lysosomal membrane fusion inhibition. Our study provides an initial effort to further characterize the differentially expressed genes, particularly hypothetical proteins, in the early phase of infection to enhance our understanding of the molecular actions that impair phago-lysosomal fusion.

In the past, only one study has been published describing *Brucella* genes expressed intracellularly (68). Using a differential fluorescence induction approach, the

authors identified 34 ORFs differentially activated within macrophages at 4 h PI. From these 34 ORF only 9 were identified based on similarity with other bacterial sequences in GenBank. In agreement with our results, the *Brucella* genes identified were involved in adaptation to intracellular environmental conditions. Together, these two studies reflect that even in 2 different cell types, *Brucella* undergo adaptation in the first 4 h PI.

Two studies using microarray technology have been published describing host response to *Brucella* infection (69, 104). There were 148 genes differentially transcribed in a murine macrophage cell line infected with *B. abortus* at 4 h PI (69). In general, genes associated with immune and inflammatory response were up-regulated, genes involved in cell cycle/cell division/proliferation and differentiation, and intracellular trafficking were down-regulated while genes involved in apoptosis were equally distributed. These data are consistent with our microarray results, except for the pattern of expression of genes involved in immune response. This difference could be related to the fact that macrophages are cells directly involved in the immune response while HeLa cells are not. In the other study (104), the authors evaluated the transcriptional profile of *B. melitensis*-infected murine macrophages at 4, 24 and 48 h PI, and they found that the most significant transcriptional changes happen early after infection (4 h) and return to normal in later time points (between 24 and 48 h). Even when the number of transcripts significantly differentially expressed was much higher than in our study (1,296 genes), the majority of them (81%) were down-regulated at the 4 h PI. Also consistent with our results, general cellular activities such as cell growth and maintenance, intermediate metabolism and biological process regulation were substantially suppressed. However,

He *et al.* (2006) found that immune response was up-regulated and apoptosis was clearly down-regulated. This anti-apoptotic profile observed in infected macrophages was different from our results. We were not able to differentiate whether there was a pro- or anti-apoptotic profile in *B. melitensis*-infected HeLa cells at 4 h PI. This could be due to the fact that macrophages are the primary resident cells for *Brucella* in natural infections, while epithelium is not colonized *in vivo*.

A different scenario was observed at 12 h PI where both host and pathogen transcriptional profiles were clearly up-regulated. Our interpretation of these data is that *Brucella* finish the initial adaptation period as indicated by the phagosomal membrane modification, and then *Brucella* begin replicating virtually without interfering with the host physiological metabolism. Among the major transcriptional changes observed in infected cells as compared to the non-infected ones was the up-regulation of cell-cell and cell-matrix adhesion. The up-regulation of genes involved in cell-cell contact by *Brucella* was previously reported (98), but its interpretation is unclear. *In vivo*, *Brucella* pass throughout the mucosal epithelium to colonize deeper tissues with only minimal tissue injury, therefore we hypothesize that the up-regulation of cell-cell adhesion could be a pathogen effort to avoid epithelium detachment that would prevent establishment of the infection.

During the last stage of *in vitro* infection in non-phagocytic cells, virulent *Brucella* is delivered to the perinuclear endoplasmic reticulum where actual bacterial multiplication occurs (179). This has been interpreted as an opportunity for *Brucella* to take advantage of the metabolites synthesized or translocated to this compartment to

supply their nutritional requirements for growth. For instance, *Legionella pneumophila*, another intracellular pathogen that impairs phago-lysosomal fusion and replicates inside macrophages similar to *Brucella*, scavenges host proteins and amino acids for nutrients (23). It has been demonstrated that *de novo* host protein synthesis is not required during intracellular *Brucella* replication (52). Our microarray data suggest that host cell protein biosynthesis process was down-regulated in infected cells 12 h PI, but the transcription of genes involved in translational processes in the pathogen is re-activated compared with 4 h PI. These results provide evidence to hypothesize that *Brucella* may inhibit, by an unknown mechanism, the host translational process to enhance amino acid availability for synthesizing their own proteins, or possibly to utilize the amino acids as a carbon source.

The influence of the epithelium in the initiation of the immune response in *Brucella* infection has been inadequately studied. *Salmonella typhimurium* is known to stimulate the Toll-like receptor signaling pathway in intestinal epithelial cells resulting in IL8 secretion and a massive neutrophil influx in the intestinal lumen (107). *Legionella pneumophila* was also reported to be able to induce secretion of several cytokines from the lung epithelium after infection that contributes to the immune response in legionellosis (206). This study found several immune-related transcripts up-regulated in *B. melitensis*-infected cells compared with control cells such as interleukin receptors, transcriptional activators of cytokines and activators of B and T cells. *Brucella* do not generate an acute inflammatory response after invasion *in vivo* (1). The down-regulation of 2 potent pro-inflammatory cytokines transcripts (IL8 and IL18) seems to reaffirm this

idea, but there were also two potent chemoattractants (C5 and CXCL16) up-regulated that would suggest the opposite effect. The up-regulation of immune-stimulatory transcripts like IFN γ together with CD28 and CD86 antigen molecules would further suggest that *Brucella*-infected epithelium-like cells initially induce a Th-2 immune response. Additionally, the up-regulation of other transcripts indicates cellular and humoral immune response activation (ICOSLG, CD8B1, CTLA4, CD24, TNFRSF17). This is the first time that transcripts involved in immune and inflammatory response generated from *Brucella*-infected non-phagocytic cells are reported. These data suggest some participation of the epithelium in the onset of immune response in brucellosis which will need to be further addressed. On the pathogen side, only one functional annotated gene (*acrB*) and some uncharacterized transport systems with possible implication in *Brucella* protection from deleterious host and environmental factor effects were observed to be up-regulated at 12 h PI. The role of these up-regulated defense-encoded genes in *Brucella* intracellular survival and how they interact with the host counterpart also deserve to be more carefully studied.

MAPK1 was among many transcripts involved in signaling pathways up-regulated in infected HeLa cells at 12 h PI. The MAPK signaling cascade, represented by 3 well characterized subfamilies of MAPKs (ERK1/2, JNK and p38), has been implicated in bacterial internalization (223) and intracellular survival and replication (107, 173, 207). Jimenez-Bagues *et al.* (2005) demonstrated the importance that the integrity of the MEK - MAPK - ERK 1/2 pathway has on the elimination of rough *B. suis* in macrophages (121). To identify the importance of this MAPK signaling pathway

in *B. melitensis* invasion and intracellular survival in HeLa cells, we used 2 different siRNA molecules to knock-down MAPK1 expression. Our results confirmed that the internalization of *Brucella* decreased more than 60% when the gene was knocked-down with one siRNA molecule (ID1449), but not with the other siRNA molecule (ID1544). The difference observed cannot be attributed to the MAPK1 gene expression, because qRT-PCR showed that the gene was more than 90% down-regulated compared with non-transfected cells. Interestingly, negative control transfected cells had higher numbers of internalized bacteria than the control, an effect that can be attributed to the transfecting reagent. Therefore, if the transfecting reagent's effect on the internalization process were subtracted, the number of invasive bacteria would be lower in both MAPK1 siRNA-transfected cells. Previous studies have reported that pretreatment of HeLa cells with PD098059, a ERK1/2 pathway inhibitor, resulted in a 50% decrease in *Brucella* internalization (98). In the same study the participation of GTPases of the Rho/Rac/Cdc42 subfamily in *B. abortus* internalization in non phagocytic cells was demonstrated. MAPK1 is in a downstream pathway activated by these small GTPase subfamily proteins (208). It is reasonable to believe that disruption of this signaling pathway will affect the invasion process. Later in our experiment, we observed that *Brucella* replicate intracellularly during the first 4 h PI in both MAPK1-knocked down cell cultures (even at higher rate than in control or negative transfected cells) but not at the later time point. Two papers demonstrated that *Brucella* LPS is not potent in stimulating the MAPK signaling pathways in macrophages (117, 121), suggesting that this may be one of the many reasons why virulent smooth *Brucella* would survive

intracellularly. This suggests that the interruption of MAPK pathway does not affect the fate of smooth *Brucella* in macrophages. In our experiments, MAPK1 was 3.7 fold up-regulated, but it has previously been shown that the magnitude of the expression response may not be the most useful indicator of biological significance of the gene (151). Contrary to those studies, we observed an interference in *B. melitensis* intracellular survival after 4 h PI, possibly because of the role of MAPK1 activation and its participation in bacterial virulence is different in phagocytic than in non-phagocytic cells. Alternatively, the inhibition of MAPK1 might enhance the activity of other transcriptional regulators of the MAPK pathway which may have increased inhibitory effects on the ability of *Brucella* to survive and replicate. Based on our data and the wide spectrum of cellular processes that MAPK1 participates, more experiments are needed to define the role of MAPK1 in *Brucella* pathogenesis.

In summary, we have characterized in parallel the temporal transcriptional profile of the host and the *Brucella melitensis* for the first time in an *in vitro* system of infection. Our data provide specific genes and pathways to further elucidate how both host and *Brucella* interact during the early infectious process to the eventual benefit of the pathogen and to the detriment of the naïve host. The integrated results permit the establishment of new hypotheses regarding the initial molecular pathogenesis of *Brucella*.

CHAPTER IV
TEMPORAL GLOBAL GENE EXPRESSION ANALYSIS OF THE *in vivo*
INITIAL INTERACTIONS OF BOTH *Brucella melitensis* AND THE BOVINE
HOST

INTRODUCTION

In vitro host:agent interaction studies are useful for generating initial hypotheses; however *in vivo* studies are required for a fuller understanding of the bacterial pathogenesis. Cattle are mainly infected by *B. abortus*, but are also infected by *B. melitensis* under specific epidemiological conditions, with similar clinical signs in both infectious processes (231). The alimentary tract is the major route of infection in the transmission of *B. melitensis* (2). Previous studies in cattle have isolated *Brucella* from different sections of the alimentary tract (30) and feces (46), revealing the possibility that brucellae survive in the varied environmental conditions of the gastrointestinal tract. The calf ligated ileal loop model is a useful model for the study of *in vivo* host:agent initial interaction (204), an area that has not been studied in brucellosis. The goal of this study was to characterize the morphological changes and the parallel temporal transcription profiles of *B. melitensis* and the bovine host during their initial interaction in an effort to understand how this interaction modulates the outcome of the initial infectious process.

MATERIALS AND METHODS

Bacterial strain, media and culture conditions. Smooth virulent *Brucella melitensis* 16M Biotype 1 (ATCC 23456) re-isolated from an aborted goat fetus was maintained as frozen glycerol stocks. An aliquot of a saturated culture was inoculated in a 200 ml Erlenmeyer flask filled with 50 ml of cell culture media [F12K medium (ATCC) supplemented with 10% heat-inactivated fetal bovine serum (HI-FBS) (ATCC)], and incubated at 37°C with 5% CO₂ overnight with shaking until the late-log growth phase (OD = 0.4) was reached. Heat-inactivated (H-I) *B. melitensis* was prepared by incubation overnight at 65°C. Concentration of the inocula, purity, and efficacy of heat killing of the *Brucella* was confirmed by plating serial dilutions on tryptic soy agar (TSA) (BD) and incubating at 37°C for 4 days.

Animal handling and surgical procedures. Four 3-week-old brucellosis-free male calves were used in these experiments. Calves were fed with milk replacer twice daily up to 24 h and water *ad libitum* up to 12 h prior to the surgery. To minimize the possibility of interference from other enteropathogens on the host gene expression profile, calves were tested for fecal excretion of *Salmonella* spp. and *Coccidium* spp. oocysts twice and only negative animals were used. All animal experiments were approved by the Texas A&M University Institutional Animal Care and Research Advisory Committee. Surgeries were performed under biosecurity level III (BSL3) conditions in USDA inspected and CDC-approved isolation buildings at the experimental farm at Texas A&M University (College Station, TX). The surgical procedures were similar to those previously described (203). Briefly, anesthesia was

induced with IV propofol (Propoflo; Abbot Laboratories, Chicago, IL) followed by placement of an endotracheal tube; animals were maintained under general anesthesia with isoflurane (Isoflo; Abbott Laboratories) for the duration of the experiment. The abdominal wall was incised, the distal ileum containing the linear Peyer's patch exteriorized, and 21 segments with length ranging from 6 to 8 cm were ligated with umbilical tape leaving 1-cm loops between them. The loops were intraluminally inoculated with 3 ml of a suspension containing 1×10^9 CFU of *B. melitensis* 16M/ml either alive (infected loops) or heat-inactivated (H-I) loops. Sterile cell culture media (F12K media supplemented with 10% HI-FBS) was injected into the control loops. The segments were replaced into the abdominal cavity, the incision temporarily closed, and reopened for collecting samples beginning at 15 min and continuing through 12 h PI. Calves were euthanatized with an intravenous over dose of sodium pentobarbital at the end of the procedures and the carcass immediately incinerated. One infected, one heat killed inoculated and one control loop were collected at 7 time points (0.25, 0.5, 1, 2, 4, 8 and 12 h post-inoculation) and samples were processed for quantitation of tissue-associated bacteria, morphology, and both host and agent gene expression profiling. Samples from the surgery room were transported in triple containment to the BSL3 for immediate processing.

Quantitation of tissue-associated *B. melitensis*. Two-6 mm biopsy punches (0.1 g) of intestinal mucosa were extracted from every infected loop, intensely washed three times in PBS to minimize extracellular bacteria, homogenized, and diluted in 1 ml of PBS. Similar procedures were followed in H-I and control loops to identify viable

Brucella as a consequence of leakage of the loops, cross-contamination during material processing or *Brucella* migration via lymphatic or blood vessels. Samples from mesenteric lymph nodes and liver were collected after the animals were euthanized. To determine the number of viable colony forming units (CFU) of *B. melitensis* in tissues, lysates were serially diluted and cultured on selective Farrell's media [TSA (BD) supplemented with *Brucella* selective supplement (Oxoid Limited, Hampshire, UK) as manufacturer's instructions] (7).

Five ml of blood were collected by aseptic venipuncture of the jugular vein into 0.75 ml of acid-citrate-dextrose (ACD) at T0 (pre-inoculation), 0.5, 1, 2, 4, 8 and 12 h time points. One ml of blood from every time point was cultured in selective bi-phasic media (7). Briefly, TSA (BD) + 1% agar (Difco, Lawrence, KS) was cooled after autoclaving to 56°C before adding the *Brucella* selective supplement (Oxoid). The molten medium was well mixed and dispensed 20 ml into 75 cm² cell culture flask (Corning). Flasks were placed to allow the media to solidify along one side. The following day tryptic soy broth (TSB) (BD) was autoclaved, cooled and *Brucella* selective supplement (Oxoid) added according to manufacturer's instructions. Fifteen ml were dispensed aseptically in each flask already containing the solid phase, and the sterility of the media was checked by overnight incubation at 37°C. Blood cultures were incubated for at least 1 month at 37°C and checked twice a week.

Morphologic studies. For morphologic analysis by light microscopy, full cross-sections of each loop including the Peyer's patch were fixed in formalin, processed

according to the standard procedures for paraffin embedding, sectioned at 5- μ m thickness, and stained with hematoxylin and eosin.

Isolation of total RNA from intestinal loops. Six to ten-6 mm biopsy punches were extracted from every loop. The mucosa of the samples were immediately dissected, minced into small pieces with a sterile scalpel, and placed in TRI-Reagent® (Ambion) (2 biopsy punches / 1 ml of reagent) and further homogenized with a tissue grinder. RNA was extracted according to TRI-Reagent manufacturer's instructions. The resultant RNA pellet was re-suspended in DEPC-treated water (Ambion) with 2% DTT and 1% RNase inhibitor (Promega). Contaminant genomic DNA was removed by RNase-free DNase I treatment (Ambion) according to the manufacturer's instructions, and samples were stored at -80°C until used. RNA concentration was quantitated by NanoDrop® ND-1000 (NanoDrop) and the RNA quality was determined using an Agilent 2100 Bioanalyzer (Agilent).

Enrichment and sense-strand amplification of *B. melitensis* total RNA from infected bovine Peyer's patches. *B. melitensis* total RNA was initially enriched and then amplified from 30 μ g of total RNA from *B. melitensis*-infected bovine Peyer's patches at 0.25, 0.5, 1, 2 and 4 h post-infection. The enrichment procedure was performed using MICROBEnrich® kit (Ambion) according to the manufacturer's instructions, and the remaining material immediately amplified, as it was previously described in Chapter III. The concentration of amplified RNA was quantitated by Nanodrop and samples stored at -80°C until used.

Isolation of total RNA and gDNA from cultures of *B. melitensis* 16M. The intracellular *B. melitensis* gene expression was compared to the gene expression of the inoculum (i.e., cultures of *B. melitensis* 16M grown in F12K media supplemented with 10% HI-FBS at late-log growth phase) and *B. melitensis* gDNA was used for normalization of the bacterial gene expression profile. Isolation of total RNA and gDNA from *Brucella* cultures was done as previously described in Chapter II.

Preparation of bovine reference RNA. Total RNA was isolated from Madin-Darby bovine kidney (MDBK) and bovine B lymphocyte (BL-3) cell lines (ATCC) and fresh bovine brain, as explained above. Cell lines were grown in 150 cm² cell culture flasks with minimum essential medium Eagle (MEME) (ATCC) supplemented with 10% HI-FBS. Bovine brain was harvested from cortex and cerebellum of a Holstein male calf immediately after euthanasia. The tissue was homogenized in ice-cold TRI-Reagent® (Ambion). RNA concentration from each sample was quantitated and bioanalyzed before and after pooling the samples. Total RNA isolated from three samples was pooled together in equal amounts, aliquoted and stored at -80°C until needed.

Construction of cDNA microarrays and annotation. Selective unique 70-mer oligonucleotide sets representing 13,257 cattle ORFs were obtained from normalized and subtracted cattle placenta and spleen cDNA libraries and based upon the earlier cDNA array platform GPL2864 (70) and subtracted cDNA libraries created from embryonic (day 36 and day 64) and extra-embryonic (day 14 to 25) tissues (NCBI libraries 15993, 15993 and 17188). Positive controls included beta actin (ACTB), glyceraldehyde-3-phosphate dehydrogenase (GAPDH), and hypoxanthine phosphoribosyltransferase

(HPRT). Exogenous spiking controls were the soybean genes chlorophyll ab binding protein (CAB), Rubisco small chain 1 (RBS1), and major latex protein (MSG). Negative controls were Cot1 DNA, genomic DNA, spotting buffer, poly-A, and water. All 70-mer oligos were printed in 150 mM phosphate buffer at 20 uM concentration in duplicate on aminosilane-coated glass slides at the W. M. Keck Center (University of Illinois at Urbana-Champaign). The oligos were annotated based on the GenBank accession number, when available.

Sample preparation and slides hybridization. The labeling and hybridization procedures for host and pathogen samples were explained in detail in the previous chapter (Chapter III). Bovine experimental samples (i.e. from infected, H-I and control loops) were co-hybridized against bovine reference RNA sample to a custom 13K bovine ESTs–70-mers oligoarray. Prior to hybridization, the microarrays were denatured by steam exposure, UV cross-linked and immersed in prehybridization buffer at 42°C for a minimum of 45 min. This was followed by four washes in distilled water, immersion in 100% isopropanol for 10 seconds, and drying by centrifugation. Slides were hybridized at 42°C for ~40 h in a dark humid hybridization chamber (Corning), then washed for 10 min at 42°C with low stringency buffer [1X SSC, 0.2% SDS] followed by two 5-min washes in higher stringency buffers [0.1X SSC, 0.2% SDS and 0.1X SSC] at room temperature with agitation.

Data acquisition and microarray data analysis. Immediately after washing, the slides were scanned using a commercial laser scanner (GenePix 4100). The genes represented as spots on the arrays were adjusted for background and normalized to

internal controls using image analysis software (GenePixPro 6.0). Genes with fluorescent signal values below background were disregarded in all analyses. Initially, pathogen and host arrays were normalized against *B. melitensis* genomic DNA as previously explained (219) and bovine reference RNA respectively. Resulting data was analyzed using Seralogix's suite of gene expression analysis and modeling tools (www.seralogix.com). Genes were determined to be significantly differential expressed based on Seralogix's Bayesian z-score method. Using this method genes are ranked and ordered according to their expression magnitudes and gene variance is computed using a Bayesian predicted variance value. The Bayesian variance is determined by using a sliding window algorithm that averages 50 variances directly on the ascending and descending ordered sides of each gene of interest. This method is used to smooth the variances across the dynamic range of intensity values. Significantly changed genes were determined with the Bayesian z-test ($p < 0.025$). At each time point, genes determined to be statistically significantly expressed on pathogen arrays hybridized with probes generated from *B. melitensis*-infected bovine samples (z-score $p < 0.025$) were subtracted from the final list of differentially expressed genes.

New computational tools developed by Seralogix were used for the identification of Biosignature Dynamic Bayesian Network modeling, mechanistic gene discovery and pattern/pathway recognition. Seralogix's Biosignature Analysis Framework is comprised of an integrated suite of software tools (XManager, XConsole & XBuilder) and relational database storage specialized for management and analysis of biosignature data.

Microarray results validation. Six randomly selected *B. melitensis* and 6

bovine genes with differential expression on microarray were analyzed by quantitative RT-PCR (qRT-PCR). Two micrograms of RNA from the same samples used for microarray hybridization were reverse transcribed into cDNA using TaqMan® (Applied Biosystems). For relative quantitation of target cDNA, samples were run in individual tubes in a SmartCycler II (Cepheid). One SmartMix bead (Cepheid) was used for 2 x 25 µl PCR reactions along with 20 ng of cDNA, 0.2X SYBR Green I dye (Invitrogen) and 0.3 µM forward and reverse primers (Sigma Genosys) designed by Primer Express Software v2.0 (Applied Biosystems) (Tables 11 and 12). For each gene tested, the individual calculated threshold cycles (Ct) were averaged among each condition and normalized to the Ct of the bovine *GAPDH* and 16S rRNA genes for host and pathogen respectively from the same cDNA samples before calculating the fold change using the $\Delta\Delta C_t$ method (Applied Biosystems Prism SDS 7700 User Bulletin #2). For each primer pair, a negative control (water) and an RNA sample without reverse transcriptase (to determine genomic DNA contamination) were included as controls during cDNA quantitation. Because our analysis considered genes differentially expressed based on z-score and not on fold-change, array data were considered valid if the fold change of each gene tested by qRT-PCR was expressed in the same direction as determined by microarray analysis.

RESULTS

Colonization of bovine Peyer's patches and systemic invasion of *B. melitensis* after intraluminal inoculation. We assessed the kinetics of *B. melitensis* 16M infection

TABLE 11. Primers for Real-time PCR analysis of genes in bovine Peyer's patch samples

GenBank accession #	Gene symbol	Gene product	Forward primers (5'-3')	Reverse primers (5'-3')
NM_173895	<i>BPI</i>	Bactericidal/permeability-increasing protein	CCTCCGAACTCACCATGAAG	TGTCCAATCTGAGCTCTCCAATAA
NM_175793	<i>MAPK1</i>	Mitochondrial-activated protein kinase 1	GGCTTGGCCCGTGTG	GGAAGATGGGCCTGTTGGA
NM_174006	<i>CCL2</i>	Chemokine (C-C motif) ligand 2	TCCTAAAGAGGCTGTGATTTTCAA	AGGGAAAGCCGGAAGAACAC
NM_173925	<i>IL8</i>	Interleukin 8	TGCTTTTTTGTTCGGTTTTTG	AACAGGCACTCGGGAATCCT
NM_174091	<i>IL18</i>	Interleukin 18	CTGGAATCAGATCACTTTGGCA	CAGGCATATCCTCAAAGACAGG
NM_001033608	<i>MIF</i>	Macrophage migration inhibitory factor	CTGCAGCCTGCACAGCAT	TTCATGTCTCGAGAAGTTGATGTAG
NM_001034034	<i>GAPDH</i>	Glyceraldehyde-3-phosphate dehydrogenase	TTCTGGCAAAGTGACATCGT	GCCTTGACTGTGCCGTTGA

TABLE 12. Primers for Real-time PCR analysis of genes in *B. melitensis* samples

Locus ID	Gene product	Forward primers (5'-3')	Reverse primers (5'-3')
BMEI0475	Cytochrome C1	GCTGCAGCGGCTAATAATGG	CGGTCAAAGCGAATGGATATAA
BMEI0526	Carbamoyl-phosphate synthase small subunit	CGGTCAGAAGGCGCAGAATA	CTCGCCAAGGATGTCACCAT
BMEI1384	Transcriptional regulator, AraC family	CGCAGTTCACCAAGGCATT	GCGTGTTCCAGAGGCGATCTT
BMEI1440	Thiol:disulfide interchange protein DsbA	CGAAATTGGCCGGTTTTACA	CCCACATCTCCTCAAACGA
BMEI1798	23S ribosomal RNA methyltransferase	CATGGGCTCGGTCTTTTCC	TGTTCAATTGCCATTATCAGGAT
BMEII0033	Channel protein virB9 homolog	CGATGCAGGTCGGCACTAAT	TGGCTGTTCCAGATGCTTTC
AF220147	16S rRNA	CCTTACGGGCTGGGCTACA	TGATCCGCGATTACTAGCGATT

after intraluminal inoculation by calculating the CFU present in the Peyer's patches at different time points. The intestinal loops were intraluminally inoculated with 3×10^9 CFU of *B. melitensis* 16M and 0.1 g of Peyer's patches collected beginning at 15 min and continuing through 12 h. Fifteen minutes post-inoculation, $\sim 10^6$ CFU/g of tissue were recovered (Fig. 15). The number of tissue-associated *B. melitensis* rose rapidly, reaching the peak (2×10^6 CFU/g of tissue) by 4 h post-inoculation, and decreasing at later time points.

To address the possibility of *Brucella* systemic invasion, blood from the jugular vein was collected and cultured. Blood samples taken from the first calf were contaminated and not considered in the final analysis of the data. Blood from the second calf was collected as early as 1 h time point while samples from the two other animals were taken from 30 min PI through the end of the procedure. All blood samples before the inoculation (T0, control) were *Brucella*-free, but *B. melitensis* was isolated from all samples after inoculation. *B. melitensis* were also isolated from mesenteric lymph nodes and liver at the 12 h time point and also isolated from control loops and loops inoculated with *B. melitensis* H-I at 8 and 12 h time points (2×10^2 to 2×10^3 CFU of *B. melitensis* / g of Peyer's patch) from 1 animal. These results indicate rapid penetration of *B. melitensis* through Peyer's patches followed by systemic distribution and organ colonization via blood and lymphatic vessels.

Morphologic findings of *B. melitensis*-infected bovine Peyer's patches. No differences in histological features were observed between control samples and H-I *B.*

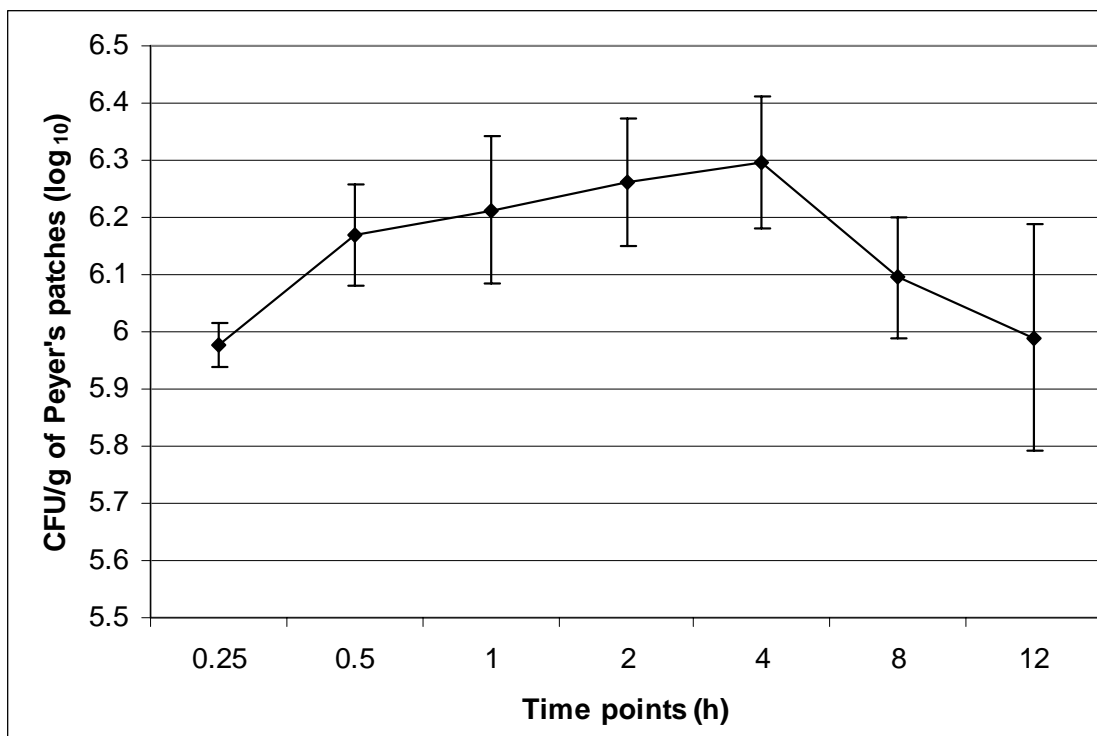


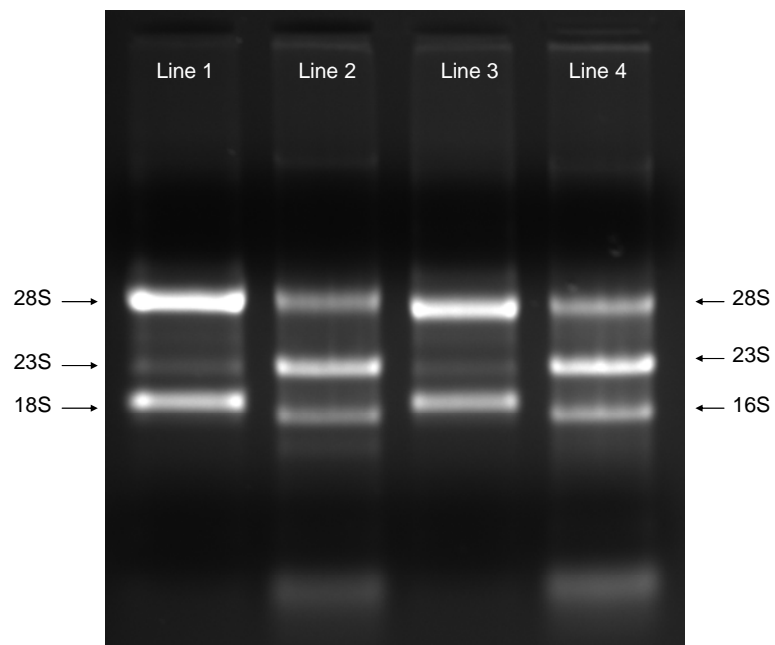
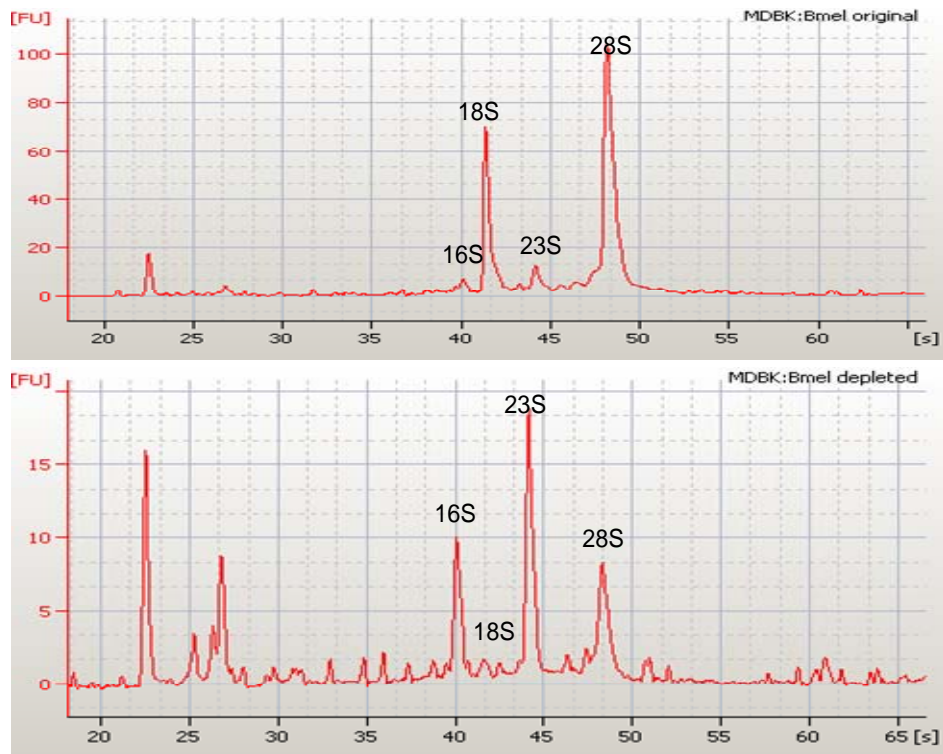
FIG. 15. Kinetics of infection with *B. melitensis* 16M. Ileal loops were intraluminally inoculated in 3 ml containing 1×10^9 CFU of *B. melitensis* 16M/ml. Tissue (Peyer's patch) samples of 0.1 g of mucosal tissue were extracted at 0.25, 0.5, 1, 2, 4, 8 and 12 h PI from every infected loop, intensively washed 3 times in PBS, macerated and diluted in 1 ml of distilled water. To determine the kinetics of the infection, macerated samples were serially diluted and cultured on Farrell's medium. Numbers of CFU recovered from bovine Peyer's patches are the average of 4 calves. Bars represent standard deviation.

melitensis-inoculated or *B. melitensis*-infected Peyer's patches or mesenteric lymph nodes in the first 12 h PI.

Enrichment procedure is useful for analysis of *B. melitensis* RNA from infected bovine tissues. Before applying the enrichment and amplification protocol described in Chapter III for characterizing the transcriptome of intracellular *Brucella*, we wanted to determine if the enrichment procedure was useful for analysis of bacterial RNA from infected bovine tissues. To answer this question a sample of 25 μg of MDBK cell line (Madin-Darby bovine kidney; ATCC) total RNA was spiked with 2 μg of *B. melitensis* total RNA (host:pathogen RNA = 12.5:1) and the mixed samples treated with MICROBEnrich® kit (Ambion) according to the instruction manual. A sample of RNA from HeLa cells spiked with *B. melitensis* RNA in the same proportions was used as a positive control. The total RNA yielded after the treatment was 3.72 μg for the HeLa:*Brucella* mix and 4 μg for the MDBK:*Brucella* mix. The integrity and composition of the samples pre and post-treatment were evaluated by agarose gel electrophoresis and Bioanalyzer analysis (Fig. 16A and B). Our results found that the enrichment procedure effectively reduced bovine RNA concentration from mixed host and pathogen samples.

***In vivo* transcriptional profiling of intracellular *B. melitensis*.** The intracellular *B. melitensis* total RNA was initially enriched and then amplified from total RNA of *B. melitensis*-infected bovine Peyer's patch samples at 0.25, 0.5, 1, 2 and 4 h post-infection. Four biological replicates of experimentally enriched and amplified RNA from every time point (n = 20) were indirectly labeled and co-hybridized against *B.*

FIG. 16. Integrity and composition of the host:pathogen RNA samples pre- and post-enrichment treatment. Twenty-five (25) μg total eukaryotic RNA from human (HeLa S3) and bovine (MDBK) cell lines were mixed with 2 μg of *Brucella melitensis* 16M RNA (ratio 12.5:1) and treated with MICROBEnrich® (Ambion) according to the instruction manual. The eukaryote:prokaryote RNA ratio of the original sample was 12.5:1 and decreased to 1:1 after the treatment. **(A)** Agarose gel electrophoresis image. Lines 1 and 2: HeLa:*B.melitensis* 16M RNA mix; lines 3 and 4: MDBK:*B.melitensis* 16M RNA mix; pre- and post-treatment respectively. **(B)** Comparison of RNA composition from a sample of MDBK:*B. melitensis* 16M pre- and post-treatment with MICROBEnrich® (Ambion) and examined on an Agilent 2100 Bioanalyzer. Ribosomal RNA subunits are indicated.

A**B**

melitensis gDNA to a custom 3.2K *B. melitensis* oligo-array. In preliminary experiments, we observed (data not shown) that some bovine transcripts cross-hybridize with probes on *B. melitensis* microarrays. To account for the possibility of this cross-hybridization in the surgery samples, the original total RNA from *B. melitensis*-infected bovine Peyer's patches (i.e. non-enriched non-amplified) (n = 20) were also hybridized against *B. melitensis* gDNA on the *B. melitensis* oligo-arrays, and those oligospots with signal were considered non-specific and eliminated from all analyses to avoid false positive pathogen gene detection. The intracellular *B. melitensis* gene expression at every time point was compared to the gene expression of the inoculum (i.e. *in vitro*-grown cultures of *B. melitensis* at late-log phase of growth) (n = 4). Based on these criteria, statistical analysis of microarray results reveal that between 720 and 822 *B. melitensis* genes were detected as differentially expressed (z-score $p < 0.025$) between 15 min and 4 h post-infection (Table 13). The ratio between up- and down-regulated genes varied from 1.1:1 to 1.4:1, and none of the genes inversed its transcriptional expression during these first 4 h PI. A group of 618 genes (19.3% of *B. melitensis* genome) that were differentially expressed in at least 4 out of 5 time points was considered the core set of genes that reflect the major changes in *B. melitensis* gene expression during the early *in vivo* bovine Peyer's patch infection and therefore important in understanding key events in the modulation of host response. From this set of 618 differentially expressed genes, 365 (59%) were up-regulated and 253 (41%) were down-regulated compared with the *in vitro* grown culture (Appendix F). Differentially expressed genes with predicted or

TABLE 13. Number of genes differentially expressed by intracellular *B. melitensis* from 15 minutes to 4 h post-infection

Time point	No. genes up-regulated	No. genes down-regulated	Total No. of genes differentially expressed
15 min	431	385	816
30 min	419	357	776
1 h	465	357	822
2 h	398	322	720
4 h	470	343	813

annotated functions were assigned to clusters of orthologous genes (COGs) functional categories according to the NCBI *Brucella melitensis* 16M genome project web page (http://www.ncbi.nlm.nih.gov/entrez/query.fcgi?db=genomeprj&cmd=Retrieve&dopt=Overview&list_uids=180). The COGs in which the greatest number of transcriptional changes occurred included, transcription, translation, amino acid transport and metabolism, energy production and conversion, and cell wall and membrane biogenesis (Fig. 17). In most of the COG categories, most genes were up-regulated except for transcription, defense, cell motility and intracellular trafficking and secretion groups, in which the opposite effect was observed. Genes assigned to nucleotide, lipid and inorganic ion transport and metabolism groups were equally distributed between those that were up- and down-regulated. There were 65 (10.5%) and 168 (27%) of the core genes differentially expressed in the first 4 h PI that had only a general predicted

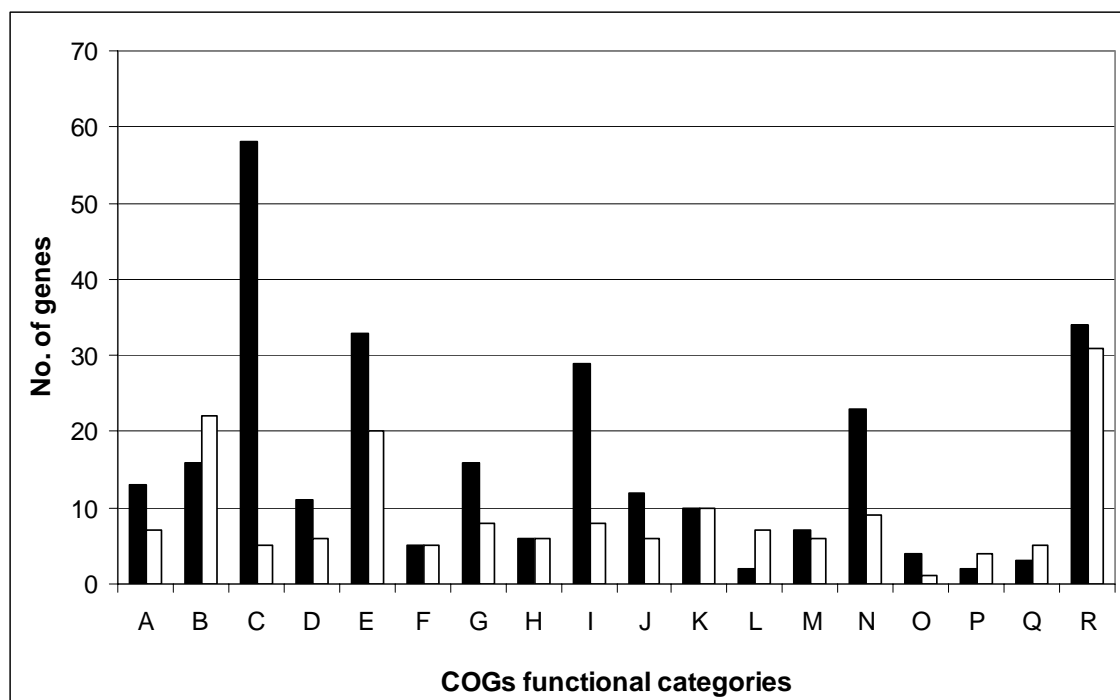


FIG. 17. Distribution of genes differentially expressed in intracellular *B. melitensis* between 15 min and 4 h post-infection categorized by COGs functional categories. Genes differentially expressed with predicted or annotated functions were assigned to clusters of orthologous genes (COG) functional categories. Functional classification is as follows: A, DNA replication, recombination and repair; B, Transcription; C, Translation, ribosomal structure and biogenesis; D, Post-translational modification and secretion, protein turnover and chaperones; E, Amino acid transport and metabolism; F, Nucleotide transport and metabolism; G, Carbohydrate transport and metabolism; H, Lipid transport and metabolism; I, Energy production and conversion; J, Coenzyme transport and metabolism; K, Inorganic ion transport and metabolism; L, Defense mechanisms; M, Signal transduction; N, Cell wall/membrane biogenesis; O, Cell division; P, Cell motility; Q, Intracellular trafficking and secretion; R, General function prediction only. There were 168 (81 up- and 87 down-regulated) differentially expressed genes with unknown function that are not included in the figure. Solid bars, up-regulated genes; open bars, down-regulated genes.

function or unknown function, respectively. This represents 37.5% of the genes differentially expressed, and may contain pathways with previously unrecognized roles in *B. melitensis* early pathogenesis.

An overview analysis of the core set of differentially expressed genes disclosed that *Brucella* actively express not only genes involved in survival under stress conditions but also genes required for intracellular multiplication during the first 4 h PI *in vivo*. The first of these activities is reflected by the up-regulation of some stress-indicator genes including a gene encoding a protein involved in DNA protection during starvation (BMEI1980), and genes encoding heat shock and chaperone proteins such as DnaJ (BMEI0047, BMEI1513), HspA (BMEI1784) and GrpE (BMEI1777). Enhanced transcription of exopolyphosphatase (BMEI0598), a regulator of adjustment to stress in *E. coli* (130), and *hfq* (BMEI0872), a gene encoding an RNA-binding protein (Host Factor I) that increase *Brucella* resistance under stress conditions (193) was also observed. Additionally, genes encoding DNA replication, cell division, translation, amino acid metabolism, and cell wall and membrane biogenesis, all of which are molecular indicators of *B. melitensis* active growth, were up-regulated. Specifically, genes whose products are involved in DNA replication like DNA polymerase (BMEI1876), chromosomal replication initiation protein (BMEI1943), DNA helicase (BMEI1485) and the single-strand binding protein (BMEI880), were also up-regulated. Moreover, four genes actively involved in control of cell division were up-regulated: *parB* (BMEI0010), *ftsA* (BMEI0584), *minC* (BMEI0927) and BMEI0213. Amino acids are not available inside intracellular vacuoles, where *Brucella* reside (132), however

amino acid biosynthesis is absolutely necessary for bacterial growth and multiplication inside intracellular vacuoles. Transcripts for proteins implicated in amino acid biosynthesis such as *ilvCDI*, *carA* and *trpB-D*, among others, were enhanced compared with the control. In addition, 58 genes that encode proteins required in translation and ribosomal structure were up-regulated, suggesting increased production of protein synthesis machinery in the first 4 h PI. Overall, these *Brucella* gene expression data are in accordance with the bacteriological studies, in which an increasing number of *Brucella* were isolated from 15 minutes to 4 h PI.

Twenty-three transcripts involved in cell wall and membrane biogenesis were also up-regulated. Among them were ORFs encoding genes involved in LPS biosynthesis (BMEI0831/0833, BMEI1037, BMEI1404, BMEI1418, BMEI1602). LPS is a well characterized *Brucella* virulence factor that participates in the inhibition of the early fusion of phagolysosome membranes and facilitates *Brucella* to survive intracellularly (184). Another major virulence element required in initial *Brucella* pathogenesis *in vitro* is *virB*, a type IV secretion system (T4SS) gene (169). In our experiment, 2 of the 11 genes of the T4SS (*virB5* and *II*) were significantly down-regulated in 4 or more time points. Another ORF (BMEI1538) encoding a hypothetical protein that was identified as important for *B. melitensis* internalization in non-phagocytic cells (Chapter II), was up-regulated from 15 min to 4 h post-infection. In general, these data confirm that recognized virulence factors were differentially expressed in the *in vivo* system of infection.

Transcriptional profile of host bovine Peyer's patches inoculated with *B. melitensis*. RNA isolated from the mucosa of the intestinal Peyer's patches inoculated with viable *B. melitensis*, H-I *B. melitensis* or culture medium (control) from 4 different animals at 0.25, 0.5, 1, 2 and 4 h PI (n = 60) was indirectly labeled and co-hybridized against bovine reference RNA on a custom 13.2K bovine oligoarray. Bioanalysis determined that RNA from the experimental samples and the reference was of good quality (RIN > 7.0, 28S/18S ratio > 1.4, OD_{260/280} > 2.0, OD_{260/230} > 1.8 for experimental samples; and RIN = 9.7, 28S/18S ratio = 2.1, OD_{260/280} = 2.01, OD_{260/230} = 1.85 for reference RNA). When hybridized on the arrays, the reference bovine RNA generated a readable signal intensity on more than 85% of the spots on the microarray (SNR > 3SD above background) and co-hybridization with experimental samples allowing comparison of bovine gene expression profiles across all treatments and time points.

Microarray analysis revealed that 1,387 bovine genes were detected as differentially expressed (z-score $p < 0.025$) in loops inoculated with virulent *B. melitensis* 16M compared with controls between 15 min and 4 h post-infection (Table 14). From these 1,387 genes, 646 (46.5%) were up- and 741 (53.5%) were down-regulated. Two different expression profiles could be distinguished in *B. melitensis*-infected host in the first 4 h post-infection. The initial expression profile, which we termed the "very early" expression profile, was characterized by up-regulated gene expression that extended from 15 min to 1 h PI, followed by a down-regulated (termed "early") transcriptional profile from 1 through 4 h PI. Of 224 differentially expressed

TABLE 14. Number of host genes differentially expressed in *B. melitensis*-infected bovine Peyer's patch from 15 min to 4 h post-infection

Time point	No. genes up-regulated	No. genes down-regulated	Total No. of genes differentially expressed
15 min	107	20	127
30 min	143	16	159
1 h	561	612	1173
2 h	65	300	365
4 h	3	5	8

genes in the “very early” host response, 196 (88%) were up- and 28 (12%) were down-regulated (Appendix G). The greatest number of transcriptional changes occurred in the transcription regulation, cell cycle/cell differentiation and proliferation, and inflammation and immune response Gene Ontology (GO) processes. After 1 h post-infection, a different set of 1,163 genes was expressed, 459 (39%) up- and 704 (61%) down-regulated (Appendix H). Genes encoding proteins implicated in transcription regulation, protein biosynthesis and protein degradation, cell cycle and cell proliferation, inflammation and immune response and general metabolism experienced the greatest transcriptional changes due to the *B. melitensis* infection (Fig. 18). Furthermore, 73 (32%; 62 up- and 11 down-regulated) and 507 (44%; 174 up- and 333 down-regulated; not shown) of the differentially expressed genes before and after 1 hour PI respectively lacked of functional annotation.

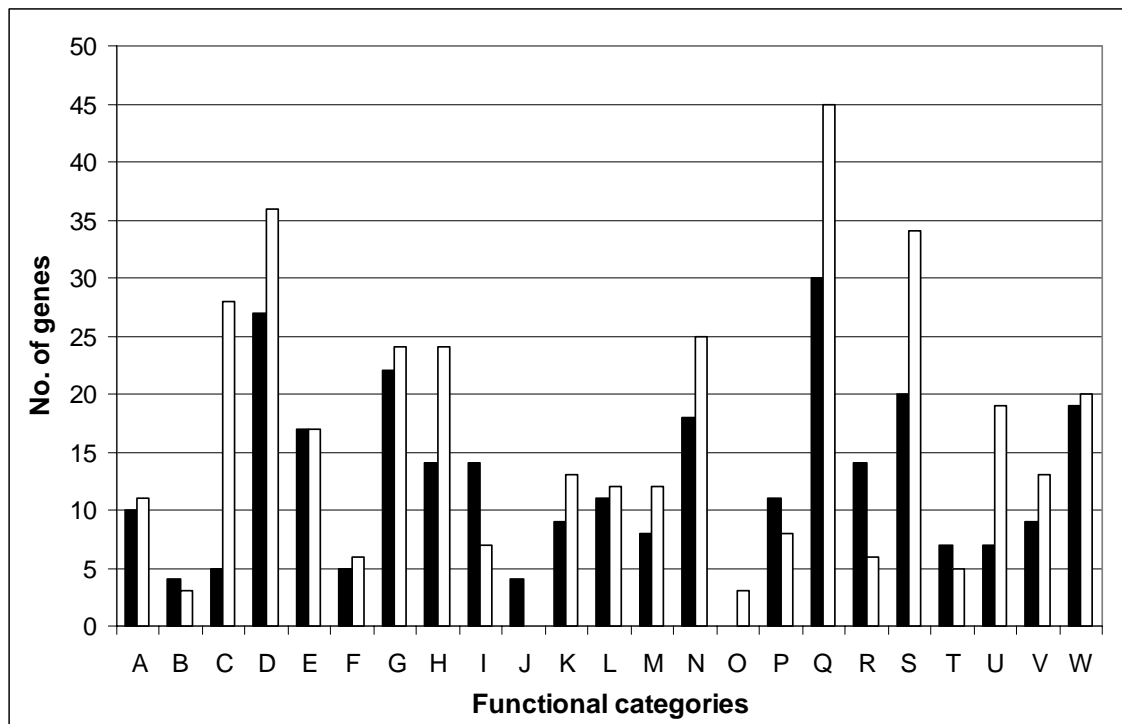


FIG. 18. Distribution of host genes differentially expressed in *B. melitensis*-infected bovine Peyer's patch after 1 h post-infection categorized by Gene Ontology. Functional classification is as follows: A, DNA replication and repair; B, Chromosome organization; C, RNA processing; D, Transcription regulation; E, Protein biosynthesis; F, Protein folding; G, Protein degradation; H, Cell cycle / cell proliferation and differentiation; I, Cell adhesion; J, Cell-cell communication; K, Cytoskeleton organization; L, Morphogenesis and development; M, Apoptosis; N, Inflammation and immune response; O, Pregnancy; P, Nervous system development and proliferation; Q, Metabolism; R, Electron transport; S, Signal transduction; T, Surface receptors; U, Transport; V, Endocytosis and intracellular trafficking; W, Other functions. Solid bars, up-regulated genes; open bars, down-regulated genes.

Inflammatory and innate immune responses are key elements in avoiding infectious disease in naïve hosts. The very early expression profile of bovine Peyer's patches infected with *B. melitensis* had a clear up-regulation of these functions that was slightly reversed later. Genes encoding proteins important in neutrophil function and NK cell bactericidal elements were initially up-regulated. For instance, 3 genes encoding neutrophil lysosomal granules such as *BPI* (bactericidal/permeability increasing-protein), one locus (Bt.78164) encoding a protein strongly similar to myeloperoxidase, and another locus (Bt.24637) encoding a product similar to azurocidin 1 were up-regulated. Also a gene (Bt.11022) whose product is involved in increasing neutrophil exocytosis and phagocytosis - induced respiratory burst activity (43) was up-regulated, as well as two other protein-encoding genes involved in NK cell activation (*TYROBP*) and dendritic cell - NK cells cross-talk (*NCR3*) (136, 232). NK cells were reported to be early participants in the impairment of intramacrophagic *Brucella* replication *in vitro* (57). Other anti-inflammatory and immune-modulator genes were differentially expressed after 1 h PI. *TLR6*, which mediates cellular response to bacterial lipoproteins, was down-regulated. Genes encoding pro-inflammatory cytokines which mediate neutrophil or eosinophil migration or their receptors such as *IL8*, *IL18*, *SDF1*, *SYK*, eotaxin and *CCR3* were down-regulated. One monocyte chemotaxis gene (*CCL2*) and one cellular receptor for chemoattractant molecules (*CCR1*) were also down-regulated. Moreover, *SOCS3*, a gene encoding a protein involved in suppression of intracellular cytokine signals, was down-regulated. Two genes, one encoding the enhanced killer of intracellular pathogens *MIF* and the other one encoding its cellular receptor (*CD74*),

were up-regulated after 1 h post-infection as well as *iNOS2A*, which encodes a potent protein involved in the defense response to intracellular bacteria. Genes involved in T lymphocyte attraction and activation were also differentially expressed in the host response to *Brucella*. Two genes encoding T cell-attractant and activating proteins such as *CD2* and a locus (Bt.37553) moderately similar to *CXCL9*, and 3 other genes such as *IL16*, linker for activation of T cells (Bt.26847) and a gene with some similarity to *CXCL11* (Bt.18368), were up-regulated in the very early and in the early host response, respectively. The chemokine *CXCL13*, important for the development of B cell areas of secondary lymphoid tissues (144) and predominantly a B cell chemoattractant, was down-regulated. In summary these data indicate that the bovine host responds to very early *Brucella* infection with an up-regulation of genes that encode lysosomal bactericidal enzymes and later turns on an anti-polymorphonuclear and anti-monocyte, but not antiT lymphocyte, chemoattractant response.

The activation of the complement system is another important non-specific host response to bacterial infection. In the very early PI response, three genes encoding components of the complement system were up-regulated. Two of them are participants of the membrane attack complex (MAC), a perforin bacterial membrane system and final product of the complement activation. Later, three genes encoding complement activation elements (*DF*, *CIR* and Bt.76479) were up-regulated, while the complement component *Iqa* was down-regulated.

Differential expression of genes coding for antigen processing and presentation molecules MHC I & II were observed in the “early”, but not in the “very early”, host

response. Two different probes on the array for the classical major histocompatibility class I antigens (*BOLA*) had lower signal in infected than in control samples, as did the *B2M* gene, a necessary element for MHC I expression (9). Alternatively, two genes (*BOLA-DRB3* and *BOLA-DOB*) which encode components of the major histocompatibility class II antigen were up-regulated while another one (*BOLA-DRA*) was down-regulated.

The inhibition of host cell apoptosis by intracellular pathogens was interpreted as a protective mechanism that prevents the bacteria from being recognized and eliminated by the host immune system. In our study, four pro-apoptotic genes (*CIDEB*, *PTGES*, one transcribed locus with moderate similarity to caspase recruitment domain [Bt.687] and another transcribed locus strongly similar to an apoptotic chromatin condensation inducer in the nucleus [Bt.9054]) were up-regulated in the very early response, and another eight pro-apoptotic genes (*TP53*, *BID*, *GRIM19*, *WWOX*, *DEDD2*, a gene similar to PLAIDD [Bt.30544], a gene similar to BCL2/adenovirus E1B 19-kDa protein-interacting protein 3 [Bt.1411], and a transcript locus moderately similar to necrosis factor receptor superfamily, member 12a [Bt.20111]) were up-regulated after 1 h of *B. melitensis* infection. Simultaneously, four anti-apoptotic genes (*BCL2A1*, a gene similar to TM2 domain containing 2 [Bt.13981], and 2 transcripts moderate similar to cell death regulator Aven [Bt.1793] and IAP repeat-containing 2 [Bt.64777]) were down-regulated in the early infection response. These data suggest that early in the infection, the host induces a cell death program to avoid *Brucella* intracellular survival and persistence.

Abortion is the principal clinical symptom of brucellosis in pregnant animals (171). Pregnancy is maintained by a delicate hormonal equilibrium involving progesterone (a pregnancy-stimulatory hormone) and prostaglandins (a delivery-inductor hormone) as the two major participants (118). In our microarray-based expression analysis a delivery-induced transcriptional profile was observed. For instance, a gene encoding for a pregnancy-associated glycoprotein 7 (*PAG7*), a protein found to be expressed in early bovine pregnancy (115), was down-regulated in the very early *Brucella*:host interaction, while 20-beta-hydroxysteroid dehydrogenase-like gene (Bt.28223) involved in prostaglandin E₂ to PGF₂α conversion, was up-regulated. After 1 h PI, a gene involved in progesterone biosynthesis (*ADAM*), one progesterone receptor (*PGRMC2*) and one inhibitor of prostaglandin effects (*PGDH*), were down-regulated. Summarizing, these data indicates an early pro-abortive transcriptional response in a *Brucella*-infected host.

Other observations arising from the evaluation of microarray data analysis after 1 h PI include the transcriptional arrest of the cell cycle and inhibition of cell proliferation and differentiation (*TP53*, *CCNE2*, *CDK10*), and the enhanced expression of cell-cell adhesion (*ITG*, *IGAL1*, *ZO3*) and cell-cell communication (*GJB1* and 6) related genes.

A much lower number of host genes were expressed in intestinal loops inoculated with heat-killed *B. melitensis* 16M. A total of 140 genes were differentially expressed in the first 4 h post-inoculation, being 78 (56%) up- and 62 (44%) down-regulated (Appendix I). Sixty-nine (49%) of the differentially expressed genes did not have a functional characterization and 25 of 71 of the expressed genes with known

functions in killed *Brucella*-inoculated tissues were also observed differentially expressed in viable *B. melitensis*-infected tissues. More genes encoding inflammatory and immune responses were differentially transcribed than any other functional category. Interestingly, 4 up-regulated genes in live *Brucella*-infected tissues from this category (*BPI*, *NCR3*, a gene similar to complement component C9 precursor [Bt.14139] and a gene with some similarity to CXCL9 [Bt.37553]), encoding NK cell and complement activation and lysosomal enzymes, were down-regulated in killed *Brucella*-inoculated Peyer's patches. Simultaneously, 2 leukocyte-chemoattractant genes, *CCL5* (RANTES) and *CCL8*, were up-regulated in tissues inoculated with heat-inactivated pathogen. Overall, these data suggest a pro-inflammatory expression profile in heat-killed *Brucella*-inoculated tissues, which is the opposite of that which was observed in live *B. melitensis*-infected tissues in the first 4 h post-infection. Similar to the pro-apoptotic expression profile observed with live *B. melitensis* infection, up-regulation of a pro-apoptotic gene similar to Death Associated Transcription Factor 1 (Bt.14503), down-regulation of the anti-apoptotic gene *BCL2A1*, and down-regulation of protein biosynthesis-involved genes could be observed in tissues inoculated with heat-killed *Brucella*. Aside from this, no other apparent biological patterns could be identified among the other 52 functional genes expressed as a consequence of the H-I pathogen inoculation during the first 4 h post-inoculation, as the remaining genes were randomly distributed among different GO processes.

Validation of microarray gene expression results by qRT-PCR. To confirm the microarray results we randomly chose 6 *B. melitensis* and 6 bovine genes

differentially expressed in the first 4 h post-infection and conducted qRT-PCR at every time point, (i.e. 60 data points). Validation of *B. melitensis* microarray results was done using cDNA reverse transcribed from the same enriched and amplified RNA samples used for microarray hybridization. Fold change relative to the inoculum and control loops was used for measuring the intracellular *B. melitensis* and bovine gene expression, respectively. Quantitative Real-time PCR results confirmed that all of the *Brucella* and host genes tested were altered in the same direction as was determined by microarray analysis (Figs. 19 and 20).

Dynamic Bayesian modeling analysis of host and pathogen microarray results reveal biosignature candidate genes. To further identify specific *B. melitensis* and bovine biological processes, pathways and gene targets for blocking *B. melitensis* early infection, a mathematical model of predictive analysis was conducted. The analysis identified 31 to 54 candidate genes important for *Brucella* early pathogenesis (Appendix J). Genes encoding proteins involved in transcription and amino acid metabolism were identified as important throughout the evaluated period (i.e. first 4 h PI), while others were only identified as essential at a specific time point. Several genes with predicted or uncharacterized function were also marked as necessary for initial *Brucella* pathogenesis in bovine Peyer's patches. This analysis suggests that *Brucella* host invasion is sustained in different biological processes, whose importance varies during the course of infection.

FIG. 19. Validation of *B. melitensis* microarray results by quantitative Real-time PCR. cDNA was synthesized from the same enriched and amplified RNA samples used for microarray hybridization. Six randomly selected ORFs that were differentially expressed by microarrays in intracellular *B. melitensis* between 15 min and 4 h PI as compared to the inoculum were validated by quantitative RT-PCR. Fold-change was normalized to the expression of *B. melitensis* 16S rRNA and calculated using the $\Delta\Delta C_t$ method. All tested genes at all time points had fold-changes altered in the same direction as microarray. Open bars represent fold-change by microarray, solid bars represent fold-change by qRT-PCR.

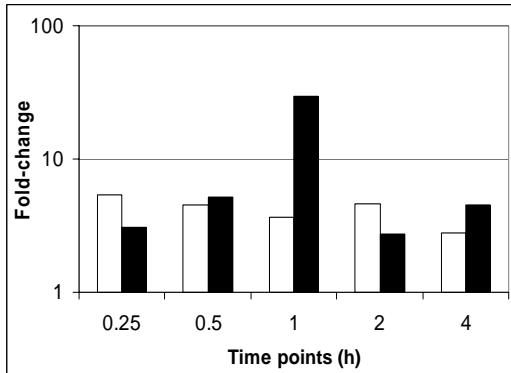
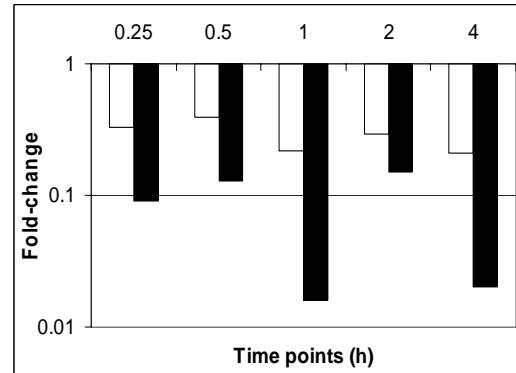
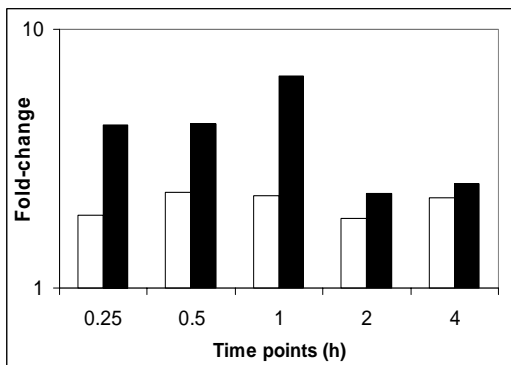
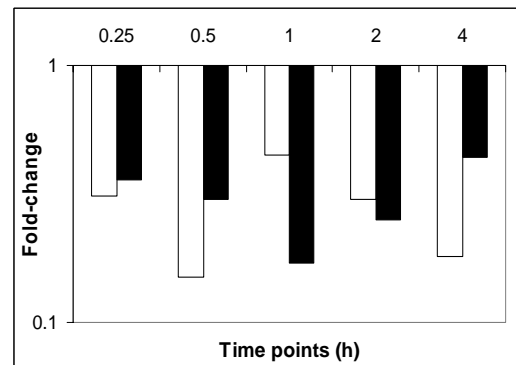
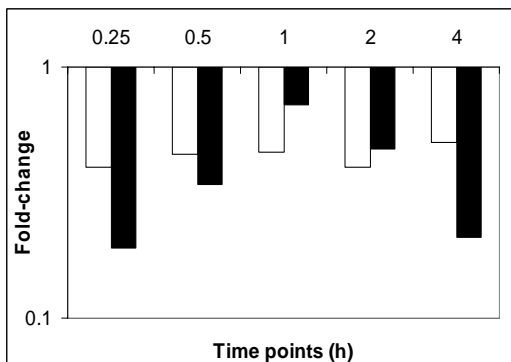
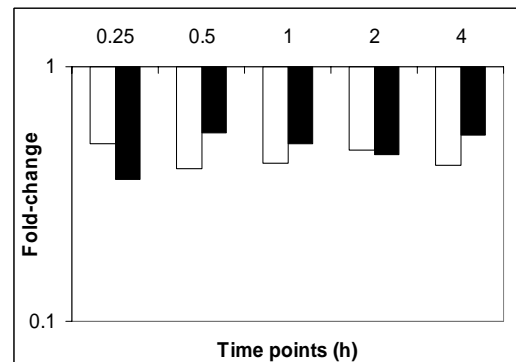
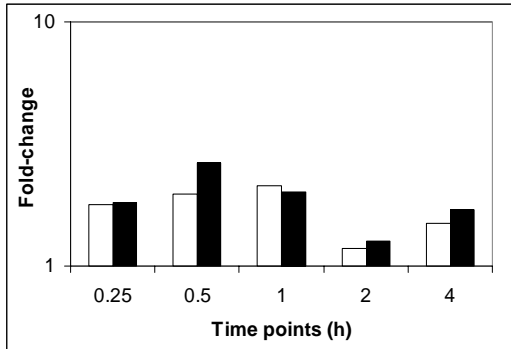
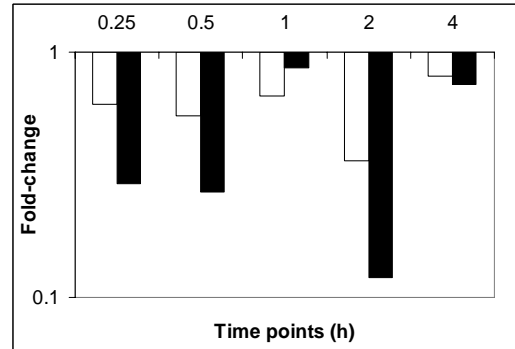
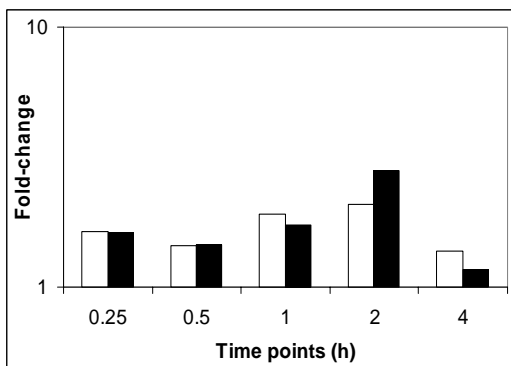
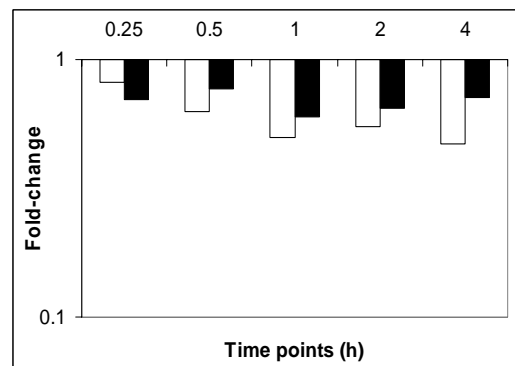
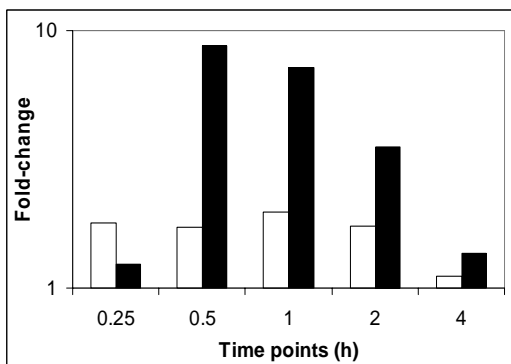
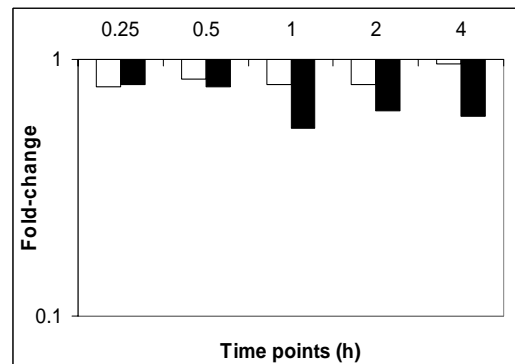
BMEI0475**BMEI1440****BMEI0526****BMEI1798****BMEI1384****BMEI0033**

FIG. 20. Validation of bovine microarray results by quantitative Real-time PCR. cDNA was synthesized from the same RNA samples used for microarray hybridization. Six randomly selected genes that were differentially expressed by microarrays in *B. melitensis*-infected bovine Peyer's patch between 15 min and 4 h PI as compared to non-infected tissues (control) extracted at the same time points were validated by quantitative RT-PCR. Fold-change was normalized to the expression of *GAPDH* and calculated using the $\Delta\Delta C_t$ method. All tested genes at all time points had fold-changes altered in the same direction in microarray and qRT-PCR. Open bars represent fold-change by microarray, solid bars represent fold-change by qRT-PCR.

BPI**CCL2****MAPK1****IL8****MIF****IL18**

Similarly, we conducted an *in silico* predictive mathematical model using the host gene expression data. The analysis identified 47 highly activated gene ontology (GO) biological processes (downloaded from Gene Ontology Consortium Database; <http://www.geneontology.org>) comprising 37 distinct mechanistic genes: 6 for “very early” and 31 for “early” infection (Table 15). Using the same bioinformatic platform, NK cell mediated cytotoxicity (hsa04650), leukocyte transendothelial migration (hsa04670), cell adhesion molecules (hsa04514), gap junction (hsa04540) and MAPK signaling (hsa04010) were identified among the top five pathways important for initial *Brucella* pathogenesis in bovine Peyer’s patches. Furthermore, genes such as *TP53* (apoptosis and Wnt signaling pathways), *ITGA4*, *ITGAL* and *VCAM1* (cell adhesion molecules, leukocyte transendothelial migration and NK cell mediated cytotoxicity pathways), *MAPK1* (MAPK signaling, NK cell mediated cytotoxicity and insulin signaling pathways), *ADCY1* and *ADRB1* (gap junction and calcium signaling pathways), *SYK* (NK cells mediated cytotoxicity) and *IL8* and *CCL2* (cytokine-cytokine receptor interaction signaling pathway) were the top 10 candidate genes that influence the outcomes of *Brucella*:host initial interaction. In summary, these data provide an important starting point for further analysis of important host biological processes, pathways and genes in *Brucella* pathogenesis.

DISCUSSION

In this study, we analyzed the kinetics of *Brucella* invasion and the global gene expression of the *Brucella melitensis*:bovine host interaction in the first 12 h post-

TABLE 15. Set of host candidate genes identified *in silico* as important for infection of bovine Peyer's patch in the first 4 hours of *Brucella*:host interaction

Unigene ID	Symbol	Gene product	Expression
Mechanistic genes at "very early" host response			
Bt.4689	<i>UCHL5</i>	Ubiquitin carboxyl-terminal hydrolase L5	Up
Bt.336	<i>TPSB1</i>	Tryptase beta 1	Up
Bt.1354	<i>MYO1A</i>	Myosin IA	Up
Bt.45674	<i>CD2</i>	CD2 antigen	Up
Bt.20121	<i>CTSD</i>	Cathepsin D (lysosomal aspartyl protease)	Up
Bt.20296	<i>SFXN2</i>	Sideroflexin 2	Up
Mechanistic genes at "early" host response			
Bt.15513	<i>SSB</i>	Sjogren syndrome antigen B (autoantigen La)	Down
Bt.18504	<i>MMP3</i>	Metalloproteinase 3 receptor	Up
Bt.4902	<i>CTSZ</i>	CTSZ protein	Up
Bt.8282	<i>DPP4</i>	Dipeptidylpeptidase IV (CD26, adenosine deaminase complexing protein 2)	Down
Bt.7938	<i>CTSS</i>	Cathepsin S	Down
Bt.1613	<i>PRSS11</i>	Protease, serine, 11 [IGF binding]	Down
Bt.24017	<i>PSMC2</i>	Proteasome (prosome, macropain) 26S subunit, ATPase 2	Down
Bt.7181	<i>CAPNS1</i>	Calpain, small subunit 1	Up
Bt.12473	<i>CDC37</i>	CDC37 homolog	Down
Bt.11942	<i>COL18a1</i>	Collagen, type XVIII, alpha 1	Up
Bt.52428	<i>CFL1</i>	Cofilin 1 (non-muscle)	Up
Bt.45570	<i>EPAS1</i>	Endothelial PAS domain protein 1	Down
Bt.4908	<i>RBBP7</i>	Retinoblastoma binding protein 7	Down
Bt.7776	<i>TPT1</i>	Tumor protein, translationally-controlled 1	Up
Bt.8140	<i>FCER1G</i>	Fc fragment of IgE, high affinity I, receptor for; gamma polypeptide	Up
Bt.44261	<i>TNFRSF8</i>	Tumor necrosis factor receptor superfamily, member 8	Up
Bt.15528	<i>MIF</i>	Macrophage migration inhibitory factor (glycosylation-inhibiting factor)	Up
Bt.62596	<i>CCR1</i>	Chemokine C-C motif receptor 1	Down
Bt.2408	<i>CCL2</i>	Chemokine (C-C motif) ligand 2	Down
Bt.42359	<i>PLA2G7</i>	Phospholipase A2, group VII	Down
Bt.2047	<i>ADM</i>	Adrenomedullin	Down
Bt.4990	<i>ACVR2B</i>	Activin A receptor, type IIB	Up
Bt.16889	<i>LTB4R</i>	Leukotriene B4 receptor	Up
Bt.167	<i>MAPK1</i>	Mitogen-activated protein kinase 1	Up
Bt.52357	<i>HRMT1L2</i>	HMT1 hnRNP methyltransferase-like 2	Up
Bt.4269	<i>OTC</i>	Ornithine carbamoyltransferase	Down
Bt.24449	<i>SDHA</i>	Succinate dehydrogenase flavoprotein subunit A	Up
Bt.23164	<i>UQCRC1</i>	UQCRC1 protein	Up
Bt.4001	<i>HMOX1</i>	Heme oxygenase (decyclizing) 1	Up
Bt.2689	<i>PRDX2</i>	Peroxiredoxin 2	Up
Bt.12916	<i>GPX3</i>	Glutathione peroxidase 3 (plasma)	Up
Bt.28278	<i>ACE2</i>	Angiotensin I converting enzyme 2 precursor	Down
Bt.32810	<i>PDLIM1</i>	PDZ and LIM domain 1 (elfin)	Down
Bt.64560		Transcribed locus	Up
Bt.43664		Transcribed locus	Up

infection using a ileal-loop model of infection. Initially, we evaluated the kinetics of invasion by *B. melitensis* in bovine Peyer's patches. The alimentary tract is the main route of invasion for *B. abortus* and *B. melitensis* (2, 171) however the portal(s) of entry is incompletely characterized. *B. abortus* was isolated from the small intestine of calves 5 h after being fed infected milk (30) and from feces of coyotes orally infected (46), which suggest that in natural conditions viable *Brucella* are able to reach the intestinal Peyer's patches. In our experiment, *Brucella* were recovered from intestinal tissue as early as 15 min post-infection, and the number of tissue-associated bacteria was maximal at 4 h PI (2×10^6 *Brucella* / g of tissue) and decreased later. The inverse relation between *Brucella* invasion and time post-infection was also observed in *B. abortus* S19-infected bovine ileal loops (1). The decreasing uptake through time was apparently related to the degeneration of *Brucella* in the intestinal lumen and consequent lack of adhesion due to surface modification. Another possibility might be the saturation of *Brucella* receptors in the epithelium, as was reported in *Salmonella* infection (21). A third reason for the decreased number of tissue-associated *Brucella* during the experiment could be the quick passage from the lumen through the tissue to the blood and lymphatic circulation. In this study, we isolated *B. melitensis* from general circulation, beginning as soon as 30 minutes after inoculation. Other bacterial pathogens such as *Salmonella*, *Yersinia* and *Shigella* also colonize and invade the host through the Peyer's patches at even higher numbers than we observed in this study (97, 235, 237), but their almost immediate presence in systemic blood after inoculation has not been reported. This data were unexpected as *B. melitensis*, thus the elucidation of the host and *Brucella* elements

responsible for this quick invasion and translocation will contribute to unraveling one of the most valuable secrets of the initial *Brucella*:host interaction.

No significant histologic differences were observed in samples taken from ileal loops inoculated with culture media (control), H-K *Brucella* or fully virulent *B. melitensis* at any of the 7 time points evaluated. Similar to these results, Mense *et al.* (2001) did not detect substantial histologic changes or inflammatory responses in the respiratory tract in mice after 1 day of intranasal inoculation of *B. melitensis* (157). In contrast a mild acute inflammation at 4, 6 and 10 h after *B. abortus* S19 inoculation was observed in another study using the ileal loop model (1). These differences could be due to differences in the *Brucella* species inoculated or to a host response to a larger inoculum (6×10^{11} vs. 3×10^9 CFU used in our study).

Brucellosis is a chronic infectious disease and most of the current research has been focused on persistence (74, 109, 248). There is little knowledge of the virulence factors that influence the establishment of infection. One of the major virulence factors described in *Brucella* spp. is the *virB* operon which encodes a T4SS. Results from *in vitro* system of infection found that *virB* is not required for cellular invasion, but its expression, which begins 15 min after the bacteria is phagocytized and reaches maximal expression at 5 h PI (212), is indispensable for intracellular survival of *Brucella* (Chapter II and III of this dissertation, (48, 169, 213)). In our *in vivo* experiment, genes from *virB* operon were down regulated. Besides *virB5* and *virB11* (Appendix F), *virB6*, *virB9* and *virB10* were also down-regulated although they are not displayed in appendix F because they were not differentially expressed in more than three time points. The down

regulation of *virB9* was also verified by qRT-PCR, confirming that the type IV secretion system was down-regulated. In addition, the transcriptional regulator *vjbR* (BMEII1116) that positively regulates the expression of the *B. melitensis virB* operon (48) was not differentially expressed in our microarray results. These data indicate that the T4SS was down-regulated in our *in vivo* model during the first 4 h PI. These results, in addition to those reported by Roux *et al.* who did not see differences in the number of *B. abortus* and *B. melitensis* WT and *virB* mutant recovered from mouse spleens in the first 3 days PI (196), suggest that *virB* apparently plays a minimal role in the initial *in vivo Brucella* pathogenesis. There may be environmental signals *in vivo* that affect the expression of the *virB* operon differently than in *in vitro* systems of infection. Identification of the host molecular targets of the T4SS will help characterize its expression *in vivo*.

The unconventional lipopolysaccharide (LPS) component of the external membrane is another well-characterized virulence factor in *Brucella* (138, 227). LPS was shown to be active in inhibition of the early fusion of the *Brucella*-containing phagosomes and lysosomes (184) and directly involved in deficient CD4⁺ T cell activation (79). In our study, several genes encoding LPS biosynthesis were up-regulated, suggesting active LPS participation during the initial *Brucella*:host interaction. It was hypothesized that LPS released during intracellular replication and death of brucellae is integrated in lipid rafts that are recycled to the cell surface, where they form macrodomains in association with MHC class II (80, 137). The segregation of MHC class II molecules in macrodomains was postulated to be a possible mechanism responsible for the down-regulation of antigen presentation following *Brucella* infection

(79, 137). In our study 2 genes encoding MHC class II antigen presentation and several others whose products are involved in T cell activation were up-regulated, which would suggest early development of a T cell immune response. The up-regulation of MHC class II molecules was observed on the cell surface of mouse macrophages recovered from *B. abortus* LPS-inoculated mice (79). Altogether the previous data reaffirm that the down regulation of T cell activation in brucellosis is not a transcriptional regulation mechanism such as that described for another intracellular pathogen causing leishmaniasis (135) nor a direct suppressive effect on T cells, but instead an antigen presenting cell surface membrane modification that impairs efficient antigen presentation (137).

Smooth brucellae were found to impair apoptosis in mononuclear cells, which was interpreted as a pathogen strategy to avoid being recognized and eliminated by the immune system (73, 86, 96). In our study, the molecular response of the host in the first 4 h PI had an apoptotic profile. Interestingly, *BCL2A1* was down-regulated in the first 4 h PI in our study in both infected tissue and tissues inoculated with H-I *B. melitensis*, but the human homolog was observed up-regulated in *B. suis*-infected human monocytes at the same time point (96). The differences observed could be due to the complexity of our model system which includes the multiple cell types present in the intestinal tract as opposed to monocytes in *in vitro* culture. Moreover, it could be interpreted as host innate immune response to prevent the establishment of persistent infection before *Brucella* interfere with the host gene expression.

A mathematical prediction model identified *Brucella* “mechanistic” candidate genes important for infection of bovine Peyer’s patches (Appendix J). Some of the candidate genes were identified as important during the whole period, while others were only identified as candidates for specific time points. Some of these genes do not occur among the core set of genes differentially expressed in the first 4 h PI because they were not detected differentially expressed in more than three time points. Among them we identified *aroC* (BMEI1506) which is necessary for biosynthesis of aromatic amino acids, and which is absolutely required for intracellular replication of *Brucella*, *Salmonella* and *Shigella* (35, 60, 82), and *lon* (BMEI0876), a stress response protease required for initial *in vivo* infection in a mouse model of brucellosis (192). Some of the mechanistic candidate genes were down-regulated, which could be interpreted in that their expression is deleterious for the pathogen’s early survival *in vivo*. These data need to be experimentally corroborated, but they suggest potential pathways for future research.

In this study, we observed that the naïve bovine host immediately responded to *Brucella* infection by enhancing the transcriptional profile that is followed by a transcriptional down-regulation. The innate immune response has been recognized as a central defense mechanism that influences the development of adaptive immunity and is a critical component of local immunity in mammals (77). “Very early” post-infection, our study found that genes encoding proteins involved in the innate immune response such as complement components, bactericidal oxygen and nitrogen intermediates and neutrophil lysosomal enzymes were up-regulated. However, the role that these gene

products play *in vivo* in the early host protection against *Brucella* infection needs to be evaluated, as previous *in vitro* studies have demonstrated that smooth brucellae are not only resistant to complement-mediated killing (72) but also inhibit neutrophil degranulation (19, 172), NK cell activity (198) and are poor inducers of the respiratory burst (188) and bactericidal nitrogen intermediates (121, 150). In contrast, some of these genes were down-regulated in H-I *B. melitensis*-inoculated Peyer's patches, which suggest that the host recognizes the pathogen as an inert element that does not need to be killed.

Elicitation of the host immune response by *Brucella* spp. was reported earlier (29, 239). In this study, down-regulation of the genes encoding the pro-inflammatory cytokines IL8 and IL18 (both confirmed by qRT-PCR) were observed after 1 h PI. The same two cytokines were also down-regulated in *B. melitensis*-infected HeLa cells at 12 h PI (Chapter III). However, IL8 mRNA expression was detected in a human macrophage cell line infected with *B. suis* in the first 5 h PI (56). This would suggest that the down-regulated expression of these 2 cytokines primarily originates in the epithelium, which supports our previous hypothesis about the active role of the epithelium in the early immune response to *Brucella* infection (Chapter III). IL8, but not IL18, is the major neutrophil chemoattractant in *in vivo* pathogenesis of *S. typhimurium*-induced enteritis (204), and its down-regulation may be one of the primary reasons why PMN infiltration is not observed in *Brucella*-infected tissues. Moreover, IL18 is also a pro-inflammatory cytokine with broader biological functions, i.e. NK cell proliferation (83), apoptosis (123), Th1/Th2 response (110), and activation of T cell proliferation

(158); its role in the onset of brucellae infection needs to be defined, being apparently dispensable for persistence (239). Eosinophils are also absent in response to *Brucella* infection. The down-regulation of the eosinophil chemoattractant, eotaxin, and its receptor *CCR3* (182) could contribute to the lack of eosinophil infiltration in *Brucella*-infected tissues. *Brucella* LPS and outer membrane proteins (OMPs) were identified as responsible for disrupting the host immune response (90, 127). In our study, several previous uncharacterized OMPs were distinguished *in silico* as candidate genes important for early *B. melitensis* virulence (Appendix J) that must be experimentally corroborated.

Monocyte migration inhibitory factor (*MIF*) is not only an important regulator of innate and adaptive immunity but also a positive regulator of other cellular activities. For instance, *MIF* is a chemoattractant for monocytes/macrophages in injured tissues through activation of *CCL2* (95). In our study *MIF* was up-regulated after 1 h PI, but *CCL2* was simultaneously down-regulated (both confirmed by qRT-PCR), which may explain the absence of monocyte infiltration in early *Brucella* infection. Furthermore, *MIF* binds *CD74* and induces the activation of the ERK1/2 MAPK cascade and PGE2 production (145). ERK1/2 (or MAPK1) is mainly involved in cell proliferation, differentiation and development (124). Dynamic Bayesian modeling analysis indicates that *MIF* and *MAPK1* are candidate genes important for *Brucella* survival in the first 4 h post-infection of the bovine Peyer's patch (Table 14). The influence of the genes and the relevance of the pathway *in vivo* must wait further experimental testing.

MIF also induces prostaglandin E2 (PGE₂) production (145). PGE₂, together with PGF₂α are potent stimulators of myometrial contraction and cervical smooth muscle relaxation, playing a major role in parturition and abortion (63, 111). In our study, not only *MIF* was up-regulated, but also *PTGES*, which converts PGH₂ to PGE₂ (116), and 20-beta-hydroxysteroid dehydrogenase-like gene (Bt.28223) involved in PGE₂ to PGF₂α conversion. The gene *PGDH*, which encodes a prostaglandin-inactivating enzyme, was down-regulated, and its down-regulation was observed during term or premature delivery (125). Interestingly, the human homolog gene was also observed down-regulated in *B. melitensis*-infected HeLa cells at 12 h PI (Chapter III). The enhanced presence of FGL2 and the decreased activity of IL8 (genes encoding these proteins were up- and down-regulated in this study, respectively) were also implicated in abortion (38, 211). The individual contribution of these genes in *Brucella*-induced abortion is unknown, but together they indicate an early pro-abortive transcriptional profile in the *B. melitensis*-infected host that deserves future study.

In summary, we characterized several phenomena during the first 4 h of the *B. melitensis*: bovine host interaction. Our results demonstrate that *Brucella* are able to invade the host via intestinal Peyer's patches and are present in systemic blood by 30 min post-infection. A common set of genes was identified as differentially expressed in *Brucella*, while two different transcriptional profiles were observed in the bovine host early in the infection. The accessibility to new techniques such as laser capture microdissection (LCM) will allow study of the temporal expression profile of both *Brucella* and host more accurately, allowing determination of how *Brucella* modify their

transcriptome inside different cell types and how these cells respond to *Brucella* infection. Increasingly powerful software and modeling approaches will facilitate the connectivity of *Brucella* effectors with host targets for better understanding of the *Brucella*:host interaction for subsequent therapeutic and vaccine research.

CHAPTER V

CONCLUSIONS

Brucella spp. are the etiologic agents of brucellosis, causing world-wide zoonotic infectious disease that results in abortion and infertility in animals and a chronic debilitating illness in humans. *Brucella melitensis* is one of the six species of the genus *Brucella* and considered potential bioterrorist agent due to its high virulence to humans. The objective of this study was to elucidate the molecular pathogenesis of brucellosis by characterizing the alterations in the transcriptome of the host and *B. melitensis* during their early interactions. The hypothesis was that the dynamics of *Brucella*:host interactions modifies gene expression levels in both genomes during the early infectious process lead to the eventual benefit of the pathogen and to the detriment of the naïve host.

To test the hypothesis and accomplish the overall objective, specific goals were elaborated. Initially, the *Brucella* invasion-associated transcriptome was characterized and relevant genes for *Brucella* invasion in non-professional phagocytic cells were identified. In these experiments, *B. melitensis* invasiveness and gene expression were found to be associated with the phase of *in vitro* growth, as illustrated phenotypically by HeLa cell internalization, and molecularly by 454 differentially expressed genes identified by cDNA microarray technology. Two of eight differentially expressed genes were confirmed to be important for internalization in non-phagocytic cells which may

indicate that approximately 25% (or about 115 genes) of the differentially expressed detected genes may participate in the invasion process.

The next specific goal was to characterize the transcriptome of *B. melitensis* and the epithelial-like HeLa cell line to identify initial strategies of the pathogen for intracellular survival and replication, and perturbations of major gene(s) modulating critical cellular pathways in the host during the initial *Brucella* infectious process. Microarray-based studies revealed that both host and pathogen had initial down-regulated expression profiles at 4 h PI that were reversed at 12 h PI. Very little is known about which effectors are utilized by *Brucella* to survive intracellularly nor which host molecules are targeted to benefit the pathogen in detriment of the naïve host. These experiments revealed numerous specific genes and pathways, thus further elucidating interactive mechanisms during the early infectious process. Two of the *in silico* identified genes were confirmed to be critical for the intracellular life style of *Brucella* in non-phagocytic cells in the first 12 h PI, validating *in silico* generated data as a powerful tool to identify invasion and survival mechanisms of *Brucella*. Future investigations should explore other specific *in silico* identified host and pathogen biological processes, pathways or genes to further characterize the initial molecular host:*Brucella* intracellular interactions.

Finally, the morphological changes and the temporal transcription profiles of both *B. melitensis* and the bovine host were investigated during their initial interactions to expand our understanding of how this interaction modulates the outcome of the infectious process. Host invasion of Peyer's patches by *B. melitensis* and the presence of

Brucella in systemic blood within 30 minutes was confirmed, and the *in vivo* transcriptional profiles of both *B. melitensis* and bovine host were characterized at multiple times during the first 4 h PI. These *in vivo* experiments generated data that conflicts with previously published *in vitro* findings. For instance, the *virB* operon was down-regulated providing evidence that it may not be essential for *in vivo* *B. melitensis* invasion. Also pro-apoptotic and anti-inflammatory expression profiles were identified in the host during the first 4 h PI, and genes encoding proteins related with interruption of pregnancy and abortion were differentially expressed. These findings can be extended by using laser capture micro dissection (LCM) to further the define pathways and genes expressed by *Brucella* in specific cell types and identify host responsive genes. By combining gene deletion mutants of *Brucella* with specific host genes knocked down by siRNA the *in vivo* host:*Brucella* interactions can be more effectively understood. As more powerful bioinformatics are developed, these new tools will connect *Brucella* effector genes with host targets for a clearer understanding of the *Brucella*:host interactions for application to improved therapeutics and vaccines.

REFERENCES

1. **Ackermann, M. R., N. F. Cheville, and B. L. Deyoe.** 1988. Bovine ileal dome lymphoepithelial cells: endocytosis and transport of *Brucella abortus* Strain 19. *Veterinary Pathology* **25**:28-35.
2. **Adams, L. G.** 2002. The pathology of brucellosis reflects the outcome of the battle between the host genome and the *Brucella* genome. *Veterinary Microbiology* **90**:553-561.
3. **Adams, L. G., and J. W. Templeton.** 1998. Genetic resistance to bacterial diseases of animals. *Rev. Sci. Tech. Off. Int. Epiz.* **17**:200-219.
4. **Alexander, B., P. R. Schmurrenberger, and R. R. Brown.** 1981. Numbers of *Brucella abortus* in the placenta, umbilicus and fetal fluid of two naturally infected cows. *Veterinary Record* **108**:500.
5. **Allen, C. A., L. G. Adams, and T. A. Ficht.** 1998. Transposon-derived *Brucella abortus* rough mutants are attenuated and exhibit reduced intracellular survival. *Infection and Immunity* **66**:1008-1016.
6. **Almirón, M., M. Martínez, N. Sanjuan, and R. A. Ugalde.** 2001. Ferrochelatase is present in *Brucella abortus* and is critical for its intracellular survival and virulence. *Infection and Immunity* **69**:6225-6230.
7. **Alton, G. G., L. M. Jones, R. D. Angus, and J. M. Verger.** 1988. Techniques for the brucellosis laboratory. Institut National de la Recherche Agronomique, Paris, France.

8. **Anderson, T. D., N. F. Cheville, and V. P. Meador.** 1986. Pathogenesis of placentitis in the goat inoculated with *Brucella abortus*. II. Ultrastructural studies. *Veterinary Pathology* **23**:227-239.
9. **Arce-Gómez, B., E. A. Jones, C. J. Barnstable, E. Solomon, and W. F. Bodmer.** 1978. The genetic control of HLA-A and B antigens in somatic cell hybrids: requirement for beta2 microglobulin. *Tissue Antigens* **11**:96-112.
10. **Arellano-Reynoso, B., N. Lapaque, S. Salcedo, G. Briones, A. E. Ciocchini, R. A. Ugalde, E. Moreno, I. Moriyón, and J. P. Gorvel.** 2005. Cyclic B-1,2-glucan is a *Brucella* virulence factor required for intracellular survival. *Nature Immunology* **6**:618-625.
11. **Arenas, G. N., A. S. Staskevich, A. Aballay, and L. S. Mayorga.** 2000. Intracellular trafficking of *Brucella abortus* in J774 macrophages. *Infection and Immunity* **68**:4255-4263.
12. **Baek, S. H., G. Rajashekara, G. Splitter, and J. P. Shapleigh.** 2004. Denitrification genes regulate *Brucella* virulence in mice. *Journal of Bacteriology* **186**:6025-6031.
13. **Bailey, A. M., M. A. Webber, and L. J. V. Piddock.** 2006. Medium plays a role in determining expression of *acrB*, *marA*, and *soxS* in *Escherichia coli*. *Antimicrobial Agents and Chemotherapy* **50**:1071-1074.
14. **Baldwin, C. L., and M. Parent.** 2002. Fundamentals of host immune response against *Brucella abortus*: what the mouse model has revealed about control of infection. *Veterinary Microbiology* **90**:367-382.

15. **Barthel, R., J. Feng, J. A. Piedrahita, D. M. McMurray, J. W. Templeton, and L. G. Adams.** 2001. Stable transfection of the bovine *NRAMP1* gene into murine RAW264.7 cells: Effect on *Brucella abortus* survival. *Infection and Immunity* **69**:3110-3119.
16. **Beier, D., and R. Gross.** 2006. Regulation of bacterial virulence by two-component systems. *Current Opinion in Microbiology* **9**:143-152.
17. **Bellaire, B. H., R. M. Roop II, and J. A. Cardelli.** 2005. Opsonized virulent *Brucella abortus* replicates within nonacidic, endoplasmic reticulum-negative, LAMP-1 positive phagosomes in human monocytes. *Infection and Immunity* **73**:3702-3713.
18. **Berlutti, F., C. Morea, A. Battistoni, S. Sarli, P. Cipriani, F. Superti, M. G. Ammendolia, and P. Valenti.** 2005. Iron availability influences aggregation, biofilm, adhesion and invasion of *Pseudomonas aeruginosa* and *Burkholderia cenocepacia*. *International Journal of Immunophatology and Pharmacology* **18**:661-170.
19. **Bertram, T. A., P. C. Canning, and J. A. Roth.** 1986. Preferential inhibition of primary granule release from bovine neutrophils by a *Brucella abortus* extract. *Infection and Immunity* **52**:285-292.
20. **Billard, E., C. Cazevielle, J. Dornand, and A. Gross.** 2005. High susceptibility of human dendritic cells to invasion by the intracellular pathogens *Brucella suis*, *B. abortus*, and *B. melitensis*. *Infection and Immunity* **73**:8418-8424.

21. **Bolton, A. J., M. P. Osborne, T. S. Wallis, and J. Stephen.** 1999. Interaction of *Salmonella choleraesuis*, *Salmonella dublin* and *Salmonella typhimurium* with porcine and bovine terminal ileum *in vivo*. *Microbiology* **145**:2431-2441.
22. **Boschiroli, M. L., S. Ouahrani-Bettache, V. Foulongne, S. Michaux-Charachon, G. Bourg, A. Allardet-Servent, C. Cazeville, J. P. Liautard, M. Ramuz, and D. O'Callaghan.** 2002. The *Brucella suis virB* operon is induced intracellularly in macrophages. *PNAS* **99**:1544-1549.
23. **Bruggemann, H., A. Hagman, M. Jules, O. Sismeiro, M. A. Dillies, C. Gouyette, F. Kunst, M. Steinert, K. Heuner, J. Y. Coppée, and C. Buchrieser.** 2006. Virulence strategies for infecting phagocytes deduced from the *in vivo* transcriptional program of *Legionella pneumophila*. *Cellular Microbiology* **8**:1228-1240.
24. **Buckley, A. M., M. A. Webber, S. Cooles, L. P. Randall, R. M. La Ragione, M. J. Woodward, and L. J. V. Piddock.** 2006. The AcrAB-TolC efflux system of *Salmonella enterica* serovar Typhimurium plays a role in pathogenesis. *Cellular Microbiology* **8**:847-856.
25. **Burse, A., H. Weingart, and M. S. Ullrich.** 2004. The phytoalexin-inducible multidrug efflux pump AcrAB contributes to virulence in the fire blight pathogen, *Erwinia amylovora*. *Molecular Plant and Microbes Interaction* **17**:43-54.
26. **Cameron, H. S., E. H. Hughes, and P. W. Gregory.** 1942. Genetic resistance to brucellosis in swine. *Journal of Animal Science* **1**:106-110.

27. **Campbell, G. A., and L. G. Adams.** 1992. The long-term culture of bovine monocyte-derived macrophages and their use in the study of intracellular proliferation of *Brucella abortus*. *Veterinary Immunology and Immunopathology* **34**:291-305.
28. **Campbell, G. A., L. G. Adams, and B. A. Sowa.** 1994. Mechanisms of binding of *Brucella abortus* to mononuclear phagocytes from cows naturally resistant or susceptible to brucellosis. *Veterinary Immunology and Immunopathology* **41**:295-306.
29. **Caron, E., T. Peyrard, S. Kohler, S. Cabane, J. P. Liautard, and J. Dornand.** 1994. Live *Brucella* spp. fail to induce tumor necrosis factor alpha excretion upon infection of U937-derived phagocytes. *Infection and Immunity* **62**:5267-5274.
30. **Carpenter, C. M.** 1924. *Bacterium abortum* invasion of the tissues of calves from the ingestion of infected milk. *The Cornell Veterinarian* **14**:16-31.
31. **Castaneda-Roldán, E. I., F. Avelino-Flores, M. Dall'Agnol, E. Freer, L. Cedillo, J. Dornand, and J. A. Girón.** 2004. Adherence of *Brucella* to human epithelial cells and macrophages is mediated by sialic acid residues. *Cellular Microbiology* **6**:435-445.
32. **Castaneda-Roldán, E. I., S. Ouahrani-Bettache, Z. Saldana, F. Avelino-Flores, M. A. Rendón, J. Dornand, and J. A. Girón.** 2006. Characterization of SP41, a surface protein of *Brucella* associated with adherence and invasion of host epithelial cells. *Cellular Microbiology* **8**:1877-1887.

33. **Celli, J., C. de Chastellier, D. M. Franchini, J. Pizarro-Cerdá, E. Moreno, and J. P. Gorvel.** 2003. *Brucella* evades macrophages killing via VirB-dependent sustained interactions with the endoplasmic reticulum. *The Journal of Experimental Medicine* **198**:545-556.
34. **Censini, S., C. Lange, Z. Xiang, J. E. Crabtree, P. Ghiara, M. Brodovsky, R. Rappuoli, and A. Covacci.** 1996. Cag, a pathogenicity island of *Helicobacter pylori*, encodes type I-specific and disease-associated virulence factors. *PNAS* **93**:14648-14653.
35. **Cersini, A., A. M. Salvia, and M. L. Bernardini.** 1998. Intracellular multiplication and virulence of *Shigella flexneri* auxotrophic mutants. *Infection and Immunity* **66**:549-557.
36. **Chain, P. S. G., D. J. Comerci, M. E. Tolmasky, F. W. Larimer, S. A. Malfatti, L. M. Vergez, F. Agüero, M. L. Land, R. A. Ugalde, and E. García.** 2005. Whole-genome analyses of speciation events in pathogenic brucellae. *Infection and Immunity* **73**:8353-8361.
37. **Chatterjee, S. S., H. Hossain, S. Otten, C. Kuenne, K. Kuchmina, S. Machata, E. Domann, T. Chakraborty, and T. Hain.** 2006. Intracellular gene expression profile of *Listeria monocytogenes*. *Infection and Immunity* **74**:1323-1338.
38. **Clark, D. A., K. Foerster, L. Fung, W. He, L. Lee, M. Mendicino, U. R. Markert, R. M. Gorczynski, P. A. Marsden, and G. A. Levy.** 2004. The fgl2 prothrombinase/fibroleukin gene is required for lipopolysaccharide-triggered

- abortions and for normal mouse reproduction. *Molecular Human Reproduction* **10**:99-108.
39. **Comerci, D. J., M. J. Martínez-Lorenzo, R. Sieira, J. P. Gorvel, and R. A. Ugalde.** 2001. Essential role of the VirB machinery in the maturation of the *Brucella abortus*-containing vacuole. *Cellular Microbiology* **3**:159-168.
40. **Corbeil, L. B., K. Blau, T. I. Inzana, K. H. Neilsen, R. H. Jacobson, R. R. Corbeil, and A. J. Winter.** 1988. Killing of *Brucella abortus* by bovine serum. *Infection and Immunity* **56**:3251-3261.
41. **Corbel, M. J.** 1997. Brucellosis: an overview. *Emerging Infectious Disease* **3**:213-221.
42. **Cossart, P., and P. J. Sansonetti.** 2004. Bacterial invasion: The paradigms of enteroinvasive pathogens. *Science* **304**:242-248.
43. **Coxon, P. Y., M. J. Rane, S. Uriarte, D. W. Powell, S. Singh, W. Butt, Q. Chen, and K. R. McLeish.** 2003. MAPK-activated protein kinase-2 participates in p38 MAPK-dependent and ERK-dependent functions in human neutrophils. *Cellular Signalling* **15**:993-1001.
44. **Crescenzi, M., and A. Giuliani.** 2001. The main biological determinants of tumor line taxonomy elucidated by a principal component analysis of microarray data. *FEBS Letters* **507**:114-8.
45. **Davidson, A. L., and J. Chen.** 2004. ATP-binding cassette transporters in bacteria. *Annual Review Biochemistry* **73**:41-68.

46. **Davis, D. S., F. C. Heck, J. D. Williams, T. R. Simpson, and L. G. Adams.** 1988. Interspecific transmission of *Brucella abortus* from experimentally infected coyotes (*Canis latrans*) to parturient cattle. *Journal of Wildlife Disease* **24**:533-537.
47. **Delpino, M. V., J. Cassataro, C. A. Fossati, F. A. Goldbaum, and P. C. Baldi.** 2006. *Brucella* outer membrane protein Omp31 is a haemin-binding protein. *Microbes and Infection* **8**:1203-1208.
48. **Delrue, R. M., C. Deschamps, S. Leonard, C. Nijskens, I. Danese, J. M. Schaus, S. Bonnat, J. Ferooz, A. Tibor, X. De Bolle, and J. J. Letesson.** 2005. A quorum-sensing regulator controls expression of both the type IV secretion system and the flagellar apparatus of *Brucella melitensis*. *Cellular Microbiology* **7**:1151-1161.
49. **Delrue, R. M., P. Lestrade, A. Tibor, J. J. Letesson, and X. De Bolle.** 2004. *Brucella* pathogenesis, genes identified from random large-scale screens. *FEMS Microbiology Letters* **231**:1-12.
50. **Delrue, R. M., M. J. Martínez-Lorenzo, P. Lestrade, I. Danese, V. Bielarz, P. Mertens, X. De Bolle, A. Tibor, J. P. Gorvel, and J. J. Letesson.** 2001. Identification of *Brucella* spp. genes involved in intracellular trafficking. *Cellular Microbiology* **3**:487-497.
51. **DelVecchio, V. G., V. Kapatral, R. J. Redkar, G. Patra, and C. Mujer.** 2002. The genome sequence of the facultative intracellular pathogen *Brucella melitensis*. *PNAS* **99**:443-448.

52. **Detilleux, P. G., B. L. Deyoe, and N. F. Cheville.** 1991. Effect of endocytic and metabolic inhibitors on the internalization and intracellular growth of *Brucella abortus* in Vero cells. *American Journal of Veterinary Research* **52**:1658-1664.
53. **Detilleux, P. G., B. L. Deyoe, and N. F. Cheville.** 1990. Entry and intracellular localization of *Brucella* spp. in Vero cells: Fluorescence and electron microscopy. *Veterinary Pathology* **27**:317-328.
54. **Detilleux, P. G., B. L. Deyoe, and N. F. Cheville.** 1990. Penetration and intracellular growth of *Brucella abortus* in nonphagocytic cells *in vitro*. *Infection and Immunity* **58**:2320-2328.
55. **Dombrecht, B., K. Marchal, J. Vanderleyden, and J. Michiels.** 2002. Prediction and overview of the RpoN-regulon in close related species of Rhizobiales. *Genome Biology* **3**:RESEARCH0076.1-0076.11.
56. **Dornand, J., A. Gross, V. Lafont, J. Liautard, J. Oliaro, and J. P. Liautard.** 2002. The innate immune response against *Brucella* in humans. *Veterinary Microbiology* **90**:383-394.
57. **Dornand, J., V. Lafont, J. Oliaro, A. Terraza, E. I. Castaneda-Roldán, and J. P. Liautard.** 2004. Impairment of intramacrophagic *Brucella suis* multiplication by human natural killer cells through a contact-dependent mechanism. *Infection and Immunity* **72**:2303-2311.
58. **Dorrell, N., P. Guigue-Talet, S. Spencer, V. Foulongne, D. O'Callaghan, and B. W. Wren.** 1999. Investigation into the role of the response regulator NtrC in the metabolism and virulence of *Brucella suis*. *Microbial Pathogenesis* **27**:1-11.

59. **Dorrell, N., S. Spencer, V. Foulongne, P. Guigue-Talet, D. O'Callaghan, and B. W. Wren.** 1998. Identification, cloning and initial characterisation of FeuPQ in *Brucella suis*: a new sub-family of two component regulatory systems. FEMS Microbiology Letters **162**:143-150.
60. **Dougan, G., S. Chatfield, D. Pickard, J. Bester, D. O'Callaghan, and D. Maskell.** 1988. Construction and characterization of vaccine strains of *Salmonella* harboring mutations in two different *aro* genes. The Journal of Infectious Diseases **158**:1329-1335.
61. **Eberl, L.** 1999. N-acyl homoserinelactone-mediated gene regulation in Gram-negative bacteria. Systematic Applied Microbiology **22**:493-506.
62. **Edmonds, M. D., A. Cloeckart, N. J. Booth, W. T. Fulton, S. D. Hagius, J. V. Walker, and P. H. Elzer.** 2001. Attenuation of a *Brucella abortus* mutant lacking a major 25 kDa outer membrane protein in cattle. American Journal of Veterinary Research **62**:1461-1466.
63. **Egarter, C. H., and P. Husslein.** 1992. Biochemistry of myometrial contractility. Bailliere's Clinical Obstetrics and Gynaecology **6**:755-769.
64. **Eggenhofer, E., R. Rachel, M. Haslbeck, and B. Scharf.** 2006. MotD of *Sinorhizobium meliloti* and related alpha proteobacteria is the flagellar-hook-length regulator and therefore reassigned as FliK. Journal of Bacteriology **188**:2144-2153.

65. **Elzer, P. H., S. D. Hagius, D. S. Davis, V. G. Del Vecchio, and F. M. Enright.** 2002. Characterization of the caprine model for ruminant brucellosis. *Veterinary Microbiology* **90**:425-431.
66. **Enright, F. M.** 1990. The pathogenesis and pathobiology of *Brucella* infection in domestic animals, p. 301-320. *In* K. Nielsen and J. R. Duncan (ed.), *Animal brucellosis*. CRC Press, Boca Raton, Florida.
67. **Ernst, F. D., E. J. Kuipers, A. Heijens, R. Sarwari, J. Stoof, C. W. Penn, J. G. Kusters, and A. H. M. van Vliet.** 2005. The nickel-responsive regulator NikR controls activation and repression of gene transcription in *Helicobacter pylori*. *Infection and Immunity* **73**:7252-7258.
68. **Eskra, L., A. Canavessi, M. Carey, and G. Splitter.** 2001. *Brucella abortus* genes identified following constitutive growth and macrophage infection. *Infection and Immunity* **69**:7736-7742.
69. **Eskra, L., A. Mathison, and G. Splitter.** 2003. Microarray analysis of mRNA levels from RAW264.7 macrophages infected with *Brucella abortus*. *Infection and Immunity* **71**:1125-1133.
70. **Everts, R. E., M. R. Band, Z. L. Liu, C. G. Kumar, L. Liu, J. J. Loor, R. Oliveira, and H. A. Lewin.** 2005. A 7872 cDNA microarray and its use in bovine functional genomics. *Veterinary Immunology and Immunopathology* **105**:235-245.
71. **Eze, M. O., L. Yuan, R. M. Crawford, C. M. Paranavitana, T. L. Hadfield, A. K. Bhattacharjee, R. L. Warren, and D. L. Hoover.** 2000. Effects of

- opsonization and gamma interferon on growth of *Brucella melitensis* 16M in mouse peritoneal macrophages in vitro. *Infection and Immunity* **68**:257-263.
72. **Fernández-Prada, C. M., M. Nikolich, R. Vemulapalli, N. Sriranganathan, S. M. Boyle, G. G. Schurig, T. L. Hadfield, and D. L. Hoover.** 2001. Deletion of *wboA* enhances activation of the lectin pathway of complement in *Brucella abortus* and *Brucella melitensis*. *Infection and Immunity* **69**:4407-4416.
73. **Fernández-Prada, C. M., E. B. Zelazowska, M. Nikolich, T. L. Hadfield, R. M. Roop II, G. L. Robertson, and D. L. Hoover.** 2003. Interactions between *Brucella melitensis* and human phagocytes: Bacterial surface O-polysaccharide inhibits phagocytosis, bacterial killing, and subsequent host cell apoptosis. *Infection and Immunity* **71**:2110-2119.
74. **Ficht, T. A.** 2003. Intracellular survival of *Brucella*: defining the link with persistence. *Veterinary Microbiology* **92**:213-223.
75. **Finlay, B. B., and P. Cossart.** 1997. Exploitation of mammalian host cell functions by bacterial pathogens. *Science* **276**:718-725.
76. **Finlay, B. B., and S. Falkow.** 1997. Common themes in microbial pathogenicity revisited. *Microbiology and Molecular Biology Reviews* **61**:136-169.
77. **Finlay, B. B., and R. E. W. Hancock.** 2004. Can innate immunity be enhanced to treat microbial infections? *Natural Reviews in Microbiology* **2**:497-504.
78. **Forbes, L. B., and S. V. Tessaro.** 2003. Evaluation of cattle for experimental infection with and transmission of *Brucella suis* biovar 4. *Journal of American Veterinary Medical Association* **222**:1252-1256.

79. **Forestier, C., F. Deleuil, N. Lapaque, E. Moreno, and J. P. Gorvel.** 2000. *Brucella abortus* lipopolysaccharide in murine peritoneal macrophages acts as a down-regulator of T cell activation. *The Journal of Immunology* **165**:5202-5210.
80. **Forestier, C., E. Moreno, J. Pizarro-Cerdá, and J. P. Gorvel.** 1999. Lysosomal accumulation and recycling of lipopolysaccharide to the cell surface of murine macrophages, an *in vitro* and *in vivo* study. *The Journal of Immunology* **162**:6784-6791.
81. **Foster, S. L., S. H. Richardson, and M. L. Failla.** 2001. Elevated iron status increases bacterial invasion and survival and alters cytokine/chemokine mRNA expression in Caco-2 human intestinal cells. *Journal of Nutrition* **131**:1452-8.
82. **Foulongne, V., G. Bourg, C. Cazeville, S. Michaux-Charachon, and D. O'Callaghan.** 2000. Identification of *Brucella suis* genes affecting intracellular survival in an *in vitro* human macrophage infection model by signature-tagged transposon mutagenesis. *Infection and Immunity* **68**:1297-1303.
83. **Frencht, A. R., E. B. Holroyd, L. Yang, S. Kim, and W. M. Yokoyama.** 2006. IL-18 acts synergistically with IL-15 in stimulating natural killer cell proliferation. *Cytokine* **35**:229-234.
84. **Fretin, D., A. Faucommier, S. Kohler, S. M. Halling, S. Léonard, C. Nijskens, J. Ferrooz, P. Lestrade, R. M. Delrue, I. Danese, J. Vandenhaute, A. Tibor, X. De Bolle, and J. J. Letesson.** 2005. The sheathed flagellum of *Brucella melitensis* is involved in persistence in a murine model of infection. *Cellular Microbiology* **7**:687-698.

85. **Galán, J. E., and D. Zhou.** 2000. Striking a balance: modulation of the actin cytoskeleton by *Salmonella*. PNAS **97**:8754-8761.
86. **Galdiero, E., C. Romano Carratelli, M. Vitiello, I. Nuzzo, E. Del Vecchio, C. Bentivoglio, G. Perillo, and F. Galdiero.** 2000. HSP and apoptosis in leukocytes from infected or vaccinated animals by *Brucella abortus*. New Microbiology **23**:271-279.
87. **García Carrillo, C.** 1990. Laboratory animal models for brucellosis studies, p. 423-442. In K. Nielsen and J. R. Duncan (ed.), Animal brucellosis. CRC Press, Boca Raton, Florida.
88. **García Carrillo, C., and R. Casas Olascoaga.** 1977. Comparison of two challenge strains used to test the potency of *Brucella abortus* vaccines. The British Veterinary Journal **133**:554-558.
89. **Ge, J., D. M. Catt, and R. L. Gregory.** 2004. *Streptococcus mutans* surface alpha-enolase binds salivary mucin MG2 and human plasminogen. Infection and Immunity **72**:6748-6752.
90. **Giambartolomei, G. H., A. Zwerdling, J. Cassataro, L. Bruno, C. A. Fossati, and M. T. Philipp.** 2004. Lipoproteins, not lipopolysaccharide, are the key mediators of the proinflammatory response elicited by heat-killed *Brucella abortus*. The Journal of Immunology **173**:4635-4642.
91. **Godfroid, F., B. Taminau, I. Danese, P. Denoel, A. Tibor, V. Weynants, A. Cloeckert, J. Godfroid, and J. J. Letesson.** 1998. Identification of the perosamine synthetase gene of *Brucella melitensis* 16M and involvement of

- lipopolysaccharide O side chain in *Brucella* survival in mice and in macrophages. *Infection and Immunity* **66**:5485-5493.
92. **Godfroid, J., A. Cloeckert, J. P. Liautard, S. Kohler, D. Fretin, K. Walravens, B. Garin-Bastuji, and J. J. Letesson.** 2005. From the discovery of the Malta fever's agent to the discovery of a marine mammal reservoir, brucellosis has continuously been a re-emerging zoonosis. *Veterinary Research* **36**:313-326.
93. **Gorvel, J. P., and E. Moreno.** 2002. *Brucella* intracellular life: from invasion to intracellular replication. *Veterinary Microbiology* **90**:281-297.
94. **Green, B. T., M. Lyte, A. Kulkarni-Narla, and D. R. Brown.** 2003. Neuromodulation of enteropathogen internalization in Peyer's patches from porcine jejunum. *Journal of Neuroimmunology* **141**:74-82.
95. **Gregory, J. L., E. F. Morand, S. J. McKeown, J. A. Ralph, P. Hall, Y. H. Yang, S. R. McColl, and M. J. Hickey.** 2006. Macrophage migration inhibitory factor induces macrophage recruitment via CC chemokine ligand 2. *The Journal of Immunology* **177**:8072-8079.
96. **Gross, A., A. Terraza, S. Ouahrani-Bettache, J. P. Liautard, and J. Dornand.** 2000. *In vitro Brucella suis* infection prevents the programmed cell death of human monocytic cells. *Infection and Immunity* **68**:342-351.
97. **Grutzkau, A., C. Hanski, H. Hahn, and E. O. Riecken.** 1990. Involvement of M cells in the bacterial invasion of Peyer's patches: a common mechanism shared by *Yersinia enterocolitica* and other enteroinvasive bacteria. *Gut* **31**:1011-1015.

98. **Guzmán-Verri, C., E. Chaves-Olarte, C. von Eichel-Streiber, I. López-Goni, M. Thelestam, S. Arvidson, J. P. Gorvel, and E. Moreno.** 2001. GTPases of the Rho subfamily are required for *Brucella abortus* internalization in nonprofessional phagocytes. *The Journal of Biological Chemistry* **276**:44435-44443.
99. **Guzmán-Verri, C., L. Manterola, A. Sola-Landa, A. Parra, A. Cloeckert, J. Garin, J. P. Gorvel, I. Moriyón, E. Moreno, and I. López-Goni.** 2002. The two-component system BvrR/BvrS essential for *Brucella abortus* virulence regulates the expression of outer membrane proteins with counterparts in members of the *Rhizobiaceae*. *PNAS* **99**:12375-12380.
100. **Haine, V., M. Dozot, J. Dornand, J. J. Letesson, and X. De Bolle.** 2006. NnrA is required for full virulence and regulates several *Brucella melitensis* denitrification genes. *Journal of Bacteriology* **188**:1615-1619.
101. **Haine, V., A. Sinon, F. Van Steen, S. Rousseau, M. Dozot, P. Lestrade, C. Lambert, J. J. Letesson, and X. De Bolle.** 2005. Systematic targeted mutagenesis of *Brucella melitensis* 16M reveals a major role for GntR regulators in the control of virulence. *Infection and Immunity* **73**:5578-5586.
102. **Halling, S. M., B. D. Peterson-Burch, B. J. Bricker, R. L. Zuerner, Z. Qing, L. L. Li, V. Kapur, D. P. Alt, and S. C. Olsen.** 2005. Completion of the genome sequence of *Brucella abortus* and comparison to the highly similar genomes of *Brucella melitensis* and *Brucella suis*. *Journal of Bacteriology* **187**:2715-2726.

103. **Harmon, B. G., L. G. Adams, J. W. Templeton, and R. Smith III.** 1989. Macrophage function in mammary glands of *Brucella abortus*-infected cows and cows that resisted infection after inoculation of *Brucella abortus*. *American Journal of Veterinary Research* **50**:459-465.
104. **He, Y., S. Reichow, S. Ramamoorthy, X. Ding, R. Lathigra, J. C. Craig, B. W. S. Sobral, G. G. Schurig, N. Sriranganathan, and S. M. Boyle.** 2006. *Brucella melitensis* triggers time-dependent modulation of apoptosis and down-regulation of mitochondrion-associated gene expression in mouse macrophages. *Infection and Immunity* **74**:5035-5046.
105. **Hegde, P., R. Qi, K. Abernathy, C. Gay, S. Dharap, R. Gaspard, J. E. Hughes, E. Snesrud, N. Lee, and J. Quackenbush.** 2000. A concise guide to cDNA microarray analysis. *BioTechniques* **29**:548-562.
106. **Heymann, P., M. Gerads, M. Schaller, F. Dromer, G. Winkelmann, and J. F. Ernst.** 2002. The siderophore iron transporter of *Candida albicans* (Sit1p/Arn1p) mediates uptake of ferrichrome-type siderophores and is required for epithelial invasion. *Infection and Immunity* **70**:5246-5255.
107. **Hobbie, S., L. M. Chen, R. J. Davis, and J. E. Galán.** 1997. Involvement of mitogen-activated protein kinase pathways in the nuclear responses and cytokine production induced by *Salmonella typhimurium* in cultured intestinal epithelial cells. *The Journal of Immunology* **159**:5550-5559.

108. **Holland, I. B., L. Schmitt, and J. Young.** 2005. Type 1 protein secretion in bacteria, the ABC-transporter dependent pathway. *Molecular Membrane Biology* **22**:29-39.
109. **Hong, P. C., R. M. Tsois, and T. A. Ficht.** 2000. Identification of genes required for chronic persistence of *Brucella abortus* in mice. *Infection and Immunity* **68**:4102-4107.
110. **Hoshino, T., R. H. Wiltrout, and H. A. Young.** 1999. IL-18 is a potent coinducer of IL-13 in NK and T cells: a new potential role for IL-18 in modulating the immune response. *The Journal of Immunology* **162**:5070-5077.
111. **Howie, A., H. A. Leaver, I. D. Aitken, L. A. Hay, I. E. Anderson, G. E. Williams, and G. Jones.** 1989. The effect of chlamydial infection on the initiation of premature labour: serial measurements of intrauterine prostaglandin E2 in amniotic fluid, allantoic fluid and utero-ovarian vein, using catheterised sheep experimentally infected with an ovine abortion strain of *Chlamydia psittaci*. *Prostaglandins, Leukotriens and Essential Fatty Acids* **37**:203-211.
112. **Hu, C. M., S. Y. Jang, J. C. Fanzo, and A. B. Pernis.** 2002. Modulation of T cell cytokine production by interferon regulatory factor-4. *The Journal of Biological Chemistry* **277**:49238-49246.
113. **Huang, L. Y., J. Aliberti, C. A. Leifer, D. M. Segal, A. Sher, D. T. Golenbock, and B. Golding.** 2003. Heat-killed *Brucella abortus* induces TNF and IL-12p40 by distinct MyD88-dependent pathways: TNF, unlike IL-12p40

- secretion, is Toll-like receptor 2 dependent. *The Journal of Immunology* **171**:1441-1446.
114. **Inglis, T. J. J., T. Robertson, D. E. Woods, N. Dutton, and B. J. Chang.** 2003. Flagellum-mediated adhesion by *Burkholderia pseudomallei* precedes invasion of *Acanthamoeba astronyxis*. *Infection and Immunity* **71**:2280-2282.
115. **Ishiwata, H., S. Katsuma, K. Kizaki, O. V. Patel, H. Nakano, T. Takahashi, K. Imai, A. Hirasawa, S. Shiojima, H. Ikawa, Y. Suzuki, G. Tsujimoto, Y. Izaike, J. Todoroki, and K. Hashizume.** 2003. Characterization of gene expression profiles in early bovine pregnancy using a custom cDNA microarray. *Molecular Reproduction and Development* **65**:9-18.
116. **Jakobsson, P. J., S. Thorën, R. Morgenstern, and B. Samuelsson.** 1999. Identification of human prostaglandin E synthase: A microsomal, glutathione-dependent, inducible enzyme, constituting a potential novel drug target. *PNAS* **96**:7220-7225.
117. **Jarvis, B. W., T. H. Harris, N. Qureshi, and G. A. Splitter.** 2002. Rough lipopolysaccharide from *Brucella abortus* and *Escherichia coli* differentially activates the same mitogen-activated protein kinase signaling pathways for tumor necrosis factor alpha in RAW 264.7 macrophage-like cells. *Infection and Immunity* **70**:7165-7168.
118. **Jenkin, G., and I. R. Young.** 2004. Mechanisms responsible for parturition; the use of experimental models. *Animal Reproduction Science* **82-83**:567-581.

119. **Jiang, X., and C. L. Baldwin.** 1993. Effects of cytokines on intracellular growth of *Brucella abortus*. *Infection and Immunity* **61**:124-134.
120. **Jiménez de Bagués, M. P., S. Dubal, J. Dornand, and A. Gross.** 2005. Cellular bioterrorism: How *Brucella* corrupts macrophage physiology to promote invasion and proliferation. *Clinical Immunology* **114**:227-238.
121. **Jiménez de Bagués, M. P., A. Gross, A. Terraza, and J. Dornand.** 2005. Regulation of the mitogen-activated protein kinases by *Brucella* spp. expressing a smooth and rough phenotype: Relationship to pathogen invasiveness. *Infection and Immunity* **73**:3178-3183.
122. **Jiménez de Bagués, M. P., A. Terraza, A. Gross, and J. Dornand.** 2004. Different responses of macrophages to smooth and rough *Brucella* spp.: Relationship to virulence. *Infection and Immunity* **72**:2429-2433.
123. **John, T., B. Kohl, A. Mobasheri, W. Ertel, and M. Shakibaei.** 2007. Interleukin-18 induces apoptosis in human articular chondrocytes. *Histology and Histopathology* **22**:469-482.
124. **Johnson, G. L., and R. Lapadat.** 2002. Mitogen-activated protein kinase pathways mediated by ERK, JNK, and p38 protein kinases. *Science* **298**:1911-1912.
125. **Johnson, R. F., C. M. Mitchell, V. Clifton, and T. Zakar.** 2004. Regulation of 15-hydroxyprostaglandin dehydrogenase (PGDH) gene activity, messenger ribonucleic acid processing, and protein abundance in the human chorion in late

- gestation and labor. *The Journal of Clinical Endocrinology & Metabolism* **89**:5639-5648.
126. **Jones, S. M., and A. J. Winter.** 1992. Survival of virulent and attenuated strain of *Brucella abortus* in normal and gamma interferon-activated murine peritoneal macrophages. *Infection and Immunity* **60**:3011-3014.
127. **Jubier-Maurin, V., R. A. Boigegrain, A. Cloeckaert, A. Gross, M. T. Alvarez-Martínez, A. Terraza, J. Liautard, S. Kohler, B. Rouot, J. Dornand, and J. P. Liautard.** 2001. Major Outer Membrane Protein Omp25 of *Brucella suis* is involved in inhibition of tumor necrosis factor alpha production during infection of human macrophages. *Infection and Immunity* **69**:4823-4830.
128. **Jumas-Bilak, E., S. Michaux-Charachon, G. Bourg, D. O'Callaghan, and M. Ramuz.** 1998. Differences in chromosome number and genome rearrangements in the genus *Brucella*. *Molecular Microbiology* **27**:99-106.
129. **Kalher, S. C.** 2000. *Brucella melitensis* infection discovered in cattle for first time, goats also infected. *Journal of American Veterinary Medical Association* **216**:648.
130. **Keasling, J. D., L. Bertsch, and A. Kornberg.** 1993. Guanosine pentaphosphate phosphohydrolase of *Escherichia coli* is a long-chain exopolyphosphatase. *PNAS* **90**:7029-7033.
131. **Kim, S., M. Watarai, Y. Kondo, J. Erdenebaatar, S. I. Makino, and T. Shirahata.** 2003. Isolation and characterization of mini-Tn5km2 insertion

- mutants of *Brucella abortus* deficient in internalization and intracellular growth in HeLa cells. *Infection and Immunity* **71**:3020-3027.
132. **Kohler, S., V. Foulongne, S. Ouahrani-Bettache, G. Bourg, J. Teyssier, M. Ramuz, and J. P. Liautard.** 2002. The analysis of the intramacrophagic virulome of *Brucella suis* deciphers the environment encountered by the pathogen inside the macrophage host cell. *PNAS* **99**:15711-15716.
133. **Kuldau, G. A., G. De Vos, J. Owen, G. McCaffrey, and P. Zambryski.** 1990. The *virB* operon of *Agrobacterium tumefaciens* pTiC58 encodes 11 open reading frames. *Molecular and General Genetics* **221**:256-266.
134. **Kusumawati, A., C. Cazeville, F. Porte, S. Bettache, J. P. Liautard, and J. Sri Widada.** 2000. Early events and implication of F-actin and annexin I associated structures in the phagocytic uptake of *Brucella suis* by the J-774A.1 murine cell line and human monocytes. *Microbial Pathogenesis* **28**:343-352.
135. **Kwan, W. C., W. R. McMaster, N. Wong, and N. E. Reiner.** 1992. Inhibition of expression of major histocompatibility complex class II molecules in macrophages infected with *Leishmania donovani* occurs at the level of gene transcription via a cyclic AMP-independent mechanism. *Infection and Immunity* **60**:2115-2120.
136. **Lanier, L. L., B. C. Corliss, J. Wu, C. Leong, and J. H. Phillips.** 1998. Immunoreceptor DAP12 bearing a tyrosine-based activation motif is involved in activating NK cells. *Nature* **391**:703-707.

137. **Lapaque, N., F. Forquet, C. de Chastellier, Z. Mishal, G. Jolly, E. Moreno, I. Moriyón, J. E. Heuser, H. T. He, and J. P. Gorvel.** 2006. Characterization of *Brucella abortus* lipopolysaccharide macrodomains as mega rafts. *Cellular Microbiology* **8**:197-206.
138. **Lapaque, N., I. Moriyón, E. Moreno, and J. P. Gorvel.** 2005. *Brucella* lipopolysaccharide acts as a virulence factor. *Current Opinion in Microbiology* **8**:60-66.
139. **Lathem, W. W., S. D. Crosby, V. L. Miller, and W. E. Goldman.** 2005. Progression of primary pneumonic plague: A mouse model of infection, pathology, and bacterial transcriptional activity. *PNAS* **102**:17786-17791.
140. **Lavigne, J. P., G. Patey, F. J. Sangari, G. Bourg, M. Ramuz, D. O'Callaghan, and S. Michaux-Charachon.** 2005. Identification of a new virulence factor, BvfA, in *Brucella suis*. *Infection and Immunity* **73**:5524-5529.
141. **Lawson, J. N., and S. A. Johnston.** 2006. Amplification of sense-stranded prokaryotic RNA. *DNA and Cell Biology* **25**:627-634.
142. **Lawson, J. N., C. R. Lyons, and S. A. Johnston.** 2006. Expression profiling of *Yersinia pestis* during mouse pulmonary infection. *DNA and Cell Biology* **25**:608-616.
143. **Lee, C. A., and S. Falkow.** 1990. The ability of *Salmonella* to enter mammalian cells is affected by bacterial growth state. *PNAS* **87**:4304-4308.
144. **Legler, D. F., M. Loetscher, R. S. Roos, I. Clark-Lewis, M. Baggiolini, and B. Moser.** 1998. B cell-attracting chemokine 1, a human CXC chemokine expressed

- in lymphoid tissues, selectively attracts B lymphocytes via BLR1/CXCR5. *The Journal of Experimental Medicine* **187**:655-660.
145. **Leng, L., C. N. Metz, Y. Fang, J. Xu, S. Donnelly, J. Baugh, T. Delohery, Y. Chen, R. A. Mitchell, and R. Bucala.** 2003. MIF signal transduction initiated by binding to CD74. *The Journal of Experimental Medicine* **197**:1467-1476.
146. **Lestrade, P., R. M. Delrue, I. Danese, C. Didembourg, B. Taminiau, P. Mertens, X. De Bolle, A. Tibor, C. M. Tang, and J. J. Letesson.** 2000. Identification and characterization of in vivo attenuated mutants of *Brucella melitensis*. *Molecular Microbiology* **38**:543-551.
147. **Lestrade, P., A. Dricot, R. M. Delrue, C. Lambert, V. Martinelli, X. De Bolle, J. J. Letesson, and A. Tibor.** 2003. Attenuated signature-tagged mutagenesis mutants of *Brucella melitensis* identified during the acute phase of infection in mice. *Infection and Immunity* **71**:7053-7060.
148. **Lissoni, P., S. Barni, G. Tancini, V. Fossati, and F. Frigerio.** 1994. Pineal- opioid system interactions in the control of immunoinflammatory responses. *Annals of the New York Academic of Science* **741**:191-196.
149. **López-Goni, I., C. Guzmán-Verri, L. Manterola, A. Sola-Landa, I. Moriyón, and E. Moreno.** 2002. Regulation of *Brucella* virulence by the two-component system BvrR/BvrS. *Veterinary Microbiology* **90**:329-339.
150. **López-Urrutia, L., A. Alonso, M. L. Nieto, Y. Bayón, A. Orduna, and M. Sánchez Crespo.** 2000. Lipopolysaccharides of *Brucella abortus* and *Brucella*

- melitensis* induce nitric oxide synthesis in rat peritoneal macrophages. *Infection and Immunity* **68**:1740-1745.
151. **Manger, I. D., and D. A. Relman.** 2000. How the host 'sees' pathogens: Global gene expression responses to infection. *Current Opinion in Immunology* **12**:215-218.
152. **Manteca, C., G. Daube, T. Jauniaux, A. Linden, V. Pirson, J. Detilleux, A. Ginter, P. Coppe, A. Kaeckenbeeck, and J. G. Mainil.** 2002. A role for the *Clostridium perfringens* beta2 toxin in bovine enterotoxaemia. *Veterinary Microbiology* **86**:191-202.
153. **Marko, N. F., B. Frank, J. Quackenbush, and N. H. Lee.** 2005. A robust method for the amplification of RNA in the sense orientation. *BMC Genomics* **6**:27.
154. **Martínez de Tejada, G., J. Pizarro-Cerdá, E. Moreno, and I. Moriyón.** 1995. The outer membranes of *Brucella* spp. are resistant to bactericidal cationic peptides. *Infection and Immunity* **63**:3054-3061.
155. **McQuiston, J. R., R. Vemulapalli, T. I. Inzana, G. G. Schurig, N. Sriranganathan, D. Fritzinger, T. L. Hadfield, R. A. Warren, N. Snellings, D. L. Hoover, S. M. Halling, and S. M. Boyle.** 1999. Genetic characterization of a Tn5-disrupted glycosyltransferase gene homolog in *Brucella abortus* and its effect on lipopolysaccharide composition and virulence. *Infection and Immunity* **67**:3830-3835.

156. **Meador, V. P., and B. L. Deyoe.** 1989. Intracellular localization of *Brucella abortus* in bovine placenta. *Veterinary Pathology* **26**:513-515.
157. **Mense, M. G., L. L. van de Verg, A. K. Bhattacharjee, J. L. Garrett, J. A. Hart, L. E. Lindler, T. L. Hadfield, and D. L. Hoover.** 2001. Bacteriologic and histologic features in mice after intranasal inoculation of *Brucella melitensis*. *American Journal of Veterinary Research* **62**:398-405.
158. **Micallef, M. J., T. Ohtsuki, K. Kohno, F. Tanabe, S. Ushio, M. Namba, T. Tanimoto, K. Torigoe, M. Fujii, M. Ikeda, S. Fukuda, and M. Kurimoto.** 1996. Interferon-gamma-inducing factor enhances T helper 1 cytokine production by stimulated human T cells: Synergism with interleukin-12 for interferon gamma production. *European Journal of Immunology* **26**:1647-1651.
159. **Molofsky, A. B., and M. S. Swanson.** 2004. Differentiate to thrive: lessons from the *Legionella pneumophila* life cycle. *Molecular Microbiology* **53**:29-40.
160. **Moreno, E., and I. Moriyón.** 2002. *Brucella melitensis*: A nasty bug with hidden credentials for virulence. *PNAS* **99**:1-3.
161. **Moreno, E., E. Stackebrandt, M. Dorsch, J. Wolters, M. Busch, and H. Mayer.** 1990. *Brucella abortus* 16S rRNA and lipid A reveal a phylogenetic relationship with members of the alpha-2 subdivision of the class Proteobacteria. *Journal of Bacteriology* **172**:3569-3576.
162. **Mounier, J., F. K. Bahrani, and P. J. Sansonetti.** 1997. Secretion of *Shigella flexneri* Ipa invasins on contact with epithelial cells and subsequent entry of the

- bacterium into cells are growth stage dependent. *Infection and Immunity* **65**:774-782.
163. **Mukherjee, S., G. Keitany, Y. Li, Y. Wang, H. Ball, E. J. Goldsmith, and K. Orth.** 2006. *Yersinia* YopJ acetylates and inhibits kinase activation by blocking phosphorylation. *Science* **312**:1211-1214.
164. **Mulero, J. J., A. M. Pace, S. T. Nelken, D. B. Loeb, T. R. Correa, R. Drmanac, and J. E. Ford.** 1999. *IL1HY1*: a novel interleukine-1 receptor antagonist gene. *Biochemical and Biophysical Research Communications* **263**:702-706.
165. **Muzny, D. M., T. A. Ficht, J. W. Templeton, and L. G. Adams.** 1989. DNA homology of *Brucella abortus* strains 19 and 2308. *American Journal of Veterinary Research* **50**:655-661.
166. **Naroeni, A., N. Jouy, S. Ouahrani-Bettache, J. P. Liautard, and F. Porte.** 2001. *Brucella suis*-impaired specific recognition of phagosomes by lysosomes due to phagosomal membrane modifications. *Infection and Immunity* **69**:486-493.
167. **Naroeni, A., and F. Porte.** 2002. Role of cholesterol and the ganglioside GM1 in entry and short-term survival of *Brucella suis* in murine macrophages. *Infection and Immunity* **70**:1640-1644.
168. **Nickerson, C. A., and C. M. Ott.** 2004. A new dimension in modeling infectious disease. *ASM News* **70**:169-175.

169. **O'Callaghan, D., C. Cazevieille, A. Allardet-Servent, M. L. Boschioli, G. Bourg, V. Foulongne, P. Frutos, Y. Kulakov, and M. Roamuz.** 1999. A homologue of the *Agrobacterium tumefaciens* VirB and *Bordetella pertussis* Ptl type IV secretion systems is essential for intracellular survival of *Brucella suis*. *Molecular Microbiology* **33**:1210-1220.
170. **Oliveira, S. C., and G. Splitter.** 1995. CD8+ type 1 CD44hi CD45 RBlo T lymphocytes control intracellular *Brucella abortus* infection as demonstrated in major histocompatibility complex class I and class II-deficient mice. *European Journal of Immunology* **25**:2551-2557.
171. **Olsen, S. C., C. O. Thoen, and N. F. Cheville.** 2004. *Brucella*, p. 309-319. In C. L. Gyles, J. F. Prescott, J. G. Songer, and C. O. Thoen (ed.), *Pathogenesis of bacterial infections in animals*, Third ed. Blackwell Publishing Ltd., Ames, Iowa.
172. **Orduna, A., C. Orduna, J. M. Eiros, M. A. Bratos, P. Gutiérrez, P. Alonso, and A. Rodríguez Torres.** 1991. Inhibition of the degranulation and myeloperoxidase activity of human polymorphonuclear neutrophils by *Brucella melitensis*. *Microbiología* **7**:113-119.
173. **Palmer, L. E., S. Hobbie, J. E. Galán, and J. B. Bliska.** 1998. YopJ of *Yersinia pseudotuberculosis* is required for the inhibition of macrophage TNF- α production and downregulation of the MAP kinases p38 and JNK. *Molecular Microbiology* **27**:953-965.

174. **Pancholi, V., P. Fontan, and H. Jin.** 2003. Plasminogen-mediated group A streptococcal adherence to and pericellular invasion of human pharyngeal cells. *Microbial Pathogenesis* **35**:293-303.
175. **Paulsen, I. T., R. Seshadri, K. Nelson, J. A. Eisen, and J. F. Heidelberg.** 2002. The *Brucella suis* genome reveals fundamental similarities between animal and plant pathogens and symbionts. *PNAS* **99**:13148-13153.
176. **Pei, J., and T. A. Ficht.** 2004. *Brucella abortus* rough mutants are cytopathic for macrophages in culture. *Infection and Immunity* **72**:440-450.
177. **Pepe, J. C., J. L. Badger, and V. L. Miller.** 1994. Growth phase and low pH affect the thermal regulation of the *Yersinia enterocolitica inv* gene. *Molecular Microbiology* **11**:123-135.
178. **Piddock, L. J. V.** 2006. Multidrug-resistance efflux pumps: not just for resistance. *Nature Reviews Microbiology* **4**:629-636.
179. **Pizarro-Cerdá, J., S. Méresse, R. G. Parton, G. van der Goot, A. Solalanda, I. López-Goni, E. Moreno, and J. P. Gorvel.** 1998. *Brucella abortus* transits through the autophagic pathway and replicates in the endoplasmic reticulum of non-professional phagocytes. *Infection and Immunity* **66**:5711-5724.
180. **Pizarro-Cerdá, J., E. Moreno, V. Sanguedolce, J. L. Mege, and J. P. Gorvel.** 1998. Virulent *Brucella abortus* prevents lysosome fusion and is distributed within autophagosome-like compartments. *Infection and Immunity* **66**:2387-2392.

181. **Plant, J. W., G. J. Eamens, and J. T. Seaman.** 1986. Serological, bacteriological and pathological changes in rams following different routes of exposure to *Brucella ovis*. Australian Veterinary Journal **63**:409-412.
182. **Ponath, P. D., S. Qin, T. W. Post, J. Wang, L. Wu, N. P. Gerard, W. Newman, C. Gerard, and C. R. Mackay.** 1996. Molecular cloning and characterization of a human eotaxin receptor expressed selectively on eosinophils. The Journal of Experimental Medicine **183**:2437-2448.
183. **Porte, F., J. P. Liautard, and S. Kohler.** 1999. Early acidification of phagosomes containing *Brucella suis* is essential for intracellular survival in murine macrophages. Infection and Immunity **67**:4041-4047.
184. **Porte, F., A. Naroeni, S. Ouahrani-Bettache, and J. P. Liautard.** 2003. Role of the *Brucella suis* lipopolysaccharide O antigen in phagosomal genesis and in inhibition of phagosome-lysosome fusion in murine macrophages. Infection and Immunity **71**:1481-1490.
185. **Rajashekara, G., J. D. Glasner, D. A. Glover, and G. Splitter.** 2004. Comparative whole-genome hybridization reveals genomic islands in *Brucella* species. Journal of Bacteriology **186**:5040-5051.
186. **Ramos, H. C., M. Rumbo, and J. C. Sirard.** 2004. Bacterial flagellins: mediators of pathogenicity and host immune responses in mucosa. TRENDS in Microbiology **12**:509-517.
187. **Ramos, J. L., M. Martínez-Bueno, A. J. Molina-Henares, W. Terán, K. Watanabe, X. Zhang, M. T. Gallegos, R. Brennan, and R. Tobes.** 2005. The

- TetR family of transcriptional repressors. *Microbiology and Molecular Biology Reviews* **69**:326-356.
188. **Rasool, O., E. Freer, E. Moreno, and C. Jarstrand.** 1992. Effect of *Brucella abortus* lipopolysaccharide on oxidative metabolism and lysozyme release by human neutrophils. *Infection and Immunity* **60**:1699-1702.
189. **Rhodius, V.** 2002. Purification of RNA from *E. coli*, p. 149-152. In D. Bowtell and J. Sambrook (ed.), *DNA microarrays*. Cold Spring Harbor Laboratory Press, Cold Spring Harbor, New York.
190. **Rittig, M. G., M. T. Alvarez-Martínez, F. Porte, J. P. Liautard, and B. Rouot.** 2001. Intracellular survival of *Brucella* spp. in human monocytes involves conventional uptake but special phagosomes. *Infection and Immunity* **69**:3995-4006.
191. **Rittig, M. G., A. Kaufmann, A. Robins, B. Shaw, H. Sprenger, D. Gemsa, V. Foulongne, B. Rouot, and J. Dornand.** 2003. Smooth and rough lipopolysaccharide phenotypes of *Brucella* induce different intracellular trafficking and cytokine/chemokine release in human monocytes. *Journal of Leukocyte Biology* **74**:1045-1055.
192. **Robertson, G. L., M. E. Kovach, C. A. Allen, T. A. Ficht, and R. M. Roop II.** 2000. The *Brucella abortus* Lon functions as a generalized stress response protease and is required for wild-type virulence in BALB/c mice. *Molecular Microbiology* **35**:577-588.

193. **Robertson, G. L., and R. M. Roop II.** 1999. The *Brucella abortus* host factor I (HF-I) protein contributes to stress resistance during stationary phase and is a major determinant of virulence in mice. *Molecular Microbiology* **34**:690-700.
194. **Roop II, R. M., B. H. Bellaire, M. W. Valderas, and J. A. Cardelli.** 2004. Adaptation of the brucellae to their intracellular niche. *Molecular Microbiology* **52**:621-630.
195. **Ross, H. M., G. Foster, R. J. Reid, K. L. Jahans, and A. P. MacMillan.** 1994. *Brucella* species infection in sea mammals. *Veterinary Record* **134**:359.
196. **Roux, C. M., H. G. Roldán, R. L. Santos, P. D. Beremand, T. L. Thomas, L. G. Adams, and R. M. Tsolis.** *Brucella* requires a functional type IV secretion system to elicit innate immune responses in mice. *Cellular Microbiology*, in press.
197. **Russell, S. M., A. D. Keegan, N. Harada, Y. Nakamura, M. Noguchi, P. Leland, M. C. Friedmann, A. Miyajima, R. K. Puri, W. E. Paul, and et al.** 1993. Interleukin-2 receptor gamma chain: A functional component of the interleukin-4 receptor. *Science* **262**:1880-1883.
198. **Salmerón, I., M. Rodríguez-Zapata, O. Salmerón, L. Manzano, S. Vaquer, and M. Alvarez-Mon.** 1992. Impaired activity of natural killer cells in patients with acute brucellosis. *Clinical Infectious Diseases* **15**:764-770.
199. **Salyers, A. A., and D. D. Whitt.** 2002. Bacterial pathogenesis: A molecular approach, Second ed. ASM Press, Washington, D.C.

200. **Samartino, L. E., R. E. Truax, and F. M. Enright.** 1994. Invasion and replication of *Brucella abortus* in three different trophoblastic cell lines. *Zentralbl Veterinarmed [B]* **41**:229-236.
201. **Sandhu, K. S., and C. L. Gyles.** 2002. Pathogenic shiga toxin-producing *Escherichia coli* in the intestine of calves. *Canadian Journal Veterinary Research* **66**:65-72.
202. **Sangari, F. J., A. Seoane, M. C. Rodriguez, J. Agüero, and J. M. García Lobo.** 2007. Characterization of the urease operon of *Brucella abortus* and assessment of its role in virulence of the bacterium. *Infection and Immunity* **75**:774-780.
203. **Santos, R. L., R. M. Tsolis, S. Zhang, T. A. Ficht, A. J. Baümler, and L. G. Adams.** 2001. *Salmonella*-induced cell death is not required for enteritis in calves. *Infection and Immunity* **69**:4610-4617.
204. **Santos, R. L., S. Zhang, R. M. Tsolis, A. J. Baümler, and L. G. Adams.** 2002. Morphologic and molecular characterization of *Salmonella typhimurium* infection in neonatal calves. *Veterinary Pathology* **39**:200-215.
205. **Sato, T., Y. Endo, M. Matsushita, and T. Fujita.** 1994. Molecular characterization of a novel serine protease involved in activation of the complement system by mannose-binding protein. *International Immunology* **6**:665-669.
206. **Schmeck, B., P. D. N'Guessan, M. Ollomang, J. Lorenz, J. Zahlten, B. Opitz, A. Flieger, N. Suttorp, and S. Hippenstiel.** 2007. *Legionella pneumophila*-

- induced NF- κ B and MAPK-dependent cytokine release by lung epithelial cells. *European Respiratory Journal* **29**:25-33.
207. **Schorey, J. S., and A. M. Cooper.** 2003. Macrophage signalling upon mycobacterial infection: The MAP kinases lead the way. *Cellular Microbiology* **5**:133-142.
208. **Scita, G., P. Tenca, E. Frittoli, A. Tocchetti, M. Innocenti, G. Giardina, and P. P. DiFiore.** 2000. Signaling from Ras to Rac and beyond: Not just a matter of GEFs. *The EMBO Journal* **19**:2393-2398.
209. **Sha, J., C. L. Galindo, V. Pancholi, V. L. Popov, Y. Zhao, C. W. Houston, and A. K. Chopra.** 2003. Differential expression of the enolase gene under *in vivo* versus *in vitro* growth conditions of *Aeromonas hydrophila*. *Microbial Pathogenesis* **34**:195-204.
210. **Shafikhani, S. H., and J. Engel.** 2006. *Pseudomonas aeruginosa* type III-secreted toxin ExoT inhibits host-cell division by targeting cytokinesis at multiple steps. *PNAS* **103**:15605-15610.
211. **Shimoya, K., N. Matsuzaki, T. Taniguchi, T. Kameda, M. Koyama, R. Neki, F. Saji, and O. Tanizawa.** 1992. Human placenta constitutively produces interleukin-8 during pregnancy and enhances its production in intrauterine infection. *Biology of Reproduction* **47**:220-226.
212. **Sieira, R., D. J. Comerci, L. I. Pietrasanta, and R. A. Ugalde.** 2004. Integration host factor is involved in transcriptional regulation of the *Brucella abortus virB* operon. *Molecular Microbiology* **54**:808-822.

213. **Sieira, R., D. J. Comerci, D. O. Sánchez, and R. A. Ugalde.** 2000. A homologue of an operon required for DNA transfer in *Agrobacterium* is required in *Brucella abortus* for virulence and intracellular multiplication. *Journal of Bacteriology* **182**:4849-4855.
214. **Sinai, A. P., P. Webster, and K. Joiner.** 1997. Association of host cell endoplasmic reticulum and mitochondria with the *Toxoplasma gondii* parasitophorous vacuole membrane: a high affinity interaction. *Journal of Cell Science* **110**:2117-2128.
215. **Smith III, R., J. C. Kapatsa, S. J. Sherwood III, T. A. Ficht, J. W. Templeton, and L. G. Adams.** 1990. Differential reactivity of bovine lymphocytes to species of *Brucella*. *American Journal of Veterinary Research* **51**:518-523.
216. **Sola-Landa, A., J. Pizarro-Cerdá, M. J. Grilló, E. Moreno, I. Moriyón, J. M. Blasco, J. P. Gorvel, and I. López-Goni.** 1998. A two-component regulatory system playing a critical role in plant pathogens and endosymbionts is present in *Brucella abortus* and controls cell invasion and virulence. *Molecular Microbiology* **29**:125-138.
217. **Spera, J. M., J. E. Ugalde, J. Mucci, D. J. Comerci, and R. A. Ugalde.** 2006. A B lymphocyte mitogen is a *Brucella abortus* virulence factor required for persistent infection. *PNAS* **103**:16514-16519.
218. **Stevens, M. P., O. Marches, J. Campbell, V. Huter, G. Franckel, A. D. Phillips, E. Oswald, and T. S. Wallis.** 2002. Intimin, Tir, and Shiga Toxin 1 do

- not influence enteropathogenic responses to shiga toxin-producing *Escherichia coli* in bovine ligated intestinal loops. *Infection and Immunity* **70**:945-952.
219. **Talaat, A. M., S. T. Howard, W. Hale IV, R. Lyons, H. Garner, and S. A. Johnston.** 2002. Genomic DNA standards for gene expression profiling in *Mycobacterium tuberculosis*. *Nucleic Acids Research* **30**:e104.
220. **Talaat, A. M., P. Hunter, and S. A. Johnston.** 2000. Genome-directed primers for selective labeling of bacterial transcripts for DNA microarray analysis. *Nature Biotechnology* **18**:679-682.
221. **Talaat, A. M., R. Lyons, S. T. Howard, and S. A. Johnston.** 2004. The temporal expression profile of *Mycobacterium tuberculosis* infection in mice. *PNAS* **101**:4602-4607.
222. **Taminiau, B., M. Daykin, S. Swift, M. L. Boschioli, A. Tibor, P. Lestrade, X. De Bolle, D. O'Callaghan, P. Williams, and J. J. Letesson.** 2002. Identification of a quorum-sensing signal molecule in the facultative intracellular pathogen *Brucella melitensis*. *Infection and Immunity* **70**:3004-3011.
223. **Tang, P., C. L. Sutherland, M. R. Gold, and B. B. Finlay.** 1998. *Listeria monocytogenes* invasion of epithelial cells requires the MEK-1/ERK-2 mitogen-activated protein kinase pathway. *Infection and Immunity* **66**:1106-1112.
224. **Templeton, J. W., and L. G. Adams.** 1990. Natural resistance to bovine brucellosis, p. 144-150. *In* L. Garry Adams (ed.), *Advances in brucellosis research*. Texas A&M University Press, College Station, Texas.

225. **Tizard, I. R.** 2004. *Veterinary immunology: An introduction*, Seventh ed. Elsevier (USA), Philadelphia.
226. **Tuanyok, A., M. Tom, J. Dunbar, and D. E. Woods.** 2006. Genome-wide expression analysis of *Burkholderia pseudomallei* infection in a hamster model of acute melioidosis. *Infection and Immunity* **74**:5465-5476.
227. **Tumurkhuu, G., N. Koide, K. Takahashi, F. Hassan, S. Islam, H. Ito, I. Mori, T. Yoshida, and T. Yokochi.** 2006. Characterization of biological activities of *Brucella melitensis* lipopolysaccharide. *Microbiology and Immunology* **50**:421-427.
228. **Ugalde, J. E., C. Czibener, M. F. Feldman, and R. A. Ugalde.** 2000. Identification and characterization of the *Brucella abortus* phosphoglucomutase gene: Role of lipopolysaccharide in virulence and intracellular multiplication. *Infection and Immunity* **68**:5716-5723.
229. **van Asten, F. J., H. G. Hendriks, J. F. Dkoninkx, and J. E. van Dijk.** 2004. Flagella-mediated bacterial motility accelerates but is not required for *Salmonella* serotype Enteritidis invasion of differentiated Caco-2 cells. *International Journal of Medical Microbiology* **294**:395-399.
230. **van der Goot, G., and T. Harder.** 2001. Raft membrane domains: From a liquid-ordered membrane phase to a site of pathogen attack. *Seminars in Immunology* **13**:89-97.
231. **Verger, J. M.** 1985. *Brucella melitensis* infection in cattle, p. 197-203. In J. M. Verger and M. Plommet (ed.), *Brucella melitensis*. Seminar in the CEC

Programme of Co-ordination of Research on Animal Pathology. The Commission of the European Communities, Brussels, Belgium.

232. **Vitale, M., M. Della Chiesa, S. Carlomagno, D. Pende, M. Arico, L. Moretta, and A. Moretta.** 2005. NK-dependent DC maturation is mediated by TNF-alpha and IFN-gamma released upon engagement of the NKp30 triggering receptor. *Immunobiology* **106**:566-571.
233. **Vizcaíno, N., A. Cloeckaert, M. S. Zygmunt, and G. Dubray.** 1996. Cloning, nucleotide sequence, and expression of the *Brucella melitensis omp31* gene coding for an immunogenic major outer membrane protein. *Infection and Immunity* **64**:3744-3751.
234. **Vogel, J. P., H. L. Andrew, S. K. Wong, and R. R. Isberg.** 1998. Conjugative transfer by the virulence system of *Legionella pneumophila*. *Science* **279**:873-876.
235. **Wassef, J. S., D. F. Keren, and J. L. Mailloux.** 1989. Role of M cells in initial antigen uptake and in ulcer formation in the rabbit intestinal loop model of shigellosis. *Infection and Immunity* **57**:858-863.
236. **Watarai, M., S. I. Makino, Y. Fujii, K. Okamoto, and T. Shirahata.** 2002. Modulation of *Brucella*-induced macropinocytosis by lipid rafts mediates intracellular replication. *Cellular Microbiology* **4**:341-355.
237. **Watson, P. R., S. M. Paulin, A. P. Bland, P. W. Jones, and T. S. Wallis.** 1995. Characterization of intestinal invasion by *Salmonella typhimurium* and

- Salmonella dublin* and effect of a mutation in the *invH* gene. *Infection and Immunity* **63**:2743.
238. **Weiss, A. A., S. D. Johnston, and D. L. Burns.** 1993. Molecular characterization of an operon required for pertussis toxin secretion. *PNAS* **90**:2970-2974.
239. **Weiss, D. S., K. Takeda, S. Akira, A. Zychlinsky, and E. Moreno.** 2005. MyD88, but not Toll-like receptors 4 and 2, is required for efficient clearance of *Brucella abortus*. *Infection and Immunity* **73**:5137-5143.
240. **Wilson, C. L., S. D. Pepper, Y. Hey, and C. J. Miller.** 2004. Amplification protocols introduce systematic but reproducible errors into gene expression studies. *BioTechniques* **36**:498-506.
241. **Wu, Q., J. Pei, C. Turse, and T. A. Ficht.** 2006. Mariner mutagenesis of *Brucella melitensis* reveals genes with previously uncharacterized roles in virulence and survival. *BMC Microbiology* **6**:102.
242. **Wyllie, S., P. Seu, and J. A. Goss.** 2002. The natural resistance-associated macrophage protein 1 Slc11a1 (formerly Nramp1) and iron metabolism in macrophages. *Microbes and Infection* **4**:351-359.
243. **Young, E. J.** 1995. An overview of human brucellosis. *Clinical Infectious Diseases* **21**:283-290.
244. **Yura, T.** 1996. Regulation and conservation of the heat-shock transcription factor sigma 32. *Genes to Cells* **1**:277-284.

245. **Zaitseva, M. B., H. Golding, M. Betts, A. Yamauchi, E. T. Bloom, L. E. Butler, L. Stevan, and B. Golding.** 1995. Human peripheral blood CD4+ and CD8+ T cells express Th1-like cytokine mRNA and proteins following *in vitro* stimulation with heat-inactivated *Brucella abortus*. *Infection and Immunity* **63**:2720-2728.
246. **Zhan, Y., J. Yang, and C. Cheers.** 1993. Cytokine response of T-cell subsets from *Brucella abortus*-infected mice to soluble brucella proteins. *Infection and Immunity* **61**:2841-2847.
247. **Zhang, S., R. L. Santos, R. M. Tsolis, S. Stender, W. D. Hardt, A. J. Bäuml, and L. G. Adams.** 2002. The *Salmonella enterica* Serotype Typhimurium effector proteins SipA, SopA, SopB, SopD, and SopE2 act in concert to induce diarrhea in calves. *Infection and Immunity* **70**:3843-3855.
248. **Zygmunt, M. S., S. D. Hagius, J. V. Walker, and P. H. Elzer.** 2006. Identification of *Brucella melitensis* 16M genes required for bacterial survival in the caprine host. *Microbes and Infection* **8**:2849-2854.

APPENDIX A

TABLE A.1. Genes significantly altered in *B. melitensis* grown in F12K tissue culture medium to late-log phase, compared to stationary phase under the same conditions

Locus ID	Gene product	SAM	Spotfire	GSpring	ANOVA
		FC			(<i>p</i>)
DNA replication, recombination and repair					
BMEI0453	MutT/NUDIX family protein	5.2	69.1	60.8	0.007082
BMEI0462	Phosphohydrolase (MutT/NUDIX family protein)	37.8	122.2	132.0	0.01818
BMEI0880	Single-strand binding protein	2.9	124.0	124.9	0.029169
BMEI0901	Resolvase	2.5	2.8	2.8	0.005101
BMEI1321	DNA polymerase, bacteriophage-type	3.1	3.8	3.9	0.008698
BMEI1362	Chromosomal replication initiator protein DnaA	3.8	300.9	449.2	0.029257
BMEI1409	Transposase	11.7	201.6	264.4	0.013443
BMEI1420	Transposase	123.0	123.0	123.0	0.009518
BMEI1422	Transposase	75.6	94.8	95.0	0.005182
BMEI1485	Replicative DNA helicase	15.2	66.6	60.5	0.024788
BMEI1815	Transposase	6.2	80.0	70.3	0.037454
BMEI1910	Recombination protein RecR	4.3	88.2	77.7	0.028354
BMEI1942	DNA polymerase III subunit beta	5.95	160.0	170.9	0.040039
BMEI0183	Transposase	5.8	8.7	9.8	0.011806
BMEI0290	DNA polymerase III subunit epsilon	4.0	55.4	76.8	0.027906
BMEI0447	Transporter	2.5	4.9	5.3	0.00539
BMEI0527	Exodeoxyribonuclease VII large subunit	4.0	112.5	111.0	0.001261
BMEI0663	Phosphohydrolase (MutT/NUDIX family protein)	98.8	141.2	152.2	0.025194
BMEI0676	DNA topoisomerase IV subunit B	2.53	2.8	2.9	0.014043
BMEI0713	Transposase	174.2	311.0	324.6	0.000368
BMEI0716	Transposase	6.4	67.6	63.1	0.041021
Transcription					
BMEI0280	RNA polymerase sigma 32 factor	-5.0	-10.0	-4.3	0.004316
BMEI0510	Leucine-responsive regulatory protein	59.4	87.2	76.0	0.004841
BMEI1098	Transcriptional regulatory protein, AsnC family	4.3	10.7	10.1	0.032585
BMEI1379	Transcriptional regulator BetI	6.0	155.2	169.8	0.008584
BMEI1384	Transcriptional regulator, AraC family	-20.0	-20.7	-17.0	0.005425
BMEI1717	Transcriptional regulator, IclR	4.3	12.2	13.3	0.006167
BMEI1758	Transcriptional activator, LuxR family	221.6	221.6	221.6	0.011148
BMEI1789	DNA-directed RNA polymerase subunit N (sigma-54 factor rpon)	7.56	113.6	92.1	0.017962
BMEI1845	Transcriptional regulatory protein, AsnC family	100.0	100.0	100.0	0.018725
BMEI0092	Replication protein B	54.4	74.6	71.5	0.017128

TABLE A.1. (continued)

Locus ID	Gene product	SAM	Spotfire	GSpring	ANOVA
			FC		(p)
BMEI10127	Acetate operon repressor	2.6	34.9	41.4	0.018305
BMEI10143	Transcriptional regulator, AraC family	13.1	120.6	110.8	0.011801
BMEI10346	Transcriptional regulatory protein, AsnC family	39.3	39.1	39.1	0.00386
BMEI10372	Transcriptional regulator, MerR family	3.9	91.5	64.7	0.039435
BMEI10383	Transcriptional regulator, GntR family	37.4	37.4	37.4	0.026822
BMEI10426	Transcriptional regulator, DeoR family	44.9	44.9	44.9	0.005492
BMEI10436	Transcriptional regulator, DeoR family	8.8	94.1	98.6	2.60E-03
BMEI10467	Transcriptional regulator, MerR family	37.0	88.1	86.1	0.021261
BMEI10520	Transcriptional regulator, MarR family	-7.2	-7.4	-6.4	0.009266
BMEI10573	Transcriptional regulator, RpiR family	56.5	103.4	109.5	0.026452
BMEI10721	Transcriptional regulator, AraC family	13.7	107.2	98.6	0.013143
BMEI10807	Transcriptional regulator, GntR family	4.4	219.3	202.1	0.007073
BMEI10902	Transcriptional regulator protein, LysR family	34.2	34.2	34.2	0.007487
BMEI11007	Transcriptional regulator, GntR family	7.0	61.0	508.9	0.001131
BMEI11077	Transcriptional regulator protein, LysR family	3.2	55.4	72.3	0.0216
BMEI11093	Glycerol-3-phosphate regulon repressor	386.5	386.5	386.5	0.004118
BMEI11135	Transcriptional regulator protein, LysR family	2.3	3.1	3.1	0.008648
Translation, ribosomal structure and biogenesis					
BMEI0277	Heat shock protein 15	2.4	3.3	3.2	0.008141
BMEI0616	tRNA delta(2)-isopentenylpyrophosphate transferase	9.4	73.7	69.1	0.005714
BMEI0890	Queuine tRNA-ribosyltransferase	5.8	174.1	212.4	0.011321
BMEI0934	ATP-dependent RNA helicase RhlE	3.4	46.4	36.4	0.032457
BMEI1671	Translation initiation factor IF-1	2.4	4.3	4.8	0.031672
BMEI1798	23S ribosomal RNA methyltransferase	164.3	171.4	172.6	0.005135
BMEI1959	Methyltransferase	213.5	213.5	213.5	0.004073
BMEI1960	Methyltransferase	8.1	85.8	89.3	0.021941
BMEI0276	Ribonuclease P	6.4	274.5	226.0	0.008062
BMEI0278	Translation initiation inhibitor	4.4	8.1	7.2	0.004336
BMEI0597	23S ribosomal RNA methyltransferase	4.4	7.8	8.4	0.012347
BMEI0890	16S ribosomal RNA m(5)C 967 methyltransferase	30.7	88.8	77.7	0.02906
Nucleotide metabolism					
BMEI0358	Deoxyuridine 5'-triphosphate nucleotidohydrolase	6.95	114.4	100.3	3.90E-05
BMEI0608	Thymidylate synthase	91.7	91.7	91.7	0.012037
BMEI1281	Dihydroorotase	2.3	2.5	2.5	0.002812
BMEI1571	Guanine deaminase	-5.1	-11.4	-4.9	0.011304
BMEI1575	Xanthine dehydrogenase	2.9	76.7	79.6	0.021288
BMEI1576	Xanthine dehydrogenase	68.3	257.3	254.9	0.000524
BMEI1639	Dihydropyrimidine dehydrogenase	94.7	123.0	122.3	0.014601
BMEI0088	Inosine-uridine preferring nucleoside hydrolase	10.5	785.5	1058.8	0.021628

TABLE A.1. (continued)

Locus ID	Gene product	SAM	Spotfire	GSpring	ANOVA (p)
			FC		
BMEI0627	Probable adenine deaminase	3.4	177.2	223.8	0.013583
Carbohydrate metabolism					
BMEI0344	Phosphoglucosamine mutase/phosphoacetylglucosamine mutase/phosphomannomutase	51.3	84.9	76.9	0.010824
BMEI0921	UDP-glucose 4-epimerase	-7.6	-11.6	-6.7	0.005944
BMEI0974	Ribose-5-phosphate isomerase A	97.5	158.0	157.0	0.008367
BMEI1237	UDP-glucose 4-epimerase	2.6	2.6	2.8	0.039446
BMEI1436	Pyruvate phosphate dikinase	5.5	67.3	58.8	0.029235
BMEI1570	Putative hydroxypyruvate reductase	3.7	116.9	114.9	0.040269
BMEI0355	D-galactose 1-dehydrogenase	4.3	85.1	111.2	0.020829
BMEI0430	Erythritol kinase	3.5	103.2	118.8	0.03274
BMEI0476	Uronate isomerase	55.8	55.8	55.8	0.017535
BMEI0568	Myo-inositol-1(or 4)-monophosphatase	2.7	4.7	4.6	0.023251
BMEI0574	Myo-inositol 2-dehydrogenase	154.3	154.3	154.3	0.023522
BMEI0724	Endoglucanase H	3.7	208.4	206.4	0.013526
BMEI0823	Glycerol kinase	58.9	58.9	58.9	0.005347
BMEI0850	GDP-fucose synthetase	6.5	285.5	453.3	0.032125
BMEI1095	L-fuculose phosphate aldolase	5.5	164.6	194.1	0.010794
Lipid metabolism					
BMEI0099	3-hydroxybutyryl-CoA dehydrogenase	3.1	10.9	11.5	0.03388
BMEI0166	Acyl-CoA thioesterase II	3.85	76.7	81.4	0.032527
BMEI0477	Monoamine oxidase regulatory protein, putative	41.3	64.1	63.4	0.035528
BMEI0688	3-hydroxyisobutyrate dehydrogenase	81.9	82.0	81.9	0.020739
BMEI0897	Glutaryl-CoA dehydrogenase	2.7	68.1	66.2	0.021585
BMEI1024	3-hydroxyisobutyrate dehydrogenase	8.8	177.8	185.3	0.018569
BMEI1235	Short-chain dehydrogenase	49.2	49.2	49.2	0.010489
BMEI1473	3-oxoacyl-(acyl carrier protein) synthase	2.3	2.4	2.4	0.003662
BMEI1478	Acyl-carrier-protein S-malonyltransferase	9.1	62.1	49.2	0.023269
BMEI1709	Oxidoreductase UcpA	2.7	3.8	3.4	0.028269
BMEI1861	Arylesterase precursor	5.2	134.7	154.4	0.029325
BMEI0047	Lysophospholipase L2	47.2	47.2	47.2	0.008023
BMEI0239	Cardiolipin synthetase	14.4	170.8	182.4	0.017839
BMEI0514	3-ketoacyl (acyl-carrier-protein) reductase	4.5	139.2	197.5	0.033898
BMEI1103	Phosphatidylglycerophosphatase B	3.6	148.1	143.9	0.02058
Amino acid metabolism					
BMEI0028	L-sorbose dehydrogenase [FAD]	13.1	76.2	63.6	0.027971
BMEI0559	5,10-methylenetetrahydrofolate reductase	2.7	3.0	2.9	0.017735
BMEI0591	Xaa-Pro aminopeptidase	94.4	144.8	134.7	0.01548

TABLE A.1. (continued)

Locus ID	Gene product	SAM	Spotfire	GSpring	ANOVA (p)
			FC		
BMEI0617	Acetolactate synthase III large subunit	54.4	146.4	125.8	0.014389
BMEI0647	Urease alpha subunit	42.7	42.7	42.7	0.021861
BMEI0706	CobC protein	46.8	46.8	46.8	0.016867
BMEI0730	Lactoylglutathione lyase	163.9	163.9	163.9	0.011144
BMEI1365	Protease II	88.2	260.5	308.2	0.015829
BMEI1380	Choline dehydrogenase	6.2	295.9	360.4	0.025683
BMEI1617	O-succinylhomoserine sulfhydrylase	-18.6	-136.3	-14.6	0.006793
BMEI1719	Sarcosine oxidase gamma subunit	4.0	27.3	10.5	0.005638
BMEI1720	Sarcosine oxidase alpha subunit	24.0	64.0	64.1	0.021308
BMEI1781	Carbamoyl-phosphate synthase large chain	22.8	124.4	148.7	0.009883
BMEI1905	Prephenate dehydratase	4.7	154.1	118.3	0.033418
BMEII0012	Oligoendopeptidase F	41.9	96.1	100.6	0.021343
BMEII0040	Glutamate synthase [NADPH] large chain	14.8	92.1	90.6	0.024754
BMEII0049	N-formylglutamate deformylase	8.6	69.6	73.0	0.020268
BMEII0134	5-carboxymethyl-2-hydroxymuconate delta-isomerase	234.53	298.8	302.4	0.002041
BMEII0135	5-carboxymethyl-2-hydroxymuconate semialdehyde dehydrogenase	3.16	9.7	10.3	0.037007
BMEII0136	Homoprotocatechuate 2,3-dioxygenase	23.7	170.7	164.3	0.026465
BMEII0404	3-isopropylmalate dehydrogenase	5.0	103.4	89.7	0.01957
BMEII0546	Metal-activated pyridoxal enzyme	2.5	2.6	2.6	0.004646
BMEII0582	Sarcosine oxidase beta subunit	77.9	147.5	151.7	0.002203
BMEII0756	N-acetylglucosamine kinase	13.7	147.8	107.9	0.018282
BMEII0907	Glutaminase	4.6	152.4	128.0	0.03523
BMEII0910	Glutamate decarboxylase beta	3.1	136.3	113.9	0.041125
BMEII0964	Asparagine synthetase B (glutamine-hydrolyzing)	14.4	331.3	323.2	0.00443
BMEII1054	ATP phosphoribosyltransferase	2.3	2.4	2.3	0.002473
BMEII1055	ATP phosphoribosyltransferase regulatory subunit	5.8	251.7	103.8	0.038745
Secondary metabolite biosynthesis, transport and metabolism					
BMEI1560	Salicylaldehyde dehydrogenase	3.9	81.9	68.3	0.023819
BMEI1860	Hypothetical transmembrane oxidoreductase	2.4	2.7	2.5	0.018287
BMEII0078	2,3-dihydroxybenzoate-AMP ligase	221.0	221.0	221.0	0.015707
BMEII0079	Isochorismatase	55.6	105.4	92.1	0.010724
BMEII0580	Probable blue-copper protein Yack precursor	2.7	6.8	7.7	0.019374
Energy production and conversion					
BMEI0475	Cytochrome C1	15.13	180.3	164.8	0.016951
BMEI0548	Flavoheмоprotein	99.2	99.2	99.2	0.004279
BMEI0836	Citrate synthase	-3.7	-5.0	-3.3	0.008278
BMEI0898	Predicted acyl-CoA transferase/Carnitine dehydratase	2.8	3.7	4.1	0.017818
BMEI1462	Cytochrome C oxidase polypeptide III	5.6	152.0	114.1	0.008024
BMEI1465	Cytochrome C oxidase polypeptide I	2.85	3.3	3.2	0.0006

TABLE A.1. (continued)

Locus ID	Gene product	SAM	Spotfire	GSpring	ANOVA (p)
			FC		
BMEI1591	Ferredoxin-NADP reductase	49.2	72.7	72.4	0.009468
BMEI2037	Phosphoenolpyruvate carboxykinase	113.9	155.7	158.2	0.021717
BMEI0135	5-carboxymethyl-2-hydroxymuconate semialdehyde dehydrogenase	3.16	9.7	10.3	0.037007
BMEI0141	Aldehyde dehydrogenase	137.2	166.5	169.7	0.004314
BMEI0241	Coniferyl-aldehyde dehydrogenase	35.8	71.0	71.6	0.024943
BMEI0246	Nitroreductase	78.7	78.7	78.7	0.000402
BMEI0255	Iron-sulfur cluster-binding protein	3.6	75.5	83.5	0.026113
BMEI0378	Formate dehydrogenase alpha chain	214.2	214.2	214.2	0.005487
BMEI0388	Piperidine-6-carboxylate dehydrogenase	5.5	106.7	101.4	0.007737
BMEI0553	Alcohol dehydrogenase	-5.3	-6.6	-4.8	0.005386
BMEI0588	Formate dehydrogenase accessory protein	11.5	66.6	56.3	0.028185
BMEI0771	Hydroxyacylglutathione hydrolase	23.4	23.4	23.4	0.000994
BMEI0876	Quinone oxidoreductase	51.5	99.7	97.6	0.005751
BMEI0950	Nitrate reductase alpha chain	193.9	282.4	290.3	0.016923
BMEI0951	Nitrate reductase beta chain	4.1	408.9	512.2	0.019189
BMEI0965	Pseudoazurin	3.8	41.8	44.0	0.016079
BMEI0973	Nitrous-oxide reductase precursor	24.8	43.0	42.2	0.03814
BMEI1005	Malate dehydrogenase	4.9	144.5	103.8	0.01867
BMEI1019	Alpha-methylacyl-CoA racemase	3.0	173.7	194.3	0.029976
BMEI1073	Cytochrome b561	31.9	31.9	31.9	0.009619
Inorganic ion transport and metabolism					
BMEI0317	Integral membrane protein	72.2	97.4	95.2	0.017047
BMEI0450	Cobalt-Zinc-Cadmium resistance protein Czcd	5.3	8.2	7.0	0.009439
BMEI0511	TRK system potassium uptake protein TrkH	7.2	67.7	49.0	0.031708
BMEI0639	CbiM protein	124.1	275.3	278.9	0.003432
BMEI0640	CbiM protein	-2.6	-3.0	-2.7	0.001693
BMEI0660	Metal chelate transport ATP-binding protein	2.4	2.5	2.5	0.007193
BMEI1988	Phosphate transport system permease protein PstC	-3.9	-3.9	-3.7	0.001835
BMEI0338	ABC transporter substrate binding protein	4.9	98.6	96.6	0.001187
BMEI0487	Nickel-binding periplasmic protein precursor	10.2	106.7	61.5	0.029493
BMEI0488	Nickel transport system permease protein NikB	10.0	88.4	73.1	0.006553
BMEI0536	Iron(III) dicitrate transport system permease protein FecD	4.2	105.8	126.6	0.013862
BMEI0567	Iron(III)-transport ATP-binding protein SfuC	7.5	383.3	497.7	0.022023
BMEI0581	Superoxide dismutase (Cu-Zn)	7.4	99.2	80.5	0.010658
BMEI0704	Bacterioferritin	3.2	3.5	4.0	0.032068
BMEI0765	Potassium efflux system protein PhaG	26.9	138.0	129.4	0.022215
BMEI0767	Potassium efflux system protein PhaE	5.3	92.0	76.3	0.024117
BMEI0883	High-affinity iron permease	13.0	151.4	64.8	0.039901
BMEI1011	Sulfite reductase (NADPH) flavoprotein alpha-component	19.9	200.1	214.6	0.010442

TABLE A.1. (continued)

Locus ID	Gene product	SAM	Spotfire	GSpring	ANOVA (p)
			FC		
BMEI1120	Iron(III)-binding periplasmic protein precursor	20.8	131.3	137.1	0.016841
Cofactor transport and metabolism					
BMEI0176	Porphobilinogen deaminase	4.1	33.0	41.5	0.006669
BMEI0177	Uroporphyrinogen-III synthetase	2.3	2.9	2.9	0.02117
BMEI0690	Cobryric acid synthase	215.6	279.7	296.5	0.020047
BMEI0700	Precorrin-3B C17-methyltransferase	2.4	2.9	2.6	0.03227
BMEI0841	Molybdopterin biosynthesis MoeA protein	-3.0	-3.2	-2.7	0.00438
BMEI0842	Molybdenum cofactor biosynthesis protein C	-5.1	-6.7	-4.5	0.007319
BMEI0886	Phosphopantetheine adenylyltransferase	73.1	73.3	73.5	0.010854
BMEI0954	2-amino-4-hydroxy-6-hydroxymethylidihydropteridine pyrophosphokinase	2.3	2.5	2.4	0.025565
BMEI1187	Riboflavin synthase subunit beta	4.1	57.9	61.1	0.017448
BMEI1517	Pyridoxamine 5'-phosphate oxidase	4.4	6.0	7.8	0.04036
BMEI1592	3-methyl-2-oxobutanoate hydroxymethyltransferase	2.5	2.6	2.6	0.023893
BMEI1735	Thiazole synthase	2.7	78.3	84.1	0.038439
BMEI1902	Molybdopterin biosynthesis enzyme	6.8	26.0	40.9	0.034044
BMEI0077	Isochorismate synthase Dhbc	17.1	70.5	58.8	0.02942
BMEI0775	Biotin synthase	18.5	97.3	106.1	0.007341
BMEI0834	Glutamate-1-semialdehyde 2,1-aminomutase	2.7	4.2	4.4	0.019027
BMEI1010	Thiamine biosynthesis lipoprotein ApbE precursor	3.2	85.8	105.2	0.028487
BMEI1044	Rivoflavin kinase/FMN adenylyltransferase	5.3	139.8	147.3	0.00776
Cell envelope, biogenesis and outer membrane					
BMEI0271	Monofunctional biosynthetic peptidoglycan transglycosylase	7.5	75.9	56.6	0.028509
BMEI0402	31 kDa outer-membrane immunogenic protein precursor	4.2	4.9	4.5	0.017121
BMEI0418	Lipooligosaccharide biosynthesis protein Lic2B	23.0	62.7	56.2	0.018425
BMEI0566	Soluble lytic murein transglycosylase	-3.6	-4.8	-3.5	0.001835
BMEI0586	UDP-3-O-[3-hydroxymyristoyl] N-acetylglucosamine deacetylase	21.1	419.8	394.4	0.001476
BMEI0786	Outer membrane protein	11.6	141.4	133.5	0.033327
BMEI0814	Penicillin-binding protein 6 (D-alanyl-D-alanine carboxypeptidase fraction C)	99.9	151.9	141.9	0.032178
BMEI0833	UDP-N-acetylglucosamine acyltransferase	70.6	145.1	156.5	0.00953
BMEI0991	RarE lipoprotein A	3.8	6.1	6.5	0.00441
BMEI1079	Lipoprotein NlpD	16.2	250.2	173.5	0.043447
BMEI1175	Putative capsule polysaccharide export protein precursor	6.5	193.0	176.1	0.020777
BMEI1414	Perosamine synthetase	133.4	156.9	161.9	0.027191
BMEI1493	Peptidoglycan binding protein (LysM domain)	3.3	55.1	61.3	0.036401
BMEI1626	N-acetylglucosaminyltransferase	4.2	89.4	92.6	0.012732
BMEI1707	Mandelate racemase	42.5	265.7	298.4	0.010775
BMEI0083	Basic membrane protein A precursor	255.3	255.3	255.3	0.000461

TABLE A.1. (continued)

Locus ID	Gene product	SAM	Spotfire	GSpring	ANOVA (p)
			FC		
BMEI0084	Basic membrane protein A precursor	156.3	156.3	156.3	0.006337
BMEI0157	Hypothetical protein	69.7	99.9	99.0	0.011761
BMEI0376	Heat resistant agglutinin 1 precursor	100.2	100.2	100.2	0.023267
BMEI0472	Membrane fusion protein MtrC	86.7	185.5	185.5	0.012122
BMEI0727	UDP-glucose 6-dehydrogenase	36.1	248.0	218.4	0.011001
BMEI0729	Cellulose synthase catalytic subunit (UDP-forming)	89.1	106.0	109.3	0.002611
BMEI0731	dTDP-glucose 4-6-dehydratase	62.1	87.4	88.3	0.001361
BMEI0836	dTDP-4-dehydroxamnose 3,5-epimerase	53.2	53.2	53.2	0.026117
BMEI1101	Bactoprenol glucosyl transferase/Bactoprenol apolipoprotein N-acyltransferase	4.3	190.3	160.5	0.026543
BMEI1128	Succinoglycan biosynthesis protein ExoM	3.6	55.8	50.1	0.00868
BMEI1130	Probable UDP-N-acetyl-D-mannosaminuronic acid transferase	76.9	83.3	83.1	0.002959
Membrane transport					
BMEI0113	Asparagine transport system permease protein	73.4	73.4	73.4	0.003179
BMEI0263	Leucine-, isoleucine-, valine-, threonine-, and alanine-binding protein precursor	3.1	10.6	10.1	0.01319
BMEI0264	Leucine-, isoleucine-, valine-, threonine-, and alanine-binding protein precursor	10.3	234.4	181.7	0.017178
BMEI0642	Urea transporter	94.4	94.4	94.4	0.003138
BMEI0654	ABC transporter ATP-binding protein	23.7	346.4	384.7	0.004751
BMEI0797	Transporter	6.9	478.8	464.2	0.010229
BMEI1022	Arginine/Ornithine-binding periplasmic protein precursor	4.2	244.4	209.7	0.017741
BMEI1041	ABC transporter ATP-binding protein	-5.0	-5.5	-3.9	0.010444
BMEI1416	O-antigen export system ATP-binding protein RfbB	207.7	207.7	207.7	0.015649
BMEI1554	Transporter, MFS superfamily	87.2	87.2	87.2	0.015542
BMEI1580	Mannitol transporter, large subunit	3.5	69.6	72.8	0.017358
BMEI1713	Maltose/maltodextrin transport ATP-binding protein MalK	234.4	437.5	458.8	0.005988
BMEI1912	Sugar transporter	44.3	89.7	87.9	0.015466
BMEI0025	Attachment mediating protein VirB1 homolog	9.0	115.3	109.3	0.010999
BMEI0027	Channel protein VirB3 homolog	2.2	165.3	141.1	0.042572
BMEI0034	Channel protein VirB10 homolog	81.6	81.6	81.6	0.025033
BMEI0038	D-serine/D-alanine/glycine transporter	35.03	236.2	243.8	0.003534
BMEI0066	High affinity branched-chain amino acid transport ATP-binding protein LivG	11.7	85.3	90.2	0.012414
BMEI0087	Sugar ABC transporter, permease protein	40.3	151.7	134.9	0.033397
BMEI0098	High affinity branched-chain amino acid transport ATP-binding protein LivF	5.6	135.9	137.1	0.014354
BMEI0099	High affinity branched-chain amino acid transport ATP-binding protein LivG	86.2	86.2	86.2	0.016303
BMEI0102	High affinity branched-chain amino acid transport system permease protein LivH	13.7	123.2	113.2	0.003106
BMEI0103	Leu/ile/val-binding protein precursor	10.2	154.4	159.9	0.008315

TABLE A.1. (continued)

Locus ID	Gene product	SAM	Spotfire	GSpring	ANOVA (p)
			FC		
BMEII0114	Sn-glycerol-3-phosphate transport system permease protein UgpE	5.9	55.6	40.7	0.008082
BMEII0144	Xylose transport system permease protein XylH	84.1	84.1	84.1	0.011375
BMEII0196	Spermidine/putrescine-binding periplasmic protein	7.7	65.8	66.1	0.02712
BMEII0200	Oligopeptide transport ATP-binding protein OppD	5.8	40.8	35.4	0.046728
BMEII0223	Oligopeptide transport ATP-binding protein OppF	69.4	69.4	69.4	0.020388
BMEII0284	Periplasmic dipeptide transport protein precursor	2.8	49.2	39.9	0.025605
BMEII0285	Dipeptide transport system permease protein DppB	6.6	262.1	306.1	0.019232
BMEII0302	Ribose transport system permease protein RbsC	3.4	44.7	25.4	0.028921
BMEII0340	High affinity branched-chain amino acid transport system permease protein LivM	4.2	4.7	4.7	1.00E-04
BMEII0342	High affinity branched-chain amino acid transport ATP-binding protein LivF	67.6	100.6	91.8	0.005617
BMEII0481	ABC transporter ATP-binding protein	6.0	303.9	289.7	0.016367
BMEII0483	ABC transporter integral membrane protein	3.0	19.3	22.0	0.01803
BMEII0517	Branched-chain amino acid transport protein AzIC	14.7	169.0	154.7	0.00594
BMEII0548	Glycine betaine/L-proline transport ATP-binding protein ProV	4.1	101.4	120.6	0.025865
BMEII0583	Iron(III)-transport ATP-binding protein SfuC	102.3	102.3	102.3	0.004557
BMEII0596	Methylenomycin A resistance protein	8.1	97.8	76.0	0.023565
BMEII0618	Xanthine/uracil permease	5.7	193.7	206.2	0.02544
BMEII0621	Sn-glycerol-3-phosphate transport system permease protein UgpC	81.4	81.4	81.4	0.02135
BMEII0622	Sn-glycerol-3-phosphate transport system permease protein UgpE	158.6	185.6	176.9	0.015793
BMEII0623	Sn-glycerol-3-phosphate transport system permease protein UgpE	-16.2	-18.0	-13.9	0.006297
BMEII0624	Sn-glycerol-3-phosphate transport system permease protein UgpA	58.3	102.1	105.0	0.014122
BMEII0628	High affinity branched-chain amino acid transport ATP-binding protein LivF	9.0	87.8	68.7	0.013577
BMEII0662	Transporter, Msf superfamily	55.2	109.0	104.0	0.015113
BMEII0691	Periplasmic oligopeptide-binding protein precursor	4.0	74.9	63.7	0.031048
BMEII0737	Oligopeptide transport system permease protein OppC	3.0	88.3	70.2	0.012229
BMEII0753	Sorbitol/mannitol transport inner membrane protein	3.4	42.2	45.3	0.039989
BMEII0755	Sugar-binding protein	2.8	9.0	8.6	0.036941
BMEII0845	Lipopolysaccharide N-acetylglucosaminyltransferase	-2.8	-3.5	-2.6	0.014534
BMEII0851	Exopolysaccharide production protein ExoF precursor	14.3	344.7	451.8	0.020084
BMEII0861	Oligopeptide transport system permease protein AppC	5.6	375.3	490.0	0.018617
BMEII0863	Oligopeptide transport ATP-binding protein AppD	8.3	128.5	79.9	0.029032
BMEII0864	Oligopeptide transport ATP-binding protein AppF	45.4	44.0	44.0	0.02127
BMEII0868	Leucine-specific binding protein precursor	235.6	396.7	402.3	0.000378
BMEII0875	Leucine-specific binding protein precursor	3.7	7.6	6.5	0.023208
BMEII0922	Spermidine/putrescine transport ATP-binding protein PotA	9.2	86.1	83.4	0.004857
BMEII1122	Iron(III)-transport system permease protein SfuB	71.7	71.7	71.7	0.003809

TABLE A.1. (continued)

Locus ID	Gene product	SAM	Spotfire	GSpring	ANOVA (p)
			FC		
Defense mechanisms					
BMEI0403	Multiple antibiotic resistance protein MarC	163.0	262.8	256.8	0.012425
BMEI0656	Daunorubicin resistance transmembrane protein	98.95	98.95	98.95	0.0151
BMEI0893	Acriflavin resistance protein B	10.46	12.4	9.8	0.00035
BMEI0380	Acriflavin resistance protein A precursor	267.76	267.76	267.76	0.009676
BMEI0382	Acriflavin resistance protein D	94.95	175.5	161.3	0.008164
BMEI0451	Type I restriction-modification system methylation	-3.6	-3.9	-3.2	0.007363
BMEI0533	Fusaric acid resistance protein FusE	15.6	145.4	161.5	0.027832
BMEI0801	Daunorubicin resistance transmembrane protein	3.2	160.2	136.7	0.021329
BMEI0914	Acriflavin resistance protein A precursor	5.4	130.8	161.9	0.030513
BMEI0916	Acriflavin resistance protein D	78.66	78.66	78.66	0.020278
Signal transduction					
BMEI0067	cAMP-dependent protein kinase regulatory subunit	2.3	2.9	2.9	0.00272
BMEI0372	Sensory transduction regulatory protein	-6.2	-7.3	-5.1	0.00684
BMEI0374	Sensory transduction histidine kinase	-3.8	-4.4	-3.6	0.003242
BMEI1328	Sensory transduction histidine kinase	3.3	131.0	122.6	0.030607
BMEI1582	Transcriptional regulatory protein DegU	37.7	46.7	43.8	0.003334
BMEI1606	Sensory transduction histidine kinase	2.8	3.3	3.0	0.023505
BMEI2034	Sensor protein ChvG	3.8	36.9	38.5	0.003834
BMEI0292	Response regulator protein	2.9	3.6	3.5	0.001663
BMEI1027	Hypothetical protein	2.4	4.1	3.9	0.011999
Post-translational modification and secretion, protein turnover and chaperones					
BMEI0643	Urease accessory protein UreD	32.4	32.4	32.4	0.012636
BMEI0644	Urease accessory protein UreG	9.3	202.1	196.6	0.029832
BMEI0645	Urease accessory protein UreF	70.1	70.1	70.1	0.026077
BMEI0646	Urease accessory protein UreE	49.7	49.7	49.7	0.001821
BMEI0783	Protease DO	49.6	188.8	162.3	0.011156
BMEI1080	Protein-L-isoaspartate O-methyltransferase	-16.3	-17.0	-15.7	0.000502
BMEI1331	Cytochrome C-type biogenesis protein CydL	4.1	158.5	164.5	0.005198
BMEI1574	XdhC protein (assists in molybdopterin insertion into xanthine dehydrogenase)	4.6	110.5	107.5	0.000469
BMEI1655	Urease accessory protein UreD	15.1	371.3	391.2	0.037834
BMEI1793	Putative protease IV	-2.5	-2.5	-2.2	0.00705
BMEI1799	Lipoprotein signal peptidase	201.8	271.9	271.6	0.00713
Cell division					
BMEI0008	Glucose-inhibited division protein B	8.8	291.7	360.0	0.017072
BMEI0010	Chromosome partitioning protein ParB	8.0	116.3	106.8	0.000631
BMEI0073	Cell division protein FtsX	7.0	208.3	260.8	4.83E-04
BMEI0470	Integral membrane protein	71.7	93.4	89.1	0.011569

TABLE A.1. (continued)

Locus ID	Gene product	SAM	Spotfire	GSpring	ANOVA (p)
			FC		
BMEI0925	Cell division topological specificity factor MinE	3.5	80.7	87.7	0.039051
Cell motility and chemotaxis					
BMEI0961	Kinesin-like protein	8.8	69.1	76.0	0.019508
BMEI0150	Flagellin	96.6	96.6	96.6	0.007312
BMEI0151	Flagellar M-ring protein FlIF	3.1	3.7	3.3	0.030285
BMEI0156	Chemotaxis MotD protein	3.0	4.1	4.0	0.000409
BMEI0164	Flagellar basal body rod modification protein	2.1	2.4	2.5	0.018005
BMEI0166	Flagellar biosynthetic protein FlhA	5.4	104.9	97.7	0.034612
BMEI1112	Flagellar motor switch protein FlhN	10.3	139.2	130.1	0.003866
General function prediction only					
BMEI0158	Acetyltransferase	48.95	77.0	78.9	0.023737
BMEI0346	Sodium/bile acid cotransporter homolog, sbf family	334.6	334.6	334.6	0.004413
BMEI0350	Acetyltransferase	3.8	50.6	29.4	0.013507
BMEI0594	Chloramphenicol acetyltransferase	191.2	191.2	191.2	0.001931
BMEI0720	Sugar fermentation stimulation protein	5.4	76.5	67.1	0.026151
BMEI0736	Ferripyochelin binding protein	4.8	200.1	195.5	0.022678
BMEI0740	Inosine-5'-monophosphate dehydrogenase	-7.4	-8.3	-6.3	0.008082
BMEI0946	NAD(FAD)-utilizing dehydrogenase	4.2	15.0	15.2	0.004063
BMEI0962	Membrane lipoprotein lipid attachment SitE containing protein	-20.7	-267.3	-16.9	0.004775
BMEI1269	Chloramphenicol-sensitive protein RarD	2.4	2.9	3.0	0.004112
BMEI1370	ATPase	3.9	57.0	61.9	0.025749
BMEI1388	Oxidoreductase	4.1	88.9	75.6	0.018948
BMEI1437	Putative hydroxylase	36.7	51.8	49.4	0.022621
BMEI1443	2-Haloalkanoic acid dehalogenase I	2.3	2.7	2.8	0.009551
BMEI1487	Colicin V production protein	4.25	109.6	136.5	0.039396
BMEI1534	Methyltransferase	-5.0	-5.2	-4.5	0.005094
BMEI1634	Phosphoglycolate phosphatase	30.2	83.5	93.0	0.02468
BMEI1822	S-formylglutathione hydrolase	2.7	3.0	3.0	0.011448
BMEI2011	2-hydroxyomuconic semialdehyde hydrolase	10.3	151.7	145.9	0.006432
BMEI0327	Phosphoglycolate phosphatase	70.5	291.1	363.5	0.043366
BMEI0829	Possible S-adenosylmethionine-dependent methyltransferase	20.0	47.3	55.5	0.036531
BMEI0838	Succinoglycan biosynthesis transport protein ExoT	12.2	84.9	91.5	0.011502
BMEI1003	Putative O-antigen transporter	2.4	2.6	2.5	0.035181
BMEI1016	Protease I	66.5	66.5	66.5	0.018129
BMEI1019	Alpha-methylacyl CoA racemase	3.0	173.7	194.3	0.029976
BMEI1052	Transporter	3.3	114.5	123.0	0.020979
BMEI1060	2,5-diketo-D-glucuronic acid reductase	7.0	237.9	189.0	0.01192

TABLE A.1. (continued)

Locus ID	Gene product	SAM	Spotfire	GSpring	ANOVA (p)
			FC		
Predicted by homology					
BMEI0804	Hypothetical cytosolic protein	-6.5	-9.0	-5.4	0.019652
BMEI1319	Hypothetical membrane spanning protein	2.9	132.1	136.8	0.020961
BMEI0261	Hypothetical cytosolic protein	30.8	31.7	31.7	0.023401
BMEI0522	Hypothetical protein	8.1	275.0	346.4	0.03065
Unknown function					
BMEI0002	Cytochrome functioning/assembly related protein	3.75	218.6	242.6	0.026103
BMEI0016	Hypothetical protein	3.0	7.4	9.2	0.035575
BMEI0018	Hypothetical cytosolic protein	2.8	3.9	3.9	0.001061
BMEI0051	Hypothetical protein	29.4	29.4	29.4	0.010789
BMEI0057	Hypothetical membrane spanning protein	2.3	2.4	2.4	0.014254
BMEI0059	Hypothetical protein	13.2	66.2	60.8	0.018855
BMEI0063	Hypothetical membrane spanning protein	4.5	108.7	102.9	0.030677
BMEI0064	Hypothetical protein	7.8	209.0	237.5	0.02241
BMEI0152	Hypothetical cytosolic protein	3.3	113.4	166.3	0.027048
BMEI0153	Hypothetical protein	3.3	108.2	104.6	0.008451
BMEI0179	Hypothetical protein	6.3	83.2	61.1	0.0013685
BMEI0217	Hypothetical protein	6.9	218.1	235.6	0.009073
BMEI0262	Hypothetical protein	2.9	106.8	126.6	0.026445
BMEI0366	Hypothetical protein	-3.9	-4.4	-3.5	0.00797
BMEI0373	Hypothetical protein	-3.5	-3.8	-3.3	0.005577
BMEI0422	Hypothetical protein	3.4	14.7	10.9	0.00701
BMEI0425	Hypothetical protein	4.0	41.8	29.3	0.00842
BMEI0431	Hypothetical protein	18.9	43.3	46.6	0.034105
BMEI0442	Hypothetical protein	112.1	222.9	214.6	0.005347
BMEI0448	Hypothetical protein	68.1	83.6	86.3	0.02205
BMEI0458	Hypothetical membrane spanning protein	26.3	195.3	182.2	0.007626
BMEI0498	Cold shock protein CspA	3.2	3.6	4.0	0.031073
BMEI0542	Hypothetical protein	3.7	68.1	60.6	0.015161
BMEI0550	Hypothetical protein	231.3	231.3	231.3	2.70E-05
BMEI0590	Hypothetical protein	72.3	250.8	259.7	0.005759
BMEI0600	Hypothetical membrane spanning protein	3.6	83.5	76.9	0.012201
BMEI0601	Hypothetical protein	5.7	100.2	80.3	0.039441
BMEI0607	Hypothetical cytosolic protein	4.5	73.8	55.8	0.034613
BMEI0620	Hypothetical protein	-6.5	-7.6	-4.7	0.01773
BMEI0638	Hypothetical protein	32.6	237.6	217.3	0.008528
BMEI0678	Low pH-induced protein A	-4.1	-6.0	-3.3	0.012169
BMEI0692	Hypothetical protein	8.9	390.0	383.9	0.000643
BMEI0798	Hypothetical protein	-15.4	-18.0	-15.4	0.001644
BMEI0805	Hypothetical protein	-36.4	-56.4	-26.5	0.003588

TABLE A.1. (continued)

Locus ID	Gene product	SAM	Spotfire	GSpring	ANOVA
			FC		(p)
BMEI0813	Hypothetical protein	-9.2	-11.1	-8.5	0.001088
BMEI0903	Hypothetical protein	4.5	93.7	84.9	0.019457
BMEI1026	Outer membrane protein E	2.8	3.7	3.9	0.023952
BMEI1028	Hypothetical protein	8.1	186.3	227.3	0.024455
BMEI1072	Hypothetical protein	-25.8	-29.3	-17.8	0.007248
BMEI1086	Hypothetical cytosolic protein	2.9	4.2	4.2	0.021914
BMEI1165	Hypothetical membrane spanning protein	28.6	30.2	30.2	0.004184
BMEI1173	Hypothetical membrane spanning protein	-2.8	-3.0	-2.8	1.92E-04
BMEI1214	Hypothetical protein	-5.4	-5.5	-4.9	0.009011
BMEI1219	Hypothetical protein	5.0	467.0	572.7	0.024323
BMEI1242	Hypothetical membrane spanning protein	-7.6	-10.9	-5.7	0.009799
BMEI1275	Hypothetical protein	3.0	37.2	35.4	1.10E-02
BMEI1298	Hypothetical cytosolic protein	11.8	199.6	187.5	0.008254
BMEI1317	Hypothetical protein	23.0	116.3	130.9	0.013377
BMEI1358	Hypothetical cytosolic protein	121.1	121.1	121.1	0.005318
BMEI1361	Hypothetical cytosolic protein	12.9	177.6	168.0	0.020648
BMEI1371	Hypothetical protein	4.8	148.3	119.3	0.041039
BMEI1417	Perosamine synthetase WbkB	225.2	338.0	140.2	0.017503
BMEI1428	Ribonuclease III	3.1	156.8	172.5	0.031964
BMEI1431	BioY protein	19.2	19.2	19.2	0.008123
BMEI1461	Zinc-finger protein	79.4	79.4	79.4	0.015544
BMEI1474	Hypothetical protein	2.8	2.9	2.8	0.022541
BMEI1507	Hypothetical protein	-4.6	-5.3	-4.7	0.000656
BMEI1508	Putative lipoprotein	2.5	99.7	94.9	0.041956
BMEI1509	Hypothetical protein	3.1	95.9	91.2	0.03679
BMEI1516	Hypothetical protein	20.4	20.4	20.4	1.18E-02
BMEI1538	Hypothetical protein	146.3	157.0	157.6	0.001598
BMEI1572	Hypothetical membrane spanning protein	49.1	87.2	70.7	0.014322
BMEI1665	Hypothetical protein	47.1	62.9	62.9	0.018253
BMEI1673	Zinc-binding protein	4.7	158.4	176.8	0.00935
BMEI1681	Hypothetical protein	2.7	86.9	108.5	0.017799
BMEI1699	Hypothetical protein	5.9	119.7	105.4	0.014791
BMEI1711	Hypothetical protein	187.0	187.0	187.0	0.008656
BMEI1761	Hypothetical protein	11.4	164.2	155.7	0.001759
BMEI1767	Hypothetical protein	3.3	22.3	21.0	0.04257
BMEI1785	Hypothetical protein	-4.6	-7.9	-4.3	0.004907
BMEI1795	Hypothetical protein	4.8	199.7	268.0	0.02577
BMEI1857	Hypothetical cytosolic protein	4.4	137.1	153.5	0.0001582
BMEI1866	Hypothetical protein	5.1	98.2	97.9	0.035802
BMEI1893	Protein YbiS precursor	148.6	148.6	148.6	0.010974
BMEI1993	Hypothetical exported protein	23.2	190.5	174.4	0.023201

TABLE A.1. (continued)

Locus ID	Gene product	SAM	Spotfire	GSpring	ANOVA (p)
		FC			
BMEI2044	Hypothetical membrane spanning protein	-2.3	-2.3	-2.1	0.006975
BMEI2049	Hypothetical protein	12.5	151.5	135.2	0.036594
BMEII0043	Hypothetical protein	38.6	102.5	81.5	0.030811
BMEII0082	Hypothetical protein	201.8	201.8	201.8	0.001519
BMEII0090	Hypothetical protein	32.8	32.8	32.8	0.018867
BMEII0094	Hypothetical protein	7.2	310.1	306.7	0.006073
BMEII0231	SlyX protein	6.9	510.9	649.5	0.016558
BMEII0237	Hypothetical protein	82.3	86.6	82.2	0.026051
BMEII0296	Hypothetical protein	26.6	158.7	145.5	0.000888
BMEII0399	Hypothetical protein	69.2	90.9	91.9	0.005163
BMEII0529	Surface protein	2.5	3.0	3.5	0.039543
BMEII0615	Hypothetical protein	-60.5	-70.5	-43.9	0.010396
BMEII0658	Hypothetical protein	15.3	193.4	179.1	0.004162
BMEII0668	Putative integral membrane protein	4.3	103.3	129.3	0.022889
BMEII0682	Oxacillin resistance-associated protein FmtC	4.7	49.2	43.4	0.027366
BMEII0733	Hypothetical protein	2.3	3.2	3.1	0.039316
BMEII0805	Hypothetical protein	4.0	140.1	116.1	0.025098
BMEII0905	Hypothetical protein	224.3	224.3	224.3	0.00956
BMEII0935	Nickel resistance protein	2.7	8.2	10.1	0.021854
BMEII0993	Hypothetical protein	30.3	30.0	30.0	0.033095
BMEII0994	Hypothetical protein	3.3	12.1	9.0	0.011808
BMEII0995	Hypothetical protein	3.1	360.2	290.1	0.023106
BMEII1013	Hypothetical cytosolic protein	5.8	243.9	262.2	0.008494
BMEII1091	Hypothetical pyridoxal phosphate biosynthesis protein	108.1	206.2	175.9	0.01675

FC = Fold-change

Negative sign (-) before the number indicates down-regulation of the gene

GSpring = GeneSpring software

SAM = Significance Analysis of Microarrays software

Spotfire = Spotfire DecisionSite 8.2 software

ANOVA = Analysis of variance

APPENDIX B

TABLE B.1. Genes significantly altered by intracellular *B. melitensis* at 4 h PI of HeLa cells, compared to the inoculum

Locus ID	Symbol	Gene product	Fold-change	p value
DNA replication, recombination and repair				
BMEI0986	<i>tatD</i>	SEC-independent protein TatD	2.48	2.24E-02
BMEI1026	<i>mutL</i>	DNA mismatch repair protein	5.27	1.51E-02
BMEI0596	<i>uvrD</i>	DNA helicase II	0.30395	9.74E-03
BMEI1946	<i>mutM</i>	Formamidopyrimidine-DNA glycosylase	0.3125	1.25E-04
Transcription				
BMEI0685		Transcriptional regulator, AraC family	3.72	2.95E-03
BMEI10226		NTA operon transcriptional regulator	5.91	2.01E-03
BMEI10642		PCA regulon regulatory protein	4.68	1.87E-03
BMEI0371	<i>sigH</i>	Regulatory factor VirF homolog	0.08425	2.55E-03
BMEI0447	<i>lrp</i>	Leucine-responsive regulatory protein	0.41667	3.91E-03
BMEI0493	<i>ompR</i>	Transcriptional regulator OmpR	0.22936	9.19E-03
BMEI0686		Transcriptional regulator, LysR family	0.2924	4.34E-03
BMEI0744	<i>nusG</i>	Transcription antitermination protein NusG	0.20284	1.09E-02
BMEI0750	<i>rpoC</i>	DNA-directed RNA polymerase, beta chain	0.20161	9.24E-03
BMEI1035	<i>rhIE-2</i>	ATP-dependent RNA helicase DEAD	0.36101	8.68E-03
BMEI10281		Transcriptional regulator, GntR family	0.32787	9.93E-03
Translation				
BMEI1073		Glucose-inhibited division protein A	3.65	2.46E-03
BMEI10260		GTP-binding protein LepA	10.01	5.11E-04
BMEI0056	<i>rpmB</i>	LSU ribosomal protein L28P	0.1938	6.04E-05
BMEI0148	<i>rimM</i>	16S ribosomal RNA processing protein RimM	0.29412	9.28E-04
BMEI0156	<i>rplS</i>	LSU ribosomal protein L19P	0.1007	1.12E-02
BMEI0191	<i>prfA</i>	Bacterial Peptide Chain Release Factor 1 (RF-1)	0.2849	8.52E-05
BMEI0201	<i>rplU</i>	LSU ribosomal protein L21P	0.29155	8.35E-03
BMEI0202	<i>rpmA</i>	LSU ribosomal protein L27P	0.23641	9.80E-03
BMEI0481		LSU ribosomal protein L25P	0.26178	8.32E-04
BMEI0491	<i>csaA</i>	Protein secretion chaperonin CsaA	0.16287	4.37E-04
BMEI0742	<i>tuf</i>	Protein Translation Elongation Factor Tu (EF-TU)	0.1297	1.27E-02
BMEI0746	<i>rplA</i>	LSU ribosomal protein L1P	0.28736	1.16E-02
BMEI0747	<i>rplJ</i>	LSU ribosomal protein L10P	0.28818	2.40E-03
BMEI0756	<i>rpsJ</i>	SSU ribosomal protein S10P	0.21834	1.00E-02
BMEI0757	<i>rplC</i>	LSU ribosomal protein L3P	0.18727	5.88E-03
BMEI0759	<i>rplW</i>	LSU ribosomal protein L23P	0.17123	3.58E-03

TABLE B.1. (continued)

Locus ID	Symbol	Gene product	Fold-change	p value
BMEI0774	<i>rpsE</i>	SSU ribosomal protein S5P	0.06623	1.83E-03
BMEI0776	<i>rplO</i>	LSU ribosomal protein L15P	0.23148	4.35E-03
BMEI0780	<i>rpsK</i>	SSU ribosomal protein S11P	0.15674	6.53E-03
BMEI0782	<i>rplQ</i>	LSU ribosomal protein L17P	0.12723	3.18E-04
BMEI0826	<i>frr</i>	Ribosome recycling factor (RRF)	0.25253	7.81E-04
BMEI0915	<i>thrS</i>	Threonyl-tRNA synthetase	0.28818	6.59E-04
BMEI0987	<i>metG</i>	Methionyl-tRNA synthetase	0.16949	6.30E-03
BMEI1168	<i>rplM</i>	LSU ribosomal protein L13P	0.31348	9.90E-03
BMEI1272	<i>cysS</i>	Cysteinyl-tRNA synthetase	0.34247	7.37E-03
BMEI1418		GDP-mannose 4,6-dehydratase / GDP-4-amino-4,6-dideoxy-D-mannose formyltransferase	0.37879	1.87E-03
BMEI1480	<i>rpsF</i>	SSU ribosomal protein S6P	0.27174	1.47E-02
BMEI2038		Peptidyl-tRNA hydrolase	0.26042	9.70E-03
Signal transduction mechanisms				
BMEI0102	<i>uspA</i>	Universal stress protein family	0.13298	9.43E-03
BMEI1128		BolA protein family	0.16	1.06E-02
BMEI1328		Sensory transduction histidine kinase	0.37175	1.11E-04
BMEI2036		Transcriptional regulatory protein ChvI	0.28409	2.47E-04
Carbohydrate transport and metabolism				
BMEII0474		Mannonate dehydratase	3.75	8.46E-03
BMEII0941		Maltose/Maltodextrin transport ATP-binding protein Malk	11.32	7.80E-03
BMEI0393		D-Ribose-binding periplasmic protein precursor	0.31847	3.45E-04
BMEI0399		Dihydroxyacetone kinase	0.23256	2.55E-02
BMEI0977		Putative sugar kinase	0.3413	6.73E-03
BMEI1997		Gluconolactonase	0.369	1.36E-02
BMEII0435		D-ribose-binding periplasmic protein precursor	0.25063	2.40E-03
BMEII0590		Sugar-binding protein	0.18868	1.58E-03
Aminoacid transport and metabolism				
BMEI0084	<i>lysA</i>	Diaminopimelate decarboxylase	2.2	1.98E-02
BMEI0256		D-amino acid dehydrogenase, small subunit	2.91	1.05E-02
BMEII0207		Dipeptide transport system permease protein DppC	6.74	5.63E-03
BMEII0909		Glutamate/gamma-aminobutyrate antiporter	3.66	1.69E-02
BMEII0922		Spermidine/Putrescine transport ATP-binding protein PotA	3.16	1.56E-02
BMEI0207	<i>proB</i>	Gamma-glutamyl kinase	0.29586	9.11E-03
BMEI0433	<i>sapA</i>	Periplasmic dipeptide transport protein precursor	0.19685	4.83E-03
BMEI0559	<i>metF</i>	5,10-methylenetetrahydrofolate reductase	0.26596	7.20E-03
BMEI0618	<i>ilvN</i>	Acetolactate synthase, small subunit	0.30211	7.87E-03
BMEI0734	<i>cysE</i>	Serine acetyltransferase	0.38462	1.31E-02
BMEI0844		Anthranilate phosphoribosyltransferase	0.26385	5.71E-03

TABLE B.1. (continued)

Locus ID	Symbol	Gene product	Fold-change	p value
BMEI1380	<i>betA</i>	Choline dehydrogenase	0.36364	9.73E-03
BMEI0012	<i>pepF</i>	Oligoendopeptidase F	0.27855	3.78E-03
BMEI0284		Periplasmic dipeptide transport protein precursor	0.34247	5.12E-03
BMEI0295		Biphenyl-2,3-diol 1,2-dioxygenase III	0.34483	1.85E-03
Nucleotide transport and metabolism				
BMEI0598		Exopolyphosphatase	7.84	7.13E-03
BMEI0931		NrdI protein	3.13	1.60E-02
BMEI0778	<i>adk</i>	Adenylate kinase	0.31348	1.85E-03
Lipid transport and metabolism				
BMEI0861		Glucose 1-dehydrogenase II	0.25253	1.14E-02
BMEI0958		Sterol binding protein	0.4065	2.12E-03
Coenzyme and inorganic ion transport and metabolism				
BMEI1438	<i>czcD</i>	Cobalt-zinc-cadmium resistance protein CzcD	3.09	1.18E-02
BMEI0998	<i>norB</i>	Nitric-oxide reductase subunit B	3.74	2.67E-03
BMEI1207		Salicylate hydroxylase	3.94	1.78E-02
BMEI0640		4-hydroxybenzoate-3-monooxygenase	22.89	6.84E-04
BMEI0050		CobT protein	0.32051	2.13E-03
BMEI0375	<i>fur</i>	Ferric uptake regulation protein	0.37594	5.58E-03
BMEI0547	<i>phnA</i>	PhnA protein	0.27933	4.92E-03
BMEI0931		Putative thiosulfate sulfurtransferase	0.04943	5.98E-03
BMEI1021		Molybdopterin-guanine dinucleotide biosynthesis protein B	0.40486	4.30E-03
BMEI1557		Arsenate reductase	0.29326	7.78E-03
BMEI1757		Omega-amino acid-pyruvate aminotransferase	0.31546	8.25E-03
BMEI0844		31 kDa outer-membrane immunogenic protein precursor	0.25575	7.59E-03
Post-translational modifications				
BMEI1440		Thiol:Disulfide interchange protein DbsA	6.57	2.61E-02
BMEI0512	<i>trxB</i>	Thioredoxin reductase	0.21097	3.21E-03
BMEI0845		Peptidyl-prolyl cis-trans isomerase D	0.36496	1.58E-03
BMEI0875	<i>clpX</i>	ATP-dependent Clp protease, ATP-binding subunit ClpX	0.2584	3.59E-03
BMEI1455		Thio:disulfide interchange protein	0.35336	3.81E-05
BMEI1649	<i>ureG</i>	Urease accessory protein UreG	0.3367	1.08E-03
BMEI1651	<i>ureE</i>	Urease accessory protein UreE	0.35587	1.05E-03
Energy production and conversion				
BMEI0949	<i>narG</i>	Respiratory nitrate reductase 1 alpha chain	142.49	1.70E-03
BMEI0974	<i>nosZ</i>	Nitrous-oxide reductase	3.32	5.47E-03
BMEI0140		2-oxoglutarate dehydrogenase E1 component	0.17857	6.13E-04
BMEI0251	<i>atpD</i>	ATP synthase beta chain	0.24631	2.36E-04

TABLE B.1. (continued)

Locus ID	Symbol	Gene product	Fold-change	p value
BMEI0791		Isocitrate dehydrogenase	0.2551	8.10E-03
BMEI1152	<i>nuoG</i>	NADH-quinone oxidoreductase chain G	0.19802	4.94E-03
Secondary metabolites biosynthesis				
BMEI0394		2-deoxy-D-glucose-3-dehydrogenase	0.40161	8.42E-03
BMEI1708		2- hydroxyhepta-2,4-diene-1,7-dioate isomerase / 5-carboxymethyl-2-oxo-hex-3-ene-1,7-dioate decarboxylase	0.1634	3.14E-04
Cell wall/membrane biogenesis				
BMEI0852		Succinoglycan biosynthesis transport protein ExoP	4.42	1.31E-02
BMEI0340		Peptidoglycan-associated lipoprotein	0.21645	1.19E-02
BMEI0454	<i>ompW</i>	Outer membrane protein W precursor	0.22831	9.75E-03
BMEI0566		Soluble lytic murein transglycosylase	0.22883	2.22E-03
BMEI0786		Outer membrane protein	0.37037	5.57E-04
BMEI1193		Cell wall degradation protein	0.28986	1.92E-02
BMEI1992	<i>rlpA</i>	Rare lipoprotein A	0.31646	3.14E-03
Cell division				
BMEI0583	<i>ftsQ</i>	Cell division protein FtsQ	0.09756	1.20E-02
BMEI0584	<i>ftsA</i>	Cell division protein FtsA	0.18149	4.60E-05
General function prediction only				
BMEI0593		SCO2 protein	2.34	2.16E-02
BMEI1458	<i>thrB</i>	Homoserine kinase	3.23	8.45E-03
BMEI0123		Exoenzymes regulatory protein AepA precursor	3.54	6.82E-03
BMEI0179		Low affinity zinc transport membrane protein	6.61	9.40E-04
BMEI0638		3-oxodipate enol-lactonase	3.29	8.23E-03
BMEI0792		Intracellular proteinase I	0.34483	9.68E-04
BMEI0796		31 kDa immunogenic protein precursor	0.33557	1.04E-03
BMEI1110		Secretion activator protein	0.21368	1.12E-02
BMEI1495		Lysine decarboxylase	0.21322	4.88E-03
BMEI1951		Putative hydrolase	0.23419	5.62E-03
BMEI0479		ABC transporter substrate-binding protein	0.22075	2.10E-03
BMEI0806		Putative transmembrane protein	0.33898	4.84E-04
Unknown function				
BMEI0731		Cold shock protein	3.3	6.70E-03
BMEI1454		Hypothetical protein	4.06	2.37E-03
BMEI1539		Hypothetical protein	17.34	6.49E-04
BMEI1896		Hypothetical membrane spanning protein	6.46	1.41E-02
BMEI0262		Hypothetical protein	3.76	7.06E-03
BMEI1131		Hypothetical protein	2.71	2.24E-02

TABLE B.1. (continued)

Locus ID	Symbol	Gene product	Fold-change	p value
BMEI0100		Hypothetical protein	0.14025	5.16E-03
BMEI0119		Hypothetical protein	0.37879	8.81E-03
BMEI0144		Hypothetical exported protein	0.21008	1.04E-03
BMEI0222		Carbonic anhydrase	0.21834	1.13E-02
BMEI0287		Hypothetical protein	0.38911	1.57E-03
BMEI0299		Hypothetical protein	0.01643	2.03E-03
BMEI0323		Probable transport ATP-binding protein MsbA	0.12063	6.89E-03
BMEI0445		Oxalate/formate antiporter	0.03421	1.40E-02
BMEI0497		Hypothetical membrane spanning protein	0.28736	6.59E-03
BMEI0521		Hypothetical protein	0.25253	6.15E-03
BMEI0535		Hypothetical protein	0.40161	6.69E-03
BMEI0668		Calcium binding protein	0.29326	1.10E-02
BMEI0724		Hypothetical protein	0.23981	4.46E-03
BMEI0732		Hypothetical cytosolic protein	0.4329	7.06E-03
BMEII0754		Sugar-binding protein	0.32154	4.73E-03
BMEII0755		Sugar-binding protein	0.3861	8.90E-04
BMEI0885		Hypothetical protein	0.2457	5.36E-03
BMEI1031		Hypothetical protein	0.34843	2.49E-02
BMEI1072		Hypothetical protein	0.19646	7.57E-03
BMEI1226		Hypothetical cytosolic protein	0.33113	1.17E-02
BMEI1242		Hypothetical membrane spanning protein	0.32051	2.81E-03
BMEI1435		Polysaccharide deacetylase	0.45045	1.38E-02
BMEI1745		Hypothetical protein	0.30864	1.21E-03
BMEI1761		Hypothetical protein	0.1996	1.21E-02
BMEI1893		Protein YbiS precursor	0.38168	1.43E-05
BMEII0279		Hypothetical membrane spanning protein	0.2439	1.41E-02
BMEII0335		Hypothetical protein	0.37037	3.86E-03
BMEII0471		Hypothetical protein	0.35842	5.00E-03
BMEII0581	<i>sodC</i>	Superoxide dismutase (Cu-Zn)	0.08606	1.75E-02
BMEII0609		Hypothetical protein	0.22422	7.44E-03
BMEII0615		Hypothetical protein	0.29326	2.42E-02
BMEII0991		Hypothetical membrane spanning protein	0.24331	1.16E-02

Fold-change below 1 indicates down-regulation of the gene expression

Genes were ordered in cluster of ortholog groups (COGs) functional categories (downloaded from NCBI/genome projects/bacteria/*B. melitensis*) with adaptations

APPENDIX C

TABLE C.1. Genes significantly altered by intracellular *B. melitensis* at 12 h PI of HeLa cells, compared to the inoculum

Locus ID	Symbol	Gene product	Fold-change	p value
DNA replication, recombination and repair				
BMEI0988	<i>holA</i>	DNA polymerase III, delta subunit	4.58	1.23E-02
BMEI1818	<i>hrpB</i>	ATP-dependent helicase HrpB	2.82	1.00E-02
BMEI0332	<i>ruvC</i>	Holliday junction resolvase	0.274	8.97E-04
Transcription				
BMEI0169		Transcriptional regulator, GntR family/Aminotransferase Class-I	2.61	1.01E-02
BMEI0320		Transcriptional regulator, GntR family	2.38	7.42E-03
BMEI0604		Transcriptional regulator, tetR family	5.87	6.99E-03
BMEI0299		Transcriptional regulator, IclR family	5.92	5.80E-03
BMEI0346	<i>asnC</i>	Transcriptional regulatory protein, AsnC family	3.31	4.42E-03
BMEI0426	<i>deoR</i>	Transcriptional regulator, DeoR family	3.34	2.22E-03
BMEI0486	<i>nikR</i>	Nickel-responsive regulator NikR	3.54	1.64E-02
BMEI1949		Transcriptional regulator, MarR family	0.2882	1.40E-02
Translation				
BMEI1953		Aspartyl-tRNA synthetase	2.74	4.01E-03
BMEI1959		Methyltransferase	2.74	1.29E-02
BMEI2005	<i>pheS</i>	Phenylalanyl-tRNA synthetase, alpha chain	2.91	6.83E-03
BMEI0202	<i>rpmA</i>	LSU ribosomal protein L27P	0.1848	9.17E-03
BMEI0759	<i>rpIW</i>	LSU ribosomal protein L23P	0.4202	3.10E-03
BMEI0823	<i>rpsB</i>	SSU ribosomal protein S2P	0.1721	6.09E-03
BMEI1199		Arginyl-tRNA-protein transferase	0.216	1.48E-02
BMEI1267	<i>ksgA</i>	Dimethyladenosine transferase	0.1927	1.59E-02
Defense mechanisms				
BMEI1645	<i>AcrB</i>	Acriflavin resistance protein B	3.84	4.01E-03
Signal transduction mechanisms				
BMEI1336	<i>phoQ</i>	Sensor protein PhoQ	2.14	8.16E-03
BMEI1582	<i>degU</i>	Transcriptional regulatory protein DegU	4.79	1.47E-02
BMEI0190	<i>ptsP</i>	Phosphoenolpyruvate-protein phosphotransferase PtsP	0.0739	6.75E-03
BMEI2027		Alkaline phosphatase synthesis sensor protein PhoR	0.2632	1.73E-03
Cell wall / membrane biogenesis				
BMEI1304		Outer membrane Porin F precursor	3.51	3.91E-04
BMEI1426		Putative undecaprenyl-phosphate alpha-N-acetylglucosaminyltransferase	3.74	3.60E-03

TABLE C.1. (continued)

Locus ID	Symbol	Gene product	Fold-change	p value
BMEI1556		Integral membrane protein	3.75	8.68E-03
BMEI10376		Heat resistant agglutinin 1 protein	2.69	1.48E-02
BMEI10728		Cellulose synthase catalytic subunit (UDP-forming)	5.48	1.44E-03
BMEI0633		Integral membrane protein	0.33	4.51E-03
Cell motility				
BMEI10156	<i>motD</i>	Chemotaxis MotD protein	3.7	9.36E-03
Cell division				
BMEI0583	<i>ftsQ</i>	Cell division protein FtsQ	0.1776	5.10E-03
Energy production and conversion				
BMEI0898		Predicted acyl-CoA transferases/carnitine dehydratase	2.32	8.98E-03
BMEI10141		Aldehyde dehydrogenase	2.99	8.80E-03
BMEI10185	<i>dld</i>	D-lactate dehydrogenase	5.22	1.64E-02
BMEI10786		NADH dehydrogenase	3	5.76E-03
BMEI10949	<i>narG</i>	Respiratory nitrate reductase 1, alpha chain	103.31	6.94E-03
BMEI10974	<i>nosZ</i>	Nitrous-oxide reductase	3.81	2.94E-04
BMEI11062		(S)-2-hydroxy-acid oxidase subunit GlcE	2.52	1.18E-02
BMEI10474	<i>petB</i>	Cytochrome B	0.365	3.32E-03
BMEI11152	<i>nuoG</i>	NADH-quinone oxidoreductase chain G	0.1842	1.07E-02
BMEI11157	<i>nuoB</i>	NADH-quinone oxidoreductase chain B	0.1988	3.87E-03
Carbohydrate transport and metabolism				
BMEI10106		Xylose repressor	6.25	8.57E-03
BMEI10624	<i>ugpA</i>	Sn-glycerol-3-phosphate transport system permease UgpA	3.48	1.49E-02
BMEI10857		N-acetylmannosamine-6-phosphate 2-epimerase / N-acetylmannosamine kinase	2.63	4.62E-03
BMEI11119		Multidrug resistance protein B	2.76	4.49E-03
Amino acid transport and metabolism				
BMEI0124	<i>argJ</i>	Bifunctional ornithine acetyltransferase/N-acetylglutamate synthase protein	3.6	6.13E-03
BMEI0649	<i>ureA</i>	Urease gamma subunit	10.57	8.57E-03
BMEI1309		Histidinol-phosphate aminotransferase	3.66	1.05E-02
BMEI1627		Arginine-binding periplasmic protein	4.55	8.73E-03
BMEI1722		Sarcosine oxidase beta subunit	3.62	1.96E-02
BMEI1728	<i>proW</i>	Glycine betaine/L-proline transport system permease ProW	3.39	4.58E-03
BMEI10070		Leucine-, isoleucine-, valine-, threonine-, and alanine-binding protein precursor	7.61	1.08E-02
BMEI10196		Spermidine/putrescine-binding periplasmic protein	3.1	7.71E-03
BMEI10249		Dihydrodipicolinate reductase	2.64	1.19E-02
BMEI10631	<i>livM</i>	High-affinity branched-chain amino acid transport system permease protein LivM	3.09	8.73E-03
BMEI1166		O-acetylhomoserine sulfhydrylase/O-acetylserine sulfhydrylase	0.2083	7.58E-03

TABLE C.1. (continued)

Locus ID	Symbol	Gene product	Fold-change	p value
BMEI0038	<i>cycA</i>	D-serine/D-alanine/glycine transporter	0.1905	9.93E-03
Lipid transport and metabolism				
BMEI0022		3-hydroxybutyryl-CoA dehydratase	4.37	3.54E-03
BMEI0552		Lysophospholipase L2	4.95	2.78E-03
BMEI1521	<i>acdA</i>	Acyl-CoA dehydrogenase	2.32	4.93E-03
BMEI1922		Acetoacetyl-CoA synthetase	3.12	1.19E-02
BMEI0062	<i>fabG</i>	Probable carbonyl reductase (NADPH)	2.64	1.13E-02
Coenzyme and inorganic ion transport and metabolism				
BMEI1438	<i>czcD</i>	Cobalt-zinc-cadmium resistance protein CzcD	3.01	7.71E-03
BMEI1517	<i>pdxH</i>	Pyridoxamine 5-phosphate oxidase	4.8	1.06E-02
BMEI0105	<i>frpB</i>	Iron-regulated outer membrane protein FrpB	2.65	6.57E-03
BMEI0580		Probable blue-copper protein Yack precursor	2.38	7.02E-04
BMEI0776	<i>bioF</i>	8-amino-7-oxononanoate synthase	3.08	5.50E-03
BMEI0798		Nitrate transport ATP-binding protein NrtC	3.64	4.17E-03
BMEI0001	<i>hemE</i>	Uroporphyrinogen decarboxylase	0.2604	6.33E-03
BMEI0675	<i>cysW</i>	Sulfate transport system permease protein CysW	0.2137	9.34E-03
General function prediction only				
BMEI0361		ABC transporter ATP-binding protein/ABC transporter permease protein	3.93	5.05E-03
BMEI0697		Transporter, DME family	3.95	1.20E-02
BMEI0852		Methyltransferase	3.68	1.05E-03
BMEI0981		Phosphoglycolate phosphatase	3.52	9.27E-03
BMEI1284		Hypothetical protein-tyrosine phosphatase	2.59	1.78E-02
BMEI1323		Transporter, DME family	3.61	5.30E-04
BMEI1578		Glyoxylate induced protein	2.93	1.28E-02
BMEI1743		ABC transporter ATP-binding protein	4.81	5.54E-04
BMEI0618		Xanthine/uracil permease	3.03	8.02E-04
BMEI0335		4-hydroxybenzoyl-CoA thioesterase family active site	0.2062	2.45E-03
BMEI0554		Glutamine synthetase	0.369	1.09E-02
BMEI0806		Putative transmembrane protein	0.4132	1.24E-02
Unknown function				
BMEI0304		Hypothetical cytosolic protein	7.22	1.66E-03
BMEI0903		Hypothetical protein	2.77	8.20E-03
BMEI0907		Hypothetical protein	5.47	1.10E-02
BMEI1470		Protein YicC	5.54	1.51E-03
BMEI1472		Hypothetical protein	2.38	2.31E-03
BMEI1562		Hypothetical protein	2.63	6.11E-03
BMEI1711		Hypothetical protein	3.52	4.24E-03
BMEI1854		Hypothetical protein	5.01	2.88E-03

TABLE C.1. (continued)

Locus ID	Symbol	Gene product	Fold-change	p value
BMEI1856		Hypothetical exported protein	3.46	1.04E-02
BMEI1860		Hypothetical transmembrane oxidoreductase	3.27	2.10E-03
BMEI0147		Putative integral membrane protein	3.66	3.12E-03
BMEI0149		Extracellular serine protease	3.02	7.18E-03
BMEI0191		Hypothetical protein	5.52	3.38E-03
BMEI0197	<i>pncA</i>	Glu/asp-tRNAamidotransferase subunit A	2.99	6.37E-03
BMEI0357		2-dehydro-3-deoxygalactonokinase	2.61	6.32E-03
BMEI0403		Conserved cytosolic protein	3.09	8.65E-04
BMEI0459		Hypothetical protein	4.46	7.73E-03
BMEI0693		Hypothetical cytosolic protein	3.25	6.98E-03
BMEI0725		Hypothetical protein	3.42	6.32E-03
BMEI0917		Hypothetical protein	4.05	4.45E-03
BMEI0955		Hypothetical protein	5.08	7.98E-03
BMEI0967	<i>nosX</i>	NosX	2.52	3.66E-03
BMEI1046		Hypothetical protein	13.95	1.44E-02
BMEI1072		Hypothetical protein	3.08	1.30E-02
BMEI0331		Hypothetical protein	0.2375	1.14E-03
BMEI0495		Hypothetical protein	0.116	4.56E-03
BMEI0536		Periplasmic immunogenic protein	0.2488	9.79E-03
BMEI1221		Hypothetical cytosolic protein	0.266	3.37E-03
BMEI1261		Leucyl aminopeptidase	0.112	6.22E-03
BMEI1509		Hypothetical protein	0.3597	8.59E-03
BMEI0015		Homospermidine synthase	0.2717	7.14E-03
BMEI0417		Hypothetical protein	0.3257	6.75E-03

Fold-change below 1 indicates down-regulation of the gene expression

Genes were ordered in cluster of ortholog groups (COGs) functional categories (downloaded from NCBI/genome projects/bacteria/*B. melitensis*) with adaptations

APPENDIX D

TABLE D.1. Host genes significantly altered in *B. melitensis*-infected HeLa cells at 4 h PI, compared to non-infected cells

Symbol	Gene product	Fold-change	z-score
DNA replication and repair			
ORC5L	Origin recognition complex, subunit 5	0.66221	-3.468948
POLD3	Polymerase, delta 3	0.77873	-2.428154
TOP2B	Topoisomerase (DNA) II beta	0.73286	-2.756899
ERCC5	Excision repair cross-complementing rodent repair deficiency,	0.73272	-2.51055
GADD45G	Growth arrest and DNA-damage-inducible, gamma	0.78274	-2.32859
H2AFJ	H2A histona family, member J	0.71104	-3.294313
Transcription regulation			
EWSR1	Ewing sarcoma breakpoint region 1	1.2874	2.2920873
PGBP1	Polyglutamine binding protein 1	1.44462	3.3070653
CXXC5	CXXC finger 5	0.73896	-2.725255
ETV1	ETS translocation variant 1	0.76232	-2.406796
EBF2	Early B-cell factor 2	0.77475	-2.369549
EN2	Engrailed 2	0.76205	-2.30452
HOXB9	Homeo box B9	0.75307	-2.408951
JMJD2A	Jumonji domain containing 2A	0.75587	-2.385624
MEF2B	Monocyte-specific enhancer factor 2B	0.65713	-3.849618
MLL5	Mixed-lineage leukemia protein 5 (Drosophila)	0.77121	-2.377747
NR4A1	Nuclear receptor subfamily 4, group A, member 1	0.55428	-5.284012
RFX3	Regulatory factor X 3	0.76687	-2.375122
TBX3	T-box 3	0.77082	-2.245508
THRAP5	Thyroid hormone receptor associated protein 5	0.74269	-2.357621
SOX10	Sex determining region Y, box 10	0.77109	-2.344628
ZNF134	Zinc finger protein 134	0.76556	-2.362746
ZNF189	Zinc finger protein 189	0.76975	-2.269084
ZNF202	Zinc finger protein 202	0.76388	-2.420872
ZNF257	Zinc finger protein 257	0.75757	-2.591762
RNA processing			
CPSF2	Cleavage and polyadenylation specific factor 2	1.31753	2.3680842
SNRPF	Small nuclear ribonucleoprotein F	1.37152	3.036003
U2AF1	U2 small nuclear RNA auxiliary factor 1	1.33886	2.6185748
DHX36	DEAH (Asp-Glu-Ala-His) box polypeptide 36	0.44245	-7.318729
Protein biosynthesis			
EIF5	Eukaryotic translation initiation factor 5	1.26522	2.4960049
MTIF2	Mitochondrial translation initiation factor	0.77088	-2.434161
RPL6	Ribosomal protein L6	0.76423	-2.577655
RPL41	Ribosomal protein L41	0.76695	-2.468626
Cell cycle / cell proliferation			
AIM2	Absent in melanoma 2 (Interferon inducible protein AIM2)	1.30578	2.4723298
CDK4	Cyclin-dependent kinase 4	1.29321	2.2839838

TABLE D.1. (continued)

Symbol	Gene product	Fold-change	z-score
EVI2B	Ectopic viral integration site 2B protein	1.60363	3.6896678
JUND	Jun D proto-oncogen	1.65212	4.3907758
LRP16	LRP 16 protein	1.588	3.8477827
PIWIL2	Piwi-like 2 (Drosophila)	1.31844	2.2969718
CTBP1	C-terminal binding protein 1	1.47444	3.8582533
ABL1	v-abl Abelson murine leukemia viral oncogene homolog 1	0.73293	-2.855903
MYB	v-myb myeloblastosis viral oncogene homolog (avian)	0.66196	-3.522326
DCX	Doublecortex	0.76191	-2.298506
EMP2	Epithelial membrane protein 2	0.78335	-2.252619
EPS8	Epidermal growth factor receptor kinase substrate EPS8	0.64176	-3.723731
HPGD	Hydroxyprostaglandin dehydrogenase 15 (NAD)	0.74688	-2.456055
IGF2	Insulin-like growth factor II	0.75238	-2.548235
NDRG1	N-myc downstream regulated gene 1	0.76004	-2.300189
PLGF	Placenta growth factor	0.70274	-3.097604
RBBP4	Retinoblastome-binding protein 4	0.72108	-2.927198
RUNX3	Runt-related transcription factor 3	0.77929	-2.286013
THRA	Thyroid hormone receptor alpha	0.74799	-2.456245
TIMP1	TIMP metalloproteinase inhibitor 1	0.75154	-2.517132
TPD52	Tumor protein D52	0.76654	-2.548088
ZNF3612	Zinc finger protein 36, C3H type-like 2	0.75922	-2.282861
Cell adhesion			
CD34	Hemopoietic progenitor cell antigen CD34	1.44534	3.4986467
CD47	CD47 antigen	1.32438	2.2968414
THBS1	Thrombospondin 1	1.62538	4.7191228
LAMC1	Laminin, gamma 1	0.69363	-3.198841
Apoptosis			
TFPT	TCF3 (E2A) fusion partner	0.76716	-2.324711
CASP8	Caspase 8	0.77249	-2.261711
BCAP31	B-cell receptor-associated protein 31	0.75787	-2.501483
RUNX3	Runt-related transcription factor 3	0.77929	-2.286013
SERINC3	Serine incorporator 3	0.74665	-2.576057
Immune and inflammatory response			
BDKRB2	Bradykinin receptor B2	1.58372	4.2821552
F3	Coagulation factor III	1.3538	2.4746753
C5	Complement component 5	0.77757	-2.309976
CD24	CD 24 molecule	0.69982	-3.106687
CD46	CD 46 molecule	0.75207	-2.54949
CXCL1	Chemokine (C-X-C motif) ligand 1	0.6915	-3.16797
DEFB126	Defensin b 126	0.76296	-2.301419
IFITM3	Interferon induced transmembrane protein 3	0.74363	-2.699258
MASP1	Mannan-binding lectin serine protease 1	0.7236	-2.626426
Intracellular trafficking			
SDCCAG3	Serologically defined colon cancer antigen 3	1.30104	2.4627789
AAAS	Achalasia, adrenocortical insufficiency, alacrimia	0.76584	-2.424322
GOLGA2	Golgi autoantigen, subfamily A2	0.75279	-2.473068
RAB11FIP2	RAB 11 family interacting protein 2	0.76208	-2.405119
EEA1	Early endosome antigen 1	0.74407	-2.462189

TABLE D.1. (continued)

Symbol	Gene product	Fold-change	z-score
Signal transduction			
FARP2	FERM, RhoGEF and pleckstrin domain protein 2	0.74497	-2.465998
AVPI1	Arginine vasopressin-induced 1	0.7752	-2.306763
MAP3K7IP1	Mitogen-activated protein kinase kinase kinase 7 interacting protein 1 Guanine nucleotide binding protein (G protein), alpha inhibiting activity polypeptide 2	0.76936	-2.313994
GNAI2		0.76428	-2.549902
GKAP1	G kinase anchoring protein 1	0.77107	-2.297608
RICS	Rho GTPase-activating protein	0.76216	-2.242356
Metabolism			
HYAL1	Hyaluronoglucosaminidase	6.57069	15.496092
MMP11	Matrix metalloproteinase 11	1.30574	2.4432546
HEXA	Hexosaminidase A (alpha polypeptide)	0.71608	-3.026842
APOA2	Apolipoprotein A-II	0.7216	-2.843429
GPT	Glutamic-pyruvate transaminase	0.75646	-2.36531
HMGCR	3-hydroxy-3-methylglutaryl-coenzyme A reductase	0.74266	-2.534719
LDLR	Low density lipoprotein receptor	0.78663	-2.327002
LPIN1	Lipin 1	0.76441	-2.348436
CPE	Carboxypeptidase E	0.76493	-2.356092
POMGNT1	Protein O-linked mannanose beta1,2-N-acetylglucosaminyltransferase	0.75945	-2.413648
STK23	Serine/threonine kinase 23	0.75774	-2.24361
TDO2	Tryptophan 2,3-dioxygenase	0.68774	-3.478427
DPH1	DPH1 homolog (S. cerevisiae)	0.75977	-2.323451
Cytoskeleton organization			
ACTC	Actin, alpha	1.3233	2.5042674
ALPL	Alkaline phosphatase, liver	1.50242	3.3968313
WFDC2	WAP four-disulfide core domain 2	1.38431	3.0092823
EPB41	Erythrocyte membrane protein band 4.1	0.73614	-2.797787
KRT1	Keratin 1	0.74833	-2.905533
PFN1	Profilin 1	0.79711	-2.358022
Other functions			
COMT	Catechol-O-methyltransferase	0.73715	-2.844418
GSTP1	Glutathione S-transferase pi	0.66415	-3.53081
KCND1	Potassium voltage-gated channel, member 1	0.64367	-3.630932
SFXN4	Sideroflexin 4	0.78375	-2.429203
CP	Ceruloplasmin	0.71908	-2.770096
CHGA	Chromogranin A	0.74525	-2.399948
FGA	Fibrinogen, A alpha polypeptide	0.68628	-3.100724
AGGF1	Angiogenic factor with G patch and FHA domains 1	0.73601	-2.758494
DKK3	Dickkopf homolog 3 (Xenopus laevis)	0.71877	-2.760573
EXT2	Exostosin (multiple) 2	0.76486	-2.310001
SPANXA1	Sperm protein associated with the nucleus, X-linked, family member A1	0.66837	-3.450173
ITIH4	Inter-alpha (globulin) inhibitor H4	0.62762	-4.345992
CCDC91	Coil-coil domain containing 91	1.27627	2.3041053
TRIM31	Tripartite motif-containing 31	1.63875	4.2126431
KLHL9	Kelch-like 9 (Drosophila)	0.6772	-3.211075
SDCCAG10	Serologically defined colon cancer antigen 10	0.72702	-2.735052
STAMBPL1	STAM binding protein-like 1	0.76121	-2.390359
TULP1	Tubby-like protein 1	1.26614	2.3308962

TABLE D.1. (continued)

Symbol	Gene product	Fold-change	z-score
PROM1	Prominin 1	0.77602	-2.246849
PDE6D	Phosphodiesterase 6D	0.76868	-2.334084
Unknown function			
HSPC135	Transcribed locus	1.459	3.2731334
Hs 153687	Transcribed locus	1.60324	3.4042936
Hs 155566	Transcribed locus	5.86847	14.652094
Hs 157441	Transcribed locus	1.53434	3.6155001
Hs 197081	Transcribed locus	1.30886	2.4470698
Hs 24087	Transcribed locus	1.60473	4.2862217
Hs 356537	Transcribed locus	1.38542	3.0144897
Hs 405564	Transcribed locus	1.24741	2.2522462
Hs 408576	Transcribed locus	1.32242	2.3248019
Hs 415220	Transcribed locus	1.55965	4.1941278
Hs 448968	Transcribed locus	1.34355	2.3754105
Hs 512640	Transcribed locus	1.44503	3.5539992
MGC16121	Hypothetical protein MGC16121	1.56738	3.8964986
MGC50853	Hypothetical protein MGC50853	1.32824	2.355143
MT1M	Metallothionein 1M	1.33285	2.5995546
NICN1	Nicolin 1	1.31822	2.2914136
gb:AI025496	Transcribed locus	1.32677	2.4950966
gb:H46666	Transcribed locus	1.35682	2.4532232
gb:R52934	Transcribed locus	1.39486	2.7219361
gb:W51760	Similar to Heparin-binding growth factor precursor 2	1.649	4.3171207
ACBD5	Acyl-Coenzyme A binding domain containing 5	0.74403	-2.432968
C14orf147	Transcribed locus	0.75143	-2.687003
C20orf62	Transcribed locus	0.7356	-2.897555
FLJ 20097	Transcribed locus	0.73823	-2.513384
FLJ37478	Transcribed locus	0.55793	-5.503183
Hs 108338	Transcribed locus	0.74758	-2.675371
Hs 1987	Transcribed locus	0.70571	-2.822536
Hs 83341	Transcribed locus	0.76519	-2.535004
KIAA0664	Transcribed locus	0.74777	-2.470381
TMEM140	Transmembrane protein 140	0.77583	-2.323219
gb:AA775845	Transcribed locus	0.77458	-2.387821
gb:AI190209	Transcribed locus	0.74974	-2.556592
gb:BE874451	Transcribed locus	0.66936	-3.788126
gb:H62594	Similar to contains Alu repetitive elements	0.76084	-2.700185

Negative sign (-) before the z-score numbers and fold-change below 1 indicate down-regulation of the gene expression

APPENDIX E

TABLE E.1. Host genes significantly altered in *B. melitensis*-infected HeLa cells at 12 h PI, compared to non-infected cells

Symbol	Gene product	Fold-change	z-score
DNA replication and repair			
ARID1A	AT rich interactive domain A1	1.53432145	3.45093586
POLK	Polymerase kappa	1.36535226	2.50694601
RAD51L1	Rad51-like 1 (<i>S. cerevisiae</i>)	1.34005034	2.31790911
RAD9B	RAD9 homolog B (<i>S. cerevisiae</i>)	1.31959503	2.53651239
TDP1	Tyrosyl-DNA phosphodiesterase/alkaline phosphatase D	1.33670838	2.38178397
POLE3	Polymerase, epsilon 3	0.65504295	-3.03419011
RNA processing			
CPEB2	Cytoplasmic polyadenylation element binding protein 2	1.41515313	2.98643844
CPSF2	Cleavage and polyadenylation specific factor 2	1.50438478	3.51843933
DDX12	DEAD/H box polypeptide 12	1.4437683	3.07058803
DHX15	DEAD box polypeptide 15	1.42903951	3.10560287
HNRPM	Heterogeneous nuclear ribonucleoprotein M	1.39416622	2.60652989
RNASE4	Ribonuclease 4	2.26949857	6.55731176
SNRPE	Small nuclear ribonucleoprotein E	1.50133566	3.26020646
SPOP	Speckle-type POZ protein	1.66683916	4.24989545
SFRS11	Splicing factor, arginine/serine-rich 11	1.41167802	2.54044576
XRN2	5'-3' exoribonuclease 2	1.38551554	2.77519719
DDX3Y	DEAD box protein 3, Y-chromosomal	0.7306879	-2.24863398
DDX1	DEAD box polypeptide 1	0.66094854	-3.29437546
DHX36	DEAD box polypeptide 36	0.57712856	-4.44245846
LSM3	LSM3 homolog U6 small nuclear RAN associated (<i>S. cerevisiae</i>)	0.65127981	-2.97093082
SNRPF	Small nuclear ribonucleoprotein F	0.63368679	-3.24226412
NOLA2	Nucleolar protein family A, member 2	0.65828881	-2.52074599
Transcription regulation			
ATF2	Activating transcription factor 2	1.43924458	3.04524649
AFF4	AF4/FMR2 family, member 4	1.36337646	2.68183479
CRSP3	Cofactor required for Sp1 transcriptional activation, subunit 3	1.36166754	2.78728324
CXXC5	CXXC finger 5	1.39493444	2.65395049
ETV1	EST translocation variant 1	1.5087615	3.20185387
ETV5	EST translocation variant 5	1.48650053	3.09294328
EWSR1	Ewing sarcoma breakpoint region 1	1.38353697	2.60823252
FOXJ1	Forkhead fox J1	1.40614468	2.95790085
FOXA3	Forkhead box A3	1.3879332	2.5191127
FOXI1	Forkhead box I1	1.32758513	2.5839967
HDAC6	Histone deacetylase 6	1.28801616	2.34362069
HES1	Hairy and enhancer of split 1 (<i>Drosophila</i>)	1.65541258	3.29231548
HSF4	Heat shock transcription factor 4	1.4143357	2.76784744
KLF12	Kruppel-like factor 12	1.31467392	2.64400586
KLF6	Kruppel-like factor 6	1.62447841	4.2310962
KLF9	Kruppel-like factor 9	1.58421741	3.86748496
NCOR2	Nuclear receptor corepressor 2	1.35875196	2.44483547

TABLE E.1. (continued)

Symbol	Gene product	Fold-change	z-score
NRIP1	Nuclear receptor interacting protein 1	1.58573658	3.53376861
PWP1	PWP1 homolog (<i>S. cerevisiae</i>)	1.65195601	4.3407906
RUNX1	Runt-related transcription factor 1	1.36609236	2.77118801
SOX4	SRY-box containing gene 4	1.36844765	2.62059973
TCF7	Transcription factor 7	1.47637634	3.51251753
TCFL5	Transcription factor-like 5	1.53719257	3.44044927
TFAP4	Transcription factor AP-4	1.52469015	3.92040619
TLE1	Transducin-like enhancer protein 1	1.66097678	4.79954223
ZNF148	Zinc finger protein 148	1.35028795	2.4495498
ZNF154	Zinc finger protein 154	1.49868713	3.2498285
ZNF25	Zinc finger protein 25	1.35972547	2.48145445
ZNF257	Zinc finger protein 257	1.78503777	4.8307937
ZNF350	Zinc finger protein 350	1.33624881	2.4110275
ZNF516	Zinc finger protein 516	1.33031517	2.28218382
ZNF539	Zinc finger protein 539	1.65134444	4.06973236
ZNF562	Zinc finger protein 562	1.35179955	2.561984
ZNF588	Zinc finger protein 588	1.5441345	3.43947161
ZNF711	Zinc finger protein 711	1.48458433	3.23903503
ZNF77	Zinc finger protein 77	1.4429681	2.71418556
ZNF85	Zinc finger protein 85	1.39072222	2.5222804
ZNF93	Zinc finger protein 93	1.75314079	4.97421035
ZSCAN2	Zinc finger and SCAN domain containing 2	1.34368311	2.78814967
ZBTB7A	Zinc finger and BTB domain containing 7A	1.30347568	2.27027589
ZFP64	Zinc finger protein 64	1.35889496	2.60905321
DR1	Down-regulator of transcription 1	0.72412681	-2.58629918
CRSP6	Cofactor required for Sp1 transcriptional activation, subunit 6	0.69365641	-3.29408341
GTF2A2	General transcription factor IIA, 2	0.59151487	-4.70473678
HIF1A	Hypoxia-inducible factor 1 alpha	0.75572392	-2.34033564
LBX2	Ladybird homeobox homolog 2 (<i>Drosophila</i>)	0.73465781	-2.45051559
MAFG	v-maf musculoaponeurotic fibrosarcoma oncogen homolog G (avian)	0.63249762	-3.48412529
NPM1	Nucleophosmin	0.64128313	-3.55471191
RDBP	RD RNA binding protein	0.65307586	-3.8351949
RELA	v-rel reticuloendotheliosis viral oncogen homolog A	0.7484415	-2.41428433
TRIM25	Tripartite motif-containing 25	0.73494299	-2.57053527
Protein biosynthesis			
EIF3S2	Eukaryotic translation initiation factor 3, subunit 2 beta	1.29839183	2.33339833
RPL15	Ribosomal protein L15	1.55955374	2.76556456
RPS6KB1	Ribosomal protein S6 kinase, 70kDa, polypeptide 1	1.41461526	2.91887674
BXDC2	Brix domain containing 2	0.62778446	-2.63289232
EIF1AX	Eukaryotic translation initiation factor 1A, X-linked	0.63624377	-3.21042145
EIF4G2	Eukaryotic translation initiation factor 4 gamma, 2	0.66276356	-2.9289305
EIF5A	Eukaryotic translation initiation factor 5A	0.63919136	-3.80973593
EIF3S1	Eukaryotic translation initiation factor 3, subunit 1 alpha	0.59292889	-3.27564382
ETF1	Eukaryotic translation termination factor 1	0.69935248	-2.96492683
RARS	Arginyl-tRNA synthetase	0.72623583	-2.52859147
KARS	Lysyl-tRNA synthetase	0.7096688	-2.80301925
MRRF	Mitochondrial ribosome recycling factor	0.67015086	-3.14898986
MTIF2	Mitochondrial translational initiation factor 2	0.71972669	-3.09158056
MRPS2	Mitochondrial ribosomal protein S2	0.68009218	-2.80356902

TABLE E.1. (continued)

Symbol	Gene product	Fold-change	z-score
MRPS21	Mitochondrial ribosomal protein S21	0.74624741	-2.49683403
RPL35	Ribosomal protein L35	0.63007113	-2.41985813
RPL6	Ribosomal protein L6	0.70632771	-2.34652836
RPS27A	Ribosomal protein S27A	0.64516206	-2.29586512
RPSA	Ribosomal protein SA	0.60634426	-2.62094334
Protein folding and secretion			
DNAJB6	DNAJ (Hsp40) homolog, subfamily B, member 6	1.32912642	2.27378249
DNAJB9	DNAJ (Hsp40) homolog, subfamily B, member 9	1.48277505	3.2645933
CCT3	Chaperonin containing TCP1, subunit 3	0.69482582	-3.20058906
CCT5	Chaperonin containing TCP1, subunit 5	0.58798466	-2.78201688
PPIF	Peptidylprolyl isomerase F	0.68140944	-2.28713363
Protein degradation			
CPE	Carboxipeptidase E	1.79432184	4.26864274
CTSB	Cathepsin B	2.10685177	6.59857524
DET1	De-etiolated homolog 1 (Arabidopsis)	1.34185917	2.31541883
PRSS1	Protease, serine, 1	2.48033721	6.23311521
PRSS7	Protease, serine, 7	1.46481556	3.2570814
QPCT	Glutaminyl-peptide cyclotransferase	2.73103881	7.70652938
UCHL1	Ubiquitin carboxyl-terminal esterase L1	1.58948645	3.92859894
USP34	Ubiquitin specific protease 34	1.33982461	2.48385939
UBE2D3	Ubiquitin-conjugating enzyme E2 D3	1.48941968	3.01468981
USP15	Ubiquitin specific protease 15	1.41530897	2.86048378
USP32	Ubiquitin specific protease 32	1.62895059	4.38396107
PSMA3	Proteasome subunit, alpha type, 3	0.72243294	-2.95342313
PSMB7	Proteasome subunit, beta type, 7	0.54451429	-3.18438138
PSMD2	Proteasome, 26S subunit, non-ATPase, 2	0.77223605	-2.37960134
UBE2M	Ubiquitin-conjugating enzyme E2M	0.64486165	-3.35493238
UBQLN1	Ubiquilin 1	0.74116747	-2.598481
UCHL3	Ubiquitin carboxyl-terminal esterase L3	0.69807835	-2.9856338
Cell cycle / cell proliferation			
CCND1	Cyclin D1	1.57244336	4.17721854
CCNG1	Cyclin G1	1.38747381	2.37289798
CCNJL	Cyclin J-like	1.38294191	2.457603
CDC2L2	Cell division cycle 2-like 2	1.45305789	2.92941568
CDC2L6	Cell division cycle 2-like 6	1.37873476	2.685863
CHES1	Check point suppressor 1	1.3736702	2.52626936
EGR1	Early growth response protein 1	1.56166189	4.16011838
MAPK1	Mitogen-activated protein kinase 1	3.75962187	10.1187443
MDM4	Mdm4, transformed 3T3 cell double minute 4	1.32454138	2.65653248
S100A12	S100 calcium-binding protein A12	1.5744013	3.26919462
TP53	Tumor protein p53	1.38940668	2.91713307
CYLD	Cylindromatosis	1.34009448	2.3118973
GAS2	Growth-arrest specific protein 2	1.4326843	2.75504528
KLK10	Kallikrein-related peptidase 10	1.3822572	2.8595219
CDK5RAP3	CDK5 regulatory subunit associated protein 3	1.37763166	2.65243917
DDR2	Discoidin domain receptor family, member 2	1.30900128	2.46134716
ERBB3	v-erb-B2 erythroblastic leukemia viral oncogene homolog 3 (avian)	1.52956178	3.39757225
FOS	v-fos FBJ murine osteosarcoma viral	1.3343976	2.78526197

TABLE E.1. (continued)

Symbol	Gene product	Fold-change	z-score
MYB	v-myb myeloblastosis viral oncogen homolog (avian)	1.77265465	4.16701161
SRC	v-src sarcoma viral oncogen homolog (avian)	1.41008744	2.26239951
FGF5	Fibroblast growth factor 5	1.31957471	2.36670783
FGFR2	Fibroblast growth factor receptor 2	1.40397966	2.61505016
GAB1	GRB2-associated binder 1	1.36552448	2.9423508
HOXC10	Homeobox C10	1.37954251	2.46726183
IGF2	Insulin-like growth factor II	2.25163425	5.33288161
PDGFRA	Platelet-derived growth factor receptor, alpha	2.62226	7.44349863
PIM1	Pim 1 oncogen	1.68315464	4.07710952
VEGF	Vascular endothelial growth factor	1.46844684	3.20649729
MCC	Mutated in colorectal cancers	1.3282819	2.39548411
MDF1	MyoD family inhibitor	1.31553577	2.39609787
GPC1	Glypican 1	1.74226479	4.42631559
GPC3	Glypican 3	4.31796195	12.1236823
DCBLD2	Discoidin, CUB and LCCL domain containing 2	1.43402004	3.07271434
DUSP6	Dual specificity phosphatase 6	1.75209287	4.39842565
ESR1	Estrogen receptor 1	1.37283953	2.51066343
GPNUMB	Glycoprotein nmb	3.51891919	8.98178452
IGFBP2	Insulin-like growth factor binding protein 2	1.81273375	5.08259798
IGFBP3	Insulin-like growth factor binding protein 3	2.98629032	9.67892132
MNT	Max binding protein	1.4117326	2.80414686
PPP2R4	Protein phosphatase 2A, regulatory subunit B	1.34272531	2.426593
PRRX1	Paired related homeobox 1	1.43787825	2.64686109
ATR	Ataxia telangiectasia and Rad3 related	0.75153017	-2.42279103
BCAR3	Breast cancer anti-estrogen resistance 3	0.62224344	-3.32951623
CSE1L	Chromosome segregation 1-like	0.66164997	-3.51980099
CSNK1G1	Casein kinase 1, gamma 1	0.6920897	-2.55745827
CRIP1	Cysteine-rich protein 1	0.64118677	-3.5967121
FGF7	Fibroblast growth factor 7	0.66223796	-3.5487114
GFRL1	Fibroblast growth factor receptor-like 1	0.72437967	-2.25652156
GSPT1	G1 to S phase transition protein 1 homolog	0.72030679	-2.98713414
JUND	junD proto-oncogene	0.79195892	-2.24327777
KPNA2	Karyopherin alpha 2	0.73440135	-2.73694357
MYC	v-myc myelocytomatosis viral oncogene homolog (avian)	0.57465018	-4.52724227
PA2G4	Proliferation-associated 2G4, 38kDa	0.64663808	-2.28389357
PTP4A1	Protein tyrosine phosphate type IV A, member 1	0.57636246	-2.88660231
PBK	PDZ binding kinase	0.75089718	-2.31791396
RSN	Restin	0.71425977	-2.76001253
S100A1	S100 calcium-binding protein A1	0.71484421	-2.71094875
S100A10	S100 calcium-binding protein A10	0.57534683	-3.2566169
S100A6	S100 calcium-binding protein A6	0.44447501	-6.83542389
TIMP1	TIMP metalloproteinase inhibitor 1	0.55557917	-4.83106403
IFRD2	Interferon-related developmental regulator 2	0.64864023	-3.06355135
NME1	Non-metastatic cells 1	0.72388559	-2.60204105
PPP2CA	Protein phosphatase 2, catalytic subunit, alpha	0.7433722	-2.51476873
S100A11	S100 calcium-binding protein A11	0.5360633	-5.10001361
TM4SF4	Transmembrane 4 L six family member 4	0.71445433	-2.82152881
Cell adhesion			
ADD2	Adducin 2	1.36268875	2.57327759
CAMK2N1	Calcium/calmodulin-dependent protein kinase II inhibitor 1	2.1118672	5.79943898

TABLE E.1. (continued)

Symbol	Gene product	Fold-change	z-score
CDH1	Cadherin 1, type 1, E-cadherin	1.47555734	3.0703373
CDH11	Cadherin 11, type 2, OB-cadherin (osteoblast)	1.49677177	3.09468838
CDH3	Cadherin 3, type 1, P-cadherin (placental)	1.32676655	2.31457101
CDH6	Cadherin 6, type 2, K-cadherin (fetal kidney)	1.42473285	2.68191677
CEACAM5	Carcinoembryonic antigen-related cell adhesion molecule 5	1.75298794	4.89237531
COL18A1	Collagen, type 18 alpha 1	1.3172008	2.27979411
COL2A1	Collagen, type II, alpha 1	1.3465128	2.31639156
COL4A2	Collagen, type IV, alpha 2	1.43979161	2.82579349
COL6A3	Collagen, type VI, alpha 3	1.37667037	2.40449901
CTNND2	Catenin, delta 2	1.33512987	2.26972992
CD47	CD47 molecule	1.72974107	4.74776656
CDH16	Cadherin 16	1.46639152	3.16430826
CELSR3	Cadherin, EGF LAG seven-pass G-type receptor 3 (Drosophila)	1.33284108	2.42262456
CNTNAP2	Contactin associated protein-like 2	1.47861211	2.55162029
COL9A2	Collagen, type IX, alpha 2	1.35802216	2.53199352
EMILIN1	Elastin microfibril interfacier 1	2.07733039	5.69432799
EVL	Ena-vasodilator stimulate phosphoprotein	1.34955719	2.37186796
FN1	Fibronectin 1	1.37314257	2.66920781
HSPG2	Heparan sulfate preteoglycan 2	1.31472717	2.39974994
ITGA8	Integrin, alpha 8	1.43333526	2.65995252
ITGAL	Integrin, alpha L	1.43358588	3.10683665
ITGB3	Integrin, beta 3	1.46017223	3.20715914
ITGB7	Integrin, beta 7	2.15294983	5.34984602
LGALS4	Lectin, galactose binding, soluble 4	1.63503341	4.32995983
MFAP4	Microfibrillar-associated glycoprotein 4	1.45533536	3.37036407
SDC2	Syndecan 2	1.75117147	3.97432168
THBS1	Thrombospondin 1	1.56670076	3.75380685
THBS4	Thrombospondin 4	1.46778099	3.25578429
TACSTD1	Tumor-associated calcium signal transducer	1.50098222	3.58500634
ARHGDIB	Rho GDP dissociation inhibitor (GDI) beta	1.97906828	5.66077213
EPDR1	Ependymin related protein 1	0.62791651	-3.59372943
L1CAM	L1 cell adhesion molecule	0.68134811	-3.02852759
Cytoskeleton organization			
AMOT	Angiomotin	1.54917681	2.95610436
DCN	Decorin	1.56279152	3.76246873
CDC42EP3	CDC42 effector protein 3	1.57361287	3.55821634
MARCKS	Myristoylated alanine-rich C-kinase substrate	2.1935282	6.50294642
LCP1	Lymphocyte cytosolic protein 1	2.22514114	6.70170921
MAP1B	Microtubule-associated protein 1B	3.31310641	9.90914709
MARK3	MAP/microtubule affinity-regulating kinase 3	1.49409928	3.22446335
NEB	Nebulin	1.34490503	2.34471577
NEBL	Nebulette	1.3528287	2.45863066
PFN2	Profilin 2	1.49893635	3.20677329
RHOJ	Ras homolog gene family, member J	1.40640567	2.83502338
SGCD	Sarcoglycan, delta	1.43996636	2.92209503
SGCE	Sarcoglycan, epsilon	1.33583061	2.62940388
VIL1	Villin 1	1.73805376	4.00208029
MYO10	Myosin X	1.34557864	2.48487963
SNTB1	Syntrophin, beta 1	1.56927548	3.66966483
TPM1	Tropomyosin 1 (alpha)	1.40102582	2.56540417

TABLE E.1. (continued)

Symbol	Gene product	Fold-change	z-score
ABLIM1	Actin-binding LIM protein 1	0.78650662	-2.25814895
FOXC1	Forkhead box C1	0.71322099	-2.70445188
KRT18	Keratin 18	0.44141382	-4.28403717
KRT20	Keratin 20	0.66154362	-3.17430657
MYO1E	Myosin IE	0.7559879	-2.27954326
PFN1	Profilin 1	0.61523229	-3.39803745
TMOD3	Tropomodulin 3	0.61542961	-3.44982659
CART1	Cartilage paired-class homeoprotein 1	0.755282	-2.42938519
ppl	Periplakin	0.69637454	-2.89259009
Development			
ANGPT1	Angiotensinogen 1	1.4969981	2.99551335
DZIP1	DAZ interacting protein 1	1.49156858	3.21413194
SERPINA5	Serine proteinase inhibitor, clade A, member 5	1.94498944	4.77288373
SERPINA7	Serine proteinase inhibitor, clade A, member 7	1.48472277	3.03158298
HEXIM1	Hexamethylene bis-acetamide inducible 1	1.34123051	2.24340197
KRT5	Keratin 5	1.35600707	2.4337124
DIP2A	Disco-interacting protein 2 homolog A (Drosophila)	1.31093057	2.37805422
DLK1	Delta-like 1 homolog (Drosophila)	1.73041517	4.68237492
DLL3	Delta-like 3 (Drosophila)	1.54072658	3.61336602
GHR	Growth hormone receptor	1.60952377	3.57737179
LMO2	LIM domain only 2	1.52550575	2.83605201
NUMB	Numb homolog (Drosophila)	1.49151173	2.76240141
PPAP2B	Phosphatidic acid phosphatase type 2B	1.95397032	5.26227155
PLXNC1	Plexin C1	1.66635044	3.97535569
DKK3	Dickkopf homolog 3 (Xenopus laevis)	2.33885695	6.40724114
CSRP1	Cysteine and glycine-rich protein 1	0.6879742	-2.91519832
Apoptosis			
BCL2	B-cell CLL/lymphoma 2	1.39721031	2.92720266
BIRC4	Baculoviral IAP repeat-containing 4	1.47475976	3.12549012
DAD1	Defender against cell death 1	1.36053336	2.37186354
BNIP3I	BCL2/adenovirus E1B 19kDa-interacting protein 3-like	1.65399425	4.17577146
CD38	CD38 molecule	1.56697161	3.47040907
MDM4	Mdm4, transformed 3T3 cell double minute 4	1.32454138	2.65653248
MAGEH1	Melanoma antigen, family H, member 1	1.67045487	4.16928454
PRG1	Proteoglycan 1, secretory granule	1.66053857	4.10784106
TP53BP2	Tumor protein p53 binding protein, 2	1.29338127	2.36915684
BCL2L1	BCL2-like 1	0.72210355	-2.78702097
BIRC3	Baculoviral IAP repeat-containing 3	0.75013452	-2.4869422
BAG1	BCL2-associated athanogen 1	0.73222617	-2.53752448
CSE1L	Chromosome segregation 1-like	0.66164997	-3.51980099
TEGT	Testis enhanced gene transcript	0.60705412	-3.6307224
MCL1	Myeloid cell leukemia sequence 1	0.63062629	-3.88173901
ANXA1	Annexin A1	0.42901542	-4.81455638
CASP1	Caspase 1	0.69636311	-3.25735884
Immuno and Inflammatory response			
AHSG	Alpha-2-HS-Glycoprotein	3.93303463	11.3953659
BDKRB2	Bradykinin receptor B2	1.32775448	2.48659283
C2	Complement component 2	1.41090764	2.62835721

TABLE E.1. (continued)

Symbol	Gene product	Fold-change	z-score
C5	Complement component 5	1.38553768	2.34831937
CCL16	Chemokine (C-C motif) ligand 16	1.36068668	2.63295429
CD1C	CD1c molecule	1.39280467	2.5395196
CD8B1	CD8 molecule, beta 1	1.45102614	3.0873735
CD24	CD24 molecule	1.73283937	4.1015192
CD28	CD28 molecule	1.58821172	3.63784665
CD84	CD84 molecule	1.30121962	2.26534313
CD86	CD86 molecule	1.43250073	2.81126283
COLEC10	Collectin sub-family member 10	1.31773552	2.37642842
CTLA4	Cytotoxic T-lymphocyte associated protein 4	1.52297843	3.44617889
CMTM7	CKLF-like MARVEL transmembrane domain containing 7	1.37425969	2.85340126
FPRL2	Formyl peptide receptor-like 2	1.49834282	3.54572797
HLA-A	Major histocompatibility complex, class I, A	1.31863973	2.49841716
HLA-B	Major histocompatibility complex, class I, B	1.46325155	3.07795523
HLA-DQA1	Major histocompatibility complex, class II, DQ alpha 1	1.3095408	2.47766477
HLA-DRB1	Major histocompatibility complex, class II, DR beta 1	1.42660068	2.73997063
IGLL1	Immunoglobulin lambda-like polypeptide 1	3.92222738	12.9721865
IKBKAP	Inhibitor of kappa B-cells, kinase complex-associated protein	1.36727964	2.53348658
IL1F5	Interleukin 1 family, member 5	1.33380579	2.48904754
IL1R1	Interleukin 1 receptor, type 1	1.41913355	2.80514327
IL2RG	Interleukin 2 receptor, gamma	1.83847323	5.10022215
IRF4	Interferon regulatory factor 4	1.49865927	3.06580757
ICOSLG	Inducible T-cell co-stimulator ligand	1.49361984	3.57674597
IGJ	Immunoglobulin joining chain	5.56342293	11.2948463
LYZ	Lysozyme	2.36619324	7.01251088
NCF1	Neutrophil cytosolic factor 1	1.32149752	2.34952369
NFIL3	Nuclear factor, interleukin 3 regulated	1.31910484	2.63331256
TNFRSF17	Tumor necrosis factor receptor superfamily, member 17	1.39478379	2.88500711
ANXA1	Annexin A1	0.42901542	-4.81455638
CD46	CD46 molecule	0.70189729	-2.82131293
CD59	CD59 molecule, complement regulatory protein	0.47079519	-4.31038972
CRIP1	Cysteine-rich protein 1	0.64118677	-3.5967121
DAF	Decay acceleratin factor for complement (CD55 molecule)	0.74589635	-2.62878615
F3	Coagulation factor III	0.56049858	-5.11722015
IFIT1	Interferon-induced protein with tetratricopeptide repeats 1	0.44180147	-6.71630506
IFIT2	Interferon-induced protein with tetratricopeptide repeats 2	0.63468656	-3.35102169
IFITM2	Interferon-induced transmembrane protein 2	0.56652492	-3.92969628
IFITM3	Interferon induced transmembrane protein 3	0.69497068	-2.30372743
IL18	Interleukin 18	0.59304953	-4.23492351
IL8	Interleukin 8	0.68783796	-3.01058498
IFI30	Interferon, gamma-inducible protein 30	0.75522337	-2.35041666
KLRC3	Killer cell lectin-like receptor subfamily C, member 3	0.63774985	-3.46947982
SOCS1	Suppressor of cytokine signaling 1	0.69881711	-3.02963162
Nervous system development and proliferation			
CDK5RAP1	CDK5 regulatory subunit associated protein 1	1.34486228	2.5146975
DCT	Dopachrome tautomerase	3.98044135	11.581189
MDK	Midkine	1.8252039	4.46656528
NGFRAP1	Nerve growth factor receptor associated protein 1	1.30715829	2.53392347
MYEF2	Myelin basic protein expression factor 2	1.45559037	3.42963605
NES	Nestin	1.77741941	4.90787046

TABLE E.1. (continued)

Symbol	Gene product	Fold-change	z-score
NGFR	Nerve growth factor receptor	1.38314993	2.59344061
NRG3	Neuregulin 3	1.37672522	3.18463153
SEMA3C	Semaphorin 3C	1.71485936	5.18370452
ROBO1	Roundabout, axon guidance receptor, homolog 1 (Drosophila)	1.45648671	3.11902941
CLN8	Ceroid-lipofuscinosis, neuronal 8	1.38711102	2.33800532
RTN4	Reticulon 4	1.4467759	2.89293079
HPCAL1	Hippocalcin-like 1	1.33684274	2.42743985
NP1P	Nuclear pore complex interacting protein	1.75648993	4.00162409
EFNB3	Ephrin B3	1.45069469	2.45079187
NPFF	Neuropeptide FF-amide peptide precursor	1.38598666	2.70015539
PIK4CA	Phosphoinositide-3-kinase, catalytic, alpha polypeptide	1.46819621	3.40721939
PPFIA4	Protein tyrosine phosphatase, receptor-type, f polypeptide, interating protein, alpha 4	1.50512565	3.39738862
CHRNA3	Cholinergic receptor nicotinic alpha polipeptide 3	1.43895608	3.50046108
CPLX2	Complexin 2	1.31909405	2.54753348
NTS	Neurotensin	3.57038253	10.0185218
SV2B	Synaptic vesicle glycoprotein 2B	1.33280448	2.5143609
GDI1	GDP dissociation inhibitor 1	1.38759786	2.8244956
SORL1	Sortilin-related receptor, L1	1.44122535	2.90976483
CRABP2	Cellular retinoic acid-binding protein II	1.49554488	3.21555239
CRX	Cone-rod homeobox protein	1.44234535	3.11630575
LUM	Lumican	3.32532992	8.95013489
RABGGTA	Rab geranylgeranyltransferase alpha subunit	1.3354206	2.31244659
BBS5	Bardet-Biedl syndrome 5	1.32451727	2.38463048
TRIOBP	TRIO and F-actin binding protein	1.4290213	2.98409845
SNAP25	Synaptosomal-associated protein 25	0.65161648	-3.42986776
SLC6A15	Solute carrier family 6, member 15	0.43735625	-5.72640287
Metabolism			
Nucleic acids			
AK3L1	Adenylate kinase 3 like 1	1.35868119	2.39545282
ENPP3	Ectonucleotide pyrophosphatase/phosphodiesterase 3	1.34726476	2.49657784
NME4	Non-metastatic cells 4	1.43488069	3.17587834
NT5E	5'-nucleotidase, ecto	1.46971975	3.54922515
PAPSS2	3'-phosphoadenosine 5'-phosphosulfate synthase 2	1.38552039	2.67899937
CTPS	CTP synthase	0.58207028	-3.76632256
TYMS	Thymidylate synthase	0.73111215	-2.36865469
HPRT1	Hypoxanthine phosphoribosyltransferase	0.63435195	-3.88587975
PRPS2	Phosphoribosyl pyrophosphate synthetase 2	0.63515259	-2.59969318
Carbohydrates			
CHST2	Carbohydrate sulfotransferase 2	1.50579224	3.32723512
HK1	Hexokinase 1	1.91382216	5.71558137
HS3ST3B	Heparan sulfate (glucosamine) 3-O-sulfotransferase 3B1	1.41454494	2.66426755
HYAL1	Hyaluronoglucosaminidase 1	3.03443775	8.09165151
HAS2	Hyaluronan synthase 2	1.73087125	4.10218405
IDS	Iduronate 2-sulfatase	1.48393298	3.12853776
MPI	Mannose phosphate isomerase	1.42562129	3.08417271
PDK3	Pyruvate dehydrogenase kinase, isoenzyme 3	1.30900038	2.32661045
CHGN	Chondroitin beta 1, 4 N-acetylgalactosaminyltransferase	0.6936003	-2.79525741
SLC35A1	Solute carrier family 35, member 1	0.7108504	-2.83837696

TABLE E.1. (continued)

Symbol	Gene product	Fold-change	z-score
Lipids			
APOB	Apolipoprotein B	4.53711173	11.2637478
APOA2	Apolipoprotein A2	3.70707679	10.2811419
CAV1	Caveolin 1	1.88129671	5.30126973
FDFT1	Farnesyl-diphosphate farnesyltransferase 1	1.39131233	2.87158262
SC4MOL	Sterol-C4-methyl oxidase-like	1.40718068	2.78833567
ACSS2	Acyl-CoA synthetase short-chain family member 2	1.3178339	2.67107162
APOC2	Apolipoprotein C2	1.55208711	3.62817828
ASAH1	N-acylsphingosine amidohydrolase 1	1.33415623	2.48474078
BBOX1	Butyrobetaine (gamma), 2-oxoglutarate dioxygenase	1.51376845	3.23128431
ELOVL2	Elongation of very long chain fatty acids-like 2	1.40900097	2.61191543
LPIN1	Lipin 1	1.30417895	2.26170236
LRP10	Low density lipoprotein receptor-related protein 10	1.35588214	2.44136741
PCCA	Propionyl coenzyme A carboxylase, alpha	1.30481396	2.38066018
VLDLR	Very low density lipoprotein receptor	2.16157571	6.40017845
OSBP2	Oxysterol binding protein 2	0.69107939	-2.80857689
Amino acids			
DDC	DOPA decarboxylase	1.3427939	2.28005408
DMGDH	Dimethylglycine dehydrogenase	1.39081017	2.72445958
GATM	Glycine amidinotransferase	1.31521292	2.30747407
OAT	Ornithine aminotransferase	1.37152958	2.74254232
ASL	Argininosuccinate Lyase	1.63073996	3.91862349
ASNS	Asparagine synthetase	1.51767554	3.78542345
DDOST	Dolichyl-diphosphooligosaccharide-protein glycosyltransferase	1.51487156	3.53884923
GLDC	Glycine dehydrogenase (decarboxylatin)	1.34037049	2.50461897
GLS	Glutaminase	1.34936818	2.71093841
CCDC91	Coil-coil domain containing 91	1.34899065	2.41416936
ODC1	Ornithine decarboxylase	0.64562492	-3.15950612
SDF2	Stromal cell-derived factor 2	0.70229373	-3.15978524
TM4SF3	Transmembrane 4 superfamily member 3	0.51737057	-5.24922684
FNTB	Farnesyltransferase, CAAX box, beta	0.64221781	-3.5238036
Coenzymes metabolism			
BTD	Biotinidase	1.499606	3.67518414
FBP1	Folate binding protein 1	1.53282551	3.54352971
FOLR2	Folate receptor 2	0.69630437	-3.20992386
FOLR1	Folate receptor 1	0.76058393	-2.44230841
General metabolism			
NAGK	N-acetylglucosamine kinase	1.42600673	2.86490201
ITIH2	Inter-alpha (globulin) inhibitor H2	2.91856162	7.09241628
MAOA	Monoamine oxidase A	1.56885897	3.48886458
ALDH1A1	Aldehyde dehydrogenase 1 family, member A1	1.74987649	4.51026047
HIBCH	3-hydroxyisobutyryl-coenzyme A hydrolase	1.30016245	2.30890812
PPARD	Peroxisome proliferative activated receptor, delta	1.34562962	2.59824078
ALOX12	Arachidonate 12-lipoxygenase	1.31775469	2.2884762
CA11	Carbonic anhydrase XI	1.29432748	2.24233123
CASD1	CAS1 domain containing 1	1.33719212	2.28231182
NNMT	Nicotinamide N-methyltransferase	0.61712849	-3.85390281
FVT1	Follicular variant translocation protein 1	0.75644557	-2.59695465

TABLE E.1. (continued)

Symbol	Gene product	Fold-change	z-score
TCA			
IDH3A	Isocitrate dehydrogenase 3 alpha	0.71572209	-2.55178195
LDHA	Lactate dehydrogenase A	0.71729902	-2.73084932
Eletron transport			
ATP11A	ATPase, class VI, Type 11A	1.37744631	2.63982716
ATP8B2	ATPase, class I, type 8B, member 2	1.35041019	2.33334146
CYB5A	Cytochrome b5 type A (microsomal)	1.55043029	3.29428238
CYP27A1	Cytochrome p450, family 27, subfamily A, polypeptide 1	1.36702215	2.92581736
FMO5	Flavin containing monooxygenase 5	1.4669254	2.96883815
NDUFB3	NADH dehydrogenase (Ubiquinone) flavoprotein 3	1.40768279	2.91966216
NDUFB1	NADH dehydrogenase (Ubiquinone) flavoprotein 1	1.35528831	2.64889472
STEAP1	Six transmembrane epithelial antigen of the prostate 1	1.96768815	5.22293885
ATP5I	ATP synthase, H+ transporting, mitochondrial F0 complex	0.73130093	-2.86327607
ATP5J2	ATP synthase, H+ transporting, mitochondrial F0 complex, subunit F2	0.72132806	-2.83400209
COX7B2	Cytochrome c oxidase subunit VIIb2	0.5815765	-3.10704942
ETF A	Electron transfer flavoprotein alpha-subunit precursor	0.74312287	-2.38255574
HCCS	Holocytochrome c synthase	0.57075552	-5.10020156
TXNL5	Thioredoxin-like 5	0.74463801	-2.54202603
Surface receptors			
ADRBK2	Adrenergic receptor beta, kinase 2	1.43442795	2.6287744
ASGR2	Asialoglycoprotein receptor 2	1.40161663	2.90118968
EDNRB	Endothelin receptor type B	1.47142258	3.17921931
GRB7	Growth factor receptor bound protein 7	1.32299783	2.43281461
OPRL1	Opiate receptor-like 1	1.31161818	2.32493003
PLA2R1	Phospholipase A2 receptor 1	1.76374038	4.68431754
PTPRZ1	Protein tyrosine phosphatase, receptor-type, Z polypeptide 1	1.44525561	2.64621592
CD200	CD200 molecule	1.80610218	3.77848999
Signal transduction			
APBB1IP	Amyloid beta (A4) precursor protein-binding, family B, member 1 interacting protein	1.4647806	3.35222881
ARHGAP15	Rho GTPase activating protein 15	1.83182457	5.00696334
ARHGAP18	Rho GTPase activating protein 18	1.41434193	2.63185089
CNIH4	Cornichon homolog 4 (Drosophila)	1.51225761	3.54321999
CSNK1G2	Casein kinase 1, gamma 2	1.32886635	2.26393768
GPR161	G protein-coupled receptor 161	1.50989873	3.48762387
GNG2	Guanine nucleotide binding protein, gamma 2	1.54097189	3.65347611
GPR143	G protein-coupled receptor 143	1.35368956	2.47775237
INPP4B	Inositol polyphosphate-4-phosphatase, type II	1.54861704	4.20432562
LPHN2	Latrophilin 2	1.55306859	3.30453342
MPDZ	Multiple PDZ domain protein	1.50571283	3.46603738
PIK3C3	Phosphoinositide-3-kinase, class 3	1.38787937	2.66435422
PIK3CG	Phosphoinositide-3-kinase, catalytic, gamma polypeptide	1.81382367	4.33332906
PIK3R1	Phosphoinositide-3-kinase, regulatory subunit, polypeptide 1	1.59656768	3.54225972
PLCB4	Phospholipase C, beta 4	1.31542978	2.32344275
PRKAR1A	Protein kinase, cAMP-dependent, regulatory, type I alpha	1.43757154	3.25542087
PRKD3	Protein kinase D3	1.3454365	2.79819669
RAB30	Rab30, member RAS oncogene family	1.37405128	2.6425958

TABLE E.1. (continued)

Symbol	Gene product	Fold-change	z-score
RASGRP2	Ras guanyl releasing protein 2	1.30941025	2.24290377
RAB3GAP2	RAB3 GTPase activating protein subunit 2	1.37992076	2.72664696
RAP2B	RAP2B, member of RAS oncogen family	1.30897022	2.53237368
RASSF4	Ras association domain family 4	1.32134789	2.32855869
RGL1	RAL guanine nucleotide dissociation stimulator-like 1	1.56453607	3.19491149
SH2D1A	SH2 domain protein 1A	1.45954309	3.04705319
TPTE	Transmembrane phosphate with tensin homology	1.6530772	3.94957843
WSB1	WD repeat and SOCS box-containing 1	1.72004535	4.48196458
RGS2	Regulator of G-protein signalling 2	0.54509321	-5.27130607
RHOC	Ras homolog gene family, member C	0.73329149	-2.73281877
RHOF	Ras homolog gene family, member F	0.58739484	-3.13224783
RAI3	Retinoic acid induced 3	0.42262328	-6.13242229
WDR5	WD repeat domain 5	0.65798724	-2.90534861
SH2D4A	SH2 domain containing 4A	0.61310313	-3.92385828
Transport			
ABCG2	ATP-binding cassette, sub-family G, member 2	1.43755663	2.83030926
KCNH8	Potassium voltage-gated channel, subfamily H, member 8	1.39093245	2.55614003
PDPN	Podoplanin	1.3853533	2.4383033
RHAG	Rh-associated glycoprotein	2.21134892	6.1047486
SLC2A14	Solute carrier family 2, member 14	1.39908252	2.43649873
SLC9A7	Solute carrier family 9, member A7	1.32075865	2.36520355
SLC13A5	Solute carrier family 13, member 5	1.38708512	2.70201508
SLC25A36	Solute carrier family 25, member 36	1.40386266	2.9032339
SLC36A3	Solute carrier family 36, member 3	1.31714821	2.28263811
SLC43A1	Solute carrier family 43, member 1	1.36705916	2.68377439
SLC44A4	Solute carrier family 44, member 4	1.46503723	3.4473516
SLC4A3	Solute carrier family 4, member 3	1.53222799	3.41760562
TOMM40	Translocase of outer mitochondrial membrane 40 homolog (yeast)	1.87417375	5.01940063
TRPC1	Transient receptor potential cation channel, subfamily C, member1	1.52843966	3.42222961
TRPM1	Transient receptor potential cation channel, subfamily M, member1	1.45942239	3.1891183
CP	Ceruloplasmin	2.15175794	5.68997276
FTH1	Ferritin, heavy polypeptide 1	0.65502243	-2.33685813
FTMT	Ferritin mitochondrial	0.64162349	-2.32467712
KCNK1	Potassium channel, subfamily K, member 1	0.76022069	-2.27483854
MTCH2	Mitochondrial carrier homolog 2 (C. elegans)	0.78205611	-2.25929331
PLP2	Proteolipid protein 2	0.42372356	-7.24495193
SGK	Serum/glucocorticoid regulated kinase	0.57105637	-3.92424421
Endocytosis and intracellular trafficking			
AP1S2	Adaptor-related protein complex 1, sigma 2 subunit	1.52440155	3.19621278
COG8	Component of oligomeric golgi complex 8	1.46134492	3.05920623
EXOC4	Exocyst complex component 4	1.49997571	3.25142779
GOLGA2	Golgi autoantigen, golgi subfamily A, 2	1.40892463	2.87713287
GOLGA8A	Golgi autoantigen, golgi subfamily A, 8A	1.55191477	3.40998883
KDELRL3	KDEL endoplasmic reticulum protein retention receptor 3	1.34135887	2.44771414
M6PRBP1	Mannose-6-phosphate receptor binding protein 1	1.34143036	2.42061974
STX7	Syntaxin 7	1.45031769	3.1616294
SNX9	Sorting nexin 9	1.33261237	2.31777377
SYTL2	Synaptotagmin-like 2	1.94777692	5.16749699
TLOC1	Translocation protein 1	1.36905438	2.72626598

TABLE E.1. (continued)

Symbol	Gene product	Fold-change	z-score
VPS11	Vacuolar protein sorting 11 (yeast)	1.32652323	2.32376442
PICALM	Phosphatidylinositol binding clathrin assembly protein	0.70161119	-2.81106818
TMED2	Transmembrane emp24 domain trafficking protein 2	0.66271615	-2.87984175
Skeletal development			
ALPL	Alkaline phosphatase, liver	1.54932151	3.6288474
COMP	Cartilage oligomeric matrix protein	1.38479396	2.68595317
ENAM	Enamelin	2.7900519	7.51967567
MGP	Matrix Gla protein	1.75538219	4.86503301
SPARC	Secreted protein acidic and rich in cysteine	3.88613122	10.6819484
SPP1	Secreted phosphoprotein 1	3.21141268	10.1456247
TNFRSF11B	Tumor necrosis factor receptor superfamily, member 11b	1.78366558	4.39802099
STC1	Stanniocalcin 1	1.40063078	2.85229563
VDR	Vitamin D3 receptor	1.33776292	2.41708464
BMP2	Bone morphogenetic protein 2	0.74330416	-2.61239007
Blood coagulation			
EFEMP2	EGF-containing fibulin-like extracellular matrix protein 2	1.32588096	2.32864565
F7	Coagulation factor VII	1.74156023	4.80480432
FGA	Fibrinogen, A alpha polypeptide	1.75926095	4.57347696
FGG	Fibrinogen, gamma polypeptide	2.05458225	5.44521082
Other functions			
ALAD	Aminolevulinate, delta-, dehydratase	1.32699147	2.35293334
FECH	Ferrochelatase	1.41518748	2.99521549
HBG1	Hemoglobin, gamma A	9.28434474	17.672231
NOX4	NADPH oxidase 4	1.40532609	2.73494326
RCN1	Reticulocalbin 1	0.72115746	-2.34261783
PRDX6	Peroxiredoxin 6	1.31262834	2.27499884
SEPP1	Selenoprotein P, plasma 1	5.39862299	14.1782683
PRDX1	Peroxiredoxin 1	0.61920071	-2.51102794
ADH6	Alcohol dehydrogenase 6 (class V)	1.27253883	2.27743271
AGT	Angiotensinogen	2.3094322	6.97514445
AFP	Alpha-fetoprotein	5.65569314	11.9631022
ALB	Albumin	3.78573358	8.80240457
PDE4B	Phosphodiesterase 4B	1.60244828	3.90158206
PDE4DIP	Phosphodiesterase 4D interacting protein	1.46822461	3.19671564
PDE5A	Phosphodiesterase 5A	1.39223303	2.61934907
PDE7A	Phosphodiesterase 7A	1.46417191	3.05559312
ADCK4	AARF domain containing kinase 4	1.43181342	2.94427016
CD3D	CD3d molecule, delta	2.57848218	7.46910708
ENPP2	Ectonucleotide pyrophosphatase/phosphodiesterase 2	1.51887873	2.82755567
FCER1G	FC-epsilon-receptor gamma subunit	1.41840593	2.79377546
GPX3	Glutathione peroxidase 3	1.51394359	3.13299008
PEX6	Peroxisomal biogenesis factor 6	1.30679434	2.31735651
OPTN	Optineurin	1.42360136	2.36924095
PKIG	Protein kinase inhibitor, gamma	1.34610402	2.36923763
PKIB	Protein kinase inhibitor, beta	1.68975865	3.92398926
PSG9	Pregnancy specific beta-1-glycoprotein 9	1.39997832	2.55802365
RNF144	Ring finger protein 144	1.60564901	3.61246968
SCRN1	Secernin 1	1.53132664	3.73580579

TABLE E.1. (continued)

Symbol	Gene product	Fold-change	z-score
ST6GAL1	ST6 beta-galactosamide alpha-2,6-sialyltransferase 1	1.894161	4.74431473
TANK	TRAF family member-associated NFKB activator	1.36600355	2.51119771
TFF1	Trefoil factor 1	1.76124013	4.65933284
TTR	Transthyretin	1.4944669	2.94968394
WT1	Wilms' tumor protein	1.48859889	3.06063609
ANTXR1	Anthrax toxin receptor 1	0.71055456	-2.80189381
CUTC	CutC cooper transporter homolog (E. coli)	0.74205523	-2.37245576
DCTN6	Dynactin 6	0.75646073	-2.60291864

325 up- & 81 down-regulated genes of Unknown function were not listed

Negative sign (-) before the z-score numbers and fold-change below 1 indicate down-regulation of the gene expression

APPENDIX F

TABLE F.1. Core set of genes differentially expressed by intracellular *B. melitensis* in the first 4 h post infection of bovine Peyer's patch, compared to the inoculum

Locus ID	Symbol	Gene product	Expression
Replication, recombination and repair			
BMEI0537		Integrase/recombinase	Down
BMEI0728	<i>recJ</i>	Single-stranded-DNA-specific exonuclease RecJ	Down
BMEI0787	<i>recA</i>	RecA protein	Up
BMEI0877		DNA-binding protein Hu-alpha	Up
BMEI0880		Single-strand binding protein	Up
BMEI1052		Transposase	Down
BMEI1093		Exodeoxyribonuclease III	Up
BMEI1399		Transposase	Up
BMEI1408		Transposase	Down
BMEI1412		Transposase	Up
BMEI1442		A/G-specific adenine glycosylase	Down
BMEI1444		Adenine-specific methyltransferase	Up
BMEI1485	<i>dnaB</i>	Replicative DNA helicase	Up
BMEI1661		Recombinase	Down
BMEI1794	<i>ihfB</i>	Integration host factor beta subunit	Up
BMEI1801	<i>mutS</i>	DNA mismatch repair protein	Down
BMEI1876		DNA polymerase III, alpha chain	Up
BMEI1943		Chromosomal replication initiation protein	Up
BMEI1980		DNA protection during starvation protein	Up
BMEI0712		Transposase	Up
Transcription			
BMEI0003	<i>rho</i>	Transcription termination factor Rho	Up
BMEI0010	<i>parB</i>	Chromosome partitioning protein ParB	Up
BMEI0253		Transcriptional regulator, MarR family	Up
BMEI0279		Transcriptional regulator CarD family	Up
BMEI0280	<i>rpoH</i>	RNA polymerase sigma factor	Up
BMEI0320		Transcriptional regulator, GntR family	Down
BMEI0410		Transcriptional regulator, MerR family	Up
BMEI0446		Transcriptional regulator, MarR family	Up
BMEI0494		Transcriptional regulatory protein PetP	Down
BMEI0532	<i>rpoD</i>	RNA polymerase sigma factor	Up
BMEI0626		Transcriptional regulator, GntR family	Up
BMEI0744	<i>nusG</i>	Transcription antitermination protein NusG	Up
BMEI0749	<i>rpoB</i>	DNA-directed RNA polymerase beta subunit	Up
BMEI0750	<i>rpoC</i>	DNA-directed RNA polymerase beta' subunit	Up
BMEI0785		Transcriptional regulatory protein	Up
BMEI1297	<i>rpoZ</i>	DNA-directed RNA polymerase omega subunit	Up
BMEI1364		Transcriptional regulatory protein MucR	Up
BMEI1384		Transcriptional regulator, AraC family	Down
BMEI1582		Transcriptional regulatory protein DegU	Down
BMEI1641		Transcriptional regulator, TetR family	Down
BMEI1642		Transcriptional regulator, TetR family	Down

TABLE F.1. (continued)

Locus ID	Symbol	Gene product	Expression
BMEI1885		Transcriptional regulatory protein, LysR family	Down
BMEI2050		Transcriptional regulator	Down
BMEII0104		Transcriptional regulator, AraC family	Down
BMEII0128		Transcriptional regulator	Down
BMEII0299		Transcriptional regulator, IclR family	Down
BMEII0370		Histidine utilization repressor	Down
BMEII0372		Transcriptional regulator, MerR family	Down
BMEII0486		NikR nickel-responsive regulator NikR	Down
BMEII0563		Proline dehydrogenase transcriptional activator	Up
BMEII0807		Transcriptional regulator, GntR family	Down
BMEII0820		ALS operon regulatory protein	Down
BMEII0858		Transcriptional regulator, GntR family	Down
BMEII0878		Transcriptional regulator, GntR family	Down
BMEII0966		Transcription regulator, Crp family	Down
BMEII0975		Regulatory protein NosR	Down
BMEII0985		Ribitol operon repressor	Down
BMEII1077		Transcriptional regulatory protein, LysR family	Down
Translation, ribosomal structure and biogenesis			
BMEI0056	<i>rpmB</i>	Ribosomal protein L28	Up
BMEI0156	<i>rplS</i>	Ribosomal protein L19	Up
BMEI0171		Ribosomal protein L11 methyltransferase	Down
BMEI0201	<i>rplU</i>	Ribosomal protein L21	Up
BMEI0202	<i>rpmA</i>	Ribosomal protein L27	Up
BMEI0272	<i>rpmF</i>	Ribosomal protein L32	Up
BMEI0294		LSU ribosomal protein L36P	Up
BMEI0322	<i>rpmE</i>	Ribosomal protein L31	Up
BMEI0428	<i>trmU</i>	tRNA (5-methylaminomethyl-2-thiouridylate)-methyltransferase	Down
BMEI0463		Poly(A) polymerase / tRNA nucleotidyltransferase	Down
BMEI0479		GTP-binding protein	Up
BMEI0481	<i>rplY</i>	50S ribosomal protein L25	Up
BMEI0745	<i>rplK</i>	Ribosomal protein L11	Up
BMEI0746	<i>rplA</i>	Ribosomal protein L1	Up
BMEI0752	<i>rpsL</i>	Ribosomal protein S12	Up
BMEI0753	<i>rpsG</i>	Ribosomal protein S7	Up
BMEI0755		Elongation factor Tu	Up
BMEI0756	<i>rpsJ</i>	Ribosomal protein S10	Up
BMEI0757	<i>rplC</i>	Ribosomal protein L3	Up
BMEI0758	<i>rplD</i>	Ribosomal protein L4	Up
BMEI0759	<i>rplW</i>	Ribosomal protein L23	Up
BMEI0760	<i>rplB</i>	Ribosomal protein L2	Up
BMEI0761	<i>rpsS</i>	Ribosomal protein S19	Up
BMEI0762	<i>rplF</i>	Ribosomal protein L22	Up
BMEI0763	<i>rpsC</i>	30S ribosomal protein S3	Up
BMEI0764	<i>rplP</i>	Ribosomal protein L16	Up
BMEI0765	<i>rpmC</i>	Ribosomal protein L29	Up
BMEI0768	<i>rplX</i>	50S ribosomal protein L24	Up
BMEI0770	<i>rpsN</i>	30S ribosomal protein S14	Up
BMEI0771	<i>rpsH</i>	30S ribosomal protein S8	Up
BMEI0772	<i>rplV</i>	Ribosomal protein L6	Up
BMEI0773	<i>rplR</i>	50S ribosomal protein L18	Up

TABLE F.1. (continued)

Locus ID	Symbol	Gene product	Expression
BMEI0775	<i>rpmD</i>	50S ribosomal protein L30	Up
BMEI0776	<i>rplO</i>	LSU ribosomal protein L15P	Up
BMEI0779	<i>rpsM</i>	Ribosomal protein S13/S18	Up
BMEI0780	<i>rpsK</i>	Ribosomal protein S11	Up
BMEI0782	<i>rplQ</i>	Ribosomal protein L17	Up
BMEI0823	<i>rpsB</i>	30S ribosomal protein S2	Up
BMEI0826		Ribosome releasing factor	Up
BMEI0915		Threonyl-tRNA synthetase	Up
BMEI1054		Peptide chain release factor 2	Up
BMEI1057		Ribonuclease E / Zinc metalloprotease	Up
BMEI1133	<i>rpsD</i>	Ribosomal protein S4	Up
BMEI1168	<i>rplM</i>	50S ribosomal protein L13	Up
BMEI1184		Small protein A	Up
BMEI1199		Arginyl-tRNA-protein transferase	Up
BMEI1203		Ribonuclease D	Up
BMEI1247		Ribonuclease precursor	Up
BMEI1272	<i>cysS</i>	Cysteinyl-tRNA synthetase	Up
BMEI1418		GDP-mannose 4,6-dehydratase / GDP-4-amino-4,6-dideoxy-D-mannose formyltransferase	Up
BMEI1480	<i>rpsE</i>	30S ribosomal protein S6	Up
BMEI1483	<i>rplI</i>	50S ribosomal protein L9	Up
BMEI1529	<i>glyS</i>	Glycyl-tRNA synthetase beta subunit	Up
BMEI1798		23S ribosomal RNA methyltransferase	Down
BMEI1862		2'-5' RNA ligase	Up
BMEI1962	<i>rpsO</i>	Ribosomal protein S15	Up
BMEI2008		50S ribosomal protein L35	Up
BMEI2010		Translation initiation factor IF-3	Up
BMEI0276		Ribonuclease P	Up
BMEI0332	<i>rpsU</i>	Ribosomal protein S21	Up
BMEI0661	<i>rpmG</i>	Ribosomal protein L33	Up
BMEI0812	<i>def</i>	Peptide deformylase	Down
BMEI1055		Histidyl-tRNA synthetase	Up
Posttranslational modification, protein turnover, chaperones			
BMEI0047		Molecular chaperones (DnaJ family)	Up
BMEI0517		Glutathione S-transferase	Up
BMEI0874	<i>clpP</i>	ATP-dependent Clp protease proteolytic subunit	Up
BMEI1030		Protein-L-isoaspartate O-methyltransferase	Up
BMEI1129		Glutaredoxin	Up
BMEI1172	<i>ctaA</i>	Cytochrome C oxidase assembly protein COX15	Up
BMEI1331	<i>cycL</i>	Cytochrome C-type biogenesis protein CycL precursor	Down
BMEI1440		Thiol:disulfide interchange protein DsbA	Down
BMEI1513	<i>dnaJ</i>	Chaperone protein DnaJ	Up
BMEI1650		Urease accessory protein UreF	Down
BMEI1777	<i>grpE</i>	GrpE protein	Up
BMEI1784		Small heat shock protein HspA	Up
BMEI1804	<i>glnD</i>	PII uridylyl-transferase	Up
BMEI1851	<i>cmcC</i>	Heme exporter protein C	Down
BMEI0230	<i>msrA</i>	Peptide methionine sulfoxide reductase	Down
BMEI0294	<i>gst</i>	Glutathione S-transferase	Down
BMEI0577		Alkyl hydroperoxide reductase c22 protein	Up

TABLE F.1. (continued)

Locus ID	Symbol	Gene product	Expression
Amino acid transport and metabolism			
BMEI0025		L-sorbose dehydrogenase (FAD)	Down
BMEI0105		L-asparaginase II	Down
BMEI0124	<i>argJ</i>	Bifunctional ornithine acetyltransferase/N-acetylglutamate synthase protein	Down
BMEI0189		Aspartate kinase	Up
BMEI0207	<i>proB</i>	Gamma-glutamyl kinase	Up
BMEI0231		NAD-specific glutamate dehydrogenase	Up
BMEI0256		D-amino acid dehydrogenase small subunit	Up
BMEI0257		Proline racemase	Up
BMEI0258	<i>livH</i>	High affinity branched-chain amino acid transport system permease protein LivH	Up
BMEI0259	<i>livM</i>	High affinity branched-chain amino acid transport system permease protein LivM	Up
BMEI0261	<i>livF</i>	High affinity branched chain amino acid transport ATP-binding protein BraG	Up
BMEI0433	<i>oppA</i>	Periplasmic dipeptide transport protein precursor	Up
BMEI0435	<i>dppB</i>	Dipeptide transport system permease protein DppB	Up
BMEI0441	<i>proX</i>	Glycine betaine/L-proline-binding protein ProX	Up
BMEI0526	<i>carA</i>	Carbamoyl-phosphate synthase small subunit	Up
BMEI0617	<i>ilvI</i>	Acetolactate synthase III large subunit	Up
BMEI0624	<i>ilvC</i>	Ketol-acid reductoisomerase	Up
BMEI0734	<i>cysE</i>	Serine acetyltransferase	Up
BMEI0844	<i>trpD</i>	Anthranilate phosphoribosyltransferase	Up
BMEI0978	<i>glnB</i>	Nitrogen regulatory protein P-II	Up
BMEI1192		Serine hydroxymethyltransferase	Up
BMEI1211	<i>gltL</i>	General L-amino acid-binding periplasmic protein AapJ precursor	Up
BMEI1261		Leucyl aminopeptidase	Up
BMEI1308		Histidinol-phosphate aminotransferase	Down
BMEI1309		Histidinol-phosphate aminotransferase	Down
BMEI1495		Lysine decarboxylase	Up
BMEI1643		N-carbamoyl-L-amino acid amidohydrolase	Up
BMEI1721		Sarcosine oxidase delta subunit	Down
BMEI1722		Sarcosine oxidase beta subunit	Down
BMEI1774		Lactoylglutathione lyase, putative	Up
BMEI1848	<i>ilvD</i>	Dihydroxy-acid dehydratase	Up
BMEI1869		Homoserine/homoserine lactone efflux protein	Down
BMEI1888		Lactoylglutathione lyase	Up
BMEI2018	<i>trpB</i>	Tryptophan synthase subunit beta	Up
BMEII0012	<i>pepF</i>	Oligoendopeptidase F	Up
BMEII0016		Homospermidine synthase	Down
BMEII0061		2-oxoisovalerate dehydrogenase alpha and beta subunit	Down
BMEII0136		Homoprotocatechuate 2,3-dioxygenase	Down
BMEII0195	<i>potC</i>	Spermidine/putrescine transport system permease protein PotC	Down
BMEII0249		Dihydrodipicolinate reductase	Down
BMEII0295		Biphenyl-2,3-diol 1,2-dioxygenase III	Up
BMEII0348		4-aminobutyrate aminotransferase	Down
BMEII0351		Acetolactate synthase large subunit	Down
BMEII0560		Glycine cleavage system protein H	Up
BMEII0582		Sarcosine oxidase beta subunit	Up
BMEII0741		D-aminopeptidase	Up
BMEII0783		Na(+)-linked D-alanine glycine permease	Up
BMEII0862		Dihydrodipicolinate synthase	Up

TABLE F.1. (continued)

Locus ID	Symbol	Gene product	Expression
BMEI0863	<i>appD</i>	Oligopeptide transport ATP-binding protein AppD	Down
BMEI0874	<i>livG</i>	High-affinity branched-chain amino acid transport system permease protein LivH / High affinity branched-chain amino acid transport ATP-binding protein livG	Down
BMEI0875	<i>livK</i>	Leucine-specific binding protein precursor	Down
BMEI0923	<i>potD</i>	Spermidine/putrescine-binding periplasmic protein	Down
BMEI0950	<i>narG</i>	Nitrate reductase alpha chain	Down
Nucleotide transport and metabolism			
BMEI0476		Adenine phosphoribosyltransferase	Up
BMEI0778	<i>adk</i>	Adenylate kinase	Up
BMEI0849	<i>pirG</i>	CTP synthetase	Up
BMEI1256		Nucleoside diphosphate kinase	Up
BMEI1430		Ureidoglycolate hydrolase	Down
BMEI0420		Thymidylate synthase	Down
BMEI0598		Exopolyphosphatase	Up
BMEI0617		Xanthine/uracil permease	Down
BMEI0888		5'-methylthioadenosine/S-adenosylhomocysteine nucleosidase	Down
BMEI0930	<i>nrdE</i>	Ribonucleotide-diphosphate reductase alpha subunit	Down
Carbohydrate transport and metabolism			
BMEI0399		Dihydroxyacetone kinase	Up
BMEI0605		Bicyclomycin resistance protein	Up
BMEI0664	<i>rbsC</i>	Sugar transport system permease protein	Down
BMEI0667	<i>fucU</i>	Fucose operon FucU protein	Up
BMEI0726	<i>glpX</i>	GlpX protein	Up
BMEI0851		Enolase	Up
BMEI0927		Multidrug resistance protein B	Down
BMEI1036		ATP-NAD kinase	Up
BMEI1116		Ribulose-phosphate 3-epimerase	Up
BMEI1395	<i>rfbA</i>	Mannose-1-phosphate guanylyltransferase	Up
BMEI1436		Pyruvate phosphate dikinase	Up
BMEI1636		Glucose-6-phosphate isomerase / glucose-6-phosphate 1-epimerase	Up
BMEI1716		Trehalose/maltose binding protein	Up
BMEI1997		Gluconolactonase	Up
BMEI0089	<i>rbsK</i>	Ribokinase	Up
BMEI0106		Xylose repressor	Down
BMEI0300	<i>rbsA</i>	Ribose transport ATP-binding protein RbsA	Down
BMEI0360	<i>rbsB</i>	Multiple sugar-binding periplasmic receptor ChvE precursor	Up
BMEI0474		Mannonate dehydratase	Down
BMEI0621	<i>ugpC</i>	Glycerol-3-phosphate ABC transporter, ATP-binding protein	Up
BMEI0795		Multidrug resistance protein B	Up
BMEI0850		GDP-fucose synthetase	Down
BMEI0940	<i>malK</i>	Maltose/maltodextrin transport ATP-binding protein MalK	Down
BMEI1092		Hydroxypyruvate isomerase	Down
Lipid transport and metabolism			
BMEI0021		Acetyl CoA:Acetoacetyl CoA transferase alpha subunit	Down
BMEI0238		Acetyl-CoA synthetase	Up
BMEI0827	<i>uppS</i>	Undecaprenyl pyrophosphate synthetase	Up
BMEI0832		(3R)-hydroxymyristoyl-[acyl carrier protein] dehydratase	Up

TABLE F.1. (continued)

Locus ID	Symbol	Gene product	Expression
BMEI1024		3-hydroxyisobutyrate dehydrogenase	Down
BMEI1062	<i>accB</i>	Acetyl-CoA carboxylase	Up
BMEI1112		3-oxoacyl-(acyl carrier protein) synthase	Down
BMEI1113	<i>fabF</i>	3-oxoacyl-(acyl carrier protein) synthase	Up
BMEI1512		Enoyl-(acyl carrier protein) reductase	Up
BMEI0214		Enoyl-CoA hydratase	Down
BMEI0495		Acyl-CoA dehydrogenase	Down
BMEI0645		3-oxoadipate CoA-transferase subunit B	Down
Energy production and conversion			
BMEI0076		Inorganic pyrophosphatase	Up
BMEI0137		Malate dehydrogenase	Up
BMEI0161	<i>shdA</i>	Succinate dehydrogenase	Up
BMEI0248	<i>atpH</i>	ATP synthase subunit D	Up
BMEI0249	<i>atpA</i>	ATP synthase subunit A	Up
BMEI0250	<i>atpG</i>	ATP synthase subunit C	Up
BMEI0251	<i>atpD</i>	ATP synthase subunit B	Up
BMEI0252	<i>atpC</i>	ATP synthase subunit epsilon	Up
BMEI0278		Ferredoxin II	Up
BMEI0473		Ubiquinol-cytochrome C reductase iron-sulfur subunit	Up
BMEI0475		Cytochrome C1	Up
BMEI0791		Isocitrate dehydrogenase	Up
BMEI0836		Citrate synthase	Up
BMEI0854	<i>pdhA</i>	Pyruvate dehydrogenase E1 component alpha subunit	Up
BMEI0911		NifU protein	Down
BMEI0928		Acetate CoA-transferase alpha subunit	Up
BMEI0959		Ferredoxin, 2Fe-2S K04755 ferredoxin, 2Fe-2S	Up
BMEI1148	<i>nuoK</i>	NADH dehydrogenase kappa subunit	Up
BMEI1150	<i>nuoI</i>	NADH dehydrogenase subunit I	Up
BMEI1152	<i>nuoG</i>	NADH dehydrogenase gamma subunit	Up
BMEI1153	<i>nuoF</i>	NADH-quinone oxidoreductase chain F	Up
BMEI1154	<i>nuoE</i>	ATP synthase subunit E	Up
BMEI1155	<i>nuoD</i>	NADH dehydrogenase delta subunit	Up
BMEI1157	<i>nuoB</i>	NADH-quinone oxidoreductase chain B	Up
BMEI1158	<i>nuoA</i>	NADH dehydrogenase alpha subunit	Up
BMEI1320		Electron transfer flavoprotein-ubiquinone oxidoreductase precursor	Up
BMEI1466	<i>coxB</i>	Cytochrome C oxidase polypeptide II	Up
BMEI1543	<i>atpF</i>	ATP synthase subunit B	Up
BMEI1855	<i>acnA</i>	Aconitate hydratase	Up
BMEI1903		Cytochrome c-552	Up
BMEI0124		Aldehyde dehydrogenase	Down
BMEI0141		Aldehyde dehydrogenase	Down
BMEI0242		Aldehyde dehydrogenase	Down
BMEI0744		Dihydrolipoamide dehydrogenase	Down
BMEI0768		NADH dehydrogenase subunit N	Down
BMEI0880		Acetate kinase	Down
BMEI1068		Cytochrome c2 precursor	Down
Coenzyme transport and metabolism			
BMEI0177		Uroporphyrinogen-III synthetase	Up
BMEI0209	<i>nadD</i>	Nicotinic acid mononucleotide adenyltransferase	Up

TABLE F.1. (continued)

Locus ID	Symbol	Gene product	Expression
BMEI0221		Pyridoxine kinase	Down
BMEI0286		Putative nucleotide-binding protein	Up
BMEI0329		Thiamine-phosphate pyrophosphorylase	Up
BMEI0347		Phosphoserine aminotransferase	Up
BMEI0467		Coproporphyrinogen III oxidase	Up
BMEI0546		Metal-activated pyridoxal enzyme	Up
BMEI0695	<i>cobN</i>	Cobaltochelataase	Up
BMEI0696	<i>cobA</i>	Cob(II)yrinic acid a,c-diamide adenosyltransferase	Up
BMEI0954		2-amino-4-hydroxy-6-hydroxymethylidihydropteridine pyrophosphokinase	Down
BMEI0956		Dihydropteroate synthase	Down
BMEI1144		Biotin-protein ligase	Up
BMEI1207		Salicylate hydroxylase	Down
BMEI1464		Protoheme IX farnesyltransferase	Down
BMEI2012		Benzoate membrane transport protein	Up
BMEI10110		Choline-sulfatase	Down
BMEI10589	<i>ribH</i>	Riboflavin synthase subunit beta	Up
Inorganic ion transport and metabolism			
BMEI0044		CBS domain containing protein	Down
BMEI0569		Manganese transport protein MntH	Up
BMEI0622	<i>kup</i>	KUP system potassium uptake protein	up
BMEI0640		CbiM protein	Up
BMEI0675	<i>cysW</i>	Sulfate transport system permease protein <i>cysW</i>	Up
BMEI0790		Alkaline phosphatase	Up
BMEI0869	<i>trkA</i>	Trk system potassium uptake protein TrkA	Up
BMEI0882	<i>phnN</i>	Phosphonates transport ATP-binding protein PhnN	Down
BMEI0931		Putative thiosulfate sulfurtransferase	Up
BMEI1021		Molybdopterin-guanine dinucleotide biosynthesis protein B	Up
BMEI1986	<i>pstB</i>	Phosphate transport ATP-binding protein PstB	Down
BMEI10105	<i>frpB</i>	Iron-regulated outer membrane protein FrpB	Down
BMEI10581	<i>sodC</i>	Superoxide dismutase (Cu-Zn)	Up
BMEI10566	<i>sfuB</i>	Iron(III)-transport system permease protein SfuB	Down
BMEI10606	<i>fatD</i>	Ferric anguibactin transport system permease protein FatD	Down
BMEI10766	<i>phaF</i>	PhaF potassium efflux system protein	Down
BMEI10797		ABC transporter substrate-binding protein	Down
BMEI10962	<i>tauC</i>	Taurine transport permease protein TauC	Up
BMEI10972		Copper-binding periplasmic protein precursor	Down
BMEI11011		Sulfite reductase (NADPH) flavoprotein alpha-component	Down
Defense mechanisms			
BMEI0945		6-aminohexanoate-dimer hydrolase	Down
BMEI0984		Beta-(1->2)glucan export ATP-binding protein NdvA	Up
BMEI1138		Lipoprotein releasing system ATP-binding protein LolD	Down
BMEI1630	<i>acrA</i>	Acriflavin resistance protein A precursor	Down
BMEI1645	<i>acrB</i>	Acriflavin resistance protein B	Down
BMEI1742		ABC transporter ATP-binding protein	Up
BMEI10452		Type I restriction-modification enzyme, S subunit	Down
BMEI10473	<i>acrF</i>	Acriflavin resistance protein F	Down
BMEI10916	<i>acrD</i>	Acriflavin resistance protein D	Down

TABLE F.1. (continued)

Locus ID	Symbol	Gene product	Expression
Signal transduction mechanism			
BMEI0372		Two-component response regulator	Up
BMEI0492	<i>cpxA</i>	Osmolarity sensor protein EnvZ	Down
BMEI0867	<i>ntrY</i>	Nitrogen regulation protein NtrY	Up
BMEI0868	<i>ntrX</i>	Nitrogen assimilation regulatory protein NtrX	Up
BMEI0949		DnaK suppressor protein homolog	Up
BMEI1624	<i>phoR</i>	Phosphate regulon sensor protein PhoR	Down
BMEI1751		Two-component response regulator	Down
BMEI1863		Low molecular weight phosphotyrosine protein phosphatase	Up
BMEI1975	<i>phoH</i>	PhoH protein	Up
BMEI2035	<i>chvG</i>	Sensor protein ChvG	Down
BMEII0659		Two component response regulator	Up
BMEII0853		Two component response regulator	Down
BMEII1009		C-di-GMP phosphodiesterase A	Down
Cell wall/membrane biogenesis			
BMEI0214		Tail-specific protease	Up
BMEI0223		Membrane-bound lytic murein transglycosylase B	Up
BMEI0271	<i>mtgA</i>	Monofunctional biosynthetic peptidoglycan transglycosylase	Down
BMEI0340		Peptidoglycan-associated lipoprotein	Up
BMEI0421		Pleiotropic regulatory protein	Up
BMEI0579	<i>murG</i>	UDP-N-acetylenolpyruvoylglucosamine reductase	Up
BMEI0580		UDP-N-acetylmuramate--L-alanine ligase	Up
BMEI0717		22 kDa outer membrane protein precursor	Up
BMEI0830		Outer membrane protein	Up
BMEI0831		LpxD UDP-3-O-[3-hydroxymyristoyl] glucosamine N-acyltransferase	Up
BMEI0833		Acyl-(acyl-carrier-protein)-UDP-N- acetylglucosamine O-acyltransferase	Up
BMEI0913	<i>dacA</i>	Penicillin-binding protein 6 (D-alanyl-D-alanine carboxypeptidase fraction C)	Up
BMEI0998		Glycosyltransferase	Up
BMEI1007		25 kDa outer-membrane immunogenic protein precursor	Up
BMEI1029		Outer membrane protein TolC	Up
BMEI1037		Glycosyltransferase involved in cell wall biogenesis	Up
BMEI1056		N-acetylmuramoyl-L-alanine amidase	Up
BMEI1079	<i>nlpD</i>	Lipoprotein NlpD	Up
BMEI1096		Succinoglycan biosynthesis protein Exol	Down
BMEI1249		25 kDa outer-membrane immunogenic protein precursor	Up
BMEI1404		Mannosyltransferase	Up
BMEI1602		Glycosyltransferase	Up
BMEI1829		25 kDa outer-membrane immunogenic protein precursor	Up
BMEI1830		25 kDa outer-membrane immunogenic protein precursor	Up
BMEI0374	<i>alr</i>	Alanine racemase, catabolic	Down
BMEII0827		Glucose-1-phosphate cytidyllyltransferase	Down
BMEII0837		Glycosyl transferase	Down
BMEII0840		Glycosyltransferase involved in cell wall biogenesis	Down
BMEII0844		31 kDa outer-membrane immunogenic protein precursor	Up
BMEII0846		Glycosyl transferase	Down
BMEII0847		Glycosyl transferase	Down
BMEII0848		GDP-mannose 4,6-dehydratase	Down
Cell division			
BMEI0213		Membrane proteins related to metalloendopeptidase	Up

TABLE F.1. (continued)

Locus ID	Symbol	Gene product	Expression
BMEI0584	<i>ftsA</i>	Cell division protein FtsA	Up
BMEI0633	<i>crcB</i>	Camphor resistance protein CrcB	Up
BMEI1132		ATPase of the PP superfamily	Down
BMEI0927	<i>minC</i>	Septum formation inhibitor	Up
Cell motility			
BMEI0324	<i>motB</i>	Flagellar motor protein	Up
BMEI0156	<i>motD</i>	Chemotaxis MotD protein	Down
BMEI0163		Flagellum biosynthesis repressor	Up
BMEI1105	<i>fliL</i>	Flagellum-specific ATP synthase FliL	Down
BMEI1107	<i>flgF</i>	Flagellar basal-body rod protein FlgF	Down
BMEI1112	<i>fliN</i>	Flagellar motor switch protein FliN	Down
Intracellular trafficking and secretion			
BMEI0339	<i>tolB</i>	Translocation protein TolB precursor	Up
BMEI0364	<i>exbD</i>	Biopolymer transport ExbD protein	Down
BMEI0777	<i>secY</i>	Preprotein translocase SecY	Up
BMEI1873		Cell surface protein	Down
BMEI2055	<i>secB</i>	Export protein SecB	Up
BMEI0029	<i>virB5</i>	Attachment mediating protein virB5 homolog	Down
BMEI0035	<i>virB11</i>	ATPase virB11 homolog	Down
BMEI0148		Extracellular serine protease	Down
General function prediction only			
BMEI0020		Glucose-fructose oxidoreductase precursor	Down
BMEI0125		Acetyltransferase	Down
BMEI0129		Hydroxyacylglutathione hydrolase, mitochondrial	Down
BMEI0183		Competence protein F	Down
BMEI0222		Carbonic anhydrase	Up
BMEI0240		Fusaric acid resistance protein FusB / fusaric acid resistance protein FusC	Up
BMEI0244		Transaldolase	Up
BMEI0282		Zinc metalloprotease	Up
BMEI0293		2-hydroxy-6-oxo-2,4-heptadienoate hydrolase	Down
BMEI0356		Type 1 capsular polysaccharide biosynthesis protein J	Up
BMEI0420		Oxidoreductase	Up
BMEI0452		Putative phosphohydrolase, lcc family	Down
BMEI0506		Transporter, DME family	Up
BMEI0587		ComL, competence lipoprotein	Up
BMEI0630	<i>phzF</i>	Phenazine biosynthesis protein PhzF	Down
BMEI0634		Integral membrane protein	Up
BMEI0668		Calcium binding protein	Up
BMEI0709		4-hydroxyphenylacetate 3-monooxygenase	Up
BMEI0712		CbiG protein / precorrin-3B C17-methyltransferase	Up
BMEI0796		31 kDa immunogenic protein precursor	Up
BMEI0852		Methyltransferase	Up
BMEI0862	<i>cinA</i>	Putative competence-damage protein	Up
BMEI0872	<i>hfq</i>	RNA-binding protein Hfq	Up
BMEI0917		Nitroreductase family	Up
BMEI0946		NAD(FAD)-utilizing dehydrogenases	Down
BMEI0951		Amino acid regulated cytosolic protein	Up
BMEI0970		Diacylglycerol kinase	Up

TABLE F.1. (continued)

Locus ID	Symbol	Gene product	Expression
BMEI0977		Putative sugar kinase	Up
BMEI0995		Secretion activator protein	Down
BMEI1042		ABC transporter ATP-associated protein	Up
BMEI1067		Acetyltransferase	Down
BMEI1095		Hypothetical protein	Up
BMEI1110		Secretion activator protein	Up
BMEI1134		Extensin-like protein	Down
BMEI1143		Metal dependent hydrolase	Down
BMEI1185		HppA membrane-bound proton-translocating pyrophosphatase	Up
BMEI1231		NADH-ubiquinone oxidoreductase 18 KD subunit	Up
BMEI1276		Phosphohydrolase (mutT/nudix family protein)	Down
BMEI1376		Death on curing protein	Down
BMEI1470		Protein YicC	Up
BMEI1504		Acetylspermidine deacetylase	Down
BMEI1520		Response regulator protein	Up
BMEI1541		Transporter	Up
BMEI1556		Integral membrane protein	Down
BMEI1625		UDP-galactose-lipid carrier transferase	Down
BMEI1634		Phosphoglycolate phosphatase	Up
BMEI1790		ABC transporter ATP-binding protein	Up
BMEI1872		Cell surface protein	Up
BMEI1877		Hemolysin III	Down
BMEI1973		CBS domain containing protein	Up
BMEI1978		Ribosomal-protein-alanine acetyltransferase	Up
BMEII0129		Hydrolase family protein	Down
BMEII0149		Extracellular serine protease	Down
BMEII0179		Low affinity zinc transport membrane protein	Down
BMEII0272		Phosphoglycolate phosphatase	Down
BMEII0440		dTDP-glucose 4,6-dehydratase	Down
BMEII0463		Putative ICC-like phosphoesterases	Down
BMEII0465		Permease	Down
BMEII0499		Succinoglycan biosynthesis protein Exol	Down
BMEII0836		dTDP-4-dehydrorhamnose 3,5-epimerase	Down
BMEII0838		Succinoglycan biosynthesis transport protein ExoT	Down
BMEII0865		1-carboxy-3-chloro-3,4-dihydroxycyclo hexa-1,5-diene dehydrogenase	Up
BMEII0999		Nitric-oxide reductase cytochrome C chain	Down
BMEII1035		Serine protease	Down
BMEII1096		Putative tartrate transporter	Down
Unknown function			
BMEI0004		Hypothetical cytosolic protein	Down
BMEI0016		Hypothetical protein	Down
BMEI0031		Hypothetical cytosolic protein	Down
BMEI0064		Hypothetical protein	Up
BMEI0071		Hypothetical protein	Down
BMEI0088		Hypothetical protein	Up
BMEI0098		Hypothetical protein	Down
BMEI0117		Hypothetical protein	Down
BMEI0119		Hypothetical protein	Up
BMEI0134		Hypothetical protein	Down
BMEI0146		Hypothetical protein	Down

TABLE F.1. (continued)

Locus ID	Symbol	Gene product	Expression
BMEI0154		Hypothetical membrane spanning protein	Down
BMEI0186		Hypothetical cytosolic protein	Down
BMEI0210		lojap protein family	Up
BMEI0216		Hypothetical protein	Down
BMEI0220		Hypothetical protein	Down
BMEI0224		Hypothetical protein	Up
BMEI0290		Hypothetical cytosolic protein	Up
BMEI0298		Hypothetical protein	Down
BMEI0330		OpgC	Up
BMEI0362		Hypothetical protein	Down
BMEI0373		Hypothetical protein	Down
BMEI0376		Hypothetical protein	Up
BMEI0390		Hypothetical cytosolic protein	Up
BMEI0404		Hypothetical protein	Down
BMEI0427		Hypothetical protein	Up
BMEI0458		Hypothetical membrane spanning protein	Down
BMEI0490		Hypothetical cytosolic protein	Down
BMEI0497		Hypothetical membrane spanning protein	Up
BMEI0498		Cold shock protein CspA	Up
BMEI0514		Hypothetical protein	Up
BMEI0521		Hypothetical protein	Up
BMEI0567		Hypothetical protein	Up
BMEI0603		Hypothetical protein	Up
BMEI0620		Hypothetical protein	Down
BMEI0625		Hypothetical protein	Up
BMEI0629		Hypothetical protein	Down
BMEI0631		Hypothetical protein	Down
BMEI0641		Hypothetical protein	Down
BMEI0670		Putative membrane-associated alkaline phosphatase	Down
BMEI0722		Hypothetical protein	Down
BMEI0735		Hypothetical protein	Up
BMEI0751		Hypothetical protein	Up
BMEI0788		Hypothetical protein	Up
BMEI0805		Hypothetical protein	Up
BMEI0815		ATP-dependent Clp protease adaptor protein ClpS	Up
BMEI0821		Hypothetical protein	Up
BMEI0822		Hypothetical protein	Up
BMEI0848		Probable carnitine operon oxidoreductase CaiA	Up
BMEI0853		Hypothetical protein	Up
BMEI0860		Hypothetical cytosolic protein	Up
BMEI0870		Hypothetical protein	Up
BMEI0871		Hypothetical protein	Up
BMEI0885		Hypothetical protein	Up
BMEI0907		Hypothetical protein	Down
BMEI0957		Hypothetical protein	Up
BMEI0973		Hypothetical protein	Up
BMEI0996		Hypothetical protein	Up
BMEI1000		Hypothetical protein	Up
BMEI1004		Hypothetical protein	Up
BMEI1011		Hypothetical protein	Down
BMEI1013		Hypothetical membrane spanning protein	Down

TABLE F.1. (continued)

Locus ID	Symbol	Gene product	Expression
BMEI1031		Hypothetical protein	Up
BMEI1077		Hypothetical protein	Up
BMEI1101		Hypothetical protein	Up
BMEI1119		Hypothetical cytosolic protein	Down
BMEI1162		Hypothetical protein	Up
BMEI1176		Hypothetical protein	Up
BMEI1182		Hypothetical cytosolic protein	Down
BMEI1220		Hypothetical protein	Up
BMEI1222		Hypothetical protein	Up
BMEI1230		Hypothetical cytosolic protein	Up
BMEI1310		Hypothetical membrane spanning protein	Down
BMEI1313		Hypothetical cytosolic protein	Up
BMEI1340		Phage host specificity protein	Down
BMEI1341		Phage host specificity protein	Down
BMEI1343		Hypothetical protein	Down
BMEI1344		Hypothetical protein	Down
BMEI1345		Phage minor tail protein H	Down
BMEI1349		Phage portal protein	Down
BMEI1350		Phage DNA packaging protein	Down
BMEI1363		Hypothetical cytosolic protein	Down
BMEI1375		Hypothetical protein	Up
BMEI1453		Diguanylate cyclase/phosphodiesterase domain 2 (EAL)	Down
BMEI1501		Transglycosylase associated protein	Up
BMEI1515		17 kDa common-antigen	Up
BMEI1524		Hypothetical protein	Down
BMEI1525		Helix-turn-helix protein, CopG family	Up
BMEI1538		Hypothetical protein	Up
BMEI1539		Hypothetical protein	Down
BMEI1578		Glyoxylate induced protein	Down
BMEI1584		Invasion protein B	Up
BMEI1610		Hypothetical cytosolic protein	Down
BMEI1619		HslO HSP33-like chaperonin	Down
BMEI1647		Hypothetical protein	Down
BMEI1664		Hypothetical cytosolic protein	Down
BMEI1667		Hypothetical cytosolic protein	Down
BMEI1676		Hypothetical protein	Down
BMEI1681		Hypothetical protein	Up
BMEI1688		Hypothetical protein	Up
BMEI1691		Hypothetical membrane spanning protein	Down
BMEI1696		Hypothetical membrane spanning protein	Down
BMEI1698		Hypothetical protein	Down
BMEI1705		Hypothetical protein	Down
BMEI1724		Hypothetical protein	Up
BMEI1763		Hypothetical protein	Down
BMEI1783		Hypothetical membrane spanning protein	Up
BMEI1785		Hypothetical protein	Up
BMEI1792		Hypothetical periplasmic protein	Up
BMEI1795		Hypothetical protein	Up
BMEI1812		Hypothetical protein	Up
BMEI1865		Hypothetical protein	Up
BMEI1918		Hypothetical cytosolic protein	Up

TABLE F.1. (continued)

Locus ID	Symbol	Gene product	Expression
BMEI1929		Hypothetical protein	Down
BMEI1933		Hypothetical protein	Up
BMEI1947		Hypothetical cytosolic protein	Down
BMEI1991		Hypothetical protein	Up
BMEI2016		Hypothetical protein	Up
BMEII0008		Hypothetical protein	Down
BMEII0037		Hypothetical cytosolic protein	Down
BMEII0073		Hypothetical protein	Up
BMEII0091		Replication protein C	Down
BMEII0118		Hypothetical protein	Down
BMEII0157		Hypothetical protein	Down
BMEII0187		Hypothetical cytosolic protein	Down
BMEII0188		Hypothetical cytosolic protein	Down
BMEII0211		Penicillin acylase	Down
BMEII0238		HdeD protein	Down
BMEII0262		Hypothetical protein	Down
BMEII0277		Hypothetical protein	Up
BMEII0279		Hypothetical membrane spanning protein	Up
BMEI0368		Hypothetical protein	Up
BMEII0398		Sec-independent protein translocase protein TatC	Down
BMEII0434		Hypothetical protein	Up
BMEII0442		Hypothetical membrane spanning protein	Up
BMEII0464		Hypothetical membrane associated protein	Down
BMEII0516		Hypothetical protein	Down
BMEII0522		Hypothetical protein	Down
BMEII0552		Hypothetical protein	Up
BMEII0555		Hypothetical cytosolic protein	Down
BMEII0595		Hypothetical protein	Up
BMEII0652		Hypothetical protein	Up
BMEII0692		Hypothetical membrane associated protein	Up
BMEII0705		Hypothetical protein	Up
BMEII0709		Hypothetical protein	Up
BMEII0726		Hypothetical protein	Down
BMEII0749		Hypothetical protein	Down
BMEII0789		Hypothetical protein	Down
BMEII0829		Possible S-adenosylmethionine-dependent methyltransferase	Down
BMEII0833		Hypothetical protein	Down
BMEII0841		Hypothetical protein	Down
BMEII0877		Hypothetical protein	Down
BMEII0886		Hypothetical protein	Down
BMEII0906		Protein HdeA precursor	Up
BMEII0919		Hypothetical protein	Up
BMEII0933		Hypothetical protein	Up
BMEII0936		Hypothetical protein	Down
BMEII0989		Hypothetical protein	Down
BMEII0992		MRP protein homolog A	Down
BMEII1013		Hypothetical cytosolic protein	Down
BMEII1024		CIS,CIS-muconate transport protein	Down
BMEII1030		Putative lipoprotein	Up
BMEII1046		Hypothetical protein	Up
BMEII1059		Protein YbiS precursor	Down

TABLE F.1. (continued)

Locus ID	Symbol	Gene product	Expression
BMEII1067		Hypothetical cytosolic protein	Up
BMEII1071		Hypothetical protein	Down
BMEII1079		Hypothetical protein	Down
BMEII1138		Hypothetical protein	Down

Genes were ordered in cluster of ortholog groups (COGs) functional categories (downloaded from NCBI/genome projects/bacteria/*B. melitensis*) with adaptations

APPENDIX G

TABLE G.1. Host genes differentially expressed in *B. melitensis*-infected bovine Peyer's patches during the first hour post-infection, compared to non-infected tissue

Oligo sequence ID	Unigene ID	Symbol	Gene product	Expression
DNA replication and repair				
CR452654	Bt.1184	<i>APEX2</i>	Apurinic/apyrimidinic endonuclease 2	Up
BF044044	Bt.46083	<i>CGI-41</i>	CGI-41 protein	Up
AW464155	Bt.16022	<i>SMARCAL1</i>	SWI/SNF related, matrix associated, actin dependent regulator of chromatin, subfamily a-like 1	Up
BF039990	Bt.76849		Similar to DNase1-Like III protein	Up
CN437632	Bt.25809		Similar to downregulated in ovarian cancer 1	Down
Chromosome organization				
CR453453	Bt.51509		Transcribed locus, moderately similar to XP_001075299.1 H1 histone family, member X [Rattus norvegicus]	Up
CK952836	Bt.10510	<i>H2AFX</i>	H2A histone family, member X	Up
RNA processing				
CK771600	Bt.3261		Transcribed locus, strongly similar to XP_546630.2 elaC homolog 2 [Canis familiaris]	Up
DR749310	Bt.21472		Similar to splicing factor, arginine/serine-rich 16 (Suppressor of white-apricot homolog 2)	Up
AY563745	Bt.48707		Similar to related to CPSF subunits 74 kDa (MGC128672)	Up
BC103457	Bt.18030		Similar to SH3 domain-binding protein SNP70	Up
Transcription regulation				
CN436893	Bt.46244	<i>CDX2</i>	Caudal-type homeobox transcription factor 2	Up
AW466208	Bt.29568	<i>EAF2</i>	ELL associated factor 2 (EAF2)	Up
BF041568	Bt.45294		Similar to elongation factor RNA polymerase II-like 3	Up
AY318753	Bt.16536	<i>HNF4G</i>	Hepatocyte nuclear factor 4 gamma	Up
BF440215	Bt.9027	<i>NFKBIA</i>	Nuclear factor of kappa light polypeptide gene enhancer in B-cells inhibitor, alpha	Up
AW345084	Bt.30875	<i>HOXC11</i>	Homeo box C11, mRNA (incomplete sequence)	Up
AW461981	Bt.1686		Transcribed locus, strongly similar to XP_548832.2 DNA segment on chromosome X and Y (unique) 155 expressed sequence isoform 1 [Canis familiaris]	Up
CN441669	Bt.21965		Transcribed locus, strongly similar to XP_854273.1 Zinc finger protein 358 [Canis familiaris]	Up
BC109904	Bt.27825		Similar to zinc finger protein 414	Up
BM362847	Bt.77958		Transcribed locus, strongly similar to XP_220921.3 similar to aiolos [Rattus norvegicus]	Up
CN436168	Bt.33949		Transcribed locus, strongly similar to XP_001068534.1 similar to Ewing sarcoma breakpoint region 1 isoform EWS isoform 5	Up

TABLE G.1. (continued)

Oligo sequence ID	Unigene ID	Symbol	Gene product	Expression
BF042964	Bt.6148	<i>STAT6</i>	Signal transducer and activator of transcription 6, interleukin-4 induced	Up
CN442245	Bt.9198		Transcribed locus, weakly similar to XP_001058638.1 HIV TAT specific factor 1 [Rattus norvegicus]	Up
AW463092	Bt.18791		Transcribed locus, strongly similar to XP_216633.4 metastasis associated 3 [Rattus norvegicus]	Up
AW461405	Bt.4606		Similar to Kruppel-like factor 6	Up
DR697576	Bt.65045	<i>SETD8</i>	SET domain containing (lysine methyltransferase) 8	Up
CR453442	Bt.934		Transcribed locus, moderately similar to XP_001065863.1 PHD finger protein 20 (Hepatocellular carcinoma-associated antigen 58 homolog) [Rattus norvegicus]	Down
Protein biosynthesis				
BF045013	Bt.49029	<i>UTP14C</i>	UTP14, U3 small nucleolar ribonucleoprotein, homolog C (yeast)	Up
BM361943	Bt.20487	<i>MRPL28</i>	Similar to 39S ribosomal protein L28, mitochondrial precursor (L28mt) (MRP-L28) (Melanoma antigen p15) (Melanoma-associated antigen recognized by T lymphocytes)	Down
Intracellular protein transport				
BM362579	Bt.3152		Similar to endoplasmic reticulum protein 29 precursor	Up
BT021891	Bt.1494	<i>GGA1</i>	Golgi associated, gamma adaptin ear containing, ARF binding protein 1 isoform 1	Up
BF042266	Bt.1494	<i>GGA1</i>	Golgi associated, gamma adaptin ear containing, ARF binding protein 1 isoform 1	Up
BF040787	Bt.28252		Transcribed locus, strongly similar to NP_003756.1 syntaxin 10 [Homo sapiens]	Up
CN435987	Bt.4048	<i>STXBP1</i>	Syntaxin binding protein 1	Down
Protein folding and secretion				
CB458419	Bt.19205		Transcribed locus, moderately similar to XP_858724.1 DnaJ (Hsp40) homolog, subfamily C, member 11 isoform 2 [Canis familiaris]	Up
CK845963	Bt.6680	<i>FKBP2</i>	Similar to FK506-binding protein 2 precursor (Peptidyl-prolyl cis-trans isomerase)	Up
AW465477	Bt.4415	<i>HSPB1</i>	Heat shock 27kDa protein 1	Up
NM_174143	Bt.4695	<i>PIGR</i>	Polymeric immunoglobulin receptor	Up
BF042163	Bt.57833	<i>SCAMP4</i>	Secretory carrier membrane protein 4	Up
Protein degradation				
CK950309	Bt.77784		Transcribed locus, moderately similar to NP_063947.1 transmembrane protease, serine 4 [Homo sapiens]	Up
NM_174202	Bt.336	<i>TPSB1</i>	Tryptase beta 1	Up
NM_174481	Bt.4689	<i>UCHL5</i>	Ubiquitin carboxyl-terminal hydrolase L5	Up
CK955446	Bt.9636	<i>SPINK1</i>	Serine protease inhibitor, Kazal type 1	Up
CK961416	Bt.9625		Transcribed locus, weakly similar to XP_854581.1 Serine protease inhibitor Kazal-type 4 precursor (Peptide PEC-60 homolog) [Canis familiaris]	Up

TABLE G.1. (continued)

Oligo sequence ID	Unigene ID	Symbol	Gene product	Expression
CR453031	Bt.28262		Transcribed locus, weakly similar to XP_534433.1 similar to Elafin precursor (Elastase-specific inhibitor) (ESI) (Skin-derived antileukoproteinase) (SKALP) (WAP four-disulfide core domain protein 14) (Protease inhibitor WAP3) [Canis familiaris]	Up
CN437618	Bt.76319		Transcribed locus, moderately similar to XP_001065510.1 Ubiquitin carboxyl-terminal hydrolase 40 (Ubiquitin thiolesterase 40) (Ubiquitin-specific processing protease 40) (Deubiquitinating enzyme 40) [Rattus norvegicus]	Up
Cell cycle / cell differentiation and proliferation				
CK943568	Bt.49472	<i>AGR2</i>	Anterior gradient 2, homolog	Up
AJ293900	Bt.29719	<i>EGR4</i>	Early growth response 4	Up
BM363411	Bt.17081		Similar to Rhombotin-2	Up
CR452401	Bt.13110	<i>MDFI</i>	MyoD family inhibitor	Up
CN441928	Bt.4307		Transcribed locus, strongly similar to XP_542335.2 Rho-related GTP-binding protein RhoG (Sid 10750) [Canis familiaris]	Up
BE757891	Bt.52956		Transcribed locus, moderately similar to XP_419263.1 mitogen-activated protein kinase 12 isoform 1 [Gallus gallus]	Up
CR453045	Bt.1286	<i>RARRES2</i>	Retinoic acid receptor responder 2	Up
BM364258	Bt.43053	<i>SEPT11</i>	Septin 11	Up
BF039597	Bt.16930		Transcribed locus, moderately similar to XP_001076127.1 B-cell leukemia/lymphoma 3 [Rattus norvegicus]	Up
BC103128	Bt.11341	<i>NNAT</i>	Neuronatin	Down
CK963451	Bt.45679		Transcribed locus, weakly similar to XP_363162.1 protein MG08746.4 [Magnaporthe grisea 70-15]	Down
	Bt.64848	<i>YWHAZ</i>	Tyrosine 3-monooxygenase/tryptophan 5-monooxygenase activation protein, zeta polypeptide	Down
Cytoskeleton organization				
BM363541	Bt.351	<i>CORO1A</i>	Coronin, actin binding protein, 1A	Up
BM363211	Bt.6089		Similar to kaptin	Up
CR452106	Bt.55923		Transcribed locus, strongly similar to NP_113915.1 LIM motif-containing protein kinase 1	Up
NM_174395	Bt.1354	<i>MYO1A</i>	Myosin IA	Up
BM361850	Bt.59716		Transcribed locus, strongly similar to NP_055973.1 ankyrin repeat domain protein 15; kidney ankyrin repeat-containing protein [Homo sapiens]	Up
BM430199	Bt.56652		Transcribed locus, moderately similar to NP_775151.1 20 [Rattus norvegicus]	Up
Cell adhesion				
AW462342	Bt.6074	<i>CLDN3</i>	Claudin 3	Up
CR454875	Bt.51822		Transcribed locus, strongly similar to NP_001847.2 alpha 1 type XVI collagen precursor; collagen XVI, alpha-1 polypeptide [Homo sapiens]	Up
NM_174748	Bt.8130	<i>ITGA4</i>	Integrin, alpha 4 (antigen CD49D, alpha 4 subunit of VLA-4 receptor)	Up
CK973750	Bt.80510		Transcribed locus, moderately similar to NP_037107.1 galactoside-binding, soluble, 4 (galectin 4) [Rattus norvegicus]	Up

TABLE G.1. (continued)

Oligo sequence ID	Unigene ID	Symbol	Gene product	Expression
DR697630	Bt.13362	<i>TSPAN1</i>	Tetraspanin-1	Up
NM_174399	Bt.5166	<i>NCAM1</i>	Neural cell adhesion molecule 1	Down
BF042923	Bt.7220	<i>LSP1</i>	Similar to lymphocyte-specific protein 1 (MGC142338)	Down
Apoptosis				
CN794327	Bt.21648	<i>CIDEB</i>	Similar to Cell death activator CIDE-B (Cell death-inducing DFFA-like effector B)	Up
BM361824	Bt.687		Transcribed locus, moderately similar to XP_221961.3 caspase recruitment domain family member 11 [Rattus norvegicus]	Up
CN433496	Bt.9054		Transcribed locus, strongly similar to XP_240178.3 apoptotic chromatin condensation inducer in the nucleus (Acinus) [Rattus norvegicus]	Up
	Bt.8953	<i>PTGES</i>	Prostaglandin E synthase	Up
Immune and inflammatory response				
BM363735	Bt.49700	<i>AIF1</i>	Allograft inflammatory factor 1	Up
BM365194	Bt.20164	<i>C1QB</i>	Complement component 1, q subcomponent, B chain	Up
CR551837	Bt.21736		Transcribed locus, moderately similar to XP_520228.1 complement component 5 [Pan troglodytes]	Up
BC105174	Bt.14139		Similar to Complement component C9 precursor	Up
BF043775	Bt.103	<i>BPI</i>	Bactericidal/permeability-increasing protein	Up
BF706855	Bt.78164		Transcribed locus, strongly similar to NP_000241.1 myeloperoxidase [Homo sapiens]	Up
BF601278	Bt.24637		Similar to azurocidin 1 preproprotein	Up
BF040406	Bt.11022		Transcribed locus, strongly similar to NP_116584.2 mitogen-activated protein kinase-activated protein kinase 2 isoform 2 [Homo sapiens]	Up
BM363549	Bt.55288	<i>NCR3</i>	Similar to natural cytotoxicity triggering receptor 3	Up
BM363697	Bt.8939	<i>TYROBP</i>	TYRO protein tyrosine kinase binding protein	Up
CB464199	Bt.33292	<i>STAT1</i>	Signal transducer and activator of transcription 1	Up
BM364871	Bt.76115	<i>FGL2</i>	Fibrinogen-like 2	Up
BF044744	Bt.8227	<i>MAIL</i>	Molecule possessing ankyrin repeats induced by lipopolysaccharide (MAIL), homolog of mouse	Up
CK774743	Bt.45674	<i>CD2</i>	CD2 antigen	Up
BM362452	Bt.37553		Transcribed locus, moderately similar to XP_526582.1 small inducible cytokine B9 precursor; monokine induced by gamma interferon [Homo sapiens]	Up
CR452037	Bt.80577		Transcribed locus, moderately similar to XP_001063501.1 tumor necrosis factor receptor superfamily, member 11a [Rattus norvegicus]	Down
NM_205787	Bt.25528	<i>PTP</i>	Pancreatic thread protein	Down
Surface receptors				
NM_174011	Bt.49707	<i>CD3E</i>	Antigen CD3E, epsilon polypeptide (TIT3 complex)	Up
NM_174266	Bt.4436	<i>CD79A</i>	CD79A antigen (immunoglobulin-associated alpha)	Up
CB468269	Bt.20540		Transcribed locus, strongly similar to XP_850416.1 CD79B antigen isoform 1 [Canis familiaris]	Up
BF044748	Bt.12274		Protein tyrosine phosphatase, receptor type, G	Up
BM361923	Bt.52082	<i>ARRB1</i>	Arrestin, beta 1	Up
CR454049	Bt.4693	<i>ADRBK1</i>	Adrenergic, beta, receptor kinase 1	Up

TABLE G.1. (continued)

Oligo sequence ID	Unigene ID	Symbol	Gene product	Expression
BM365343	Bt.9510	<i>TIMD4</i>	T-cell immunoglobulin and mucin domain containing 4 (TIMD4)	Up
Pregnancy				
BC102264	Bt.28223 Bt.259	<i>PAG7</i>	20-beta-hydroxysteroid dehydrogenase-like Pregnancy-associated glycoprotein 7	Up Down
Intracellular signal transduction				
DR697486	Bt.21018	<i>CSNK1E</i>	Casein kinase 1, epsilon	Up
AJ696239	Bt.48141		Similar to cAMP responsive element modulator	Up
CR452358	Bt.39665		Transcribed locus, strongly similar to XP_515921.1 G protein-coupled receptor 155 [Pan troglodytes]	Up
DV918428	Bt.76522		Transcribed locus, strongly similar to NP_065871.2 PREX1 protein [Homo sapiens]	Up
AY124008	Bt.76198	<i>PTK9L</i>	Protein tyrosine kinase 9-like (A6-related protein)	Up
CK953727	Bt.12645		Similar to Ras-related protein RAB15	Up
BC102327	Bt.8189		Similar to Ran-specific GTPase-activating protein (Ran binding protein 1) (RANBP1) (HpaII tiny fragments locus 9a protein)	Up
CB170921	Bt.4310		Transcribed locus, strongly similar to XP_545702.2 Regulator of G-protein signaling 1 (RGS1) (Early response protein 1R20) (B-cell activation protein BL34) isoform 1 [Canis familiaris]	Up
BF043554	Bt.6067		Transcribed locus, strongly similar to XP_548447.2 SH2 domain containing 3C isoform 2 isoform 2 [Canis familiaris]	Up
DY096353	Bt.59664	<i>MAP4K1</i>	Mitogen-activated protein kinase kinase kinase kinase 1 (MAP4K1)	Up
CN432715	Bt.68727		Transcribed locus, strongly similar to XP_243623.3 Mitogen-activated protein kinase kinase kinase 7 interacting protein 1 [Rattus norvegicus]	Up
AW463722	Bt.21193		Transcribed locus, moderately similar to NP_001030092.1 B-lineage lymphoma c [Rattus norvegicus]	Up
BM364434	Bt.15678		Transcribed locus, moderately similar to NP_055265.1 SHP2-interacting transmembrane adaptor protein [Homo sapiens]	Up
BM363771	Bt.78550		Membrane tyrosine phosphatase (cd45)	Up
Metabolism				
Carbohydrates				
BI775802	Bt.60417	<i>CLP-1</i>	Chitinase-like protein 1 (CLP-1)	Up
CN435752	Bt.46035		Similar to Fructose-bisphosphate aldolase B (Liver-type aldolase)	Up
BM363586	Bt.49614	<i>ALDOC</i>	Aldolase C, fructose-bisphosphate	Down
Lipids				
NM_174242	Bt.49157	<i>APOA1</i>	Apolipoprotein A1	Up
NM_001001175	Bt.7741	<i>APOC3</i>	Apolipoprotein C-III	Up
CB431786	Bt.59123		Similar to myo-inositol 1-phosphate synthase A1	Up
BF045303	Bt.20496	<i>OSBPL2</i>	Oxysterol-binding protein-like protein 2 isoform 2	Up
BM363855	Bt.37581	<i>PLA2G2D4</i>	Calcium-dependent phospholipase A2 PLA2G2D4	Up

TABLE G.1. (continued)

Oligo sequence ID	Unigene ID	Symbol	Gene product	Expression
Amino acids				
CN439230	Bt.20121	<i>CTSD</i>	Cathepsin D (lysosomal aspartyl protease)	Up
AW464108	Bt.24605		Transcribed locus, moderately similar to NP_004112.1 gamma-glutamyltransferase-like activity 1 [Homo sapiens]	Up
CR452225	Bt.16774		Transcribed locus, strongly similar to XP_538655.2 glycine dehydrogenase [decarboxylating], mitochondrial precursor (Glycine decarboxylase)	Up
AW465225	Bt.45287		Similar to glutathione transferase zeta 1	Up
DR697552	Bt.20369		Similar to proline dehydrogenase (oxidase) 1	Up
Nucleotides				
CR452228	Bt.5439		Transcribed locus, strongly similar to XP_544332.2 dihydropyrimidinase related protein-3 (DRP-3) (Unc-33-like phosphoprotein) (ULIP protein) (Collapsin response mediator protein 4) (CRMP-4)	Up
General metabolism				
AV607074	Bt.19064		Transcribed locus, moderately similar to XP_534255.2 biotinidase precursor [Canis familiaris]	Up
CR455833	Bt.29206		Similar to CG14648-PA	Up
Ion transport				
NM_174276	Bt.194	<i>CLIC5</i>	Chloride intracellular channel 5	Up
AW358407	Bt.20296	<i>SFXN2</i>	Sideroflexin 2	Up
CK960601	Bt.28307		Transcribed locus, moderately similar to NP_001002968.1 ileal sodium/bile acid cotransporter [Canis familiaris]	Up
CK846142	Bt.22759		Similar to solute carrier family 40, member 1 (Ferroportin-1) (Iron-regulated transporter 1)	Up
AF508807	Bt.73273	<i>SLC5A1</i>	Solute carrier family 5 (sodium/glucose cotransporter), member 1 (SLC5A1)	Up
DV887766	Bt.44386		Transcribed locus, strongly similar to XP_868392.1 solute carrier family 25 (mitochondrial carrier; phosphate carrier), member 23 isoform 3 [Canis familiaris]	Up
NM_174540	Bt.172	<i>GABRA1</i>	Gamma-aminobutyric acid (GABA) A receptor, alpha 1	Down
Electron transport				
NM_174724	Bt.5029	<i>ATP5H</i>	ATP synthase, H ⁺ transporting, mitochondrial F0 complex, subunit d	Up
BM362197	Bt.4558	<i>CYBB</i>	Cytochrome b-245, beta polypeptide [chronic granulomatous disease]	Up
BF044616	Bt.47439		Transcribed locus, strongly similar to NP_110437.2 thioredoxin domain containing 5 isoform 1; thioredoxin related protein	Up
CN441199	Bt.25241		Transcribed locus, strongly similar to XP_547307.2 mucolipin 2 [Canis familiaris]	Down
Other functions				
BC103101	Bt.49205	<i>GMFG</i>	Glia maturation factor, gamma	Up
BF043702	Bt.10027	<i>CEACAM1</i>	Carcinoembryonic antigen-related cell adhesion molecule 1	Up
BC102496	Bt.48849	<i>ETHE1</i>	Similar to ETHE1 protein	Up

TABLE G.1. (continued)

Oligo sequence ID	Unigene ID	Symbol	Gene product	Expression
BM431520	Bt.28227		Transcribed locus, weakly similar to XP_001076797.1 similar to mucin 17 [Rattus norvegicus]	Up
BP111364	Bt.12140		Transcribed locus, moderate similar to NP_149038.1 mucin 13, epithelial transmembrane [Homo sapiens]	Up
NM_174462	Bt.8126	<i>SFTPC</i>	Surfactant, pulmonary-associated protein C	Up
BF043667	Bt.11788		Muscleblind-like 2 (Drosophila) (MBNL2), mRNA, incomplete 3' cds	Down
BC113321	Bt.33127	<i>ANXA8</i>	Annexin A8	Down
			Unknown function	
CN432436			mRNA sequence	Up
AW461357			PREDICTED: Homo sapiens hypothetical protein LOC649277 (LOC649277), mRNA	Up
AY563847			mRNA complete sequence	Up
AY563876			mRNA complete sequence	Up
BF041945			mRNA sequence	Up
BF042201			mRNA sequence	Up
BF044141			PREDICTED: Bos taurus similar to Proteinase activated receptor 4 precursor (PAR-4), mRNA	Up
BF045250			mRNA sequence	Up
BF046297	BF046297		mRNA sequence	Up
	Bt.10529		Transcribed locus, moderately similar to NP_001014186.1 protein LOC361729 [Rattus norvegicus]	Up
CR452752	Bt.11855	<i>COX4NB</i>	Similar to Neighbor of COX4	Up
CB440232	Bt.12609		Transcribed locus	Up
CN438935	Bt.12732		PREDICTED: Bos taurus similar to Suppressor/Enhancer of Lin-12 family member (sel-10) (LOC616020), mRNA	Up
DR697309	Bt.12944		Hypothetical protein MGC127568	Up
CK848330	Bt.13367		Transcribed locus	Up
CK971966	Bt.13721		Transcribed locus, moderately similar to XP_574585.1 similar to transmembrane protein 16D [Rattus norvegicus]	Up
BF046097	Bt.1633		Similar to CG31957-PA	Up
CN439347	Bt.20220		Transcribed locus	Up
CR552577	Bt.21092		Transcribed locus, strongly similar to XP_860597.1 PREDICTED: similar to nudE nuclear distribution gene E homolog like 1 (A. nidulans) isoform B isoform 3 [Canis familiaris]	Up
CV798766	Bt.22408		Transcribed locus	Up
CR456138	Bt.26523		Transcribed locus, moderately similar to XP_533005.2 PREDICTED: similar to ALMS1 [Canis familiaris]	Up
BM364898	Bt.27364		Transcribed locus	Up
CK848330	Bt.27713		Transcribed locus	Up
DR697653	Bt.28171		Hypothetical LOC616560	Up
BM363396	Bt.28517		Transcribed locus, weakly similar to XP_370586.1 PREDICTED: hypothetical protein XP_370586 [Homo sapiens]	Up
CK955406	Bt.29106		Transcribed locus	Up
CN434957	Bt.30368		Transcribed locus	Up
DR697494	Bt.33157		Transcribed locus	Up
CR454151	Bt.3352		Transcribed locus	Up

TABLE G.1. (continued)

Oligo sequence ID	Unigene ID	Symbol	Gene product	Expression
DR697435	Bt.3546		Transcribed locus, moderately similar to NP_001014238.1 protein LOC363227 [Rattus norvegicus]	Up
CR454523	Bt.37350	<i>CRYGC</i>	Crystallin, gamma C	Up
CN433087	Bt.40425	<i>MGC137951</i>	Similar to CG14353-PA	Up
CN436507	Bt.42091		Transcribed locus, weakly similar to XP_363777.1 protein MG01703.4 [Magnaporthe grisea 70-15]	Up
CR553946	Bt.43143		Transcribed locus Bos taurus	Up
BF041490	Bt.45497		Transcribed locus, strongly similar to XP_342937.1 similar to RIKEN cDNA D030015G18 [Rattus norvegicus]	Up
BF045949	Bt.48862		Proline synthetase co-transcribed bacterial homolog protein	Up
AY563754	Bt.53373		Transcribed locus	Up
BF043518	Bt.56758		Transcribed locus, strongly similar to NP_062126.3 tyrosine phosphatase, non-receptor type 5 [Rattus norvegicus]	Up
AW266954	Bt.634		Transcribed locus	Up
BF039755	Bt.6436		Transcribed locus, weakly similar to NP_997256.1 chromosome 10 open reading frame 99 [Homo sapiens]	Up
AW465810	Bt.65260		Butyrate response factor 2 (ZFP36L2)	Up
AY563880	Bt.66499		mRNAcomplete sequence	Up
BF042192	Bt.66528		Transcribed locus, moderately similar to XP_546163.2 similar to Group XIIB secretory phospholipase A2-like protein precursor (Group XIII secretory phospholipase A2-like protein) (GXIII sPLA2-like) (GXIIIB) [Canis familiaris]Bos taurus, 1 sequence(s)	Up
BF046389	Bt.66575		Transcribed locus Bos taurus	Up
BF440171	Bt.6781		Transcribed locus Bos taurus	Up
CN439346	Bt.69334		Transcribed locus Bos taurus	Up
CR550880	Bt.7468		Transcribed locus	Up
BE683354	Bt.7639		Transcribed locus, moderately similar to XP_541742.2 PREDICTED: similar to CG11986-PA isoform 1 [Canis familiaris]	Up
	Bt.78057		Transcribed locus	Up
CR452941	Bt.80635		Transcribed locus, weakly similar to XP_369999.1 protein MG06514.4 [Magnaporthe grisea 70-15]	Up
CR552274	Bt.9097		Hypothetical protein LOC57655 (GRAMD1A)	Up
CB424527			mRNA sequence	Up
CN437025			mRNA sequence	Up
CN437967			mRNA sequence	Up
CR452335			mRNA sequence	Up
CR453443			mRNA sequence	Up
CR455536			PREDICTED: Bos taurus similar to Iroquois-class homeodomain protein IRX-4 (Iroquois homeobox protein 4) (Homeodomain protein IRXA3) (LOC614900), mRNA	Up
BM362799	Bt.20356		Transcribed locus, moderately similar to NP_001019411.1 protein LOC291675 [Rattus norvegicus]	Up
CR453802	Bt.77643		Transcribed locus, weakly similar to NP_001017375.1 phosphoprotein, mpp8 [Rattus norvegicus]	Up
CK394179	Bt.58024		Transcribed locus	Up

TABLE G.1. (continued)

Oligo sequence ID	Unigene ID	Symbol	Gene product	Expression
CK979128	Bt.65012		Transcribed locus, moderately similar to NP_446101.1 transmembrane protein 1 [Rattus norvegicus]	Up
CN436261			mRNA sequence	Up
BF046022			mRNA sequence	Down
CR553683	Bt.13778		Transcribed locus	Down
AW267095	Bt.22633		Transcribed locus	Down
CN436791	Bt.30413		Transcribed locus	Down
CN439053	Bt.30510		Transcribed locus	Down
CR456291	Bt.32761		Transcribed locus	Down
CR552210	Bt.3376	<i>GBL</i>	G protein beta subunit-like	Down
CB425308	Bt.6087		Transcribed locus, strongly similar to XP_516815.1 PREDICTED: similar to transmembrane 4 superfamily member 1; membrane component, chromosome 3, surface marker 1; tumor-associated antigen L6 [Pan troglodytes]	Down
DR749302	Bt.64984		Transcribed locus, strongly similar to XP_001060645.1 similar to downregulated in renal cell carcinoma isoform 2 [Rattus norvegicus]	Down
CN433241	Bt.67490		Transcribed locus Bos taurus	Down
CN435725	Bt.74624	<i>MLL</i>	Similar to MLLT11 protein	Down

APPENDIX H

TABLE H.1. Host genes differentially expressed in *B. melitensis*-infected bovine Peyer's patches after one hour post-infection, compared to non-infected tissue

Oligo sequence ID	Unigene ID	Symbol	Gene product	Expression
DNA replication and repair				
NM_174427	Bt.4749	<i>POLD1</i>	Polymerase (DNA directed), delta 1, catalytic subunit 125kDa	Up
NM_174428	Bt.5282	<i>POLD2</i>	Polymerase (DNA directed), delta 2, regulatory subunit 50kDa	Up
BI541210	Bt.20817		Transcribed locus, strongly similar to NP_058633.1 polymerase (DNA-directed), alpha [Homo sapiens]	Up
CN433291	Bt.10510	<i>H2AFX</i>	H2A histone family, member X	Up
DR697479	Bt.47468		Transcribed locus, weakly similar to NP_986566.1 [Erethocium gossypii]	Up
BM364987	Bt.24693		Transcribed locus, moderately similar to NP_068741.1 Fanconi anemia, complementation group E [Homo sapiens]	Up
CV798789	Bt.76662		cDNA clone MGC:139804 IMAGE:8282843	Up
CN433185	Bt.12876		Transcribed locus, strongly similar to NP_000225.1 DNA ligase I [Homo sapiens]	Up
BF041685	Bt.20450		Transcribed locus, strongly similar to XP_540761.2 cryptochrome 2 (photolyase-like) [Canis familiaris]	Up
CO888038	Bt.4215		Excision repair cross-complementing rodent repair deficiency, complementation group 2 protein; malignancy-associated protein [Homo sapiens]	Up
CN433360	Bt.20277		Transcribed locus, moderately similar to XP_534241.2 DNA topoisomerase II, beta isozyme [Canis familiaris]	Down
CN438188	Bt.14643	<i>RAD17</i>	Similar to RAD17 homolog	Down
CN439458	Bt.55499		Similar to paraspeckle protein 1	Down
CN441968	Bt.28179		Transcribed locus, strongly similar to NP_115519.1 zinc finger, RAN-binding domain containing 3; 4933425L19Rik [Homo sapiens]	Down
CN436133	Bt.9810		Transcribed locus, strongly similar to XP_540212.2 DNA polymerase epsilon subunit 4 [Canis familiaris]	Down
AW289217	Bt.12578		Transcribed locus, strongly similar to NP_002544.1 origin recognition complex subunit 5 isoform 1; origin recognition complex, subunit 5 (yeast homolog)-like [Homo sapiens]	Down
BF039466	Bt.17967		Transcribed locus, strongly similar to XP_544336.2 uracil-DNA glycosylase 2 isoform a [Canis familiaris]	Down
CN439685	Bt.49518	<i>MCM7</i>	Minichromosome maintenance protein 7	Down
CK394174	Bt.62454	<i>H3F3A</i>	H3 histone, family 3A	Down
CR453487	Bt.3750	<i>S100A11</i>	S100 calcium binding protein A11 (calgizzarin)	Down
CR455462	Bt.49109	<i>MGC128567</i>	Similar to replication protein A3, 14kDa	Down
Chromosome organization				
BF043528	Bt.4638	<i>SMARCB1</i>	SWI/SNF related, matrix associated, actin dependent regulator of chromatin, subfamily b, member 1 (SMARCB1)	Up
AW463379	Bt.38062		Transcribed locus, moderately similar to NP_071789.1 attachment factor B [Rattus norvegicus]	Up
BM363362	Bt.22333		Similar to HP1-BP74	Up
CN435397	Bt.18798	<i>NASP</i>	Nuclear autoantigenic sperm protein (histone-binding)	Up

TABLE H.1. (continued)

Oligo sequence ID	Unigene ID	Symbol	Gene product	Expression
CN437487	Bt.76210		Transcribed locus, strongly similar to XP_227444.3 similar to SET domain ERG-associated histone methyltransferase [Rattus norvegicus]	Down
CN436405	Bt.27318		Transcribed locus, strongly similar to XP_229124.3 Smarca1 protein [Rattus norvegicus]	Down
BF041479	Bt.51581		Transcribed locus, strongly similar to NP_062036.2 1 [Rattus norvegicus]	Down
RNA processing				
CN433309	Bt.15722	<i>FBL</i>	Fibrillarin	Up
BF040218	Bt.76570		Transcribed locus, strongly similar to NP_006377.2 DEAD box polypeptide 17 isoform p82; probable RNA-dependent helicase p72; DEAD/H (Asp-Glu-Ala-Asp/His) box polypeptide 17 (72kD) [Homo sapiens]	Up
AW462347	Bt.15762		Similar to tRNA-dihydrouridine synthase 2-like	Up
BF045266	Bt.22762		Similar to U1 small nuclear ribonucleoprotein A (U1 snRNP protein A) (U1A protein) (U1-A)	Up
CN435437	Bt.70615		Transcribed locus, strongly similar to XP_001063720.1 small nuclear ribonucleoprotein polypeptide G [Rattus norvegicus]	Up
CR453324	Bt.33504		Transcribed locus, moderately similar to XP_001058353.1 U11/U12 snRNP 48K [Rattus norvegicus]	Down
CB445726	Bt.21871		Transcribed locus, strongly similar to XP_418176.1 U6 snRNA-associated Sm-like protein LSm7 [Gallus gallus]	Down
CR454324	Bt.65106		Similar to PDZ domain containing 6	Down
CR453923	Bt.77200		Transcribed locus, strongly similar to XP_535238.2 DEAH (Asp-Glu-Ala-His) box polypeptide 29 [Canis familiaris]	Down
CR452146	Bt.27146	<i>CPSF6</i>	Cleavage and polyadenylation specific factor 6	Down
AW462196	Bt.4077	<i>CPSF2</i>	Cleavage and polyadenylation specific factor 2, 100kDa	Down
CN438395	Bt.49583		Similar to DEAQ RNA-dependent ATPase	Down
CN439678	Bt.34334		Transcribed locus, strongly similar to XP_215739.3 formin binding protein 11 [Rattus norvegicus]	Down
CN440452	Bt.9783		Transcribed locus, strongly similar to XP_228701.3 RNA helicase [Rattus norvegicus]	Down
CN433615	Bt.65284		Transcribed locus, strongly similar to XP_851746.1 Nucleolar RNA helicase II (Nucleolar RNA helicase Gu) (RH II/Gu) (DEAD-box protein 21) [Canis familiaris]	Down
CN442388	Bt.3040	<i>SERBP1</i>	SERPINE1 mRNA binding protein 1	Down
CN441379	Bt.18263		Transcribed locus, strongly similar to Ser/Arg-related nuclear matrix protein	Down
BF042942	Bt.77649		Transcribed locus, strongly similar to XP_214053.2 Putative pre-mRNA splicing factor RNA helicase (DEAH box protein 15) [Rattus norvegicus]	Down
BF043575	Bt.9055	<i>TRMU</i>	Similar to tRNA (5-methylaminomethyl-2-thiouridylate)-methyltransferase 1	Down
BF440514	Bt.43563		Hypothetical gene supported by BC069011	Down
BF440242	Bt.41473		Similar to fragile X mental retardation 1	Down
BT021017	Bt.4620	<i>PCBP1</i>	Poly(rC) binding protein 1	Down
BC107553	Bt.38355	<i>SFRS6</i>	Splicing factor, arginine/serine-rich 6	Down
CN436610	Bt.3377		Similar to DEAD (Asp-Glu-Ala-Asp) box polypeptide 48	Down
CR454453	Bt.23170	<i>HNRPF</i>	Heterogeneous nuclear ribonucleoprotein F	Down

TABLE H.1. (continued)

Oligo sequence ID	Unigene ID	Symbol	Gene product	Expression
BF041133	Bt.10199	<i>HNRPC</i>	Heterogeneous nuclear ribonucleoprotein C (C1/C2)	Down
CN441824	Bt.61931		Transcribed locus, weakly similar to XP_367160.1 protein MG07085.4 [Magnaporthe grisea 70-15]	Down
BF044406	Bt.48320		Similar to splicing factor p54	Down
AW462759	Bt.41342		Similar to RNA-binding region (RNP1, RRM) containing 2 (predicted)	Down
CR452378	Bt.18313		Transcribed locus, strongly similar to XP_852169.1 splicing factor, arginine/serine-rich 14 isoform 1 [Canis familiaris]	Down
CR452942	Bt.49361	<i>FUSIP1</i>	FUS interacting protein (serine/arginine-rich) 1	Down
CR550423	Bt.15513	<i>SSB</i>	Sjogren syndrome antigen B (autoantigen La)	Down
U83008	Bt.14661	<i>ELAC1</i>	ElaC homolog 1 (<i>E. coli</i>)	Down
Transcription regulation				
AW266874	Bt.4851		Similar to transcriptional regulator protein	Up
CR451866	Bt.14038	<i>NT5C</i>	5', 3'-nucleotidase, cytosolic	Up
CR455869	Bt.34468	<i>MTF2</i>	Metal response element binding transcription factor 2	Up
CN434628	Bt.80550		Transcribed locus, strongly similar to NP_446244.1 LIM binding factor homolog [Rattus norvegicus]	Up
CN437285	Bt.41503		Similar to cytoplasmic nuclear factor of activated T-cells 4	Up
BF041444	Bt.45162		Transcribed locus, strongly similar to XP_512184.1 nuclear factor of activated T-cells, cytosolic component 1; NFAT transcription complex cytosolic component [Pan troglodytes]	Up
CN437384	Bt.80575		Transcribed locus, strongly similar to XP_001069461.1 Homeobox protein Hox-C9 (Hox-3.2) isoform 2 [Rattus norvegicus]	Up
BF045946	Bt.6669		Transcribed locus, strongly similar to NP_055028.2 homeo box D9 [Homo sapiens]	Up
DN282097	Bt.45247		Transcribed locus, weakly similar to XP_854664.1 zinc finger protein 75 [Canis familiaris]	Up
BF046240	Bt.10189		Transcribed locus, strongly similar to XP_533171.2 zinc finger protein 91 isoform 1 isoform 1 [Canis familiaris]	Up
AW462887	Bt.10173		Transcribed locus, strongly similar to NP_955459.1 zinc finger protein 64 isoform d; zinc finger protein 338 [Homo sapiens]	Up
CK950589	Bt.26862		Transcribed locus, moderately similar to XP_540750.2 zinc finger protein 408 [Canis familiaris]	Up
DR749266	Bt.12205		Transcribed locus, moderately similar to XP_544486.2 zinc finger protein 593 [Canis familiaris]	Up
CR452704	Bt.9141		Transcribed locus, strongly similar to NP_666288.1 CCR4-NOT transcription complex, subunit 3 [Mus musculus]	Up
AW463970	Bt.4009	<i>MTA1</i>	Metastasis associated 1	Up
BM363285	Bt.49602	<i>TNIP1</i>	Nef-associated factor 1	Up
AW461580	Bt.1662		Transcribed locus, strongly similar to XP_859184.1 megakaryoblastic leukemia 1 protein isoform 5 [Canis familiaris]	Up
CR453213	Bt.36917	<i>TRIM38</i>	Tripartite motif-containing 38	Up
BF045219	Bt.44514		Similar to protein phosphatase 1, regulatory (inhibitor) subunit 13 like	Up
CR451784	Bt.5242	<i>SSRP1</i>	Structure-specific recognition protein 1	Up
CR551087	Bt.74747		Transcribed locus, moderately similar to XP_227009.2 heterogeneous nuclear ribonucleoprotein K	Up

TABLE H.1. (continued)

Oligo sequence ID	Unigene ID	Symbol	Gene product	Expression
CR452705	Bt.23529		Transcribed locus, strongly similar to XP_536425.2 activated RNA polymerase II transcriptional coactivator [Canis familiaris]	Up
BM365730	Bt.59240		Similar to SP140 nuclear body protein	Up
CK946422	Bt.2268	<i>LASS4</i>	LAG1 longevity assurance homolog 4	Up
DT848843	Bt.59250		Transcribed locus, strongly similar to NP_005332.1 GLI-Kruppel family member HKR3 [Homo sapiens]	Up
CB442177	Bt.51623		Transcribed locus, moderately similar to XP_539481.2 nuclear factor (erythroid-derived 2)-like 3 [Canis familiaris]	Up
CN787113	Bt.20425	<i>GTF2E2</i>	General transcription factor IIE, polypeptide 2, beta 34kDa	Up
CR550783	Bt.53763	<i>NR2F2</i>	Nuclear receptor subfamily 2, group F, member 1	Down
CR550616	Bt.11325		Transcribed locus, strongly similar to XP_543051.2 activity-dependent neuroprotector isoform 1 [Canis familiaris]	Down
CR453558	Bt.33613	<i>SSBP2</i>	Single-stranded DNA binding protein 2	Down
CN436724	Bt.17324	<i>NFE2L2</i>	Nuclear factor (erythroid-derived 2)-like 2	Down
CR454351	Bt.48498		Transcribed locus, moderately similar to XP_001081621.1 helicase with zinc finger domain isoform 2 [Rattus norvegicus]	Down
CR455811	Bt.36422		Transcribed locus, moderately similar to XP_574241.1 Zfp1 protein [Rattus norvegicus]	Down
AW465775	Bt.62231		Transcribed locus, strongly similar to XP_001077663.1 zinc ring finger protein 1 [Rattus norvegicus]	Down
CN439477	Bt.64680		Transcribed locus, weakly similar to XP_853644.1 zinc finger protein 91 (HPF7, HTF10) [Canis familiaris]	Down
CN438154	Bt.14262		Transcribed locus, moderately similar to XP_533370.2 zinc finger protein 407 [Canis familiaris]	Down
CN438588	Bt.55996		Transcribed locus, strongly similar to XP_001070473.1 nuclear receptor coactivator 1 (NCoA-1) [Rattus norvegicus]	Down
AW465215	Bt.28984		Transcribed locus, strongly similar to XP_535440.2 MAX-interacting protein [Canis familiaris]	Down
BF042975	Bt.42395		Similar to LBP-1a=transcription factor binding to initiation site of HIV-1 (alternatively spliced)	Down
BF043277	Bt.10953		Similar to TSC22 domain family protein 1 (Transforming growth factor beta 1 induced transcript 4 protein) (Regulatory protein TSC-22) (TGFB stimulated clone 22 homolog) (Cerebral protein 2)	Down
BF044371	Bt.5469	<i>SURB7</i>	Similar to SRB7 suppressor of RNA polymerase B homolog	Down
BF440358	Bt.13902		Transcribed locus, strongly similar to NP_001008722.1 consensus sequence binding protein 1 (predicted) [Rattus norvegicus]	Down
BM365270	Bt.29952		Transcribed locus, strongly similar to transcriptional repressor NAC1 [H.s.]	Down
CV798817	Bt.14560		Similar to short form transcription factor C-MAF	Down
AW461546	Bt.59779		Transcribed locus, strongly similar to NP_062189.1 musculoaponeurotic fibrosarcoma oncogene family, protein B [Rattus norvegicus]	Down
BF044727	Bt.48975	<i>MED4</i>	Mediator of RNA polymerase II transcription, subunit 4 homolog (yeast)	Down
BF040723	Bt.12854		Similar to TATA box binding protein-like protein 1 (TBP-like protein 1) (TATA box binding protein-related factor 2) (TBP-related factor 2) (21-kDa TBP-like protein)	Down
BF440163	Bt.49104	<i>EED</i>	Embryonic ectoderm development protein	Down

TABLE H.1. (continued)

Oligo sequence ID	Unigene ID	Symbol	Gene product	Expression
AW462462	Bt.22999		Transcribed locus, strongly similar to NP_004372.3 cAMP responsive element binding protein-like 1; Creb-related protein [Homo sapiens]	Down
CN436757	Bt.28148		Transcribed locus, strongly similar to XP_538914.2 Forkhead box protein P4 (Fork head-related protein like A) [Canis familiaris]	Down
CR454537	Bt.23598	<i>POLR1D</i>	Polymerase (RNA) I polypeptide D, 16kDa	Down
CN438915	Bt.76715		Transcribed locus, strongly similar to NP_891847.1 myeloid/lymphoid or mixed-lineage leukemia 5 [Homo sapiens]	Down
BF039367	Bt.50935		Transcribed locus, strongly similar to NP_071585.1 Sam68-like protein SLM-2 [Rattus norvegicus]	Down
BF440342	Bt.5788		Transcribed locus, strongly similar to XP_001080272.1 ETS domain-containing protein Elk-3 (ETS-related protein NET) (ETS-related protein ERP) [Rattus norvegicus]	Down
AW462147	Bt.61520		Transcribed locus, strongly similar to XP_541963.2 cofactor required for Sp1 transcriptional activation, subunit 7, 70kDa [Canis familiaris]	Down
BF045698	Bt.49606		Similar to XAP-5 protein	Down
BF041691	Bt.51416	<i>HBP1</i>	HMG-box transcription factor 1	Down
BM363624	Bt.26220		Transcribed locus, strongly similar to v-rel reticuloendotheliosis viral oncogene homolog A	Down
AW465659	Bt.12647		Transcribed locus, strongly similar to XP_001080653.1 mediator of RNA polymerase II transcription, subunit 9 homolog [Rattus norvegicus]	Down
CN435519	Bt.16917		Transcribed locus, moderately similar to XP_509442.1 MondoA [Pan troglodytes]	Down
CN439520	Bt.4184	<i>HIF1A</i>	Hypoxia-inducible factor 1, alpha subunit (basic helix-loop-helix transcription factor)	Down
AJ696239	Bt.48141		Similar to cAMP responsive element modulator	Down
CK955473	Bt.52726		Transcribed locus, strongly similar to XP_543008.2 hepatocyte nuclear factor 4 alpha isoform a isoform 1 [Canis familiaris]	Down
Protein biosynthesis				
CR550906	Bt.33930	<i>EEF1A2</i>	Eukaryotic translation elongation factor 1 alpha 2	Up
CR455062	Bt.35903	<i>EIF1AX</i>	Eukaryotic translation initiation factor 1A, X-linked	Up
CR551876	Bt.2249	<i>EIF4E2</i>	Similar to eukaryotic translation initiation factor 4E-like 3	Up
CR456180	Bt.49332	<i>TARS</i>	Similar to threonyl-tRNA synthetase	Up
AW463888	Bt.43860	<i>FARS2</i>	Similar to phenylalanyl-tRNA synthetase, mitochondrial precursor (Phenylalanine--tRNA ligase) (PheRS)	Up
AW465478	Bt.21727		Transcribed locus, strongly similar to NP_004452.1 phenylalanine-tRNA synthetase-like protein; phenylalanine-tRNA synthetase alpha-subunit; phenylalanine-tRNA synthetase-like [Homo sapiens]	Up
CN441874	Bt.44540		Transcribed locus, weakly similar to XP_361064.1 protein MG03607.4 [Magnaporthe grisea 70-15]	Up
CN435490	Bt.20025	<i>MRPL21</i>	Similar to mitochondrial ribosomal protein L21	Up
BF042958	Bt.47838	<i>MRPL24</i>	Similar to mitochondrial ribosomal protein L24	Up
BF046336	Bt.4900	<i>MRPS5</i>	Similar to mitochondrial ribosomal protein S5	Up
CR451830	Bt.9242		Transcribed locus, moderately similar to XP_548346.2 mitochondrial ribosomal protein L41 (predicted) [Canis familiaris]	Up
CR456168	Bt.22248		RPL13 protein-like	Up

TABLE H.1. (continued)

Oligo sequence ID	Unigene ID	Symbol	Gene product	Expression
AW464060	Bt.23981	<i>RPL12</i>	Ribosomal protein L12	Up
BM362760	Bt.22568	<i>RPL29</i>	Ribosomal protein L29	Up
CR453525	Bt.7908	<i>RPS6</i>	Ribosomal protein S6	Up
BM363753	Bt.11697		Similar to 60S ribosomal protein L35	Up
AW266961	Bt.7648		Similar to ribosomal protein S19	Up
CN437563	Bt.21351	<i>EIF2S3</i>	Similar to eukaryotic translation initiation factor 2, subunit 3, structural gene X-linked	Down
AW267040	Bt.5471	<i>EIF4G2</i>	Eukaryotic translation initiation factor 4 gamma, 2	Down
CN433201	Bt.21295		Transcribed locus, strongly similar to XP_543492.2 eukaryotic translation initiation factor 4E transporter (eIF4E transporter) [Canis familiaris]	Down
BF043574	Bt.21351		Similar to eukaryotic translation initiation factor 2, subunit 3, structural gene X-linked	Down
CN434717	Bt.48825	<i>EIF3S6</i>	Eukaryotic translation initiation factor 3, subunit 6 48kDa	Down
CN437842	Bt.65927		Transcribed locus, moderately similar to XP_226707.4 elongation factor G 2, mitochondrial precursor (mEF-G 2) (Elongation factor G2) [Rattus norvegicus]	Down
CN432384	Bt.22038		Transcribed locus, strongly similar to XP_866928.1 arginyl-tRNA synthetase isoform 3 [Canis familiaris]	Down
CN437058	Bt.59370		Transcribed locus, strongly similar to NP_056155.1 leucyl-tRNA synthetase 2, mitochondrial precursor;	Down
CN435019	Bt.10387	<i>ABCF1</i>	leucine-tRNA ligase; leucine transylase [Homo sapiens] ATP-binding cassette, sub-family F (GCN20), member 1	Down
BF440250	Bt.76165		Transcribed locus, weakly similar to XP_359792.1 protein MG04985.4 [Magnaporthe grisea 70-15]	Down
BF045126	Bt.64764	<i>MRPS25</i>	Mitochondrial 28S ribosomal protein S25	Down
CR452009	Bt.45917		Transcribed locus, moderately similar to XP_508954.1 mitochondrial ribosomal protein L51	Down
CR454801	Bt.49151		Similar to 60S ribosomal protein L17 (L23) (Amino acid starvation-induced protein) (ASI)	Down
CR452611	Bt.15460	<i>RPS3</i>	Ribosomal protein S3	Down
CR551597	Bt.8462	<i>RPLP0</i>	Ribosomal protein, large, P0	Down
BF440544	Bt.2191		Similar to ribosomal protein S27, cytosolic - human	Down
BM363457	Bt.64475	<i>RPL6</i>	Ribosomal protein L6	Down
Protein folding				
CN432290	Bt.76948		Transcribed locus, weakly similar to NP_985611.1 [Eremothecium gossypii]	Up
BM364159	Bt.55432	<i>FKBP11</i>	FK506 binding protein 11, 19 kDa	Up
BM363860	Bt.20070	<i>SIL1</i>	SIL1 homolog, endoplasmic reticulum chaperone (S. cerevisiae)	Up
BF040464	Bt.23263	<i>HSP90AB1</i>	Heat shock 90kDa protein 1, beta	Up
BM364981	Bt.1430	<i>PFDN5</i>	Prefoldin 5	Up
CN436671	Bt.26818		Transcribed locus, strongly similar to XP_532518.2 DnaJ (Hsp40) homolog, subfamily B, member 9 [Canis familiaris]	Down
CN437208	Bt.59854	<i>PPIA</i>	Peptidylprolyl isomerase A (cyclophilin A)	Down
CN433513	Bt.77630		Transcribed locus, strongly similar to NP_005376.2 natural killer-tumor recognition sequence [Homo sapiens]	Down
CN433111	Bt.35339	<i>HSPA9B</i>	Heat shock 70kDa protein 9B (mortalin-2)	Down
AW462623	Bt.16330		Similar to GrpE protein homolog 2, mitochondrial precursor (Mt-GrpE#2)	Down
CN440377	Bt.28845	<i>CCT3</i>	T-complex protein 1, gamma subunit (TCP-1-gamma)	Down

TABLE H.1. (continued)

Oligo sequence ID	Unigene ID	Symbol	Gene product	Expression
Protein degradation				
AW463522	Bt.58848	<i>UCHL1</i>	Ubiquitin carboxy-terminal hydrolase L1	Up
BF041154	Bt.7631		Ubiquitin specific peptidase 5 (isopeptidase T) (USP5), mRNA, incomplete 3' cds	Up
CN786388	Bt.2294	<i>UBE1L</i>	Ubiquitin-activating enzyme E1-like	Up
CK776819	Bt.79993		Transcribed locus, strongly similar to XP_543159.2 ubiquitin-specific protease 12-like 1 [Canis familiaris]	Up
BF042633	Bt.10807		Transcribed locus, moderately similar to XP_533174.1 ubiquitin-conjugating enzyme E2L 6 isoform 1 [Canis familiaris]	Up
BM361936	Bt.32465		Similar to Ubiquitin-conjugating enzyme E2 J2 (Non-canonical ubiquitin conjugating enzyme 2) (NCUBE2)	Up
BF045963	Bt.2915		Similar to Ubiquitin-conjugating enzyme E2 T (Ubiquitin-protein ligase T) (Ubiquitin carrier protein T)	Up
AW462624	Bt.4902	<i>CTSZ</i>	CTSZ protein	Up
BF046162	Bt.46077	<i>CPA5</i>	Similar to carboxypeptidase A5	Up
BM363286	Bt.29297	<i>CAPN13</i>	Calpain 13	Up
CR552780	Bt.7040	<i>PSMB1</i>	Proteasome (prosome, macropain) subunit, beta type, 1	Up
BM362302	Bt.3624	<i>PSMB10</i>	Proteasome (prosome, macropain) subunit, beta type, 10	Up
CR455154	Bt.8062	<i>PSMC5</i>	Proteasome (prosome, macropain) 26S subunit, ATPase, 5	Up
BF041904	Bt.17968		Similar to 26S proteasome non-ATPase regulatory subunit 8 (26S proteasome regulatory subunit S14)	Up
CN439748	Bt.43820	<i>PRSS15</i>	ATP-dependent Lon protease	Up
AW462384	Bt.1722		Transcribed locus, weakly similar to XP_226175.3 mind bomb [Rattus norvegicus]	Up
BF041804	Bt.77192		Transcribed locus, strongly similar to XP_533702.2 Xaa-Pro dipeptidase (X-Pro dipeptidase) [Canis familiaris]	Up
DT824345	Bt.77217		Transcribed locus, strongly similar to NP_005459.1 N-acetylated alpha-linked acidic dipeptidase-like 1 [Homo sapiens]	Up
BF603068	Bt.24739		Transcribed locus, moderately similar to XP_001077083.1 neutrophil elastase [Rattus norvegicus]	Up
AF135232	Bt.18504	<i>MMP3</i>	Metalloproteinase 3 receptor	Up
DR697439	Bt.63794	<i>BMSC-UbP</i>	Bone marrow stromal cell-derived ubiquitin-like protein	Up
CN432461	Bt.12304	<i>ISG15</i>	Interferon-stimulated protein, 15 kDa	Up
BM362485	Bt.48919	<i>PSMB9</i>	Proteasome subunit beta type 9	Down
CN437905	Bt.48909	<i>PSMC4</i>	Proteasome (prosome, macropain) 26S subunit, ATPase, 4	Down
BM365916	Bt.24017	<i>PSMC2</i>	Proteasome (prosome, macropain) 26S subunit, ATPase 2	Down
BM364855	Bt.53697	<i>PSMB8</i>	Proteasome subunit, beta type 8	Down
CR452517	Bt.52452	<i>PSME1</i>	Proteasome activator 28 alpha subunit	Down
CR453736	Bt.77042		Transcribed locus, strongly similar to XP_547643.2 mind bomb homolog 1 [Canis familiaris]	Down
CR452352	Bt.15687		Similar to hect domain and RLD 4	Down
CR552096	Bt.30905		Transcribed locus, strongly similar to NP_973717.1 [Rattus norvegicus]	Down
CN434103	Bt.80549		Transcribed locus, strongly similar to XP_511577.1 SMAD specific E3 ubiquitin protein ligase 2; E3 ubiquitin ligase SMURF2 [Pan troglodytes]	Down
CN437394	Bt.76260	<i>ADAMTSL4</i>	Thrombospondin repeat containing 1	Down

TABLE H.1. (continued)

Oligo sequence ID	Unigene ID	Symbol	Gene product	Expression
CR456240	Bt.48960	<i>UBL4A</i>	Ubiquitin-like 4A	Down
AW465059	Bt.53978	<i>USP15</i>	Ubiquitin specific peptidase 15	Down
AW465929	Bt.55273	<i>UBE2E3</i>	Ubiquitin-conjugating enzyme E2E 3	Down
BF440277	Bt.49039	<i>UBD</i>	Similar to ubiquitin D	Down
BM445341	Bt.5070	<i>UBC</i>	Polyubiquitin	Down
CN437184	Bt.16935		Similar to Sentrin-specific protease 2 (Sentrin/SUMO-specific protease SENP2) (SMT3-specific isopeptidase 2) (Smt3ip2) (Axam2) [Canis familiaris]	Down
BF043307	Bt.12014		Transcribed locus, moderately similar to XP_545298.2 N-acetylated alpha-linked acidic dipeptidase 2 [Canis familiaris]	Down
BF039836	Bt.45767		Similar to CNDP dipeptidase 2 (metallopeptidase M20 family) (predicted)	Down
AW464210	Bt.8282	<i>DPP4</i>	Dipeptidylpeptidase IV (CD26, adenosine deaminase complexing protein 2)	Down
CR451940	Bt.12194	<i>FBXW2</i>	F-box and WD-40 domain protein 2 (FBXW2)	Down
CR452920	Bt.41339	<i>RNF8</i>	Ring finger protein 8	Down
BF043610	Bt.1613	<i>PRSS11</i>	Protease, serine, 11 [IGF binding]	Down
BF440339	Bt.7938	<i>CTSS</i>	Cathepsin S	Down
BF045684	Bt.27994	<i>ANPEP</i>	Alanyl (membrane) aminopeptidase	Down
Cell cycle / cell proliferation and differentiation				
CR453197	Bt.55596		Transcribed locus, strongly similar to NP_571977.1 kinase inhibitor 2C (p18, inhibits CDK4) [Rattus norvegicus]	Up
AW461358	Bt.63446		Similar to Interferon-induced 35 kDa protein (IFP 35)	Up
BF040980	Bt.58473		Transcribed locus, strongly similar to XP_545921.2 Max dimerization protein 4 isoform 1 [Canis familiaris]	Up
CN438129	Bt.149	<i>IGFBP2</i>	Insulin-like growth factor binding protein 2, 36kDa	Up
CN432245	Bt.9958	<i>IGFBP6</i>	Insulin-like growth factor-binding protein 6	Up
BF042760	Bt.59584	<i>GAK</i>	Cyclin G associated kinase	Up
DR749213	Bt.4267	<i>MIA</i>	Melanoma inhibitory activity	Up
CR453343	Bt.7181	<i>CAPNS1</i>	Calpain, small subunit 1	Up
BM365942	Bt.49712	<i>TP53</i>	p53 tumor suppressor phosphoprotein	Up
BF039606	Bt.56334	<i>MAD2L1</i>	MAD2 mitotic arrest deficient-like 1 (yeast)	Up
BF041588	Bt.20229	<i>TBFG4</i>	Transforming growth factor beta regulator 4	Up
NM_174385	Bt.5011	<i>LTBP2</i>	Latent transforming growth factor beta binding protein 2	Up
NM_174435	Bt.2813	<i>PRKCA</i>	Protein kinase, C alpha	Up
AU233257	Bt.11071		Transcribed locus, strongly similar to XP_543975.2 leucine zipper, putative tumor suppressor 2 [Canis familiaris]	Up
CN438167	Bt.3383		Similar to Transcription factor Dp-1 (E2F dimerization partner 1) (DRTF1-polypeptide-1)	Down
CR451824	Bt.27716	<i>NOV</i>	Nephroblastoma overexpressed	Down
CN440114	Bt.74621		Transcribed locus, moderately similar to XP_001079831.1 proto-oncogene tyrosine-protein kinase ABL1 (p150) (c-ABL) (Abelson murine leukemia viral oncogene homolog 1) [Rattus norvegicus]	Down
BF045140	Bt.24497	<i>FGFR1OP</i>	FGFR1 oncogene partner 1	Down
BF043260	Bt.5750		Similar to carcinoma related gene	Down
CK960109	Bt.37175	<i>CCNE2</i>	Cyclin E2	Down

TABLE H.1. (continued)

Oligo sequence ID	Unigene ID	Symbol	Gene product	Expression
CR550550	Bt.20570		Similar to cyclin-dependent kinases regulatory subunit 1 (CKS-1) (Sid 1334)	Down
CK769923	Bt.7907	<i>CDK10</i>	Similar to cyclin-dependent kinase (CDC2-like) 10	Down
AW463849	Bt.28600	<i>RBM22</i>	RNA binding motif protein 22	Down
CN442154	Bt.58299	<i>CAMK2D</i>	Calcium/calmodulin-dependent protein kinase II, delta	Down
BM366553	Bt.7519		Transcribed locus, moderately similar to NP_058888.1 differentiation, sphingolipid G-protein-coupled receptor, 5 [Rattus norvegicus]	Down
CR451837	Bt.23576		Transcribed locus, strongly similar to NP_002586.2 PCTAIRE protein kinase 2 [Homo sapiens]	Down
CR453819	Bt.49763	<i>PNN</i>	Pinin, desmosome associated protein	Down
AW465475	Bt.28337		Transcribed locus, strongly similar to NP_057217.2 insulin induced protein 2; INSIG2 membrane protein [Homo sapiens]	Down
BF043720	Bt.6705		Transcribed locus, strongly similar to NP_008994.1 TBC1 domain family, member 8 (with GRAM domain); vascular Rab-GAP/TBC-containing; BUB2-like protein 1 [Homo sapiens]	Down
BM362277	Bt.10855		Similar to regulator of G-protein signaling 2	Down
AF305199	Bt.74168	<i>IGFBP3</i>	Insulin-like growth factor binding protein 3	Down
AW289255	Bt.19650		Similar to cell division cycle 7-related protein kinase (CDC7-related kinase)	Down
CR453568	Bt.12473	<i>CDC37</i>	CDC37 homolog	Down
AW461388	Bt.23999		Transcribed locus, weakly similar to XP_363890.1 protein MG01816.4 [Magnaporthe grisea 70-15]	Down
CN434391	Bt.13476		Transcribed locus, strongly similar to NP_612565.1 kinesin family member 23 isoform 1; mitotic kinesin-like 1; kinesin-like 5 (mitotic kinesin-like protein 1) [Homo sapiens]	Down
CN440232	Bt.37915		Transcribed locus, moderately similar to XP_534964.2 kinesin family member 11 [Canis familiaris]	Down
CB423716	Bt.22733		Transcribed locus, moderately similar to NP_001017470.1 protein LOC367153 [Rattus norvegicus]	Down
BF046203	Bt.4831	<i>NDP52</i>	Nuclear domain 10 protein	Down
Cell adhesion				
NM_198221	Bt.13022	<i>ITGAL</i>	Integrin, alpha L (antigen CD11A (p180), lymphocyte function-associated antigen 1; alpha polypeptide)	Up
AJ535320	Bt.35830	<i>ITGAM</i>	Integrin alpha M	Up
BF041132	Bt.9972	<i>ITGB6</i>	Integrin beta6	Up
CR454674	Bt.4615	<i>ITGB2</i>	Integrin, beta 2 (antigen CD18 subunit (p95), lymphocyte function-associated antigen 1, integrin B2)	Up
BF041823	Bt.5372	<i>ICAM1</i>	Intercellular adhesion molecule 1 (CD54), human rhinovirus receptor	Up
BM365946	Bt.2657	<i>URP2</i>	UNC-112 related protein 2	Up
AW464620	Bt.2573	<i>CD9</i>	CD9 antigen (p24)	Up
BF040131	Bt.59823	<i>ZO3</i>	Tight junction protein 3	Up
BF042339	Bt.12589		Transcribed locus, moderately similar to XP_001061082.1 Laminin alpha-3 chain precursor (Nicein alpha subunit) isoform 1 [Rattus norvegicus]	Up
BI540051	Bt.33617		Transcribed locus, strongly similar to NP_032755.1 catenin (cadherin associated protein), delta 2 [Mus musculus]	Up
CR454750	Bt.32490	<i>CLSTN3</i>	Calsyntenin 3	Up
CR453007	Bt.58521		Similar to claudin 5	Up

TABLE H.1. (continued)

Oligo sequence ID	Unigene ID	Symbol	Gene product	Expression
BF040930	Bt.11942	<i>COL18a1</i>	Collagen, type XVIII, alpha 1	Up
DR697468	Bt.61880		Transcribed locus, strongly similar to NP_604447.1 type V, alpha 1 [Rattus norvegicus]	Up
CR553272	Bt.46833		Transcribed locus, strongly similar to NP_000349.1 transforming growth factor, beta-induced [Homo sapiens]	Down
CN435002	Bt.7380	<i>COL12A1</i>	Collagen, type XII, alpha 1	Down
CR452494	Bt.53485	<i>COL1A2</i>	Collagen, type I, alpha 2	Down
BF043071	Bt.28231	<i>CLDN7</i>	Similar to Claudin-7	Down
CN441870	Bt.7043	<i>VCAM1</i>	Vascular cell adhesion molecule 1	Down
CR455078	Bt.64827	<i>CDH1</i>	Cadherin 1, type 1, E-cadherin (epithelial)	Down
CN438657	Bt.23618	<i>SPON1</i>	Spondin 1, (f-spondin) extracellular matrix protein	Down
Cell-cell communication				
BF045641	Bt.35935	<i>GJB6</i>	Gap junction protein, beta 6 (connexin 30)	Up
BF042809	Bt.17182		Transcribed locus, moderately similar to XP_539605.2 gap junction protein, beta 5 (connexin 31.1) [Canis familiaris]	Up
CR550859	Bt.516	<i>GJB1</i>	Gap junction protein, beta 1, 32 kD [connexin 32]	Up
BE237149	Bt.5976		Transcribed locus, moderately similar to XP_539604.1 Gap junction beta-4 protein (Connexin 30.3) [Canis familiaris]	Up
Cytoskeletal organization				
CR454452	Bt.36476		Similar to gamma adducin (Adducin-like protein 70)	Up
CN440623	Bt.79717		Transcribed locus, strongly similar to myosin-1C	Up
AW461752	Bt.52428	<i>CFL1</i>	Cofilin 1 (non-muscle)	Up
DR697464	Bt.57772	<i>ACTN1</i>	Similar to actinin, alpha 1	Up
AW463298	Bt.59155	<i>KRT19</i>	Cytokeratin 19	Up
DT815327	Bt.6141	<i>DES</i>	Desmin	Up
BM366406	Bt.55987	<i>TPM3</i>	Tropomyosin 3	Up
CN432869	Bt.11149	<i>VIM</i>	Vimentin	Up
CN441758	Bt.23146	<i>MYH8</i>	Myosin, heavy polypeptide 8, skeletal muscle, perinatal	Up
CR452914	Bt.3684	<i>ACTR2</i>	ARP2 (actin-related protein 2, yeast) homolog	Down
CN440821	Bt.56769	<i>WASPIP</i>	Wiskott-Aldrich syndrome protein interacting protein	Down
AW461549	Bt.57467	<i>ANK3</i>	Similar to ankyrin 3	Down
CN433500	Bt.13391	<i>CAPZA2</i>	Capping protein (actin filament) muscle Z-line, alpha 2	Down
CN437939	Bt.4329	<i>SVIL</i>	Supervillin	Down
CR451851	Bt.23180	<i>PFN1</i>	Profilin 1	Down
CR553471	Bt.38667		Actin, cytoplasmic 2	Down
CR451994	Bt.48990	<i>CAP1</i>	CAP, adenylate cyclase-associated protein 1 (yeast)	Down
CR552253	Bt.64976	<i>CALD1</i>	Caldesmon, smooth muscle	Down
CR453003	Bt.2847	<i>MYL6</i>	Myosin, light peptide 6, alkali, smooth muscle and non-muscle	Down
BF043297	Bt.76268		Transcribed locus, strongly similar to XP_236444.3 myosin VI [Rattus norvegicus]	Down
CB438714	Bt.18044		Transcribed locus, strongly similar to XP_533351.2 kinesin heavy chain isoform 5C [Canis familiaris]	Down
CN438269	Bt.61392		Transcribed locus, strongly similar to NP_034310.1 fibulin 1 [Mus musculus]	Down

TABLE H.1. (continued)

Oligo sequence ID	Unigene ID	Symbol	Gene product	Expression
Morphogenesis and development				
CR451786	Bt.44967		Transcribed locus, moderately similar to NP_114452.1 1 [Rattus norvegicus]	Up
CN436901	Bt.2886	<i>DKKL1</i>	Dickkopf-like protein 1	Up
BF039742	Bt.37857		Transcribed locus, strongly similar to XP_001060983.1 Wolf-Hirschhorn syndrome candidate 1 [Rattus norvegicus]	Up
BF046291	Bt.48832	<i>MESDC2</i>	Mesoderm development candidate 2	Up
CR552730	Bt.4235		Transcribed locus, weakly similar to XP_342600.2 alpha-3 type IX collagen [Rattus norvegicus]	Up
CN440721	Bt.18467		Transcribed locus, weakly similar to XP_517386.1 T-cell receptor alpha enhancer-binding protein, short form - human [Pan troglodytes]	Up
DR749253	Bt.47429		Transcribed locus, strongly similar to XP_001078859.1 FERMRhoGEF (Arhgef) and pleckstrin domain protein 1 [Rattus norvegicus]	Up
BF044858	Bt.20145	<i>PX19</i>	Px19-like protein	Up
NM_174403	Bt.7422	<i>NR5A1</i>	Nuclear receptor subfamily 5, group A, member 1	Up
AW430313	Bt.76414		Transcribed locus, moderately similar to NP_055595.2 cullin 7 [Homo sapiens]	Up
DR697687	Bt.5219	<i>TCF21</i>	Transcription factor 21	Up
CN434722	Bt.13780		Transcribed locus, strongly similar to sprouty homolog 1	Down
AW464650	Bt.16749		Similar to plexin A3	Down
AW465346	Bt.10941		Transcribed locus, moderately similar to NP_060858.2 muscleblind-like 3 isoform G [Homo sapiens]	Down
AW464984	Bt.4908	<i>RBBP7</i>	Retinoblastoma binding protein 7	Down
BF045944	Bt.13880		Transcribed locus, strongly similar to XP_507795.1 Dickkopf related protein-1 precursor (Dkk-1)	Down
CR553196	Bt.5223	<i>DLK1</i>	Delta-like homolog (Drosophila)	Down
BM087872	Bt.28900		Similar to annexin XIIIb	Down
BF044804	Bt.62052	<i>SOX6</i>	Similar to SOX6	Down
DR697405	Bt.45570	<i>EPAS1</i>	Endothelial PAS domain protein 1	Down
CK951897	Bt.65686		Transcribed locus, strongly similar to XP_858787.1 Jagged-1 precursor (Jagged1) (hJ1) [Canis familiaris]	Down
BF440263	Bt.1424		Transcribed locus, strongly similar to NP_004226.2 Kruppel-like factor 4 (gut); endothelial Kruppel-like zinc finger protein [Homo sapiens]	Down
NM_174302	Bt.81	<i>CYLC1</i>	Cylicin, basic protein of sperm head cytoskeleton 1	Down
Apoptosis				
CN440401	Bt.30544		Similar to p75-like apoptosis-inducing death domain protein PLAIDD	Up
DR697322	Bt.1411		Similar to BCL2/adenovirus E1B 19-kDa protein-interacting protein 3	Up
BF041764	Bt.2386	<i>DEDD2</i>	Similar to death effector domain-containing DNA binding protein 2	Up
BF046452	Bt.20111		Transcribed locus, moderately similar to NP_851600.1 necrosis factor receptor superfamily, member 12a [Rattus norvegicus]	Up
CR454566	Bt.62236	<i>WWOX</i>	WW domain-containing oxidoreductase	Up
CN441881	Bt.49187	<i>GRIM19</i>	Cell death-regulatory protein GRIM19	Up
BF044468	Bt.7776	<i>TPT1</i>	Tumor protein, translationally-controlled 1	Up
BF041733	Bt.35629	<i>BID</i>	BH3 interacting domain death agonist	Up
CR550989	Bt.48127	<i>TIA1</i>	Similar to TIA1 protein	Down

TABLE H.1. (continued)

Oligo sequence ID	Unigene ID	Symbol	Gene product	Expression
CN434930	Bt.32255	<i>PDCD5</i>	Similar to programmed cell death protein 5 (TFAR19 protein) (TF-1 cell apoptosis related gene-19 protein)	Down
CR454209	Bt.14155	<i>PDCD10</i>	Similar to programmed cell death 10	Down
BF043121	Bt.45655	<i>STK17B</i>	Similar to serine/threonine-protein kinase 17B (DAP kinase-related apoptosis-inducing protein kinase 2)	Down
BF045339	Bt.61869	<i>CYCS</i>	Similar to cytochrome c, somatic	Down
AW465842	Bt.1793		Transcribed locus, moderately similar to XP_001080523.1 cell death regulator Aven [Rattus norvegicus]	Down
AW464030	Bt.4675	<i>MX1</i>	Myxovirus (influenza) resistance 1, (murine homolog)	Down
BF440414	Bt.11884	<i>BCL2A1</i>	B-cell leukemia/lymphoma 2 related protein A1	Down
BF040981	Bt.13981		Similar to TM2 domain containing 2	Down
CB538194	Bt.64777		Transcribed locus, moderately similar to NP_068520.1 IAP repeat-containing 2 [Rattus norvegicus]	Down
BF045590	Bt.20494		Transcribed locus, strongly similar to NP_036366.2 RING1 and YY1 binding protein; Ring1 interactor RYBP; YY1 and E4TF1 associated factor 1; apoptin-associated protein 1 [Homo sapiens]	Down
CN440606	Bt.12183	<i>RRAGA</i>	Ras-related GTP binding A	Down
Immuno and Inflammatory response				
AF081273	Bt.45933	<i>IL4R</i>	Interleukin-4 receptor alpha chain	Up
BE808976	Bt.49236	<i>IL11RA</i>	Interleukin 11 receptor, alpha	Up
BM366533	Bt.26527	<i>IL16</i>	Interleukin 16	Up
BM362640	Bt.26847		Linker for activation of T cells	Up
CK959898	Bt.18368		Transcribed locus, weakly similar to NP_891997.1 (C-X-C motif) ligand 11 [Rattus norvegicus]	Up
BM363136	Bt.27680		Transcribed locus, strongly similar to NP_997498.2 cytokine [Rattus norvegicus]	Up
CR452319	Bt.8140	<i>FCER1G</i>	Fc fragment of IgE, high affinity I, receptor for; gamma polypeptide	Up
AW461905	Bt.41326	<i>DF</i>	D component of complement (adipsin)	Up
CK959382	Bt.68981		Transcribed locus, weakly similar to NP_001037692.1 component factor h-like 1 [Rattus norvegicus]	Up
CN436532	Bt.43647	<i>C1R</i>	Complement component 1, r subcomponent	Up
CB434668	Bt.76479		Transcribed locus, strongly similar to NP_006601.2 mannan-binding lectin serine protease 2 [Homo sapiens]	Up
CR452765	Bt.15528	<i>MIF</i>	Macrophage migration inhibitory factor (glycosylation-inhibiting factor)	Up
AW463930	Bt.46809		Similar to CD74 antigen	Up
BF045350	Bt.5356	<i>BoLA-DRB3</i>	Major histocompatibility complex, class II, DRB3	Up
AB117946	Bt.53299	<i>BOLA-DOB</i>	Major histocompatibility complex, class II, DO beta	Up
BF041352	Bt.23126	<i>NOS2A</i>	Nitric oxide synthase 2A (inducible, hepatocytes)	Up
CB224338	Bt.9360		Similar to Calgranulin A (Migration inhibitory factor-related protein 8) (MRP-8)	Up
CK770058	Bt.44261	<i>TNFRSF8</i>	Tumor necrosis factor receptor superfamily, member 8	Up
CR452792	Bt.1577	<i>C1QA</i>	Complement component 1, q subcomponent, alpha polypeptide	Down
AJ535317	Bt.79131	<i>CD21</i>	Complement receptor type 2	Down
NM_205773	Bt.24326		Eotaxin	Down
AY574996	Bt.80445	<i>CCR3</i>	C-C motif chemokine receptor 3	Down
AY575855	Bt.62596	<i>CCR1</i>	Chemokine C-C motif receptor 1	Down
BF043950	Bt.2408	<i>CCL2</i>	Chemokine (C-C motif) ligand 2	Down
BM364516	Bt.2524	<i>SDF1</i>	Stromal cell-derived factor 1	Down

TABLE H.1. (continued)

Oligo sequence ID	Unigene ID	Symbol	Gene product	Expression
CN792099	Bt.28088	<i>CXCL13</i>	Chemokine (C-X-C motif) ligand 13-like	Down
BF074924	Bt.9468	<i>SYK</i>	Spleen tyrosine kinase	Down
BF039564	Bt.49740	<i>IL8</i>	Interleukin 8	Down
BM364841	Bt.24247		Transcribed locus, weakly similar to NP_476541.1 10 receptor, alpha [Rattus norvegicus]	Down
CN439007	Bt.234	<i>IL18</i>	Interleukin 18 (interferon-gamma-inducing factor)	Down
AW465344	Bt.49121	<i>IL22RA1</i>	Interleukin 22 receptor, alpha 1	Down
BF440593	Bt.74191	<i>IGJ</i>	Immunoglobulin J chain	Down
BF440378	Bt.143	<i>NCF2</i>	Neutrophil cytosolic factor 2 [65kD, human : chronic granulomatous disease, autosomal 2]	Down
BM364912	Bt.46153		Transcribed locus, weakly similar to XP_854209.1 osteoclast inhibitory lectin isoform 1 [Canis familiaris]	Down
BM365025	Bt.55988		Similar to SAM domain and HD domain-containing protein 1 (Dendritic cell-derived IFNG-induced protein) (DCIP) (Monocyte protein 5) (MOP-5)	Down
CB459644	Bt.24959		Transcribed locus, weakly similar to NP_001770.1 antigen, (lymphocyte function-associated antigen 3) [Homo sapiens]	Down
CN439508	Bt.15157	<i>CNIH</i>	Cornichon-like isoform 1	Down
AW461498	Bt.42359	<i>PLA2G7</i>	Phospholipase A2, group VII (platelet-activating factor acetylhydrolase, plasma)	Down
DN825756	Bt.12775	<i>BOLA</i>	Classical MHC class I antigen	Down
CN999995	Bt.12775	<i>BOLA</i>	Classical MHC class I antigen	Down
BF440417	Bt.5269	<i>B2M</i>	Beta-2-microglobulin	Down
BM362427	Bt.8552	<i>BOLA-DRA</i>	Major histocompatibility complex, class II, DR alpha	Down
BF046359	Bt.1548		Transcribed locus, moderately similar to XP_533874.2 gamma-interferon inducible lysosomal thiol reductase precursor (Gamma-interferon-inducible protein IP-30) [Canis familiaris]	Down
Pregnancy				
CR456002	Bt.2047	<i>ADM</i>	Adrenomedullin	Down
CK845888	Bt.43717	<i>PGDH</i>	Hydroxyprostaglandin dehydrogenase 15-(NAD)	Down
BF042058	Bt.30437	<i>PGRMC2</i>	Progesterone receptor membrane component 2	Down
Nervous system development and proliferation				
BF045655	Bt.54949		Similar to huntingtin-associated protein 1	Up
CR453582	Bt.361	<i>SLC1A3</i>	Solute carrier family 1 (glial high affinity glutamate transporter), member 3	Up
NM_173884	Bt.3864	<i>TH</i>	Tyrosine hydroxylase	Up
CB442833	Bt.16310		Transcribed locus, strongly similar to XP_508369.1 dJ68D18.1.2 (solute carrier family 1 (glial high affinity glutamate transporter) member 2) [Pan troglodytes]	Up
CR552897	Bt.49592		Similar to protein CGI-38	Up
CR452742	Bt.53943		Similar to ectoderm-neural cortex-1 protein (ENC-1) (p53-induced protein 10) (Nuclear matrix protein NRP/B)	Up
BM363307	Bt.78537		Transcribed locus, moderately similar to NP_060719.3 CDK5 regulatory subunit associated protein 2; CDK5 activator-binding protein C48 [Homo sapiens]	Up
CR451719	Bt.69592		Transcribed locus, strongly similar to NP_001002953.1 related with YRPW motif 1 [Canis familiaris]	Up

TABLE H.1. (continued)

Oligo sequence ID	Unigene ID	Symbol	Gene product	Expression
CR452081	Bt.76692		Transcribed locus, strongly similar to NP_443100.1 immunoglobulin superfamily, member 8; CD81 partner 3 [Homo sapiens]	Up
CR455513	Bt.56845		Transcribed locus, strongly similar to XP_532931.2 cysteine rich transmembrane BMP regulator 1 (chordin like) [Canis familiaris]	Up
NM_174229	Bt.517	<i>ADCY1</i>	Adenylate cyclase 1 (brain)	Up
CR454056	Bt.22534		Transcribed locus, moderately similar to NP_058733.1 myelin protein 22 [Rattus norvegicus]	Down
AW463945	Bt.41007	<i>GABARAPL2</i>	GABA(A) receptor-associated protein-like 2	Down
NM_174272	Bt.4231	<i>CHRNE</i>	Cholinergic receptor, nicotinic, epsilon polypeptide	Down
CN438259	Bt.21731		Similar to drebrin (Developmentally regulated brain protein)	Down
BF043908	Bt.3940		Similar to transcription factor 12	Down
CR455649	Bt.275	<i>NEDD8</i>	Neural precursor cell expressed, developmentally down-regulated 8	Down
AW464306	Bt.48322		Similar to developmentally regulated RNA-binding protein 1 (RB-1)	Down
CR453508	Bt.46270		Transcribed locus, strongly similar to XP_540253.2 nescient helix loop helix 2 [Canis familiaris]	Down
Metabolism				
Amino acids				
CR454264	Bt.5422	<i>PYCR1</i>	Pyrroline-5-carboxylate reductase-like	Up
BF042101	Bt.49106	<i>SHMT2</i>	Serine hydroxymethyltransferase 2 (mitochondrial)	Up
BE682393	Bt.16050		Similar to mitochondrial glutamate carrier 1	Up
AW461608	Bt.27135		Similar to Kynurenine--oxoglutarate transaminase I (Kynurenine aminotransferase I) (KATI) (Glutamine--phenylpyruvate transaminase) (Glutamine transaminase K) (GTK) (Cysteine-S-conjugate beta-lyase)	Up
AW465008	Bt.52357	<i>HRMT1L2</i>	HMT1 hnRNP methyltransferase-like 2	Up
CR451970	Bt.4269	<i>OTC</i>	Ornithine carbamoyltransferase	Down
BF046362	Bt.49448	<i>OAT</i>	Similar to Ornithine aminotransferase, mitochondrial precursor (Ornithine--oxo-acid aminotransferase)	Down
CR453522	Bt.26471		Transcribed locus, strongly similar to NP_056962.2 ornithine decarboxylase antizyme inhibitor; antizyme inhibitor [Homo sapiens]	Down
CN437959	Bt.20701		Transcribed locus, strongly similar to NP_858058.1 O-linked GlcNAc transferase isoform 1; O-GlcNAc transferase p110 subunit; uridinediphospho-N-acetylglucosamine	Down
CN438569	Bt.57999		Transcribed locus, strongly similar to XP_862154.1 carbamoyl-phosphate synthetase 1, mitochondrial isoform 30 [Canis familiaris]	Down
CN439799	Bt.52500	<i>ST3GAL-V</i>	Alpha 2,3-sialyltransferase	Down
BF043883	Bt.25099	<i>PSPH</i>	Similar to phosphoserine phosphatase	Down
CR455498	Bt.4733	<i>PHGDH</i>	Phosphoglycerate dehydrogenase	Down
CR454540	Bt.16072	<i>SERINC2</i>	Serine incorporator 2	Down
Nucleic acids				
BF045425	Bt.1087		Transcribed locus, strongly similar to XP_521542.1 3'-phosphoadenosine 5'-phosphosulfate synthase 2 [Pan troglodytes]	Up
BF041430	Bt.42575	<i>UCK1</i>	Similar to Uridine-cytidine kinase 1	Up

TABLE H.1. (continued)

Oligo sequence ID	Unigene ID	Symbol	Gene product	Expression
DR697437	Bt.48820	<i>DERA</i>	Similar to Putative deoxyribose-phosphate aldolase (Phosphodeoxyriboaldolase) (Deoxyriboaldolase) (DERA)	Down
BF045108	Bt.34369		Transcribed locus, strongly similar to XP_856623.1 ribose-phosphate pyrophosphokinase II (Phosphoribosyl pyrophosphate synthetase II) (PRS-II) isoform 4 [Canis familiaris]	Down
BM363371	Bt.31640	<i>OAS1</i>	2',5'-oligoadenylate synthetase 1, 40/46kDa	Down
CR452386	Bt.61486		Transcribed locus, weakly similar to XP_453052.1 protein product [Kluyveromyces lactis]	Down
DR697447	Bt.65253		Transcribed locus, weakly similar to NP_983600.1 [Eremothecium gossypii]	Down
CR454063	Bt.5340	<i>NBR-A</i>	Nucleoside-diphosphate kinase NBR-A	Down
CR452418	Bt.18730	<i>DHFR</i>	Dihydrofolate reductase	Down
Carbohydrates				
AW465422	Bt.22533		Transcribed locus, strongly similar to NP_036627.1 A [Rattus norvegicus]	Up
BF042384	Bt.62233		Transcribed locus, moderately similar to XP_001077726.1 carbohydrate sulfotransferase 5 (N-acetylglucosamine 6-O-sulfotransferase 3)	Up
CN440595	Bt.5061		Transcribed locus, moderately similar to NP_000280.1 phosphofructokinase, muscle; Phosphofructokinase, muscle type [Homo sapiens]	Up
CN440641	Bt.59986		Similar to ketohexokinase	Up
BM363300	Bt.12474	<i>GALE</i>	UDP-galactose-4-epimerase	Up
CN434306	Bt.49794	<i>PDHB</i>	Pyruvate dehydrogenase (lipoamide) beta	Up
AW463251	Bt.11825		Transcribed locus, strongly similar to NP_001015032.2 N-acetylgalactosaminyltransferase 3 [Rattus norvegicus]	Down
CN437656	Bt.44041		Similar to Aldehyde dehydrogenase, mitochondrial precursor (ALDH class 2) (ALDH1) (ALDH-E2)	Down
CR455987	Bt.20235		Similar to N-acetylglucosamine-6-sulfatase precursor (G6S) (Glucosamine-6-sulfatase)	Down
CR454616	Bt.57867		Similar to Alpha-N-acetylgalactosaminidase precursor (Alpha-galactosidase B)	Down
CN437540	Bt.49587	<i>GPI</i>	Glucosephosphate isomerase	Down
CB165214	Bt.13737	<i>GALK2</i>	Similar to N-acetylgalactosamine kinase (GalNAc kinase) (Galactokinase 2)	Down
Lipids				
BE480377	Bt.61867		Similar to carnitine acetyltransferase isoform 1 precursor	Up
CB223494	Bt.28966	<i>PLA2G2A</i>	Phospholipase A2 group IIA-like	Up
CN441201	Bt.12	<i>FABP1</i>	Fatty acid binding protein 1, liver	Up
CR454069	Bt.76327		Transcribed locus, strongly similar to NP_689572.1 carnitine palmitoyltransferase 1C; carnitine palmitoyltransferase I related C [Homo sapiens]	Up
BF040744	Bt.24308		Transcribed locus, moderately similar to NP_446126.1 hydroxylase [Rattus norvegicus]	Up
BF040540	Bt.31329	<i>PNPLA6</i>	Patatin-like phospholipase domain containing 6	Up
BF039919	Bt.46917		Hypothetical LOC768330 (LOC768330)	Up
CR551554	Bt.34980	<i>APOE</i>	Apolipoprotein E	Up
CR451929	Bt.2342	<i>CDS2</i>	Similar to phosphatidate cytidyltransferase 2	Down
CR453248	Bt.61205		Transcribed locus, weakly similar to XP_363106.1 protein MG08690.4 [Magnaporthe grisea 70-15]	Down

TABLE H.1. (continued)

Oligo sequence ID	Unigene ID	Symbol	Gene product	Expression
CN435714	Bt.56578		Transcribed locus, strongly similar to XP_538788.1 ceramide glucosyltransferase (Glucosylceramide synthase) (GCS) (UDP-glucose:N-acylsphingosine D-glucosyltransferase) (UDP-glucose ceramide glucosyltransferase) (GLCT-1)	Down
CN438868	Bt.4909	<i>TCAP</i>	Titin-cap	Down
CN441562	Bt.18340		Similar to choline/ethanolaminephosphotransferase 1	Down
BF039216	Bt.49359	<i>DEGS1</i>	Similar to degenerative spermatocyte homolog 1, lipid desaturase	Down
CN439703	Bt.22589		Transcribed locus, moderately similar to XP_342341.1 group XII-1 phospholipase A2 [Rattus norvegicus]	Down
CN438214	Bt.1539		Transcribed locus, moderately similar to NP_000396.2 GM2 ganglioside activator protein [Homo sapiens]	Down
CK770880	Bt.62243		Transcribed locus, strongly similar to NP_058864.1 phospholipase C, gamma 2 [Rattus norvegicus]	Down
CF613729	Bt.23226	<i>ACADSB</i>	Acyl-Coenzyme A dehydrogenase, short/branched chain	Down
BF044267	Bt.37818	<i>ACACB</i>	Acetyl-CoA carboxylase, type beta	Down
General metabolism				
CN435970	Bt.20720	<i>CES2</i>	Carboxylesterase 2	Up
AW461717	Bt.49713	<i>CKMT1</i>	Creatine kinase, mitochondrial 1 (ubiquitous)	Up
BM363130	Bt.53580	<i>SEPX1</i>	Selenoprotein X, 1	Up
BF039387	Bt.20141		Similar to Hydroxyacylglutathione hydrolase (Glyoxalase II) (GLX II)	Up
BF042117	Bt.21822		Similar to Aldehyde dehydrogenase 3B1	Up
AW461432	Bt.13628		Transcribed locus, strongly similar to XP_534370.2 transglutaminase 3 precursor [Canis familiaris]	Up
BF044308	Bt.44647	<i>NADK</i>	NAD kinase	Up
CK838210	Bt.9081		Similar to Selenocysteine lyase	Up
CN433788	Bt.56538		Transcribed locus, moderately similar to XP_848651.1 phosphotriesterase related protein (Parathion hydrolase-related protein) isoform 2 [Canis familiaris]	Down
CN434037	Bt.49673	<i>GSTM1</i>	Glutathione S-transferase M1	Down
CN436549	Bt.3314		Similar to Pleckstrin homology domain containing, family M (with RUN domain) member 1	Down
CN441882	Bt.15996	<i>ACAS2L</i>	Acetyl-Coenzyme A synthetase 2 (AMP forming)-like	Down
BF045987	Bt.43990		Similar to ATPase, H+ transporting, V0 subunit D isoform 2	Down
BF044672	Bt.64780		Transcribed locus, strongly similar to NP_005902.1 methionine adenosyltransferase II, alpha [Homo sapiens]	Down
CF766726	Bt.67756		Transcribed locus, strongly similar to NP_078771.1 carbonic anhydrase 13 [Mus musculus]	Down
AW463631	Bt.69	<i>NDUFA1</i>	NADH dehydrogenase (ubiquinone) 1 alpha subcomplex, 1, 7.5kDa	Down
BF042402	Bt.11993		Similar to dehydrogenase/reductase SDR family member 8 precursor (17-beta-hydroxysteroid dehydrogenase 11) (17-beta-HSD 11)	Down
AW464695	Bt.4113		Transcribed locus, strongly similar to XP_534612.2 COP9 signalosome complex subunit 8 (Signalosome subunit 8) (SGN8) (JAB1-containing signalosome subunit 8) (COP9 homolog) (hCOP9) [Canis familiaris]	Down

TABLE H.1. (continued)

Oligo sequence ID	Unigene ID	Symbol	Gene product	Expression
TCA				
BF042003	Bt.24449	<i>SDHA</i>	Succinate dehydrogenase flavoprotein subunit A	Up
AW464637	Bt.3809	<i>LDHA</i>	Lactate dehydrogenase A	Down
CN439286	Bt.13487		Similar to 6-phosphogluconate dehydrogenase (decarboxylating)	Down
Eletron transport				
CR551153	Bt.665	<i>CYP2D6</i>	Cytochrome P450, family 2, subfamily D, polypeptide 6	Up
DR697628	Bt.3985	<i>CYP17</i>	Cytochrome P450, subfamily XVII	Up
CR453506	Bt.16025	<i>COX4</i>	Cytochrome c oxidase subunit 4	Up
CN440220	Bt.63247		Transcribed locus, moderately similar to NP_001032415.1 dehydrogenase (ubiquinone) 1 beta subcomplex, 4, 15kDa [Rattus norvegicus]	Up
BF043169	Bt.2562	<i>GRP58</i>	Glucose regulated protein 58kD	Up
CR455817	Bt.231	<i>TXN</i>	Thioredoxin	Up
AW464776	Bt.5288	<i>TXN2</i>	Thioredoxin 2	Up
CN441299	Bt.74430	<i>TXNDC4</i>	Thioredoxin domain containing 4 (endoplasmic reticulum)	Up
CN441116	Bt.49189	<i>NDUFV2</i>	NADH dehydrogenase flavoprotein 2 (24kD) [ubiquinone] [NADH-ubiquinone reductase 24 kDa mitochondrial]	Up
CN437522	Bt.5483	<i>NDUFS8</i>	NADH dehydrogenase (ubiquinone) Fe-S protein 8, 23kDa (NADH-coenzyme Q reductase)	Up
BF039175	Bt.76309		Similar to NADH:ubiquinone oxidoreductase MLRQ subunit homolog	Up
BF044713	Bt.20	<i>NDUFA7</i>	NADH dehydrogenase (ubiquinone) 1 alpha subcomplex, 7, 14.5kDa	Up
BM363889	Bt.23164	<i>UQCRC1</i>	UQCRC1 protein	Up
NM_176654	Bt.4211	<i>ATP6V1B1</i>	ATPase, H+ transporting, V1 subunit B, isoform 1	Up
CN441269	Bt.62703		Similar to ATP synthase, H+ transporting, mitochondrial F1 complex, alpha subunit, isoform 1, cardiac muscle	Down
AV612395	Bt.8845	<i>ACAD9</i>	Acyl-Coenzyme A dehydrogenase family, member 9	Down
CK773196	Bt.25731		Transcribed locus, moderately similar to NP_080460.2 endoplasmic oxidoreductase 1 beta [Mus musculus]	Down
BM363367	Bt.27327	<i>UQCRH</i>	Similar to Ubiquinol-cytochrome c reductase complex 11 kDa protein, mitochondrial precursor (Mitochondrial hinge protein) (Cytochrome C1, nonheme 11 kDa protein) (Complex III subunit VIII)	Down
CN439862	Bt.60	<i>NDUFB2</i>	NADH dehydrogenase (ubiquinone) 1 beta subcomplex, 2, 8kDa	Down
CN442294	Bt.55686	<i>COX5A</i>	COX5A protein	Down
Signal transduction				
CR553533	Bt.10903	<i>TSE1</i>	Similar to cAMP-dependent protein kinase type I-alpha regulatory subunit (Tissue-specific extinguisher-1)	Up
CN440527	Bt.5371	<i>GAP1IP4BP</i>	RAS p21 protein activator (GTPase activating protein) 3 (Ins(1,3,4,5)P4-binding protein)	Up
CN441423	Bt.4559		Transcribed locus, strongly similar to NP_077322.1 3 [Rattus norvegicus]	Up
CN442144	Bt.3876	<i>ARL2</i>	ADP-ribosylation factor-like 2	Up
BF043403	Bt.29937	<i>CENTB1</i>	Similar centaurin beta1	Up

TABLE H.1. (continued)

Oligo sequence ID	Unigene ID	Symbol	Gene product	Expression
BF040565	Bt.8204		Transcribed locus, strongly similar to XP_509190.1 SLIT-ROBO Rho GTPase-activating protein 1 [Pan troglodytes]	Up
NM_174466	Bt.8137	<i>SOCS3</i>	Suppressor of cytokine signaling 3	Up
BM363844	Bt.11924		Transcribed locus, strongly similar to NP_001003264.1 signal recognition particle,72 kDa subunit [Canis familiaris]	Up
CB442289	Bt.8543	<i>TIMAP</i>	CAAX box protein TIMAP	Up
AW464303	Bt.12575		Similar to Ras-related protein rab-4B	Up
BF042882	Bt.20180	<i>RAB25</i>	RAB25, member RAS oncogene family	Up
CV798843	Bt.167	<i>MAPK1</i>	Mitogen-activated protein kinase 1	Up
BF045624	Bt.42665		Transcribed locus, strongly similar to NP_060241.2 PX domain containing serine/threonine kinase [Homo sapiens]	Up
BF043288	Bt.46188		Similar to cAMP-dependent protein kinase inhibitor beta	Up
NM_174229	Bt.517	<i>ADCY1</i>	Adenylate cyclase 1 (brain)	Up
NM_174647	Bt.4706	<i>PPP1R1B</i>	Protein phosphatase 1, regulatory (inhibitor) subunit 1B	Up
BI680681	Bt.78165		Transcribed locus, strongly similar to NP_001657.2 Rho GTPase activating protein 4 [Homo sapiens]	Up
AW445383	Bt.24520	<i>BLNK</i>	B-cell linker	Up
CK775260	Bt.34847		Transcribed locus, strongly similar to NP_058039.1 Rap2 interacting protein [Mus musculus]	Up
CK770933	Bt.74982		Transcribed locus, weakly similar to NP_445781.2 growth factor binding protein, acid labile subunit [Rattus norvegicus]	Up
CR452271	Bt.26628	<i>RAP2C</i>	Similar to RAP2C, member of RAS oncogene family	Down
CR453466	Bt.14122		Transcribed locus, strongly similar to XP_227600.4 protein vav-3 [Rattus norvegicus]	Down
CR452307	Bt.18279	<i>FZD3</i>	Frizzled homolog 3 (Drosophila)	Down
CN432293	Bt.43141		Transcribed locus, strongly similar to XP_544104.2 phosphodiesterase 7A isoform a isoform 1 [Canis familiaris]	Down
CN433357	Bt.36230		Transcribed locus, strongly similar to XP_543734.2 leucine-rich repeat kinase 2 [Canis familiaris]	Down
CN435008	Bt.45586		Transcribed locus, strongly similar to XP_535785.2 triple functional domain (PTPRF interacting) [Canis familiaris]	Down
CN435042	Bt.21189		Transcribed locus, strongly similar to XP_865394.1 protein kinase D2 isoform 5 [Canis familiaris]	Down
CN441383	Bt.30379	<i>CDKN3</i>	Cyclin-dependent kinase inhibitor 3 (CDK2-associated dual specificity phosphatase)	Down
BF041110	Bt.4641	<i>STAT5A</i>	Signal transducer and activator of transcription 5A	Down
BF044335	Bt.6801		Transcribed locus, strongly similar to XP_344278.2 ankyrin repeat and SOCS box-containing protein 3 [Rattus norvegicus]	Down
AW289213	Bt.53393	<i>RHOH</i>	Ras homolog gene family, member H	Down
CV798830	Bt.3504		Transcribed locus, strongly similar to XP_508296.1 related RAS viral (r-ras) oncogene homolog 2 [Pan troglodytes]	Down
CR453020	Bt.3192	<i>RABL2A</i>	RAB, member of RAS oncogene family-like 2A	Down
CN441075	Bt.44630	<i>RAB11A</i>	Similar to RAB11a, member RAS oncogene family	Down
CR454061	Bt.49090	<i>COMMD3</i>	COMM domain containing 3	Down
CR454313	Bt.60794		Transcribed locus, moderately similar to NP_036620.1 [Rattus norvegicus]	Down

TABLE H.1. (continued)

Oligo sequence ID	Unigene ID	Symbol	Gene product	Expression
AW289359	Bt.46977		Similar to dual adapter for phosphotyrosine and 3-phosphotyrosine and 3-phosphoinositide (hDAPP1) (B cell adapter molecule of 32 kDa) (B lymphocyte adapter protein Bam32)	Down
BF040319	Bt.64564		Transcribed locus, weakly similar to XP_369329.1 protein MG06135.4 [Magnaporthe grisea 70-15]	Down
CR454899	Bt.19807	<i>SCAP2</i>	SRC family associated phosphoprotein 2	Down
BF440395	Bt.16911		Transcribed locus, weakly similar to XP_360001.1 protein MG05376.4 [Magnaporthe grisea 70-15]	Down
BM362982	Bt.24347	<i>MRGPRF</i>	MAS-related GPR, member F	Down
CR452711	Bt.9450		Similar to A-kinase anchor protein 13	Down
CR452657	Bt.5451	<i>RAB5B</i>	RAB5B, member RAS oncogene family	Down
BM364131	Bt.49073	<i>CD3D</i>	Antigen CD3D, delta polypeptide (TiT3 complex)	Down
CN432988	Bt.39894		Transcribed locus, weakly similar to NP_604463.1 protein kinase I [Rattus norvegicus]	Down
BF040754	Bt.9569	<i>TACSTD1</i>	Tumor-associated calcium signal transducer 1	Down
DV780245	Bt.20562	<i>NCOA4</i>	Nuclear receptor coactivator 4	Down
NM_174765	Bt.7214	<i>COL4A3BP</i>	Collagen, type IV, alpha 3 (Goodpasture antigen) binding protein	Down
CK944372	Bt.2150		Transcribed locus, strongly similar to NP_037428.2 G-protein signalling modulator 2 (AGS3-like, C. elegans); LGN protein [Homo sapiens]	Down
AW670539	Bt.2462	<i>SH2D2A</i>	SH2 domain protein 2A	Down
CB539028	Bt.38707	<i>RAB8B</i>	RAB8B, member RAS oncogene family	Down
NM_178109	Bt.20923	<i>PRKR</i>	Protein kinase, interferon-inducible double stranded RNA dependent	Down
BF040014	Bt.64692	<i>RAB18</i>	Similar to Ras-related protein Rab-18	Down
BF440362	Bt.37348	<i>LPXN</i>	Leupaxin	Down
Surface receptors				
CR452313	Bt.56413		Transcribed locus, strongly similar to XP_001053288.1 receptor tyrosine kinase-like orphan receptor 2 [Rattus norvegicus]	Up
BF046224	Bt.2996		Transcribed locus, strongly similar to XP_536222.2 G protein-coupled receptor kinase 4 isoform alpha [Canis familiaris]	Up
BF039474	Bt.4990	<i>ACVR2B</i>	Activin A receptor, type IIB	Up
CK770943	Bt.37189	<i>BLR1</i>	Burkitt lymphoma receptor 1	Up
NM_174640	Bt.11204	<i>GPR73L1</i>	G protein-coupled receptor 73-like 1	Up
NM_175715	Bt.486	<i>ADCYAP1R1</i>	Adenylate cyclase activating polypeptide 1 (pituitary) receptor type I	Up
CB432832	Bt.16889	<i>LTB4R</i>	Leukotriene B4 receptor	Up
AJ618974	Bt.29889	<i>TLR6</i>	Toll-like receptor 6	Down
CR550392	Bt.7319		Transcribed locus, moderately similar to XP_342569.3 protein tyrosine phosphatase, receptor type, T [Rattus norvegicus]	Down
CR456081	Bt.15558	<i>GRM7</i>	Similar to metabotropic glutamate receptor 7 precursor (mGluR7)	Down
NM_174547	Bt.4538	<i>GUCY2C</i>	Guanylate cyclase 2C [heat stable enterotoxin receptor]	Down
NM_174051	Bt.541	<i>ESR2</i>	Estrogen receptor 2 (ER beta)	Down
Transport				
CN437574	Bt.7980	<i>LASP1</i>	LIM and SH3 protein 1	Up

TABLE H.1. (continued)

Oligo sequence ID	Unigene ID	Symbol	Gene product	Expression
AW461699	Bt.11804		Transcribed locus, strongly similar to XP_538934.2 ATP-binding cassette, sub-family C, member 10 [Canis familiaris]	Up
AW464787	Bt.63034		Transcribed locus, weakly similar to XP_368776.1 protein MG00468.4 [Magnaporthe grisea 70-15]	Up
AW464903	Bt.64977	<i>SLC02B1</i>	Organic anion transporting polypeptide 2b1	Up
BF039974	Bt.53065		Similar to copper chaperone for superoxide dismutase (Superoxide dismutase copper chaperone)	Up
NM_174221	Bt.5067	<i>ABCA4</i>	ATP-binding cassette, sub-family A (ABC1), member 4	Up
BF046658	Bt.49082	<i>TIMM50</i>	Translocase of inner mitochondrial membrane 50 homolog	Up
CN435414	Bt.1143	<i>LAPTM4B</i>	Similar to lysosomal associated protein transmembrane 4 beta	Down
CN441107	Bt.15708	<i>MON1A</i>	MON1 homolog A (yeast)	Down
BF046414	Bt.8872	<i>ATP2B1</i>	ATPase, Ca ⁺⁺ transporting, plasma membrane 1	Down
CB424419	Bt.27240		Transcribed locus, moderately similar to XP_543087.2 solute carrier organic anion transporter family, member 4A1 (Organic anion transporting polypeptide E) (OATP-E) [Canis familiaris]	Down
CK774482	Bt.759	<i>SLC4A2</i>	SLC4A2 anion exchanger	Down
CN792196	Bt.46115	<i>SLC7A9</i>	Solute carrier family 7 (cationic amino acid transporter, y ⁺ system), member 9	Down
AW464260	Bt.19972		Transcribed locus, moderately similar to NP_005064.1 solute carrier family 15 (oligopeptide transporter), member 1; peptide transporter HPEPT1 [Homo sapiens]	Down
BF044502	Bt.77860		Transcribed locus, strongly similar to NP_112410.1 carrier family 20 (phosphate transporter), member 1 [Rattus norvegicus]	Down
NM_174655	Bt.19	<i>SLC24A1</i>	Solute carrier family 24, member 1	Down
CN442091	Bt.45842	<i>SLC27A1</i>	Solute carrier family 27 (fatty acid transporter), member 1	Down
BF040441	Bt.6359		Transcribed locus, strongly similar to NP_742063.1 carrier family 30 (zinc transporter), member 4 [Rattus norvegicus]	Down
CN433928	Bt.9238	<i>SLC38A2</i>	Solute carrier family 38, member 2	Down
BF044778	Bt.8735	<i>TIMM22</i>	Translocase of inner mitochondrial membrane 22 homolog	Down
BF044937	Bt.29968	<i>ENSA</i>	Endosulfine alpha	Down
AW462521	Bt.51973	<i>ABCG2</i>	ATP-binding cassette, sub-family G, member 2	Down
AW289347	Bt.5346		Transcribed locus, weakly similar to XP_362105.1 protein MG04550.4 [Magnaporthe grisea 70-15]	Down
AW487381	Bt.24395		Transcribed locus, strongly similar to NP_055406.2 Kv channel interacting protein 2 ; A-type potassium channel modulatory protein 2; cardiac voltage gated potassium channel modulatory subunit; Kv channel-interacting protein 2 [Homo sapiens]	Down
CK954948	Bt.29087	<i>ABCG8</i>	ATP-binding cassette sub-family G member 8	Down
BF040532	Bt.19423	<i>ABCA1</i>	ATP-binding cassette sub-family A member 1	Down
Endocytosis and Intracellular trafficking				
CN438703	Bt.41539		Transcribed locus, strongly similar to NP_002324.1 low density lipoprotein receptor-related protein 3 [Homo sapiens]	Up
CN441088	Bt.48457	<i>TNPO1</i>	Transportin 1	Up
BF043219	Bt.49381	<i>RAB1A</i>	GTP binding protein Rab1a	Up

TABLE H.1. (continued)

Oligo sequence ID	Unigene ID	Symbol	Gene product	Expression
AW465699	Bt.20269		Transcribed locus, strongly similar to NP_001654.1 ADP-ribosylation factor 6 [Homo sapiens]	Up
AW462308	Bt.49453		Similar to SEC13-like 1	Up
AW465155	Bt.11133		Similar to USE1-like protein (Hematopoietic stem/progenitor cells protein MDS032) (Putative MAPK activating protein PM26) (Protein p31) isoform 3 [Canis familiaris]	Up
BF039386	Bt.6096		Similar to conserved oligomeric Golgi complex component 2 (Low density lipoprotein receptor defect C-complementing protein)	Up
CR451981	Bt.57991	<i>TRAPPC5</i>	Trafficking protein particle complex 5	Up
BF045579	Bt.53665		Similar to NSFL1 (p97) cofactor (p47)	Up
CR455769	Bt.7758		Transcribed locus, strongly similar to NP_446006.1 clathrin assembly protein [Rattus norvegicus]	Down
CR456173	Bt.5969	<i>VPS35</i>	Vacuolar protein sorting 35 (yeast)	Down
CR451664	Bt.4070	<i>SNX1</i>	Similar to sorting nexin 1	Down
CN433789	Bt.39859		Transcribed locus, strongly similar to XP_537403.2 vesicle transport-related protein isoform a [Canis familiaris]	Down
AW465446	Bt.48523		Similar to vacuolar protein sorting 29 (Vesicle protein sorting 29)	Down
BF044109	Bt.49605		Similar to amyloid beta (A4) precursor protein-binding, family A, member 3	Down
CN436560	Bt.7175		Transcribed locus, strongly similar to NP_446230.1 importin 13 [Rattus norvegicus]	Down
AW461450	Bt.64628		Transcribed locus, strongly similar to XP_532669.2 nucleoporin Nup37 (p37) [Canis familiaris]	Down
AW464321	Bt.19243		Similar to sorting nexin 6	Down
CR451855	Bt.12416		Similar to syntaxin-5	Down
BF039953	Bt.1248		Transcribed locus, strongly similar to XP_850701.1 ADP-ribosylation factor binding protein GGA2 (Golgi-localized, gamma ear-containing, ARF-binding protein 2) [Canis familiaris]	Down
CK954544	Bt.7273		Transcribed locus, strongly similar to XP_538631.2 protein transport protein Sec24A (SEC24-related protein A) isoform 1 [Canis familiaris]	Down
CR452427	Bt.52483		Transcribed locus, strongly similar to NP_005478.2 high-mobility group protein 2-like 1 isoform a [Homo sapiens]	Down
Other functions				
AW266929	Bt.12916	<i>GPX3</i>	Glutathione peroxidase 3 (plasma)	Up
CN442255	Bt.59546	<i>WDR1</i>	WD repeat domain 1	Up
DR697417	Bt.16452	<i>PRRG2</i>	Proline rich Gla (G-carboxyglutamic acid) 2	Up
BF039730	Bt.36654	<i>SRP54</i>	Signal recognition particle 54kDa	Up
BF046378	Bt.8244		Transcribed locus, weakly similar to NP_659449.3 cyclin fold protein 1; cyclin-box carrying protein 1 [Homo sapiens]	Up
AW465190	Bt.21634		Similar to 3-mercaptopyruvate sulfurtransferase	Up
CR452840	Bt.61076	<i>ATIC</i>	5-aminoimidazole-4-carboxamide ribonucleotide formyltransferase/IMP cyclohydrolase	Up
AW461380	Bt.76489		Transcribed locus, moderately similar to XP_001079086.1 NF-kappa B inhibitor [Rattus norvegicus]	Up
CN440351	Bt.21035		Similar to S100 calcium binding protein A16	Up
BF041492	Bt.5126	<i>COMMD5</i>	COMM domain-containing protein 5	Up

TABLE H.1. (continued)

Oligo sequence ID	Unigene ID	Symbol	Gene product	Expression
BF042692	Bt.53903		Transcribed locus, strongly similar to XP_853516.1 tyrosine-protein phosphatase, non-receptor type 3 (Protein-tyrosine phosphatase H1) (PTP-H1) isoform 1 [Canis familiaris]	Up
BM366427	Bt.4001	<i>HMOX1</i>	Heme oxygenase (decyclizing) 1	Up
CK394103	Bt.1639	<i>GALNT6</i>	UDP-N-acetyl-alpha-D-galactosamine:polypeptide N-acetylgalactosaminyltransferase 6 (GalNAc-T6)	Up
CR455867	Bt.20383	<i>MGST1</i>	Microsomal glutathione S-transferase 1	Up
NM_173937	Bt.4516	<i>MIP</i>	Major intrinsic protein of lens fiber	Up
NM_174453	Bt.108	<i>RPE65</i>	Retinal pigment epithelium-specific protein (65kD)	Up
NM_174462	Bt.8126	<i>SFTPC</i>	Surfactant, pulmonary-associated protein C	Up
AJ693807	Bt.10814		Transcribed locus, moderately similar to XP_546059.2 proteinase activated receptor 1 precursor (PAR-1) (Thrombin receptor) (Coagulation factor II receptor) [Canis familiaris]	Up
CR452580	Bt.2689	<i>PRDX2</i>	Peroxiredoxin 2	Up
A34676	Bt.13106	<i>F9</i>	Coagulation factor IX	Down
CR551847	Bt.30982		Similar to calcium/calmodulin-dependent protein kinase IG	Down
CN434569	Bt.65013		Transcribed locus, moderately similar to XP_940679.1 hypothetical protein XP_940679 [Homo sapiens]	Down
CN434601	Bt.9482		Transcribed locus, weakly similar to NP_071580.1 [Rattus norvegicus]	Down
CN440242	Bt.28278	<i>ACE2</i>	Angiotensin I converting enzyme 2 precursor	Down
CN436832	Bt.24903		Transcribed locus, moderately similar to XP_545854.2 peroxisomal biogenesis factor 11A [Canis familiaris]	Down
CN440825	Bt.32810	<i>PDLIM1</i>	PDZ and LIM domain 1 (elfin)	Down
BF046111	Bt.21926		Transcribed locus, moderately similar to NP_001037709.1 outer mitochondrial membrane 34 [Rattus norvegicus]	Down
BF041041	Bt.21023	<i>AS3MT</i>	Arsenic (+3 oxidation state) methyltransferase	Down
DR697599	Bt.3362		Transcribed locus, strongly similar to NP_032935.1 periplakin [Mus musculus]	Down
CR451915	Bt.41083		Similar to interferon induced transmembrane protein 5	Down
AW465015	Bt.45496		Similar to peroxisomal biogenesis factor 16	Down
L41691	Bt.4771	<i>RANBP2</i>	RAN binding protein 2	Down
CR454282	Bt.49339		Similar to Alcohol dehydrogenase class III chi chain (Glutathione-dependent formaldehyde dehydrogenase) (FDH)	Down
CR552774	Bt.12704	<i>AOC2</i>	Amine oxidase, copper containing 2 (retina-specific)	Down
CR551770	Bt.52556		Transcribed locus, strongly similar to XP_519126.1 calcitonin gene-related peptide-receptor component protein (CGRP-receptor component protein) [Pan troglodytes]	Down
BM364227	Bt.52556		Similar to calcitonin gene-related peptide-receptor component protein (CGRP-receptor component protein) (CGRP-RCP) (CGRP-PCP)	Down
CN433335	Bt.4067		Similar to myristoylated alanine-rich C-kinase substrate (MARCKS)	Down
BF045638	Bt.47401		Similar to serine protease inhibitor, Kunitz type, 2	Down

176 up- and 332 down-regulated genes of Unknown function were not listed

APPENDIX I

TABLE I.1. Host genes differentially expressed in *B. melitensis* heat inactivated-inoculated bovine Peyer's patch during the first 4 hours post-infection, compared to non-infected tissue

Oligo sequence ID	Unigene ID	Gene symbol	Gene product	Expression
DNA replication and repair				
BF046176	Bt.22960	<i>DNMT2</i>	DNA (cytosine-5-)-methyltransferase 2	Up
AJ677808	Bt.28672		Transcribed locus, moderately similar to XP_542244.2 double-strand break repair protein MRE11A (MRE11 homolog 1) [Canis familiaris]	Down
Chromatin modification				
BF041316	Bt.77188		Transcribed locus, strongly similar to XP_536904.2 histone acetyltransferase MYST1 [Canis familiaris]	Down
BF046031	Bt.53293		Similar to histone H3 methyltransferase DOT1	Down
NM_174200	Bt.45043	<i>TNP2</i>	Transition protein 2 (during histone to protamine replacement)	Down
RNA processing				
BF043207	Bt.21089		Transcribed locus, strongly similar to XP_512420.1 TRM1_Human Probable	Down
U83008	Bt.14661*	<i>ELAC1</i>	ElaC homolog 1 (<i>E. coli</i>)	Down
Transcription regulation				
CR551218	Bt.69615		Transcribed locus, strongly similar to XP_001073379.1 wingless-related MMTV integration site 7A isoform 2 [Rattus norvegicus]	Up
DR697591	Bt.45570*	<i>EPAS1</i>	Endothelial PAS domain protein 1	Up
CR553822	Bt.28727	<i>NFKBIL1</i>	Nuclear factor of kappa light polypeptide gene enhancer in B-cells inhibitor-like 1	Up
AW461405	Bt.4606*		Similar to Kruppel-like factor 6	Up
CR452893	Bt.65959		Transcribed locus, moderately similar to XP_539196.2 zinc finger protein 84 (Zinc finger protein HPF2) [Canis familiaris]	Down
AW465975	Bt.7079		Transcribed locus, strongly similar to XP_001066346.1 transcriptional enhancer factor TEF-3 (TEA domain family member 4) (TEAD-4) [Rattus norvegicus]	Down
CN440952	Bt.7492	<i>CREB3</i>	cAMP responsive element binding protein 3 (human)	Down
BF044910	Bt.45442		Similar to SIN3B long	Down
BI681052	Bt.78081		Transcribed locus, strongly similar to XP_548294.2 PHD finger protein 12 (PHD factor 1) (Pf1) isoform 1 [Canis familiaris]	Down
Protein biosynthesis				
CN437058	Bt.59370*		Similar to probable leucyl-tRNA synthetase, mitochondrial precursor (Leucine--tRNA ligase) (LeuRS)	Down
CN441874	Bt.44540*		Transcribed locus, strongly similar to Human Alanyl-tRNA synthetase	Down
BM361943	Bt.20487*		Similar to 39S ribosomal protein L28, mitochondrial precursor (L28mt) (MRP-L28) (Melanoma antigen p15)	Down

TABLE I.1. (continued)

Oligo sequence ID	Unigene ID	Gene symbol	Gene product	Expression
AW462348	Bt.20442		Transcribed locus, moderately similar to NP_076426.1 mitochondrial ribosomal protein L34 [Homo sapiens]	Down
Protein degradation				
BF045351	Bt.62312		Transcribed locus, strongly similar to XP_541630.2 F-box protein FBG4 isoform 1 [Canis familiaris]	Up
CN439280	Bt.2056		Transcribed locus, strongly similar to XP_533826.2 hydrolase [Canis familiaris]	Up
BF046516	Bt.26715	<i>ST14</i>	Suppression of tumorigenicity 14	Down
AW464210	Bt.8282*	<i>DPP4</i>	Dipeptidylpeptidase IV (CD26, adenosine deaminase complexing protein 2)	Down
Inflammatory and immune response				
CV576045	Bt.7541		Similar to pentraxin-related protein PTX3 precursor (Pentaxin-related protein PTX3) (Tumor necrosis factor-inducible protein TSG-14)	Up
BF046359	Bt.1548*		Transcribed locus, moderately similar to XP_533874.2 gamma-interferon inducible lysosomal thiol reductase precursor (Gamma-interferon-inducible protein IP-30) [Canis familiaris]	Up
BF440380	Bt.42822		Transcribed locus, weakly similar to NP_058716.1 IL6 receptor [Rattus norvegicus]	Up
BM363499	Bt.552	<i>CCL5</i>	Chemokine (C-C motif) ligand 5	Up
NM_174007	Bt.154	<i>CCL8</i>	Chemokine (C-C motif) ligand 8	Up
NM_183365	Bt.23155	<i>NCR1</i>	Natural cytotoxicity triggering receptor 1	Up
AV617024	Bt.29824	<i>JSP.1</i>	MHC class I JSP.1	Up
CB533935	Bt.14139*		Similar to complement component C9 precursor	Down
AJ535317	Bt.79131*	<i>cd21</i>	Complement receptor type 2	Down
BF043775	Bt.103*	<i>BPI</i>	Bactericidal/permeability-increasing protein	Down
BM362452	Bt.37553*		Transcribed locus, weakly similar to NP_663705.1 inducible cytokine B9 [Rattus norvegicus]	Down
BM363549	Bt.21431*	<i>NCR3</i>	Natural cytotoxicity triggering receptor 3	Down
NM_205787	Bt.25528*	<i>PTP</i>	Pancreatic thread protein	Down
Cell adhesion				
CR550740	Bt.40988		Similar to dermatopontin precursor (Tyrosine-rich acidic matrix protein) (TRAMP)	Up
CR456127	Bt.2696		Transcribed locus, strongly similar to NP_001788.2 cadherin 11, type 2 isoform 1 preproprotein; osteoblast cadherin; cadherin-11; OB-cadherin [Homo sapiens]	Up
CN439845	Bt.49521		Similar to platelet-endothelial tetraspan antigen 3 (PETA-3) (GP27) (Membrane glycoprotein SFA-1) (CD151 antigen)	Up
BM365343	Bt.9510*	<i>TIMD4</i>	T-cell immunoglobulin and mucin domain containing 4 (TIMD4)	Down
Cytoskeleton organization				
CR455803	Bt.45308		Transcribed locus, weakly similar to XP_360353.1 protein MG05727.4 [Magnaporthe grisea 70-15]	Up
BF046528	Bt.59065		Transcribed locus, strongly similar to XP_536692.2 hook homolog 1 (h-hook1) (hHK1) [Canis familiaris]	Up
AW463298	Bt.59155*	<i>KRT19</i>	Cytokeratin 19	Up
CR454496	Bt.24937		Transcribed locus, strongly similar to NP_001448.1 filamin B, beta (actin binding protein 278) [Homo sapiens]	Up
BM430199	Bt.56652*		Transcribed locus, moderate similar to XP_511487.1 S37780 keratin 20, type I-like, cytoskeletal - human	Up

TABLE I.1. (continued)

Oligo sequence ID	Unigene ID	Gene symbol	Gene product	Expression
NM_174395	Bt.438	<i>MYO1A</i>	Myosin IA	Down
CR552526	Bt.48647		Transcribed locus, moderately similar to NP_001013148.1 beta 2 [Rattus norvegicus]	Down
Apoptosis				
AW463573	Bt.14503		Similar to death associated transcription factor 1	Up
BF440414	Bt.11884*	<i>BCL2A1</i>	B-cell leukemia/lymphoma 2 related protein A1	Down
Metabolism				
CN437812	Bt.73269	<i>P4HA3</i>	Collagen prolyl 4-hydroxylase alpha III subunit	Up
BF043681	Bt.29367		Transcribed locus, weakly similar to NP_036903.2 [Rattus norvegicus]	Up
CR552975	Bt.315	<i>NDUFS7</i>	NADH dehydrogenase (ubiquinone) Fe-S protein 7, 20kDa	Up
CB223494	Bt.28966*	<i>PLA2G2A</i>	Phospholipase A2 group IIA-like	Up
CN441201	Bt.12*	<i>FABP1</i>	Fatty acid binding protein 1, liver	Up
CN435446	Bt.49234	<i>GPX4</i>	Glutathione peroxidase 4 (phospholipid hydroperoxidase)	Down
BM363586	Bt.49614*	<i>ALDOC</i>	Aldolase C, fructose-bisphosphate	Down
Intracellular signal transduction				
CN441896	Bt.76242		Transcribed locus, strongly similar to NP_001032635.1 RhoGEF and PH domain containing 1 [Rattus norvegicus]	Up
BM362357	Bt.20905		Transcribed locus, strongly similar to XP_576543.1 zeta-chain (TCR) associated protein kinase 70kDa [Rattus norvegicus]	Up
AW461747	Bt.35642		Transcribed locus, moderately similar to XP_001075684.1 similar to sorting nexin 22 [Rattus norvegicus]	Up
NM_174229	Bt.517*	<i>ADCY1</i>	Adenylate cyclase 1 (brain)	Up
NM_174322	Bt.5511	<i>GNA11</i>	GNA11 protein	Up
CK960359	Bt.32575	<i>RASGRP4</i>	RAS guanyl releasing protein 4 isoform 1	Up
NM_176873	Bt.16023	<i>RAB3C</i>	RAB3C, member RAS oncogene family	Up
AW415585	Bt.24461		Transcribed locus, strongly similar to XP_539166.2 adenylate cyclase 8 [Canis familiaris]	Down
CR551967	Bt.32878		Similar to islet-brain 1	Down
NM_174785	Bt.117	<i>GNG12</i>	Guanine nucleotide binding protein (G protein), gamma 12	Down
Intracellular protein transport				
CN435987	Bt.4048*	<i>STXBP1</i>	Syntaxin binding protein 1	Down
BC112867	Bt.28467		Similar to sorting nexin 8	Down
Ion transport				
CB424419	Bt.27240*		Transcribed locus, moderately similar to NP_598292.2 carrier organic anion transporter family, member 4a1 [Rattus norvegicus]	Up
CB442833	Bt.16310*		Transcribed locus, strongly similar to XP_508369.1 dJ68D18.1.2 (solute carrier family 1 (glial high affinity glutamate transporter) member 2) [Pan troglodytes]	Down
Unknown function				
CR550829			mRNA sequence	Up
CR551657			mRNA sequence	Up
CR452802	Bt.61866		Similar to Leucine-rich repeat-containing protein 8	Up
CR452775	Bt.52278		Similar to CG11388-PA	Up
CR456265			mRNA sequence	Up

TABLE I.1. (continued)

Oligo sequence ID	Unigene ID	Gene symbol	Gene product	Expression
CR553319	Bt.69622		Transcribed locus	Up
CR553013			Transcribed locus	Up
CN432282	Bt.62095	<i>YPEL4</i>	Yippee-like 4	Up
CN433027			Transcribed locus	Up
CN434647			mRNA sequence	Up
CN434725			mRNA sequence	Up
CN432585			Transcribed locus	Up
CN437147	Bt.30419		Transcribed locus	Up
CN437455	Bt.8337		Transcribed locus	Up
CN437575	Bt.73598		Transcribed locus	Up
CN438028	Bt.73608		Transcribed locus	Up
CN439347	Bt.20220		Transcribed locus	Up
CN439579	Bt.34378		Transcribed locus	Up
CN440911	Bt.30628		Transcribed locus	Up
CN441174	Bt.30634		Transcribed locus	Up
CN441793			mRNA sequence	Up
CN442181			mRNA sequence	Up
AW462087	Bt.26810	<i>EPB41L5</i>	Erythrocyte membrane protein band 4.1 like 5	Up
BF045800			mRNA sequence	Up
BF440526			mRNA sequence	Up
BM362543			mRNA sequence	Up
CB436617	Bt.27877		Transcribed locus, strongly similar to NP_036467.2 myosin IF; myosin-ID [Homo sapiens]	Up
BF046061	Bt.17337		Transcribed locus, moderately similar to XP_001077274.1 similar to F-box only protein 31 [Rattus norvegicus]	Up
AW462360			mRNA sequence	Up
AW462410			mRNA sequence	Up
CN438100	Bt.13769		Transcribed locus	Up
CN441927	Bt.30813		Transcribed locus	Up
CN440721	Bt.18467		CDNA clone IMAGE:8055185, containing frame-shift errors	Up
BF045955	Bt.59465		Transcribed locus, weakly similar to XP_001076965.1 similar to alanine-glyoxylate aminotransferase 2-like 1 [Rattus norvegicus]	Up
CK394179	Bt.58024		Transcribed locus	Up
CR553683	Bt.13778		Transcribed locus	Up
BM362443			mRNA sequence	Up
CR454045	Bt.58864	<i>GDPD5</i>	Glycerophosphodiester phosphodiesterase domain containing 5	Up
CN440585			mRNA sequence	Up
CK943568	Bt.49472	<i>agr2</i>	Anterior gradient 2 homologue	Up
CK775551	Bt.80256		Transcribed locus	Up
CK847243			mRNA sequence	Up
CK847243			mRNA sequence	Down
TC238026			mRNA sequence	Down
CR451776	Bt.43709		Hypothetical protein	Down
CR451870	Bt.21001		Similar to B-cell CLL/lymphoma 7C	Down
CR454897	Bt.13789		Transcribed locus	Down
CR552029	Bt.20478		Transcribed locus, moderately similar to XP_220593.2 similar to novel protein [Rattus norvegicus]	Down
CN432620	Bt.9518		Transcribed locus, strongly similar to XP_001055834.1 similar to phospholipase C-like 2 [Rattus norvegicus]	Down
AW463013	Bt.58877		Similar to coiled-coil domain containing 12 [Canis familiaris]	Down

TABLE I.1. (continued)

Oligo sequence ID	Unigene ID	Gene symbol	Gene product	Expression
BF041442	Bt.4582	<i>RBED1</i>	RNA binding motif and ELMO domain 1	Down
BF041187	Bt.58358		Similar to leader-binding protein 32	Down
BF044402	Bt.66549		Transcribed locus, weakly similar to XP_001071232.1 similar to synaptonemal complex central element protein 2 [Rattus norvegicus]	Down
BM364950	Bt.28267		Transcribed locus	Down
CK778378	Bt.26584		Similar to mFLJ00019 protein	Down
CV798736	Bt.37371		Bernardinelli-Seip congenital lipodystrophy 2	Down
BF044803	Bt.52325		Transcribed locus, moderately similar to XP_372723.2 RP2 protein, testosterone-regulated - ricefield mouse [Homo sapiens]	Down
CR551628	Bt.2112		Transcribed locus, weakly similar to NP_002408.3 identified by monoclonal antibody Ki-67 [Homo sapiens]	Down
CN432740	Bt.61506		Transcribed locus, weakly similar to XP_363567.1 protein MG01493.4 [Magnaporthe grisea 70-15]	Down
BF043616			mRNA sequence	Down
CK394018	Bt.15798		Transcribed locus	Down
BM363899	Bt.77395		Transcribed locus	Down
BF045344			mRNA sequence	Down
AW465301	Bt.33127	<i>ANXA8</i>	Annexin A8	Down
BM362340	Bt.37556	<i>PDDC1</i>	Parkinson disease 7 domain containing 1	Down
CR452375	Bt.49618		Similar to Protein C20orf35 (HSMNP1)	Down
CN433241	Bt.67490		Transcribed locus	Down
AV613881	Bt.31739		Transcribed locus, strongly similar to XP_535721.2 PREDICTED: similar to ABI gene family, member 3 (NESH) binding protein isoform 2 [Canis familiaris]	Down
CR452089	Bt.17274		Transcribed locus	Down

Genes labeled with * in Unigene ID column were also differentially expressed in *B. melitensis*-infected bovine Peyer's patches

APPENDIX J

TABLE J.1. Set of *B. melitensis* candidate genes identified *in silico* as important for bovine Peyer's patch infection in the first 4 h of *Brucella*:host interaction

Locus ID	Symbol	Gene product	Mechanistic candidate at				
			15 min	30 min	1 h	2 h	4 h
Replication, recombination and repair							
BMEI1794	<i>ihfB</i>	Integration host factor beta subunit				Up	Up
BMEI1980		DNA protection during starvation protein	Up	Up		Up	Up
Transcription							
BMEI0749	<i>rpoC</i>	DNA-directed RNA polymerase beta subunit	Up	Up	Up	Up	Up
BMEI0750	<i>rpoB</i>	DNA-directed RNA polymerase beta' subunit	Up	Up	Up	Up	Up
BMEI0781	<i>rpoA</i>	DNA-directed RNA polymerase alpha subunit					Up
BMEI1297	<i>rpoZ</i>	DNA-directed RNA polymerase omega subunit	Up	Up	Up	Up	Up
BMEI1377	<i>greA</i>	Transcription elongation factor GreA					Up
Translation, ribosomal structure and biogenesis							
BMEI1862		2'-5' RNA ligase					Up
Posttranslational modification, protein turnover, chaperones							
BMEI0195	<i>clpB</i>	ATP-dependent Clp protease, ATP binding subunit					Up
BMEI0236	<i>htpX</i>	Heat shock protein HtpX		Up			Up
BMEI0874	<i>clpP</i>	ATP-dependent Clp protease proteolytic subunit		Up			Up
BMEI0876	<i>lon</i>	ATP-dependent protease La		Up			Up
BMEI1777	<i>grpE</i>	GrpE protein					Up
BMEI1804	<i>glnD</i>	PII uridylyl-transferase		Up		Up	
Amino acid transport and metabolism							
BMEI0114		Asparagine-binding periplasmic protein precursor					Up
BMEI0124	<i>argJ</i>	Bifunctional ornithine acetyltransferase/N-acetylglutamate synthase protein	Dw				
BMEI0207	<i>proB</i>	Gamma-glutamyl kinase	Up	Up	Up	Up	Up
BMEI0208	<i>proA</i>	Gamma-glutamyl phosphate reductase	NDE				
BMEI0441	<i>proX</i>	Glycine betaine/L-proline-binding protein ProX					Up
BMEI0522	<i>carB</i>	Carbamoyl-phosphate synthase large subunit	Up	Up	NDE	ND	Up
BMEI0526	<i>carA</i>	Carbamoyl-phosphate synthase small subunit	Up	Up	Up	Up	Up
BMEI0624	<i>ilvC</i>	Ketol-acid reductoisomerase	Up	Up	Up		Up
BMEI0844	<i>trpD</i>	Anthranilate phosphoribosyltransferase	Up	Up	Up	Up	Up
BMEI1211	<i>gltI</i>	General L-amino acid-binding periplasmic protein AapJ precursor		Up		Up	Up
BMEI1506	<i>aroC</i>	Chorismate synthase	Up	NDE	Up		Up
BMEI1848	<i>ilvD</i>	Dihydroxy-acid dehydratase	Up	Up		Up	
BMEI1869		Homoserine/homoserine lactone efflux protein			Dw		Dw
BMEI2017	<i>trpF</i>	N-(5'-phosphoribosyl)anthranilate isomerase	Dw		Dw		
BMEI2018	<i>trpB</i>	Tryptophan synthase subunit beta	Up	Up	Up	Up	Up
BMEI0411	<i>leuD</i>	Isopropylmalate isomerase small subunit		Up			
BMEI0441	<i>argD</i>	Acetylmithine aminotransferase		Up			
BMEI0783		Na(+)-linked D-alanine glycine permease		Up		Up	Up
BMEI0871	<i>aroE</i>	Shikimate 5-dehydrogenase	Up	Up			

TABLE J.1. (continue)

Locus ID	Symbol	Gene product	Mechanistic candidate at				
			15 min	30 min	1 h	2 h	4 h
BMEI0875	<i>livK</i>	Leucine-specific binding protein precursor		Dw		Dw	Dw
BMEI0923	<i>potD</i>	Spermidine/putrescine-binding periplasmic protein		Dw			Dw
BMEI0952		Nitrate reductase delta chain	Up				
Nucleotide transport and metabolism							
BMEI0825	<i>pyrH</i>	Uridylate kinase		Up			
BMEI0849	<i>pyrG</i>	CTP synthetase	Up			Up	Up
BMEI1256		Nucleoside diphosphate kinase			Up		
BMEI1295	<i>pyrE</i>	Orotate phosphoribosyltransferase				Up	
Carbohydrate transport and metabolism							
BMEI0187		Transporter, DME family				Dw	
BMEI0927		Multidrug resistance protein B		Dw			Dw
BMEI0106		Xylose repressor				Dw	
BMEI0794		Multidrug resistance protein B		Up			
BMEI0795		Multidrug resistance protein B				Up	
Lipid transport and metabolism							
BMEI0075		1-acyl-sn-glycerol-3-phosphate acyltransferase			Dw		
BMEI0827	<i>uppS</i>	Undecaprenyl pyrophosphate synthetase		Up		Up	
BMEI1024		3-hydroxyisobutyrate dehydrogenase					Dw
BMEI1112		3-oxoacyl-(acyl carrier protein) synthase			Dw		
Energy production and conversion							
BMEI0137		Malate dehydrogenase					Up
BMEI0138	<i>sucC</i>	Succinyl-CoA synthetase beta subunit		NDE			
BMEI0278		Ferredoxin II	Up				
BMEI0791		Isocitrate dehydrogenase					Up
BMEI0836		Citrate synthase					Up
BMEI0959		Ferredoxin, 2Fe-2S K04755 ferredoxin, 2Fe-2S	Up				
BMEI1899		Cytochrome O ubiquinol oxidase subunit III	Dw				
BMEI0768		NADH dehydrogenase subunit N	Dw	Dw	Dw		
BMEI1068		Cytochrome c2 precursor	Dw				
Coenzyme transport and metabolism							
BMEI1144		Biotin--protein ligase	Up				
Inorganic ion transport and metabolism							
BMEI0077		Cation transport protein ChaC					Up
BMEI0637		Cobalt transport protein CbiQ		Dw			
BMEI0679		Potassium/proton antiporter RosB	Up		Up		Up
BMEI0105		Iron-regulated outer membrane protein FrpB				Dw	
BMEI0537	<i>FecE</i>	Iron (III) dicitrate transport ATP-binding protein FecE		Up			Up
BMEI0566	<i>sfuB</i>	IRON(III)-transport system permease protein SfuB		Dw	Dw		Dw
BMEI0581	<i>sodC</i>	Superoxide dismutase (CU-ZN)	Up		Up	Up	
BMEI0606	<i>fatD</i>	Ferric anguibactin transport system permease protein FatD					Up
BMEI0766		PhaF potassium efflux system protein	Dw	Dw	Dw		

TABLE J.1. (continue)

Locus ID	Symbol	Gene product	Mechanistic candidate at				
			15 min	30 min	1 h	2 h	4 h
Secondary metabolites biosynthesis, transport and catabolism							
BMEI0666		Short chain dehydrogenase	Up				
BMEI2012		Benzoate membrane transport protein		Up		Up	
Defense mechanisms							
BMEI0893	<i>acrB</i>	Acriflavin resistance protein B		Up			
BMEI1742		ABC transporter ATP-binding protein		Up		Up	
BMEI1743		ABC transporter ATP-binding protein		Up		Up	
BMEI0382	<i>AcrD</i>	Acriflavin resistance protein D	Dw		Dw		Dw
BMEI0916	<i>AcrD</i>	Acriflavin resistance protein D		Dw	Dw		
Cell wall/membrane biogenesis							
BMEI0135		Outer membrane lipoprotein				Up	
BMEI0223		Membrane-bound lytic murein transglycosylase B					Up
BMEI0340		Peptidoglycan-associated lipoprotein				Up	
BMEI0500		Soluble lytic murein transglycosylase					Up
BMEI0566		Soluble lytic murein transglycosylase					Up
BMEI0717		22 kDa outer membrane protein precursor	Up		Up		Up
BMEI0795	<i>murl</i>	Glutamate racemase		Up		Up	
BMEI0830		Outer membrane protein				Up	
BMEI0831		LpxD UDP-3-O-[3-hydroxymyristoyl] glucosamine N-acyltransferase				Up	
BMEI0833		Acyl-(acyl-carrier-protein)-UDP-N- acetylglucosamine O-acyltransferase				Up	
BMEI0850		2-dehydro-3-deoxyphosphooctonate aldolase		Up			
BMEI0998		Glycosyltransferase				Up	
BMEI1007		25 kDa outer-membrane immunogenic protein precursor	Up	Up	Up		Up
BMEI1029		Outer membrane protein TolC				Up	
BMEI1037		Glycosyltransferase involved in cell wall biogenesis				Up	
BMEI1249		25 kDa outer-membrane immunogenic protein precursor	Up		Up		Up
BMEI1829		25 kDa outer-membrane immunogenic protein precursor	Up	Up	Up		Up
BMEI1830		25 kDa outer-membrane immunogenic protein precursor	Up	Up	Up		Up
BMEI0827		Glucose-1-phosphate cytidyltransferase					Dw
BMEI0844		31 kDa outer-membrane immunogenic protein precursor				Up	
Intracellular trafficking and secretion							
BMEI0029	<i>virB5</i>	Attachment mediating protein VirB5 homolog	Dw	Dw			
General function prediction only							
BMEI0020		Glucose-fructose oxidoreductase precursor					Dw
BMEI0244		Transaldolase		Up			
BMEI0420		Oxidoreductase				Up	
BMEI0506		Transporter, DME family				Up	
BMEI0587		ComL, competence lipoprotein				Up	
BMEI0630	<i>phzF</i>	Phenazine biosynthesis protein PhzF				Dw	
BMEI0668		Calcium binding protein	Up	Up		Up	Up
BMEI0796		31 kDa immunogenic protein precursor				Up	

TABLE J.1. (continue)

Locus ID	Symbol	Gene product	Mechanistic candidate at				
			15 min	30 min	1 h	2 h	4 h
BMEI0970		Diacylglycerol kinase			Up		
BMEI1185		HppA membrane-bound proton-translocating pyrophosphatase	Up	Up	Up		Up
BMEI1231		NADH-ubiquinone oxidoreductase 18 KD subunit	Up				
BMEI1859		Integral membrane protein				Up	
BMEI2053		Transporter				Up	
BMEII1096		Putative tartrate transporter				Dw	
Function unknown							
BMEI0338		Hypothetical protein				Up	
BMEI0497		Hypothetical membrane spanning protein				Up	
BMEI0498	<i>cspA</i>	Cold shock protein CspA	Up	Up		Up	Up
BMEI0505		Hypothetical membrane associated protein				Up	
BMEI0518	<i>cspA</i>	Cold shock protein CspA	Up	Up			Up
BMEI0678		Low PH-induced protein A				Up	
BMEI1303		Hypothetical cytosolic protein	Up				
BMEI1349		Phage portal protein	Dw		Dw		
BMEI1510	<i>cspA</i>	Cold shock protein CspA					Up
BMEI1795		Hypothetical protein				Up	
BMEI1866		Hypothetical protein		Up			Up
BMEII0053		MG(2+) transport ATPase protein C	Dw		Dw		
BMEII0157		Hypothetical protein				Dw	
BMEII0987		NIRV precursor		Up			

Up = Up-regulated

Dw = Down-regulated

NDE = Non differentially expressed at this time point

VITA

Name: Carlos Alberto Rossetti

Place of Birth: Buenos Aires, Argentina

Educational Background: D.V.M., 1992
Facultad de Ciencias Veterinarias
Universidad de Buenos Aires, Argentina

M.S., Animal Health, 1998
Facultad de Ciencias Veterinarias
Universidad de Buenos Aires, Argentina

Professional Experience: Researcher (Jr. Investigator)
Instituto de Patobiología
Instituto Nacional de Tecnología Agropecuaria
November 1993 to the present

Permanent Address: Instituto de Patobiología, CICVyA
Instituto Nacional de Tecnología Agropecuaria
CC25
1712, Castelar, Buenos Aires
Argentina